Thermodynamics of Liquid Mixtures: Experimental and Theoretical Studies on the Thermochemical and Volumetric Behaviour of some Liquids and Liquid Mixtures

by

URSULA PENELOPE GOVENDER

B.Sc (Hons), M.Sc (University of Natal, Durban)

THESIS

submitted in fulfilment of the requirements for the Degree of

DOCTOR OF PHILOSOPHY

in the Department of Chemistry and Applied Chemistry,

UNIVERSITY OF NATAL, DURBAN

May 1996

Declaration

I hereby certify that the work presented in this thesis is the result of my own investigation under the supervision of Professor Trevor Letcher, and has never been submitted in candidature for a degree in any other university.

Penny Ursula Govender

I hereby certify that the above statement is correct.

Professor T M Letcher

The author gratefully makes the following acknowledgements:

- my supervisor, Trevor Letcher, for his guidance and infinite support during the course of this study and for introducing me into the Kingdom of Thermodynamics

- my mamoosh and guide, Professor Urszula Domanska, for her interest and moral support and for rekindling my dedication to thermodynamics in my most trying times

- Professor J C Ahluwalia from Indian Institute of Technology, India, for providing me with the opportunity to work in his laboratory, where part of this research was done

- Professor J D Raal for co-supervision, advice, stimulating discussions and assistance in the proof reading of this thesis

- my friends and colleagues in the department who have experienced the "ups and downs" with me, most especially, Warren Moollan, Ashley Nevines, Tankiso Tshlela, Hamdani Mahomed, Paul Whitehead, Magan Govender, Deresh Ramjugernath, Zarina Sayed Alley, Allison Maritz and Brenda Joshua

- the technical staff of the chemistry department, University of Natal

- my friends and colleagues at the Indian Institute of Technology, India, Satish Bharadwaj, Sandhiya Jain, Sheshank Deep, Sunil Kumar, Achintya Das and Jyotsna Sharma. Thank you for hours of stimulating discussion

- Andrezj Goldon from the Technical University of Warsaw for his interest in this research and the resultant discussions

- my family, for their constant encouragement and support

- the FRD and University of Natal for financial and travel assistance

- my fiance, who has been my only support at the worst of times. I know you were the hardest hit. Please forgive me. Thank you, always, for everything

- and finally, a glorious THANK YOU to the Lord Almighty, Always with me.

ABSTRACT

The excess molar volumes V_m^E and the excess molar enthalpies H_m^E have been determined for several binary systems at 298.15 K using an Anton Paar Digital Densitometer and a 2277 Thermal Activity Monitor, respectively. V_m^E and H_m^E have been determined over the whole composition range for three types of binary mixtures involving hydrogen bonded interactions. The three types are:

(i)   a short chain alkanol (methanol, ethanol, 1-propanol, 2-propanol) or

(ii)   a symmetrical secondary amine (di-n-ethylamine, di-n-propylamine) or

(iii)   1-alkyne (1-hexyne, 1-heptyne, 1-octyne)

with a branched chain ether (diisopropyl ether, 1,1-dimethylethyl methyl ether, 1,1-dimethylpropyl methyl ether) and a cyclic ether (tetrahydrofuran, tetrahydropyran, 1,4-dioxane).

For mixtures of (an alkanol + a branched chain ether or a cyclic ether) the results are explained in terms of the strong self association exhibited by the alkanol and the cross association of the OH·····O specific interaction. In particular for mixtures of (an alkanol + a cyclic ether) the results show trends relating to the size of the cycloether ring and the number of carbon atoms in the alkanol molecule.

For mixtures of a secondary amine + a branched chain ether or a cyclic ether the experimental results have been explained on the basis of the strong molecular interactions (NH·····O) between the weakly self associating secondary amine and the ether oxygen.

For binary mixtures of 1-alkyne + a branched chain ether the results indicate a dominance of the π·····O interaction over either the dissociation effects of the 1-alkyne (π·····π interactions) or the breakdown of the branched chain ether molecules self association.

Thermophysical property data, density ρ, cubic expansion coefficient α and isothermal compressibility κ_T, have also been determined for several aliphatic ethers from 288.15 K to 328.15 K at pressures ranging from 0.1 to 8 MPa. The molar volumes derived from the densities have been fitted to a polynomial as a function of temperature and pressure and the second order thermodynamic functions, the cubic expansion coefficient α and the isothermal compressibility κ_T determined. For all the ethers, the cubic expansion coefficients decrease with an increase in temperature or pressure while the isothermal compressibilities increase with an increase in temperature or pressure over the temperature and pressure ranges investigated. This work was carried out in the Thermodynamics laboratory of the Indian Institute of Technology in India. This data was required so that the experimental V_m^E and H_m^E data could be analyzed using modern theories of liquid mixtures.

The V_m^E and H_m^E data presented here has been subjected to the following theoretical analysis:

(i)   The Extended Real Associated Solution (ERAS) model,

(ii)   The Modified Universal Functional Activity Coefficient (UNIFAC) group contribution model and

(iii)   The simple Flory and the Prigogine Flory Patterson theory (PFP).

All the theories exhibited partial success when applied to the systems investigated here.

Excess molar volumes and excess molar enthalpies, V_m^E and H_m^E have also been determined over the whole composition range for binary mixtures involving symmetrical (a straight chain ether or ketone + a pseudo straight chain ether or a pseudo straight chain ketone) to test the applicability of the congruency theory. Not all of the mixtures satisfied the null test of the congruency principle.

Table of Contents

CONTENTS

List of Tables

Chapter Three

Page

List of Figures

Chapter Four

Chapter Seven

Page

List of Symbols

IPE	di-isopropyl ether
TBME	1,1-dimethyl ethyl methyl ether
TAME	1,1-dimethyl propyl methyl ether
THF	tetrahydrofuran
THP	tetrahydropyran
ROR'	branched chain or cyclic ether
NRTL	Non Random Two Liquid
UNIQUAC	Universal Quasichemical
UNIFAC	UNIQUAC Functional-Group Activity Coefficient
ERAS	Extended Real Associated Solution
chem	chemical contribution term of excess property
phys	physical contribution term of excess property
H_m^E	molar excess enthalpy [J·mol^{-1}]
Δh_A^*	self-association enthalpy of component A [kJ·mol^{-1}]
Δh_{AB}^*	cross-association enthalpy of component A with component B [kJ·mol^{-1}]
K_A	self-association constant of component A
K_{AB}	association constant of component A with component B
P_i^*	characteristic parameter of component i for pressure [J·cm^{-3}]
P_M^*	characteristic parameter of mixture for pressure [J·cm^{-3}]
s_i	surface to volume ratio of component i [nm^{-1}]
Δv_A^*	self-association volume of component A [cm^3·mol^{-1}]
T	temperature (K)

$\Delta v_{AB}^{\bullet}$	cross-association volume of component A with B [$cm^3 \cdot mol^{-1}$]
V_m^E	molar excess volume [$cm^3 \cdot mol^{-1}$]
$\tilde{V}_i$	reduced volume of component i
$\tilde{V}_M$	reduced volume of mixture
$\tilde{T}_i$	reduced temperature of component i
$\tilde{P}_i$	reduced pressure of component i
$V_i^{\bullet}$	molar hard core volume of component i [$cm^3 \cdot mol^{-1}$]
V	molar volume [$cm^3 \cdot mol^{-1}$]
x_i	mole fraction of component i
g_{12} *or* g_{21}	adjustable parameters for NRTL model
a_{mn} *or* a_{nm}	group interaction parameters for the UNIFAC model
R_k	group volume parameters
Q_k	group surface parameters
G_m^E *or* g_m^E	excess Gibbs energy
r and q	pure component structural parameters for the UNIQUAC model
z	co-ordination term in UNIQUAC model
u_{12}	adjustable parameter for UNIQUAC model
c	combination term in UNIQUAC and UNIFAC models
r	residual term in UNIQUAC and UNIFAC models
Z	partition function for ERAS model
r	number of segments in *r-mer* chain molecule

Greek letters

α	thermal expansion coefficient [$10^4 \cdot K^{-1}$]
δ	deviations between calculated and experimental values

Φ_i	hard core volume fraction of component i in the mixture
ϕ_{AI}	hard core volume fractions of the monomer molecules A
ϕ^0_{AI}	hard core volume fractions of the monomer molecules A in the pure liquid state
θ_i	surface fraction of component i
κ_T	compressibility coefficient [$10^{-4}\cdot MPa^{-1}$]
X_{AB}	binary van der Waals interaction parameter [$J\cdot cm^{-3}$]
Θ_i	average area fraction in UNIQUAC model
α_{12}	adjustable parameter in NRTL model
γ_i	activity coefficient of component i
Γ_i	group residual activity coefficient of component i in Modified UNIFAC model

List of Publications

1.   " Excess enthalpies and excess molar volumes of mixtures of cycloalkanes and pseudo-cycloalkanes", *T.M. Letcher, J.D. Mercer Chalmers, U.P. Govender and R. Battino*, Thermochimica Acta, **224**, 39-42, (1993)

2.   " Excess molar enthalpies and excess molar volumes of binary mixtures of 1-alkenes with 1-propanol and 2-propanol", *T.M. Letcher, J.D. Mercer Chalmers, **U.P. Govender** and S. Radloff*, Thermochimica Acta, **224**, 33-38, (1993)

3.   " Excess molar enthalpies and excess molar volumes of binary mixtures of 1-alkynes with 1-propanol and 2-propanol", *T.M. Letcher, J.D. Mercer Chalmers, **U.P. Govender** and S. Radloff*, Fluid Phase Equilibria, **91**, 313-320 (1993)

4.   "The excess molar enthalpies of (di-n-butylamine + an ether) at the temperature 298.15 K", *T.M. Letcher, U. Domanska , **P. Govender*** , The Journal of Chemical Thermodynamics, **26**, 681-689 (1994)

5.   "The excess molar volumes of (di-n-butylamine + an ether) at the temperature 298.15 K", *T.M. Letcher, U. Domanska , **P. Govender*** , The Journal of Chemical Thermodynamics, **26**, 1019-1023 (1994)

6.   **International Data Series (IDS)** Series A, Selected Data on Mixtures, "Excess Enthalpy of Dibutylamine + ethers, *T.M. Letcher, **P. Govender***, **22, No. 4,** 295-303.

7.   "The excess molar enthalpies of (an alkanol + a branched chain ether) at the temperature 298.15 K", *T.M. Letcher, Penny.U. Govender*, The Journal of Chemical Engineering Data, **40,** 997-1000 (1995)

8.   "The excess molar enthalpies of (an alkanol + a cyclic ether) at the temperature 298.15 K", *T.M. Letcher, Penny.U. Govender,* The Journal of Chemical Engineering Data, **40,** 1097(1995)

9.   "Effect of Temperature and Pressure on the Volumetric Properties of Branched and Cyclic Ethers", *U.P. Govender, T.M. Letcher, S.K. Garg, J.C. Ahluwalia,* The Journal of Chemical Engineering Data, **41,** 147 (1996)

10. "Excess molar enthalpies and excess molar volumes of ternary mixtures of ethers and ketones", *Trevor M Letcher and Penny U Govender*, Thermochimica Acta, **accepted for publication**, July 1996.

11. "The excess molar volumes of (an alkanol + a cyclic ether) at the temperature 298.15 K and application of the PFP and ERAS model", *Trevor M Letcher and Penny Govender* , Fluid Phase Equilibria, **accepted for publication**, August 1996.

12. "The excess molar volumes of (an alkanol + a branched chain ether) at the temperature 298.15 K and application of the PFP and ERAS model", *Trevor M Letcher and Penny Govender,* Journal of Chemical Engineering Data, **in preparation**, May 1996

For my parents

For always believing in me

Chapter One

Introduction

The thermodynamic excess properties and thermophysical properties are known to be useful in elucidating the nature and strength of molecular interactions that are present in liquids and liquid mixtures. Furthermore, accurate data of this type are important in the practical and theoretical use of liquid mixtures.[1-6] In industry and indeed to the chemical engineer, the determination and prediction of excess thermodynamic quantities are essential in the design and performance analysis of chemical process operations like distillation, fluid-phase separation etc.[3,7,8] The need for efficient optimisation of chemical processes have led to an increase in the demand for accurate thermodynamic data particularly in the petrochemical industry. From a theoretical point of view, the field of thermodynamics and specifically the determination of experimental excess properties is fundamental in the testing of various thermodynamic theories which may serve as a guide in the formulation of new postulates. Attempts to model real solution behaviour are important because of (i) possible interpolation of limited experimental results available for systems already studied to systems not previously studied and (ii) as an aid to understanding the nature of liquids and liquid mixtures.

The present work describes the results of thermodynamic investigations carried out at 298.15 K for mixtures concerning molecules differing vastly in size, shape and chemical

nature. The thermodynamic properties determined and discussed in this thesis are the excess molar volume, V_m^E, and excess molar enthalpy, H_m^E, for binary liquid mixtures. The mixtures include pairs of substances in which hydrogen bonded interactions involving single proton donors, can occur. The proton donors (an alkanol, a secondary amine, a 1-alkyne) investigated here were mixed with highly branched chain ether and cyclic ether molecules in order to investigate possible (-OH or -NH or -CH·····O-) interactions. The thermodynamic data determined for binary liquid mixtures of (a short chain alkanol or a secondary amine or a 1-alkyne + a branched chain ether or cyclic ether) have been used to test many of the most recent and important theoretical models as applied to associating liquids and liquid mixtures.

Excess molar volumes, V_m^E, and excess molar enthalpies, H_m^E, have been determined for twenty four binary systems at 298.15 K involving (a short chain alkanol + a branched chain ether or a cyclic ether). The alkanols used were methanol, ethanol, propan-1-ol and propan-2-ol, the branched chain ethers were di-isopropyl ether (IPE), 1,1-dimethyl ethyl methyl ether (TBME), 1,1-dimethyl propyl methyl ether (TAME) and the cyclic ethers were tetrahydofuran (THF), tetrahydropyran(THP) and 1,4-dioxane. The effect on the hydrogen bonding capability with an increase in alkyl chain length of the primary and secondary alkanol on the excess properties was observed.

Excess molar volumes, V_m^E, and excess molar enthalpies, H_m^E, have also been determined for binary systems at 298.15 K involving (a secondary amine + a branched chain ether or a cyclic ether). The secondary amines investigated were diethylamine and di-n-propylamine and the branched chain and cyclic ethers were the same as used for the alkanol mixtures. The effect of increasing the alkyl chain on the amine and the degree of branching and of ring size of the ethers on the results was investigated.

Excess thermodynamic properties have also been measured for mixtures of (1-alkyne (hex-1-yne or hept-1-yne or oct-1-yne) + a branched chain ether (IPE or TBME or TAME)). The results have been compared to previously determined results for related systems.

The effect on the excess thermodynamic properties of the $\equiv$CH$\cdots\cdots$O interactions is compared to the OH$\cdots\cdots$O and NH$\cdots\cdots$O interactions. A comparison is also made of the effect on the excess thermodynamic properties of the OH$\cdots\cdots$O and the NH$\cdots\cdots$O interaction.

Pure component thermophysical properties ie. densities, ρ, cubical expansion coefficients, α, and the isothermal compressibilities, κ_T, have been experimentally determined for branched chain and cyclic ethers differing in shape and size. These thermophysical properties were determined in order to facilitate testing the thermodynamic models used in this work. In addition, the branched chain ethers used in this work have recently been used as additives in the fuel industry and the thermophysical properties determined here could be important in designing separation processes for the new fuel mixtures. The thermophysical property data of these compounds above room temperature and at pressures above atmospheric pressure are not available in the literature. The densities, ρ, have been directly measured at temperatures from 288.15 K to 328.15 K and a pressures from 0.1 to 8 MPa. The cubical expansion coefficients, α, and the isothermal compressibilities, κ_T, have been calculated from the change in molar volume with temperature and pressure, respectively.

The study of the above mixtures has not only yielded a considerable amount of valuable and important experimental data which had not been previously reported but also afforded an opportunity to test the most important models and theories of liquid mixtures. The NRTL[14], UNIQUAC[15] UNIQUAC (ASM)[16], Modified UNIFAC[17,18], Flory[19], Flory-Prigogine-Patterson[11,12] and the Extended Real Association Solution[20,21] models have been fitted and

applied to the experimental V_m^E and H_m^E data in this thesis. In particular, a detail analysis of the Modified UNIFAC, PFP and ERAS model are investigated for the self associating components of binary mixtures used in this work.

In addition, the theory of the principle of congruence[22] as applied to multicomponent mixtures, was also tested in a novel way by mixing a symmetrical ether of side chain carbon number m with an equimolar mixture of two symmetrical ethers (a pseudo-ether) such that their average side chain carbon number was m. Excess molar enthalpies and volumes were measured using these mixtures at atmospheric pressure and at 298.15 K. The process was repeated for mixtures of ketones and pseudo-ketones[22].

Chapter Two

Excess Molar Volumes of Mixing

2.1 Introduction

The volume change on mixing of binary liquid mixtures, V_m^E, at constant pressure is of interest to a thermochemist because (a) it serves as sensitive indicator for the applicability of liquid theories to liquid mixtures and (b) from a practical point of view, reliable V_m^E results are relatively easy to obtain.[23] The volume changes on mixing of two liquids can arise from a combination of some or all of the following factors: (i) packing effects caused by a difference in the size and shape of the component species, (ii) the structural changes upon mixing ie. the changes in the correlation of molecular orientation, (iii) the difference in the intermolecular interaction energy between like and unlike molecules and (iv) formation of new chemical species including hydrogen bonded complexes. The complexity associated with the elucidation of the origin of excess volume and hence the representation of the non-ideality exhibited by binary mixtures has consequently been an area of active interest over the last two decades.[24]

In this work V_m^E's have been determined over the whole composition range at 298.15 K for binary mixtures of a short chain alkanol (methanol, ethanol, 1-propanol, 2-propanol) or a symmetrical secondary amine (diethylamine, di-n-propylamine)

or a 1-alkyne (1-hexyne, 1-heptyne, 1-octyne) with a branched chain ether (diisopropyl ether, 1,1-dimethylethyl methyl ether, 1,1-dimethylpropyl methyl ether) and/or a cyclic ether (tetrahydrofuran, tetrahydropyran, 1,4-dioxane). These mixtures reflect the possible hydrogen bonding interactions between the functional groups ie. -OH$\cdots$O, -NH$\cdots$O and $\equiv$CH$\cdots$O interactions.

All the V_m^E results are discussed in terms of possible packing associations, dissociations of the pure component species and the cross associations between the different molecules. The simple Flory and Prigogine Flory Patterson theories (PFP) was applied to the V_m^E data and the results are presented in Chapter 6. The V_m^E together with the H_m^E from Chapter 3 data have been treated in terms of the Extended Real Associated Solution (ERAS) model and the results are also presented in Chapter 6.

2.2 Measurement of Excess Molar Volumes

The excess molar volume, V_m^E, at a concentration of x_A of component A is defined as[25]

$$V_m^E = V_{(mixture)} - \{ x_A V_A^o + (1-x_A) V_B^o \} \tag{2.1}$$

where the last term is the ideal molar volume of the mixture. The volume changes for binary mixtures, V_m^E, can be determined experimentally in one of two ways, namely (i) indirectly from density (densitometric or pycnometric) measurements, or (ii) from the more direct dilatometric methods, ie. by measuring the resultant volume change upon mixing of the two components. Both these experimental methods have been extensively reviewed by Battino,[23] Letcher,[26] Handa and Benson,[24] and by Stokes and Marsh.[27,28,29]

2.2.1 Pycnometer

There is a wealth of reference in the literature of a variety of types of pycnometer.[30,31,32] One of the earliest described pycnometers was that of Scatchard, Wood and Mochel[32] and is illustrated in figure 2.1. This single arm pycnometer was used to obtain density measurements with precision of 1×10^{-4} g.cm^{-3}. Basically, this pycnometer has a bulb with a capacity of 11 cm^3, a 1 mm internal diameter precision capillary with 11 lines lightly etched around the stem, and spaced 1 mm apart.[32] During measurement, the bulb is filled using a hypodermic syringe and cannula and the composition of the mixtures have to be known with a large degree of accuracy. Many workers overcame the latter by weighing the two components into the pycnometer.[13,32]
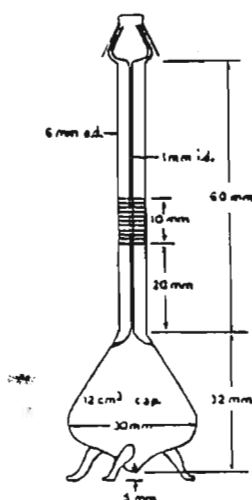
Figure 2.1. Pycnometer of Scatchard et al.[32]

Potentially serious errors could arise due to inadequate mixing, evaporation and vapour space composition, however, careful measurements with excellent accuracy and reproducibility

have been reported using this technique.[33] Wood and Brausie[31] and later Battino[34] improved on the accuracy of density measurement by the pycnometer technique by introducing and developing a mixing bottle. Battino's mixing bottle is depicted in figure 2.2. With this bottle potential errors due to evaporation of the samples is minimised. Later a bicapillary pycnometer made of Pyrex glass was developed in the laboratory of Kimura and Takagi.[35] This pycnometer had a volume capacity of approximately 3.6 cm³, capillary stems with an internal diameter of 0.5 mm. Sharp lines were scored on each stem and magnified by a travelling microscope were used as reference points. The pycnometer was allowed to stand for 20-30 minutes on the balance, before each weighing and the reproducibility for weighing was $\pm$ 0.01 mg - which gave a precision of 1 x 10^{-4} g.cm^{-3} in density measurements.[35]
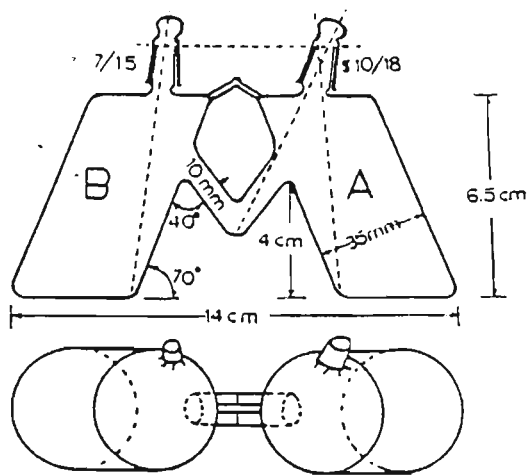
Figure 2.2. Mixing bottle of Battino [34]

2.2.2 Mechanical Oscillator Densitometers or Density Meters

The remote or external measuring cells were developed to eliminate the inherent sources of error in the pycnometer technique and to achieve the highest possible accuracy and precision of the measurement results.[36] The introduction of the remote cells offers a system for liquid measurement according to the oscillating sample tube method.[37] The density determination is based, in principle, on measuring the period of oscillation of a vibrating U-shaped sample tube which is either filled with sample or through which the sample is continuously flowing. The accuracy of this method is limited to some extent by four control factors:[38] the calibration procedure, the viscosity of the sample, the pressure of the system and the temperature control. The density of the sample is related to the resonance frequency of an electronically excited mechanical oscillator and the period of oscillation of the sample contained in the oscillator.[38] The effective mass (M) of the oscillator is composed of its own unknown mass (M_o) as well as the unknown mass of the sample, density ρ, contained in volume V and is given by

$$M = M_o - V\rho \tag{2.2}$$

The resonance frequency is given by

$$2\pi v = (c/M)^{1/2} = [c/(M_o + V\rho)]^{1/2} \tag{2.3}$$

where the mass M is attached to a spring of constant elasticity c, under the condition that the oscillator performs an undamped oscillation.[24] Rearranging and making ρ the subject of the

formula

$$\rho = -M_o / V + (c/4\pi^2 V)(1/v^2) = A + B\tau^2 \qquad (2.4)$$

where $\tau = 1/v$, ie. the period of oscillation, and A and B are constants characteristic of the oscillator. Densities are measured relative to a reference material:

$$\rho - \rho_o = B(\tau^2 - \tau_o^2) \qquad (2.5)$$

where ρ_o is the density of the reference material and τ_o is its corresponding period of oscillation.

In this work, a densitometer containing an external measuring cell designed by Kratky et al.[39] and commercially marketed by Anton Paar (Graz, Austria) was used. It consists of a U-shaped hollow borosilicate glass oscillator or sample tube, mounted in a dual wall glass cylinder filled with a gas of high thermal conductivity to facilitate a rapid temperature equilibration of the sample inside the oscillator. *B* from equation 2.5 is determined by obtaining τ with two calibration measurements with samples of known densities i.e. air and distilled water. The precision obtained in τ is 2×10^{-6} Hz^{-1}. Details of the Anton Paar vibrating tube densitometer are given in the experimental section - 2.3.2.

Recent developments by Handa and Benson et al.[24] show that in order to obtain a precision of 0.001 cm$^3 \cdot$mol^{-1} in V_m^E, the composition should be precise to five significant figures and density readings precise to six significant places. Further to this, Battino[23,57] reported that the measuring cell temperature must be controlled to $\pm$ 0.001 K to accurately determine densities to 0.00002 g$\cdot$cm^{-3}.

2.2.3 Direct Measurements - Batch Dilatometers and Continuous Dilution Dilatometers

Highly accurate measurements are obtained by direct measurements using dilatometry,[24,25] without the need for time consuming procedures such as pycnometer filling, weighing etc. and errors arising from mass, composition or temperature determination of samples. Direct dilatometric measurement of V_m^E gives a much higher ratio of accuracy to effort.[25] A suitable and simple dilatometer is shown in figure 2.3.[25] The dilatometer is filled with a hypodermic syringe. Mixing is achieved by gently rocking the dilatometer to and fro. The excess molar volume of mixing, V_m^E, is given by the relation: (neglecting small terms allowing for the effects of the change of pressure on mixing of the volumes of the liquids and of the mercury)

$$V_m^E = \Delta V/ (n_A + n_B) = A\Delta h/ (n_A + n_B) \tag{2.6}$$

where A is the cross sectional area of the capillary and n_A and n_B are the amounts of substance of A and of B.
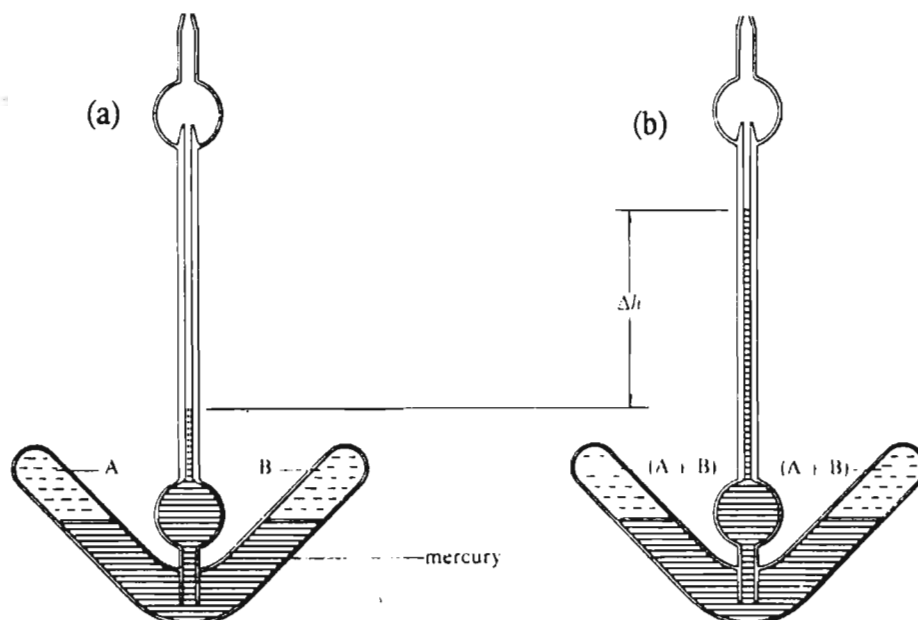
Figure 2.3 A dilatometer for measurements of volume of mixing showing (a) before mixing (b) after mixing[25]

There have been fundamentally two types of dilatometric apparatus designed for the direct measurement of volume change[24] : (i) one composition per loading of the apparatus at a single temperature or *batch dilatometers*, and (b) a number of compositions per loading at a single temperature or *continuous dilution dilatometers*.[24]

2.2.3.1 Batch Dilatometry

One of the early examples of a design for a single loading dilatometer was the apparatus by Keyes and Hildebrand in 1917.[40] As seen in figure 2.4, it consists of a U-tube with mercury filling the bottom of the vessel in order to separate the two sample components A and

B. Graduated capillaries on the two arms provided the means by which the volumes, before and after mixing, were determined. The entire mixing vessel was immersed in a thermostatted bath, and mixing was achieved by rocking the apparatus to and fro. It was reported that precision of ± 0.003 cm$^3 \cdot$mol^{-1} in V_m^E could be achieved over the temperature range 280-350 K.[41]
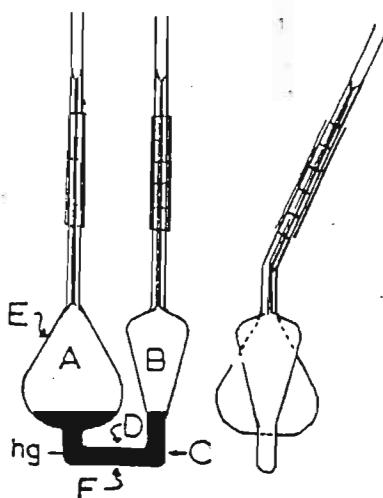
Figure 2.4 Keyes and Hildebrand dilatometer[40]

Duncan, Sheridan and Swinton[42] in their reviews, describe methods and modified dilatometer apparatus in which the precision was found to be $\pm$ 0.002 cm$^3 \cdot$mol^{-1} or $\pm$ 0.5% in V_m^E.[41,42]

Errors arising in a batch dilatometer include the failure to take into account the a compressibility correction (a 1 % possible error in V_m^E), corrections due to temperature

fluctuations and the fact that extreme care has to be taken to avoid excessive amounts of grease on the joints.[43] The primary disadvantage of the batch dilatometer was the slow speed of measurement, i.e. each loading of the dilatometer only gave a single V_m^E reading.

2.2.3.2 Continuous Dilution Dilatometry

The fundamental disadvantage of the batch dilatometer was eliminated by introduction of the many compositions per loading dilatometer ie. dilution dilatometry. The original design of the dilution dilatometer was arguably that by Geffcken, Kruis and Solana.[44] It has the mixing chamber C initially loaded with pure component A and mercury (as seen in figure 2.5). Stopcock S leads to reservoir R where pure component B is kept over mercury. The change in the mercury level upon mixing is read directly from the calibrated and graduated capillary D. The entire apparatus is kept in a thermostatted vessel. When S is opened, mercury from C forces some of component B into C via the connecting tube E. S is then closed and mixing begins. The change in level of mercury in capillary D is read directly. Increments of B are added in a similar way in order to determine V_m^E as a function of composition at one temperature.[44]
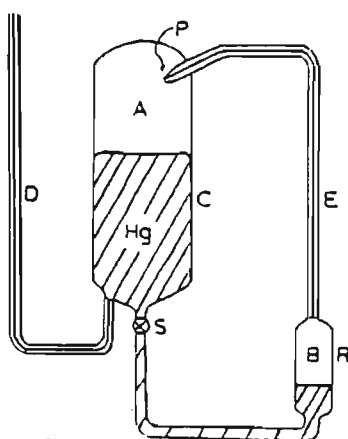
Figure 2.5 Dilution dilatometer of Geffcken, Kruis and Solana[44]

Many workers have modified and adapted Geffcken et al. original design:[43-51] Stokes et al.[49] modified the design by Geffcken et al. by having component B confined in a burette above which component A is confined in a bulb, both over mercury. The two compartments are attached to a fine stainless steel tube, and known fractions of component B enter into the bulb (containing A) by means of mercury flowing in the opposite direction via a stopcock. This design facilitates easier loading and usage.[49] Kumaran and McGlashan[50] designed a tilting dilatometer ; this tilting dilatometer is advantageous in that it reduces error because there are no taps to open and close during a measurement; rather mixing is achieved by tilting.[50] This design facilitates easier loading and calibration and allows for measurement of volume changes of any magnitude. Moreover, in the dilatometer designed by Kumaran and McGlashan,[50] the two liquids are separated by mercury at all stages of a run instead of only a diffusion boundary in a capillary as in previous dilatometer designs.[49,51] The dilatometer designed by Kumaran and McGlashan[50] is similar to the one depicted in figure 2.6 except that capillary C has a larger bore size and it has a calibrated bulb X blown at the bottom of the calibrated burette A. The presence of the bulb X eliminates the need to calibrate the mixing cell B. Before the start of the run, bulb B is filled with mercury and burette A with one of the sample components. After thermal equilibrium and with stopcock T_1 removed, mercury from B is transferred into X thus creating space of known volume in B.[50] A standard deviation of 7×10^{-4} cm^3.mol^{-1} for V_m^E for this type of dilatometer has been reported.[50]

There have been two major reported disadvantages for dilution dilatometers.[24] Firstly, relatively large volumes (50-100 cm^3) of highly purified components are required; and secondly, specifically for the dilatometers described here[49-51] , to measure a change in volume at constant pressure, a correction must be made. That is, a change in the height (Δh) of the

mercury meniscus in the capillary causes a change in the mixing cell pressure equal to $\rho g \Delta h$, where ρ = density of mercury. Errors in V_m^E of 1-2 % can accrue in this manner.[24] Tanaka et al.[52] improved on the McGlashan type dilatometer to produce a dilatometer capable of extremely sensitive and accurate precision.
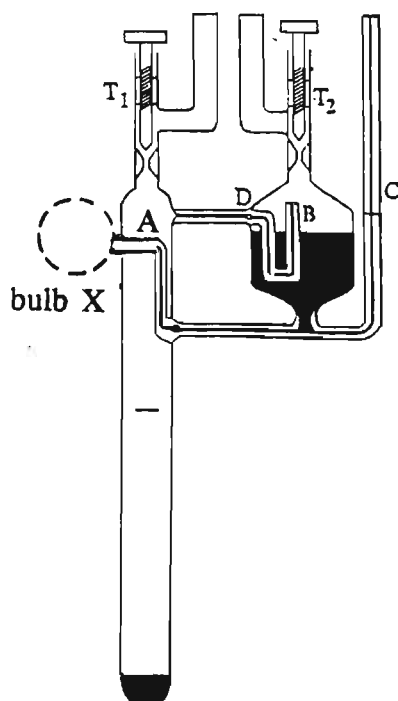
Figure 2.6 Similar designed tilting dilatometer of Kumaran and McGlashan[50]

2.2.4 Error Analysis for the V^E data obtained from density values used in this work

Appendix 1 gives the detailed manner of error analysis. In principle, to obtain a maximum error of 2×10^{-3} cm$^3 \cdot$mol^{-1} in V_m^E, the masses of the pure components must be known to a precision of 1×10^{-5} g, the τ values to 2×10^{-6} Hz^{-1} and the densities to 1×10^{-5} g$\cdot$cm^{-3}.

2.3 Experimental

2.3.1 Materials

All the liquids used in this work were tested for impurities by Gas Chromatography-Mass Spectometry(GC-MS) and Gas Liquid Chromatography(g.l.c) and were kept in a dry box before use. Some of the liquids were purified according to recommended methods.[53] A summary of the materials, their suppliers and purities used in this work are given in Table 2.1 together with density values at 298.15 K. The density results show good agreement with the literature values.[54,55]

The alkynes were fractionally distilled before use. G.l.c. analysis of the 1-alkynes showed that the impurity content was less than 0.5 mole percent.

The alkanols were purified repeatedly using previously established methods[56] in the following manner:

The alkanols were refluxed over magnesium turnings and iodine for 30 minutes and then distilled through a 150 mm lagged glass fragment-packed column. The water impurity content in the alkanols was determined by Karl Fischer titrations to be less than 0.02 mole percent. G.l.c. analyses indicated a purity of >99.8 mole percent for all the alcohols.

Diethylamine (DEA) and di-n-propylamine (DPA) were used without any further purification. Analysis of the amines by g.l.c. indicated that the total mole fraction of impurities was < 0.4 percent for each of the liquids.

The ethers were distilled before use and dried using 0.4 nm molecular sieves and degassed before measurement. The ethers were also analyzed for water content before use and in all cases the mole fraction of H_2O was determined to be < 0.01 mole percent. Analysis of the ethers by g.l.c. indicated that the total mole fraction of impurities was < 0.1 for each

of the liquids.

The instruments used for the GC-MS and g.l.c. analysis were, respectively, a Varian GC-MS and a Hewlett-Packard 5891A gas chromatograph equipped with a 3393A integrator and a 25 m carbowax capillary column. All the solvents were kept in a dry-box containing a double access door.

TABLE 2.1. Materials used, their suppliers and purities

Compound	Supplier	$\rho/(kg \cdot m^{-3})$		Purity (mole %)
		this work	literature[54,55]	
methanol	Aldrich	786.52	786.37	99.8
ethanol	Aldrich	785.12	784.93	99.8
1-propanol	Aldrich	799.74	799.60	99.5
2-propanol	Aldrich	780.93	781.26	99.5
diethylamine	Aldrich	699.69	701.60	99.5
di-n-propylamine	Aldrich	733.35	732.90	99.6
1-hexyne	BDH	711.11	710.50	99.8
1-heptyne	BDH	730.53	727.90	99.7
1-octyne	Fluka	746.57	743.10	>99
IPE	Polychem	717.84	718.20	99.0

TABLE 2.1 Continued

Compound	Supplier	$\rho/(kg \cdot m^{-3})$		Purity (mole %)
		this work	literature[54,55]	
TBME	Aldrich	734.80	735.30	>99
TAME	Janssen	765.71	765.91	>99
THF	Aldrich	881.42	881.90	99.8
THP	Aldrich	878.54	879.00	99.8
1,4-dioxane	Aldrich	1026.66	1027.90	99.5
cyclohexane	Aldrich	773.80	773.74	99.5
n-hexane	Aldrich	679.26	679.53	99.5
benzene	Aldrich	874.85	873.69	99.6

2.3.2 Apparatus Details

The V_m^E results for the binary liquid mixtures reported in this work were determined using the commercially available Anton Paar DMA 601 vibrating tube densitometer.

2.3.2.1 Equipment Description

(a) Principle of operation

The laboratory arrangement for the densitometer is shown schematically in figure 2.7. The measuring cell is contained in a separate housing and is thermally separated from the electronics. The oscillator or sample tube is made out of borosilicate glass and is fused into a dual wall glass cylinder. The space between the U-shaped sample tube and the inner wall of the dual wall is filled with a propriety gas of high thermal conductivity to facilitate a rapid temperature equilibration of the sample inside the oscillator with the thermostat liquid which flows through the dual wall cylinder around the sample tube. An additional shorter capillary tube inside the inner space of the dual wall cylinder is for the accurate determination of the measuring cell temperature by means of a temperature sensor. This capillary tube has a wall thickness of about 0.2 mm to ensure good heat transfer. In operation, the sample tube is completely filled with ± 0.7 cm^3 of sample substance then electronically excited and density measurements are determined precisely by measurement of the period of oscillation of the sample tube. The determination of density by this method is based on the measurement of the period of oscillation of the undamped vibrating tube of volume, V, which in this case is filled with sample liquid. In this way the natural frequency of the vibration of the tube is influenced by the mass and the density of the sample. For the purposes of a mathematical derivation, the system is analogous to a hollow body of mass, *M*, which is suspended by a spring with a constant elasticity, c(cf. equations 2.2 to 2.5).

In this instrument, two remote cells generate square wave signals in synchronism with the zero amplitude of the oscillating sample tube. These signals are separated by an optical isolator and are filtered from any resulting noise. The signal from any one of these sources,

depending on the operators choice, is then fed into a period meter. Time based pulses every 10^{-5} seconds permit the determination of the time lapse of a preselected number of oscillator periods and hence allow for determination of the period of vibration, τ. The resulting period is related to the sample density through equation 2.4, which is rewritten for the sake of completeness:

$$\rho = A + B\,\tau^2 \tag{2.7}$$

Constant A and B contain the spring constants of the oscillator as well as the empty oscillator's mass and that volume of the sample which participates in the oscillation. These constants are instrument constants for each individual oscillator and can be determined by two calibration measurements with samples of known density (e.g. air and deionised water).

Care should be taken not to introduce air bubbles into the sample cell during injection as fluctuating τ values can introduce errors.
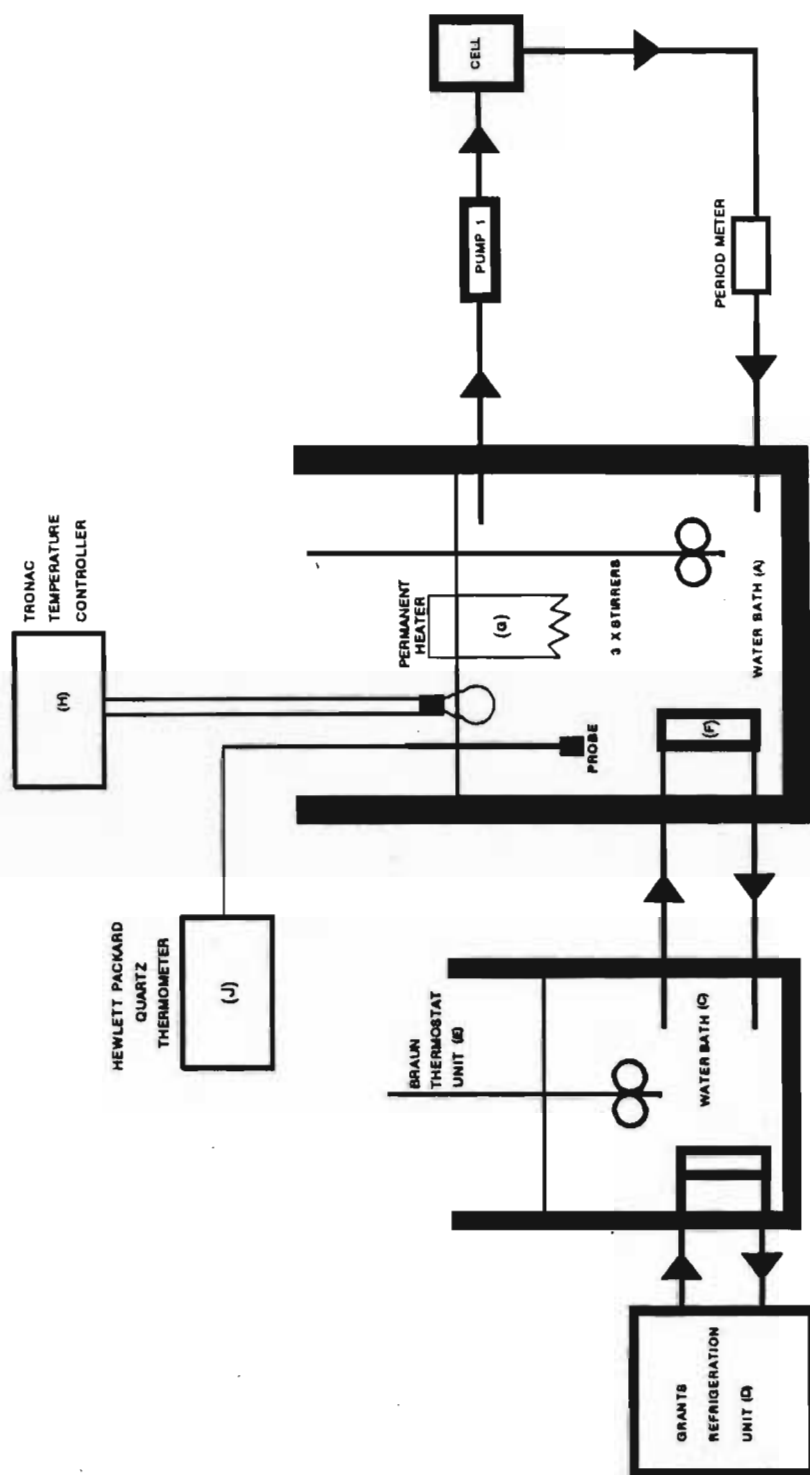
Figure 2.7 Laboratory arrangement for the densitometer

(b) Temperature Control

A diagrammatic representation of the temperature control system is shown in figure 2.7. A uniform temperature throughout the bath, A, was achieved through the use of two variable speed mechanical stirrers, B. An auxiliary cooling system, C , comprising a 50 litre water bath cooled by a Grants refrigeration coil, D, was incorporated to assist with the temperature control of the main water bath. Water from this auxiliary bath was pumped via a Haake immersion thermostat unit, E, at a rate of 2.8 litre·min^{-1} through a 4 m coiled copper tube, F, (12 mm i.d.) placed inside the primary cooling bath. Since the auxiliary bath was maintained at a temperature of approximately 1 K below the operating temperature, this arrangement served to assist the main water bath in temperature maintenance. The thermostat liquid used for both the auxiliary and the main water bath was distilled water treated with a commercially available corrosion and algae inhibitor.

The thermostat system within the main water bath consisted of a permanent rheostatted immersion heater, G, delivering up to 4 W, and a 40 W light bulb connected to a Tronac temperature controller, H. The light bulb was used because it has a very low thermal heat capacity and heat transfer is rapid. Water from the primary water bath was pumped through the water jacket by a submersible pump, I, at a rate of 3.4 litre·min^{-1}. All rubber tubing to and from the densitometer was insulated to reduce heat losses. A Hewlett Packard 2801A quartz thermometer, J, calibrated as discussed in *Appendix 2*, was employed to monitor the temperature within the main bath. An Anton Paar digital meter, linked to a thermocouple, was used to monitor the temperature in the cell.

(c) Preparation of mixtures

The pure solvents were degassed before sample solutions were made up by immersing them in a sonic bath for 20 minutes. The mixtures were made up in flasks of 5 cm^3 volume fitted with ground glass stoppers. Care was taken to first add the least volatile component to the flask, and that the completed mixture left a small vapour space - just large enough to aid mixing. The mixtures were made up just before injecting into the densitometer, and were given a vigorous shake before injection.

(d) Operation procedure for instrument and actual sample measurement

Before any experimental measurements were made, complete temperature equilibration was achieved by allowing a warm up time of at least 60 minutes. Prior to each experimental run, the cell was flushed thoroughly with absolute ethanol (>99 %) and then acetone. After flushing, compressed air was blown through the cell. A constant period value, τ, for the sample tube filled with air (in this case, the value at 298.15 K for $\tau_A = \pm 1.336100$ Hz^{-1}) was obtained. Double distilled pre-boiled(to remove dissolved air) water (used as the calibrated standard sample) was then introduced into the cell by means of a glass syringe, which was equipped with a machined teflon nozzle, ensuring a leak-proof fit at the sample cell-syringe junction. The injection process was carried out slowly, enabling the liquid to properly wet the walls of the cell, and thus reducing the risk of trapping air bubbles in the U-tube. The sample was always filled past its nodal points and the syringe was left in place, at the inlet nodal point during each measurement. The outlet nodal point of the cell was sealed with a teflon plug to reduce evaporation. The solution mixtures were introduced into the sample cell in exactly the same manner as for distilled water. With the cell illumination light off, the photoelectric portion of the excitation system was automatically activated. Each measuring cycle was

allowed to continue until a constant period value was obtained. Period values for water (reference substance) pure solvents and air were determined between each solution injection. These values were not only required for the density calculations, but also permitted a continuous check on both the sample purity and the densitometer operation. The precision of τ, judged by the repeated measurements for the same solution at different times, was estimated to be better than 2×10^{-6} Hz^{-1}. The densitometer was also tested by measuring the densities of very pure cyclohexane and n-heptane at 298.15 K. The results are listed in Table 2.1 and show good agreement with the literature values.

2.4 Results

The measured excess volumes, V_m^E are given in Tables 2.2 - 2.10 together with the deviations $, \delta V_m^E$, calculated from the Redlich-Kister polynomial

$$\delta V_m^E/(cm^3 \cdot mol^{-1}) = V_m^E/(cm^3 \cdot mol^{-1}) - x(1-x) \sum_{r=0}^{r=k} A_r (1-2x)^r \qquad (2.8)$$

where x refers to the mole fraction. The coefficients A_r were estimated by the method of unweighed least squares and are given in Table 2.11 - 2.14 respectively. The *Statgraphics 3.0* package was used to fit the equation to the data. The V_m^E results were calculated using a GWBASIC program - the details of which are given in *Appendix 3*.

TABLE 2.2 Experimental excess molar volumes, V_m^E for binary mixtures of $\{x\ C_jH_{2j+1}OH + (1-x)\ ROR'\}$ and the deviations, δV_m^E at the temperature 298.15 K. ROR' are branched chain ethers.

x	V_m^E $cm^3 \cdot mol^{-1}$	$\delta V_m^E \cdot 10^3$ $cm^3 \cdot mol^{-1}$	x	V_m^E $cm^3 \cdot mol^{-1}$	$\delta V_m^E \cdot 10^3$ $cm^3 \cdot mol^{-1}$	x	V_m^E $cm^3 \cdot mol^{-1}$	$\delta V_m^E \cdot 10^3$ $cm^3 \cdot mol^{-1}$
			$xCH_3OH + (1-x)\{CH_3CH(CH_3)\}_2O$					
0.009	-0.0425	2.6	0.745	-0.7584	-1.4	0.893	-0.4069	2.9
0.109	-0.4602	-3.9	0.778	-0.6916	4.6	0.901	-0.3781	4.5
0.349	-0.9163	3.2	0.826	-0.5919	1.9	0.923	-0.3054	5.6
0.472	-0.9868	-1.6	0.841	-0.5515	5.3	0.946	-0.2206	3.8
0.688	-0.8480	-6.8	0.874	-0.4614	4.6	0.971	-0.1232	1.9
0.733	-0.7810	-4.7						
			$xCH_3OH + (1-x)CH_3C(CH_3)_2OCH_3$					
0.127	-0.3244	-7.3	0.559	-0.6387	-4.8	0.827	-0.3861	3.5
0.156	-0.3795	-7.4	0.611	-0.6144	-2.1	0.879	-0.3068	-1.0
0.188	-0.4280	-0.9	0.690	-0.5573	-0.1	0.909	-0.2327	2.2
0.220	-0.4739	-0.6	0.710	-0.5430	-4.5	0.914	-0.2205	3.7
0.303	-0.5672	0.2	0.716	-0.5273	4.7	0.947	-0.1414	4.9
0.334	-0.5888	3.2	0.763	-0.4788	0.7	0.978	-0.0629	0.6
0.388	-0.6216	1.7	0.783	-0.4508	3.6			
0.494	-0.6373	7.7	0.794	-0.4308	8.2			
			$xCH_3OH + (1-x)CH_3CH_2C(CH_3)_2OCH_3$					
0.032	-0.0784	-4.2	0.399	-0.4459	6.3	0.837	-0.2459	1.1
0.050	-0.1130	-2.7	0.459	-0.4600	-1.9	0.751	-0.2164	1.2
0.099	-0.1994	2.2	0.489	-0.4596	-2.7	0.876	-0.2138	-5.0
0.152	-0.2805	-0.9	0.597	-0.4346	-3.9	0.895	-0.1720	1.3
0.200	-0.3315	4.3	0.669	-0.3915	3.1	0.923	-0.1318	0.5
0.232	-0.3672	-0.9	0.705	-0.3689	1.9	0.937	-0.1105	-0.3
0.282	-0.4066	-2.4	0.745	-0.3406	-0.6	0.951	-0.0890	-1.2
0.335	-0.4336	-1.3	0.788	-0.2988	1.4	0.980	-0.0389	-1.5

TABLE 2.2 Continued

x	V_m^E cm$^3\cdot$mol^{-1}	$\delta V_m^E\cdot 10^3$ cm$^3\cdot$mol^{-1}	x	V_m^E cm$^3\cdot$mol^{-1}	$\delta V_m^E\cdot 10^3$ cm$^3\cdot$mol^{-1}	x	V_m^E cm$^3\cdot$mol^{-1}	$\delta V_m^E\cdot 10^3$ cm$^3\cdot$mol^{-1}
			$xC_2H_5OH + (1-x)\{CH_3CH(CH_3)\}_2O$					
0.011	-0.0466	9.1	0.513	-0.8102	-3.6	0.767	-0.5589	6.6
0.019	-0.0972	-1.6	0.624	-0.7493	4.3	0.809	-0.4814	1.6
0.023	-0.1139	-1.9	0.632	-0.7429	4.2	0.850	-0.3967	-4.3
0.043	-0.1893	7.6	0.669	-0.7111	-1.3	0.870	-0.3478	-5.1
0.162	-0.5450	0.2	0.691	-0.6806	2.6	0.874	-0.3376	-4.4
0.219	-0.6316	9.5	0.698	-0.6703	3.5	0.927	-0.1942	2.1
0.302	-0.7281	6.5	0.727	-0.6364	-3.3	0.956	-0.1222	-2.9
0.407	-0.8042	-7.6	0.761	-0.5822	-6.5			
			$xC_2H_5OH + (1-x)CH_3C(CH_3)_2OCH_3$					
0.089	-0.1994	-4.0	0.529	-0.5182	-1.8	0.754	-0.3900	-4.8
0.161	-0.2946	-1.8	0.541	-0.5128	1.5	0.796	-0.3384	2.2
0.246	-0.3896	-2.3	0.597	-0.4978	-2.0	0.805	-0.3320	-1.7
0.341	-0.4774	-4.1	0.617	-0.4959	-9.4	0.826	-0.3023	2.6
0.399	-0.4999	4.0	0.652	-0.4686	-1.9	0.847	-0.2767	0.7
0.450	-0.5106	7.2	0.671	-0.4557	-1.9	0.879	-0.2288	2.1
0.493	-0.5150	5.4	0.682	-0.4500	-3.7	0.884	-0.2203	2.9
0.503	-0.5136	6.3	0.712	-0.4248	-1.8	0.932	-0.1424	0.3
0.520	-0.5179	0.2	0.733	-0.4077	-3.0	0.950	-0.1052	3.4
			$xC_2H_5OH + (1-x)CH_3CH_2C(CH_3)_2OCH_3$					
0.038	-0.0542	-0.1	0.399	-0.3161	-3.7	0.734	-0.2662	1.4
0.158	-0.1835	1.7	0.406	-0.3174	-3.5	0.769	-0.2447	2.9
0.169	-0.1928	1.8	0.460	-0.3280	-5.9	0.802	-0.2215	3.7
0.234	-0.2399	2.3	0.559	-0.3234	-2.0	0.847	-0.1935	-4.9
0.257	-0.2489	7.5	0.639	-0.3014	4.3	0.931	-0.1045	-5.3
0.269	-0.2579	5.2	0.710	-0.2789	0.6			

TABLE 2.2 Continued

x	V_m^E	$\delta V_m^E \cdot 10^3$	x	V_m^E	$\delta V_m^E \cdot 10^3$	x	V_m^E	$\delta V_m^E \cdot 10^3$
	$cm^3 \cdot mol^{-1}$	$cm^3 \cdot mol^{-1}$		$cm^3 \cdot mol^{-1}$	$cm^3 \cdot mol^{-1}$		$cm^3 \cdot mol^{-1}$	$cm^3 \cdot mol^{-1}$

$$x C_3H_7OH + (1-x)\{CH_3CH(CH_3)\}_2O$$

x	V_m^E	$\delta V_m^E \cdot 10^3$	x	V_m^E	$\delta V_m^E \cdot 10^3$	x	V_m^E	$\delta V_m^E \cdot 10^3$
0.036	-0.1771	-3.7	0.350	-0.9608	-6.6	0.757	-0.7745	-4.5
0.046	-0.2203	-8.0	0.423	-1.0116	-2.2	0.807	-0.6571	0.6
0.094	-0.4101	-8.3	0.517	-1.0380	-1.3	0.843	-0.5613	-0.4
0.119	-0.4896	-4.9	0.637	-0.9497	3.7	0.873	-0.4777	-2.8
0.159	-0.6027	2.1	0.675	-0.9057	2.6	0.902	-0.3842	-3.4
0.219	-0.7354	1.5	0.748	-0.7793	9.1	0.964	-0.1534	-3.3

$$x C_3H_7OH + (1-x)CH_3C(CH_3)_2OCH_3$$

x	V_m^E	$\delta V_m^E \cdot 10^3$	x	V_m^E	$\delta V_m^E \cdot 10^3$	x	V_m^E	$\delta V_m^E \cdot 10^3$
0.022	-0.0649	-1.5	0.419	-0.6466	-0.4	0.759	-0.4815	-1.0
0.061	-0.1693	-0.7	0.427	-0.6473	1.5	0.798	-0.4243	0.6
0.099	-0.2603	-1.4	0.489	-0.6624	-4.9	0.849	-0.3409	0.2
0.170	-0.3988	-0.1	0.530	-0.6540	-1.1	0.881	-0.2787	0.6
0.228	-0.4870	1.5	0.586	-0.6349	-0.6	0.893	-0.2572	-0.6
0.281	-0.5512	0.8	0.632	-0.6062	1.5	0.908	-0.2241	-0.6
0.332	-0.5975	1.5	0.691	-0.5576	1.5	0.957	-0.1126	-2.8

$$x C_3H_7OH + (1-x)CH_3CH_2C(CH_3)_2OCH_3$$

x	V_m^E	$\delta V_m^E \cdot 10^3$	x	V_m^E	$\delta V_m^E \cdot 10^3$	x	V_m^E	$\delta V_m^E \cdot 10^3$
0.147	-0.3145	1.3	0.614	-0.4529	6.5	0.839	-0.2601	2.1
0.232	-0.3819	2.7	0.669	-0.4161	3.1	0.859	-0.2314	3.3
0.302	-0.4457	1.8	0.687	-0.4055	2.8	0.885	-0.2021	-4.3
0.374	-0.4763	-8.2	0.720	-0.3795	4.9	0.968	-0.0643	-5.2
0.429	-0.4839	-9.2	0.745	-0.3614	2.2			
0.526	-0.4914	-2.1						

TABLE 2.2 Continued

x	V_m^E $cm^3 \cdot mol^{-1}$	$\delta V_m^E \cdot 10^3$ $cm^3 \cdot mol^{-1}$	x	V_m^E $cm^3 \cdot mol^{-1}$	$\delta V_m^E \cdot 10^3$ $cm^3 \cdot mol^{-1}$	x	V_m^E $cm^3 \cdot mol^{-1}$	$\delta V_m^E \cdot 10^3$ $cm^3 \cdot mol^{-1}$

$$x CH_3CH(CH_3)OH \ + \ (1\text{-}x)\{CH_3CH(CH_3)\}_2O$$

x	V_m^E	$\delta V_m^E \cdot 10^3$	x	V_m^E	$\delta V_m^E \cdot 10^3$	x	V_m^E	$\delta V_m^E \cdot 10^3$
0.041	-0.0908	9.1	0.464	-0.4854	-3.6	0.788	-0.3643	6.6
0.076	-0.1693	-1.6	0.547	-0.4860	4.3	0.841	-0.2993	1.6
0.104	-0.2184	-1.9	0.621	-0.4715	4.2	0.872	-0.2569	-4.3
0.150	-0.2798	7.6	0.671	-0.4496	-1.3	0.895	-0.2194	-5.1
0.234	-0.2741	0.2	0.702	-0.4198	2.6	0.923	-0.1757	-4.4
0.275	-0.4216	9.5	0.742	-0.4009	3.5	0.949	-0.1231	2.1
0.350	-0.4569	6.5	0.754	-0.3919	-3.3			

$$x CH_3CH(CH_3)OH \ + \ (1\text{-}x)CH_3C(CH_3)_2OCH_3$$
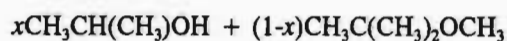
x	V_m^E	$\delta V_m^E \cdot 10^3$	x	V_m^E	$\delta V_m^E \cdot 10^3$	x	V_m^E	$\delta V_m^E \cdot 10^3$
0.044	-0.0584	-9.6	0.391	-0.2443	4.9	0.773	-0.1893	-1.1
0.088	-0.0988	-6.9	0.515	-0.2589	-0.7	0.803	-0.1724	-0.7
0.160	-0.1583	-9.0	0.627	-0.2419	0.7	0.832	-0.1472	6.1
0.200	-0.1788	-3.4	0.648	-0.2334	3.9	0.871	-0.1250	0.4
0.310	-0.2283	-4.4	0.727	-0.2112	-1.2	0.909	-0.0939	0.6
0.385	-0.2489	-0.7	0.737	-0.2134	-7.9	0.944	-0.0617	-0.4

$$x CH_3CH(CH_3)OH \ + \ (1\text{-}x)CH_3CH_2C(CH_3)_2OCH_3$$
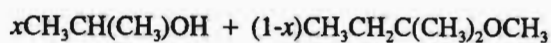
x	V_m^E	$\delta V_m^E \cdot 10^3$	x	V_m^E	$\delta V_m^E \cdot 10^3$	x	V_m^E	$\delta V_m^E \cdot 10^3$
0.019	-0.0087	-2.8	0.513	-0.1451	-2.9	0.731	-0.1302	0.8
0.055	-0.0247	5.7	0.541	-0.1430	-5.1	0.778	-0.1167	-1.7
0.124	-0.0673	1.3	0.608	-0.1448	-0.7	0.809	-0.1126	3.4
0.214	-0.1055	4.6	0.680	-0.1427	4.7	0.866	-0.0873	0.1
0.309	-0.1246	-1.5	0.694	-0.1367	0.6	0.914	-0.0603	-2.3
0.393	-0.1431	2.9	0.716	-0.1329	0.6	0.948	-0.0370	-4.3

TABLE 2.3 Experimental excess molar volumes, V_m^E for binary mixtures of $\{x\ C_jH_{2j+1}OH\ +\ (1-x)\ ROR'\}$ and the deviations, δV_m^E at the temperature 298.15 K. ROR' are cyclic ethers.

x	V_m^E $cm^3 \cdot mol^{-1}$	$\delta V_m^E \cdot 10^3$ $cm^3 \cdot mol^{-1}$	x	V_m^E $cm^3 \cdot mol^{-1}$	$\delta V_m^E \cdot 10^3$ $cm^3 \cdot mol^{-1}$	x	V_m^E $cm^3 \cdot mol^{-1}$	$\delta V_m^E \cdot 10^3$ $cm^3 \cdot mol^{-1}$
				$x CH_3OH\ +\ (1-x)\ c\text{-}(CH_2)_4O$				
0.020	-0.0100	-1.4	0.502	-0.1505	1.9	0.818	-0.1127	0.6
0.104	-0.0447	1.7	0.576	-0.1542	-0.8	0.825	-0.1096	0.7
0.140	-0.0601	2.2	0.648	-0.1485	0.5	0.839	-0.1027	2.0
0.170	-0.0772	-2.5	0.698	-0.1429	-0.2	0.897	-0.0762	1.2
0.261	-0.1092	-1.3	0.723	-0.1404	-2.2	0.948	-0.0475	-3.3
0.300	-0.1201	-0.5	0.756	-0.1306	0.4	0.981	-0.0162	1.1
0.374	-0.1359	0.9	0.764	-0.1307	-1.7			
				$x CH_3OH\ +\ (1-x)\ c\text{-}(CH_2)_5O$				
0.053	-0.0133	0.4	0.441	-0.1003	1.3	0.773	-0.0821	2.6
0.099	-0.0269	-0.1	0.521	-0.1081	-1.7	0.855	-0.0624	1.1
0.183	-0.0521	-1.4	0.535	-0.1079	-1.2	0.915	-0.0427	-0.7
0.281	-0.0749	0.7	0.631	-0.1050	0.9	0.973	-0.0203	-5.2
0.369	-0.0910	1.4	0.684	-0.0994	-0.3			
				$x CH_3OH\ +\ (1-x)\ c\text{-}(CH_2)_2O(CH_2)_2O$				
0.020	-0.0071	0.1	0.426	-0.2581	-5.8	0.816	-0.2320	-1.1
0.083	-0.0410	-0.4	0.503	-0.2758	-0.9	0.852	-0.2114	-6.5
0.121	-0.0751	-9.3	0.594	-0.2856	0.9	0.874	-0.1892	-4.5
0.191	-0.1141	2.4	0.663	-0.2819	1.9	0.905	-0.1557	-4.3
0.212	-0.1239	7.7	0.684	-0.2787	2.0	0.943	-0.1023	-1.5
0.258	-0.1603	3.2	0.712	-0.2751	-0.3	0.956	-0.0757	5.2
0.347	-0.2176	-0.7	0.755	-0.2580	3.2	0.967	-0.0502	12.8
0.379	-0.2342	-1.6	0.783	-0.2450	3.8			

TABLE 2.3 Continued

x	V_m^E	$\delta V_m^E \cdot 10^3$	x	V_m^E	$\delta V_m^E \cdot 10^3$	x	V_m^E	$\delta V_m^E \cdot 10^3$
	$cm^3 \cdot mol^{-1}$	$cm^3 \cdot mol^{-1}$		$cm^3 \cdot mol^{-1}$	$cm^3 \cdot mol^{-1}$		$cm^3 \cdot mol^{-1}$	$cm^3 \cdot mol^{-1}$

$xC_2H_5OH + (1-x)\ c\text{-}(CH_2)_4O$

x	V_m^E	$\delta V_m^E \cdot 10^3$	x	V_m^E	$\delta V_m^E \cdot 10^3$	x	V_m^E	$\delta V_m^E \cdot 10^3$
0.010	0.0063	3.3	0.400	0.0079	1.9	0.717	-0.0245	0.1
0.026	0.0088	1.6	0.464	0.0007	2.4	0.779	-0.0261	-0.1
0.053	0.0138	0.9	0.496	-0.0065	-1.1	0.830	-0.0248	0.3
0.139	0.0214	-0.9	0.564	-0.0136	-0.7	0.862	-0.0224	0.9
0.235	0.0201	-1.1	0.608	-0.0180	-0.9	0.922	-0.0173	-0.7
0.315	0.0138	-1.1	0.680	-0.0230	-0.4	0.996	-0.0002	1.0

$xC_2H_5OH + (1-x)\ c\text{-}(CH_2)_5O$

x	V_m^E	$\delta V_m^E \cdot 10^3$	x	V_m^E	$\delta V_m^E \cdot 10^3$	x	V_m^E	$\delta V_m^E \cdot 10^3$
0.028	0.0098	0.3	0.388	0.0048	1.6	0.757	-0.0260	2.5
0.054	0.0154	-0.6	0.459	-0.0089	-1.7	0.809	-0.0250	1.4
0.138	0.0247	-1.6	0.525	-0.0191	-3.2	0.810	-0.0274	-1.1
0.257	0.0217	0.6	0.578	-0.0233	-1.8	0.852	-0.0241	-1.0
0.287	0.0187	1.2	0.612	-0.0238	0.6	0.886	-0.0220	-2.6
0.372	0.0068	1.1	0.673	-0.0253	2.5	0.942	-0.0107	0.7

$xC_2H_5OH + (1-x)\ c\text{-}(CH_2)_2O(CH_2)_2O$

x	V_m^E	$\delta V_m^E \cdot 10^3$	x	V_m^E	$\delta V_m^E \cdot 10^3$	x	V_m^E	$\delta V_m^E \cdot 10^3$
0.006	0.0017	-3.1	0.334	0.1361	1.4	0.767	0.0774	-1.2
0.065	0.0487	3.2	0.439	0.1421	3.1	0.804	0.0703	2.7
0.090	0.0614	1.4	0.605	0.1213	2.2	0.843	0.0539	-0.9
0.131	0.0801	-0.6	0.636	0.1117	-1.7	0.898	0.0394	3.0
0.154	0.0897	-0.9	0.649	0.1078	-2.1	0.930	0.0227	-2.4
0.253	0.1191	-3.3	0.680	0.1012	-1.4			

TABLE 2.3 Continued

x	V_m^E cm³·mol⁻¹	$\delta V_m^E \cdot 10^3$ cm³·mol⁻¹	x	V_m^E cm³·mol⁻¹	$\delta V_m^E \cdot 10^3$ cm³·mol⁻¹	x	V_m^E cm³·mol⁻¹	$\delta V_m^E \cdot 10^3$ cm³·mol⁻¹
				$x C_3H_7OH + (1-x)\ c\text{-}(CH_2)_4O$				
0.036	-0.1771	-3.7	0.350	-0.9608	-6.6	0.757	-0.7745	-4.5
0.046	-0.2203	-8.0	0.423	-1.0116	-2.2	0.807	-0.6571	0.6
0.094	-0.4101	-8.3	0.517	-1.0380	-1.3	0.843	-0.5613	-0.4
0.119	-0.4896	-4.9	0.637	-0.9497	3.7	0.873	-0.4777	-2.8
0.159	-0.6027	2.1	0.675	-0.9057	2.6	0.902	-0.3842	-3.4
0.219	-0.7354	1.5	0.748	-0.7793	9.1	0.964	-0.1534	-3.3
				$x C_3H_7OH + (1-x)\ c\text{-}(CH_2)_5O$				
0.022	-0.0649	-1.5	0.419	-0.6466	-0.4	0.759	-0.4815	-1.0
0.061	-0.1693	-0.7	0.427	-0.6473	1.5	0.798	-0.4243	0.6
0.099	-0.2603	-1.4	0.489	-0.6624	-4.9	0.849	-0.3409	0.2
0.170	-0.3988	-0.1	0.530	-0.6540	-1.1	0.881	-0.2787	0.6
0.228	-0.4870	1.5	0.586	-0.6349	-0.6	0.893	-0.2572	-0.6
0.281	-0.5512	0.8	0.632	-0.6062	1.5	0.908	-0.2241	-0.6
0.332	-0.5975	1.5	0.691	-0.5576	1.5	0.957	-0.1126	-2.8
				$x C_3H_7OH + (1-x)\ c\text{-}(CH_2)_2O(CH_2)_2O$				
0.147	-0.3145	1.3	0.614	-0.4529	6.5	0.839	-0.2601	2.1
0.232	-0.3819	2.7	0.669	-0.4161	3.1	0.859	-0.2314	3.3
0.302	-0.4457	1.8	0.687	-0.4055	2.8	0.885	-0.2021	-4.3
0.374	-0.4763	-8.2	0.720	-0.3795	4.9	0.968	-0.0643	-5.2
0.429	-0.4839	-9.2	0.745	-0.3614	2.2			
0.526	-0.4914	-2.1						

TABLE 2.3 Continued

x	V_m^E	$\delta V_m^E \cdot 10^3$	x	V_m^E	$\delta V_m^E \cdot 10^3$	x	V_m^E	$\delta V_m^E \cdot 10^3$
	$cm^3 \cdot mol^{-1}$	$cm^3 \cdot mol^{-1}$		$cm^3 \cdot mol^{-1}$	$cm^3 \cdot mol^{-1}$		$cm^3 \cdot mol^{-1}$	$cm^3 \cdot mol^{-1}$

$$xCH_3CH(CH_3)OH + (1-x)\ c\text{-}(CH_2)_4O$$

x	V_m^E	$\delta V_m^E \cdot 10^3$	x	V_m^E	$\delta V_m^E \cdot 10^3$	x	V_m^E	$\delta V_m^E \cdot 10^3$
0.020	0.0218	0.7	0.397	0.1946	-0.9	0.735	0.1239	-3.9
0.045	0.0462	-0.4	0.458	0.1964	3.2	0.773	0.1139	0.1
0.108	0.1013	2.0	0.533	0.1864	3.2	0.833	0.0899	0.9
0.199	0.1517	-0.9	0.598	0.1651	-4.1	0.876	0.0746	4.8
0.286	0.1808	-1.6	0.651	0.1556	0.5	0.922	0.0424	-3.8
0.362	0.1934	-0.6	0.685	0.1461	1.5			

$$xCH_3CH(CH_3)OH + (1-x)\ c\text{-}(CH_2)_5O$$

x	V_m^E	$\delta V_m^E \cdot 10^3$	x	V_m^E	$\delta V_m^E \cdot 10^3$	x	V_m^E	$\delta V_m^E \cdot 10^3$
0.034	0.0414	1.6	0.440	0.2023	0.5	0.700	0.1347	-1.4
0.035	0.0383	-3.4	0.544	0.1870	2.2	0.771	0.1075	0.2
0.068	0.0807	6.1	0.549	0.1861	2.6	0.820	0.0843	-1.8
0.148	0.1361	-1.4	0.595	0.1737	2.2	0.899	0.0494	0.3
0.266	0.1861	-2.8	0.642	0.1551	-1.8	0.978	0.0200	9.1
0.350	0.2020	-0.9	0.668	0.1454	-2.5			

$$xCH_3CH(CH_3)OH + (1-x)\ c\text{-}(CH_2)_2O(CH_2)_2O$$

x	V_m^E	$\delta V_m^E \cdot 10^3$	x	V_m^E	$\delta V_m^E \cdot 10^3$	x	V_m^E	$\delta V_m^E \cdot 10^3$
0.010	0.0048	-8.6	0.376	0.2485	-2.0	0.750	0.1928	-4.0
0.055	0.0792	12.4	0.436	0.2645	4.3	0.796	0.1706	1.7
0.124	0.1327	0.9	0.500	0.2664	3.0	0.842	0.1367	-0.3
0.187	0.1686	-7.4	0.546	0.2622	1.2	0.873	0.1110	-1.9
0.258	0.2170	-1.0	0.625	0.2448	-1.9	0.950	0.0546	7.7
0.333	0.2395	-0.1	0.709	0.2161	-0.8			

TABLE 2.4 Experimental excess molar volumes, V_m^E for binary mixtures of $\{x\ CH_3CH_2NHCH_2CH_3 +$ (1-x) ROR$'\}$ and the deviations, δV_m^E at the temperature 298.15 K. ROR$'$ are branched chain ethers.

x	V_m^E cm³·mol⁻¹	$\delta V_m^E \cdot 10^3$ cm³·mol⁻¹	x	V_m^E cm³·mol⁻¹	$\delta V_m^E \cdot 10^3$ cm³·mol⁻¹	x	V_m^E cm³·mol⁻¹	$\delta V_m^E \cdot 10^3$ cm³·mol⁻¹
			$x(C_2H_5)_2NH + (1-x)\{CH_3CH(CH_3)\}_2O$					
0.030	0.0025	-1.0	0.363	0.0353	-0.2	0.645	0.0307	-1.1
0.082	0.0090	-0.7	0.400	0.0380	1.1	0.744	0.0234	-0.3
0.093	0.0106	-0.4	0.459	0.0392	1.2	0.817	0.0178	1.3
0.161	0.0185	-0.4	0.536	0.0368	-0.4	0.828	0.0164	1.0
0.219	0.0244	-0.6	0.537	0.0368	-0.3	0.917	0.0063	-0.4
0.262	0.0300	1.3	0.604	0.0329	-1.5			
			$x(C_2H_5)_2NH + (1-x)CH_3C(CH_3)_2OCH_3$					
0.007	0.0030	-0.5	0.321	0.1126	2.2	0.656	0.1130	4.4
0.046	0.0221	1.0	0.416	0.1225	-0.1	0.660	0.1088	1.0
0.083	0.0388	1.9	0.440	0.1205	-3.6	0.682	0.1036	0.2
0.139	0.0605	1.1	0.446	0.1256	1.2	0.723	0.0925	-1.6
0.162	0.0687	0.9	0.495	0.1252	0.2	0.770	0.0830	1.4
0.199	0.0801	0.2	0.545	0.1242	1.3	0.814	0.0637	-4.4
0.234	0.0893	-1.1	0.550	0.1225	-0.1	0.900	0.0396	1.0
0.258	0.0947	-1.9	0.568	0.1199	-1.0	0.989	0.0024	-2.1
0.282	0.1007	-1.6	0.572	0.1200	-0.6			
			$x(C_2H_5)_2NH + (1-x)CH_3CH_2C(CH_3)_2OCH_3$					
0.046	0.0152	-3.7	0.414	0.1044	2.5	0.702	0.0820	0.2
0.102	0.0370	-2.5	0.448	0.1036	0.4	0.753	0.0704	-1.0
0.131	0.0468	-2.4	0.480	0.1019	-1.6	0.759	0.0708	0.7
0.167	0.0606	0.5	0.500	0.1030	-0.2	0.818	0.0573	1.7
0.193	0.0641	-3.0	0.560	0.0961	-4.2	0.862	0.0437	0.1
0.261	0.0835	0.8	0.561	0.1000	-0.2	0.895	0.0328	-1.2
0.305	0.0932	2.8	0.615	0.0935	-1.5	0.957	0.0179	3.4
0.331	0.0986	4.5	0.651	0.0876	-2.6	0.970	0.0114	1.2
0.409	0.1049	3.3	0.681	0.0856	0.1	0.970	0.0044	0.7

TABLE 2.5 Experimental excess molar volumes, V_m^E for binary mixtures of $\{x\ CH_3CH_2NHCH_2CH_3 + (1-x)ROR'\}$ and the deviations, δV_m^E at the temperature 298.15 K. ROR' are cyclic ethers.

x	V_m^E $cm^3 \cdot mol^{-1}$	$\delta V_m^E \cdot 10^3$ $cm^3 \cdot mol^{-1}$	x	V_m^E $cm^3 \cdot mol^{-1}$	$\delta V_m^E \cdot 10^3$ $cm^3 \cdot mol^{-1}$	x	V_m^E $cm^3 \cdot mol^{-1}$	$\delta V_m^E \cdot 10^3$ $cm^3 \cdot mol^{-1}$
				$x(C_2H_5)_2NH + (1-x)c\text{-}(CH_2)_4O$				
0.009	-0.0029	-1.5	0.371	-0.0504	-0.4	0.710	-0.0600	-1.5
0.041	-0.0073	-1.1	0.420	-0.0546	-0.1	0.749	-0.0581	-3.1
0.064	-0.0117	-2.0	0.430	-0.0553	-0.0	0.808	-0.0513	-3.7
0.097	-0.0150	-0.3	0.455	-0.0570	0.1	0.837	-0.0421	0.7
0.180	-0.0283	-1.6	0.469	-0.0565	1.6	0.885	-0.0302	2.9
0.280	-0.0386	1.3	0.577	-0.0615	0.8	0.912	-0.0202	6.4
0.339	-0.0450	1.8	0.702	-0.0602	-1.2	0.976	-0.0061	2.2
			$x(C_2H_5)_2NH + (1-x)c\text{-}(CH_2)_5O$					
0.017	0.0090	4.5	0.247	-0.0254	1.0	0.655	-0.0716	1.0
0.019	0.0099	4.8	0.312	-0.0357	2.1	0.702	-0.0699	1.2
0.075	0.0140	1.3	0.358	-0.0446	0.1	0.782	-0.0671	-1.9
0.076	0.0139	1.4	0.399	-0.0515	-1.0	0.811	-0.0634	-1.2
0.109	0.0077	1.3	0.451	-0.0595	-1.9	0.889	-0.0502	1.6
0.126	-0.0012	-3.7	0.456	-0.0590	-0.8	0.949	-0.0355	-1.1
0.132	-0.0016	-2.4	0.567	-0.0700	0.2	0.950	-0.0307	3.1
0.198	-0.0166	-0.7	0.583	-0.0710	0.8	0.961	-0.0308	-2.5
0.235	-0.0224	1.6						
			$x(C_2H_5)_2NH + (1-x)c\text{-}(CH_2)_2O(CH_2)_2O$					
0.009	-0.0039	-1.9	0.334	-0.0800	-3.2	0.709	-0.0768	0.9
0.055	-0.0084	4.4	0.352	-0.0815	-1.8	0.738	-0.0716	0.9
0.055	-0.0134	-0.5	0.392	-0.0858	-0.6	0.797	-0.0643	-4.8
0.063	-0.0112	3.6	0.450	-0.0879	2.9	0.817	-0.0582	-3.8
0.124	-0.0302	-0.3	0.542	-0.0909	2.6	0.836	-0.0523	-2.8
0.185	-0.0463	-1.1	0.567	-0.0918	1.1	0.861	-0.0422	0.6
0.246	-0.0588	0.7	0.610	-0.0906	-0.3	0.887	-0.0311	4.3
0.290	-0.0700	-1.3	0.680	-0.0809	1.5	0.955	-0.0100	4.6

TABLE 2.6 Experimental excess molar volumes, V_m^E for binary mixtures of $\{x\ CH_3(CH_2)_2NH(CH_2)_2CH_3 + (1\text{-}x)\ ROR'\}$ and the deviations, δV_m^E at the temperature 298.15 K. ROR' are branched chain ethers.

x	V_m^E cm³·mol⁻¹	$\delta V_m^E\cdot10^3$ cm³·mol⁻¹	x	V_m^E cm³·mol⁻¹	$\delta V_m^E\cdot10^3$ cm³·mol⁻¹	x	V_m^E cm³·mol⁻¹	$\delta V_m^E\cdot10^3$ cm³·mol⁻¹
				$x(C_3H_7)_2NH + (1\text{-}x)\{CH_3CH(CH_3)\}_2O$				
0.016	-0.0102	5.5	0.301	-0.2036	3.2	0.605	-0.2114	4.4
0.099	-0.0893	1.4	0.339	-0.2191	-1.0	0.659	-0.1971	3.1
0.126	-0.1118	-0.2	0.372	-0.2237	1.7	0.697	-0.1840	2.9
0.132	-0.1182	-2.1	0.391	-0.2271	1.4	0.747	-0.1665	-0.4
0.164	-0.1407	-2.3	0.461	-0.2335	0.1	0.784	-0.1514	-3.4
0.207	-0.1653	-0.6	0.482	-0.2375	-4.2	0.838	-0.1199	-0.9
0.241	-0.1825	0.0	0.504	-0.2367	-4.6	0.869	-0.0966	3.0
0.252	-0.1880	-0.5	0.585	-0.2171	3.2	0.892	-0.0866	-2.4
0.268	-0.1942	0.2	0.596	-0.2198	-2.0	0.986	-0.0063	6.3
				$x(C_3H_7)_2NH + (1\text{-}x)CH_3C(CH_3)_2OCH_3$				
0.014	-0.0019	1.3	0.283	-0.0400	0.7	0.665	-0.0433	3.3
0.023	-0.0045	0.7	0.314	-0.0429	0.1	0.722	-0.0405	2.7
0.092	-0.0198	-1.6	0.336	-0.0449	-0.7	0.732	-0.0347	2.1
0.128	-0.0238	0.1	0.351	-0.0467	-1.6	0.845	-0.0310	-0.6
0.190	-0.0307	1.2	0.383	-0.0481	-1.4	0.856	-0.0313	-2.4
0.205	-0.0324	1.1	0.436	-0.0500	-1.5	0.905	-0.0237	-2.7
0.231	-0.0351	1.1	0.456	-0.0504	-1.4	0.934	-0.0144	1.0
0.258	-0.0381	0.6	0.533	-0.0504	-0.7	0.972	-0.0116	-4.6
0.264	-0.0386	0.6	0.601	-0.0489	-0.1	0.978	-0.0074	-1.8
				$x(C_3H_7)_2NH + (1\text{-}x)CH_3CH_2C(CH_3)_2OCH_3$				
0.010	-0.0075	3.0	0.323	-0.0020	0.1	0.657	0.0072	-1.6
0.023	-0.0274	-6.5	0.388	0.0017	1.6	0.673	0.0072	-1.4
0.024	-0.0274	-5.8	0.423	0.0041	2.3	0.681	0.0070	-1.4
0.138	-0.0199	6.5	0.453	0.0056	3.1	0.832	0.0052	2.8
0.164	-0.0165	3.8	0.479	0.0062	4.0	0.861	0.0044	2.1
0.191	-0.0143	0.0	0.555	0.0074	7.1	0.930	0.0018	-2.0
0.223	-0.0121	-3.4	0.588	0.0073	8.2	0.966	0.0012	-2.6
0.265	-0.0082	-4.7						

TABLE 2.7 Experimental excess molar volumes, V_m^E for binary mixtures of $\{x\ CH_3(CH_2)_2NH(CH_2)_2CH_3 + (1-x)\ ROR'\}$ and the deviations, δV_m^E at the temperature 298.15 K. ROR' are cyclic ethers.

x	V_m^E ($cm^3 \cdot mol^{-1}$)	$\delta V_m^E \cdot 10^3$ ($cm^3 \cdot mol^{-1}$)	x	V_m^E ($cm^3 \cdot mol^{-1}$)	$\delta V_m^E \cdot 10^3$ ($cm^3 \cdot mol^{-1}$)	x	V_m^E ($cm^3 \cdot mol^{-1}$)	$\delta V_m^E \cdot 10^3$ ($cm^3 \cdot mol^{-1}$)
			$x(C_3H_7)_2NH + (1-x)c\text{-}(CH_2)_4O$					
0.005	-0.0028	-2.4	0.287	-0.0208	0.4	0.682	-0.0284	0.3
0.010	-0.0026	-1.8	0.355	-0.0240	0.4	0.682	-0.0286	0.1
0.034	-0.0056	-3.0	0.391	-0.0258	0.1	0.784	-0.0233	1.9
0.097	-0.0082	-0.4	0.409	-0.0270	-0.5	0.884	-0.0179	-0.2
0.113	-0.0087	0.4	0.460	-0.0289	-1.0	0.923	-0.0144	-1.3
0.148	-0.0108	1.1	0.587	-0.0300	-0.6	0.955	-0.0092	-0.8
0.200	-0.0153	0.4						
			$x(C_3H_7)_2NH + (1-x)c\text{-}(CH_2)_5O$					
0.061	-0.0026	-1.6	0.275	-0.0211	0.4	0.597	-0.0538	-1.0
0.100	-0.0038	-0.6	0.297	-0.0225	1.6	0.619	-0.0540	-0.3
0.143	-0.0073	-0.5	0.390	-0.0348	0.4	0.632	-0.0542	-0.1
0.145	-0.0074	-0.4	0.440	-0.0421	-1.4	0.714	-0.0514	2.8
0.146	-0.0074	-0.4	0.485	-0.0444	0.6	0.762	-0.0494	2.6
0.196	-0.0113	0.8	0.521	-0.0495	-1.4	0.891	-0.0369	-2.6
0.213	-0.0130	1.2	0.570	-0.0528	-1.4	0.921	-0.0278	-0.9
			$x(C_3H_7)_2NH + (1-x)c\text{-}(CH_2)_2O(CH_2)_2O$					
0.033	0.0138	-2.6	0.309	0.1247	-2.6	0.588	0.1609	3.2
0.067	0.0271	-4.7	0.324	0.1361	4.0	0.624	0.1557	4.0
0.117	0.0508	-2.3	0.365	0.1400	-3.6	0.687	0.1375	0.6
0.143	0.0687	4.7	0.394	0.1491	-1.2	0.717	0.1279	-0.3
0.155	0.0655	-3.4	0.397	0.1482	-2.9	0.774	0.1028	-6.6
0.187	0.0868	5.0	0.418	0.1535	-1.5	0.861	0.0750	-1.0
0.223	0.1010	4.9	0.507	0.1603	-2.7	0.916	0.0484	-2.5
0.257	0.1088	-0.3	0.543	0.1626	0.5	0.941	0.0326	0.7
0.284	0.1182	-0.8						

TABLE 2.8 Experimental excess molar volumes, V_m^E for binary mixtures of $\{x$ 1-C_6H_{10} + $(1\text{-}x)$ ROR$'\}$ and the deviations, δV_m^E at the temperature 298.15 K. ROR$'$ is a branched chain ether.

x	V_m^E cm$^3 \cdot$mol^{-1}	$\delta V_m^E \cdot 10^3$ cm$^3 \cdot$mol^{-1}	x	V_m^E cm$^3 \cdot$mol^{-1}	$\delta V_m^E \cdot 10^3$ cm$^3 \cdot$mol^{-1}	x	V_m^E cm$^3 \cdot$mol^{-1}	$\delta V_m^E \cdot 10^3$ cm$^3 \cdot$mol^{-1}
			x1-C_6H_{10} + $(1\text{-}x)\{CH_3CH(CH_3)\}_2O$					
0.110	-0.1453	0.4	0.487	-0.3784	-1.9	0.771	-0.2699	1.4
0.226	-0.2576	2.0	0.535	-0.3731	3.1	0.832	-0.2178	-1.6
0.264	-0.2889	-0.1	0.581	-0.3708	-1.5	0.852	-0.1950	0.1
0.277	-0.2999	-2.0	0.639	-0.3519	-0.6	0.926	-0.1097	-2.5
0.365	-0.3457	1.1	0.683	-0.3278	3.1	0.983	-0.0248	0.8
0.463	-0.3764	-2.2						
			x1-C_6H_{10} + $(1\text{-}x)CH_3C(CH_3)_2OCH_3$					
0.019	-0.0254	1.9	0.407	-0.3255	-4.5	0.747	-0.2532	1.6
0.086	-0.1080	5.5	0.460	-0.3367	-6.8	0.823	-0.2048	6.0
0.163	-0.1844	7.1	0.513	-0.3369	-4.5	0.879	-0.1547	2.9
0.271	-0.2702	-1.6	0.546	-0.3295	1.3	0.929	-0.1254	-25.3
0.287	-0.2761	0.7	0.597	-0.3216	1.9	0.981	-0.0678	-39.0
0.361	-0.3118	-3.6	0.659	-0.2990	7.5			
			x1-C_6H_{10} + $(1\text{-}x)CH_3CH_2C(CH_3)_2OCH_3$					
0.034	-0.0685	-27.3	0.475	-0.2750	0.1	0.725	-0.2210	-6.0
0.119	-0.1292	-1.0	0.521	-0.2744	-1.1	0.810	-0.1580	8.3
0.263	-0.2203	4.6	0.525	-0.2759	-2.9	0.831	-0.1459	6.3
0.322	-0.2441	5.1	0.615	-0.2596	-2.9	0.921	-0.0714	5.3
0.373	-0.2623	1.4	0.689	-0.2390	-7.6	0.993	-0.0354	-27.6
0.408	-0.2668	3.3						

TABLE 2.9 Experimental excess molar volumes, V_m^E for binary mixtures of $\{x$ 1-C_7H_{12} + $(1-x)$ ROR$'\}$ and the deviations, δV_m^E at the temperature 298.15 K. ROR$'$ is a branched chain ether.

x	V_m^E $cm^3 \cdot mol^{-1}$	$\delta V_m^E \cdot 10^3$ $cm^3 \cdot mol^{-1}$	x	V_m^E $cm^3 \cdot mol^{-1}$	$\delta V_m^E \cdot 10^3$ $cm^3 \cdot mol^{-1}$	x	V_m^E $cm^3 \cdot mol^{-1}$	$\delta V_m^E \cdot 10^3$ $cm^3 \cdot mol^{-1}$

$$x1\text{-}C_7H_{12} + (1-x)\{CH_3CH(CH_3)\}_2O$$

x	V_m^E	$\delta V_m^E \cdot 10^3$	x	V_m^E	$\delta V_m^E \cdot 10^3$	x	V_m^E	$\delta V_m^E \cdot 10^3$
0.040	-0.0633	9.3	0.432	-0.4521	-0.4	0.725	-0.3570	2.1
0.083	-0.1412	2.7	0.461	-0.4572	-0.8	0.749	-0.3350	2.9
0.164	-0.2592	-0.9	0.478	-0.4484	9.3	0.834	-0.2481	-1.3
0.234	-0.3378	-2.0	0.588	-0.4465	-6.0	0.924	-0.1261	-1.8
0.265	-0.3670	3.6	0.589	-0.4418	-1.7	0.973	-0.0536	-6.9
0.369	-0.4325	-1.4	0.720	-0.3612	1.6			

$$x1\text{-}C_7H_{12} + (1-x)CH_3C(CH_3)_2OCH_3$$

x	V_m^E	$\delta V_m^E \cdot 10^3$	x	V_m^E	$\delta V_m^E \cdot 10^3$	x	V_m^E	$\delta V_m^E \cdot 10^3$
0.017	-0.0323	-2.8	0.300	-0.3315	-1.9	0.608	-0.3478	-1.9
0.070	-0.1139	-2.0	0.344	-0.3520	-3.3	0.660	-0.3207	2.6
0.143	-0.2022	1.8	0.383	-0.3589	2.0	0.700	-0.2996	1.7
0.152	-0.2149	-1.0	0.394	-0.3603	3.4	0.736	-0.2744	3.9
0.215	-0.2703	2.3	0.459	-0.3733	-1.7	0.838	-0.1953	-1.8
0.223	-0.2763	2.9	0.485	-0.3729	-1.5	0.940	-0.0885	-7.2
0.265	-0.3102	-1.1	0.526	-0.3701	-2.7	0.945	-0.0683	6.4

$$x1\text{-}C_7H_{12} + (1-x)CH_3CH_2C(CH_3)_2OCH_3$$

x	V_m^E	$\delta V_m^E \cdot 10^3$	x	V_m^E	$\delta V_m^E \cdot 10^3$	x	V_m^E	$\delta V_m^E \cdot 10^3$
0.078	-0.1517	-50.3	0.411	-0.2583	1.4	0.612	-0.2426	-7.7
0.192	-0.1985	-2.3	0.471	-0.2608	-2.0	0.732	-0.1953	-2.8
0.203	-0.1927	9.7	0.483	-0.2613	-3.4	0.808	-0.1508	2.9
0.262	-0.2175	12.8	0.517	-0.2609	-6.8	0.919	-0.0625	13.7
0.292	-0.2274	13.0	0.582	-0.2476	-5.4	0.948	-0.0438	7.7
0.338	-0.2436	8.1						

TABLE 2.10 Experimental excess molar volumes, V_m^E for binary mixtures of $\{x\ 1\text{-}C_8H_{14} + (1\text{-}x)\ ROR'\}$ and the deviations, δV_m^E at the temperature 298.15 K. ROR' is a branched chain ether.

x	V_m^E cm³·mol⁻¹	$\delta V_m^E \cdot 10^3$ cm³·mol⁻¹	x	V_m^E cm³·mol⁻¹	$\delta V_m^E \cdot 10^3$ cm³·mol⁻¹	x	V_m^E cm³·mol⁻¹	$\delta V_m^E \cdot 10^3$ cm³·mol⁻¹

$x1\text{-}C_8H_{14} + (1\text{-}x)\{CH_3CH(CH_3)\}_2O$

x	V_m^E	$\delta V_m^E \cdot 10^3$	x	V_m^E	$\delta V_m^E \cdot 10^3$	x	V_m^E	$\delta V_m^E \cdot 10^3$
0.028	-0.0653	5.1	0.380	-0.5431	-5.7	0.705	-0.4372	5.8
0.122	-0.2608	5.1	0.454	-0.5583	-4.2	0.765	-0.3800	0.2
0.218	-0.4083	2.0	0.476	-0.5549	-0.5	0.842	-0.2769	2.7
0.239	-0.4321	1.8	0.529	-0.5442	3.0	0.892	-0.2095	-7.0
0.319	-0.5082	-3.6	0.570	-0.5307	2.7	0.966	-0.0841	-14.5
0.349	-0.5249	-1.9	0.639	-0.4933	2.4			

$x1\text{-}C_8H_{14} + (1\text{-}x)CH_3C(CH_3)_2OCH_3$
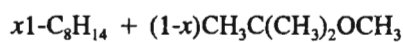
x	V_m^E	$\delta V_m^E \cdot 10^3$	x	V_m^E	$\delta V_m^E \cdot 10^3$	x	V_m^E	$\delta V_m^E \cdot 10^3$
0.027	-0.0472	3.1	0.344	-0.3830	-1.9	0.664	-0.3568	-1.5
0.051	-0.0921	-0.3	0.391	-0.3908	3.0	0.711	-0.2919	-0.7
0.203	-0.2913	-2.2	0.467	-0.3985	-0.7	0.797	-0.2202	-2.0
0.229	-0.3130	-0.5	0.504	-0.3927	0.1	0.888	-0.1254	2.0
0.280	-0.3502	-0.8	0.558	-0.3754	2.5	0.978	-0.0194	6.8
0.324	-0.3702	2.4	0.638	-0.3414	-1.3			

$x1\text{-}C_8H_{14} + (1\text{-}x)CH_3CH_2C(CH_3)_2OCH_3$

x	V_m^E	$\delta V_m^E \cdot 10^3$	x	V_m^E	$\delta V_m^E \cdot 10^3$	x	V_m^E	$\delta V_m^E \cdot 10^3$
0.031	-0.0599	-17.8	0.384	-0.2678	-0.3	0.715	-0.2073	0.7
0.111	-0.1308	-1.4	0.416	-0.2744	-3.5	0.830	-0.1404	2.3
0.179	-0.1858	-0.5	0.447	-0.2754	-3.4	0.850	-0.1313	-2.2
0.233	-0.2171	1.4	0.501	-0.2710	-1.6	0.929	-0.0649	2.1
0.288	-0.2331	10.0	0.619	-0.2445	0.6	0.977	-0.0220	0.7
0.326	-0.2541	1.3	0.621	-0.2453	-0.7			

TABLE 2.11 Coefficients A_r and standard deviations σ for [an alkanol (1) + a branched chain ether (2)] at the temperature 298.15 K by equation 2.8.

Branched Chain ether	A_0	A_1	A_2	$\sigma^{(a)}$ $cm^3 \cdot mol^{-1} \cdot 10^{-3}$
methanol				
IPE	-3.917	0.276	-0.869	4.5
TBME	-2.570	0.096	-0.479	4.4
TAME	-1.851	0.290	-0.143	3.9
ethanol				
IPE	-3.278	0.523	-0.490	13.7
TBME	-2.066	0.060	-0.226	4.7
TAME	-1.302	-0.048	-0.225	4.3
propan-1-ol				
IPE	-4.114	0.193	-0.612	8.3
TBME	-2.629	0.131	-0.247	1.6
TAME	-1.941	0.299	-0.428	7.8
propan-2-ol				
IPE	-1.952	-0.014	-0.607	4.7
TBME	-1.026	0.038	-0.232	3.7
TAME	-0.599	-0.068	-0.097	10.5

TABLE 2.12 Coefficients A_r and standard deviations σ for [an alkanol (1) + a cyclic ether (2)] at the temperature 298.15 K by equation 2.8.

Cyclic ether	A_0	A_1	A_2	A_3	$\sigma^{(a)}$ $cm^3 \cdot mol^{-1} \cdot 10^{-3}$
			methanol		
tetrahydrofuran	-0.6090	0.1087	-0.0919	0.1648	1.8
tetrahydropyran	-0.4226	0.0904	-0.0104	0.0861	2.2
1,4-dioxane	1.097	-0.4489	0.1038	-0.4477	5.2
			ethanol		
tetrahydrofuran	-0.0842	0.2382	-0.0273	0.0189	2.4
tetrahydropyran	0.0393	0.2782	0.0338	0.0741	1.5
1,4-dioxane	-0.1134	0.3551	0.0302	0.1018	2.6
			propan-1-ol		
tetrahydrofuran	-0.0236	0.2277	0.0366	0.0691	1.5
tetrahydropyran	-0.0511	0.2579	0.1314	0.0436	1.9
1,4-dioxane	0.5393	0.2002	0.0337	0.0090	2.5
			propan-2-ol		
tetrahydrofuran	0.7538	0.2799	0.1310	-0.0520	2.8
tetrahydropyran	0.7748	0.3539	0.1051	0.0364	3.7
1,4-dioxane	1.054	0.0170	0.1115	0.1974	5.6

TABLE 2.13 Coefficients A_r and standard deviations σ for [a secondary amine (1) + a branched chain or cyclic ether (2)] at the temperature 298.15 K by equation 2.8.

Branched chain or cyclic ether	A_0	A_1	A_2	A_3	$\sigma^{(a)}$ $cm^3 \cdot mol^{-1} \cdot 10^{-3}$
diethylamine					
IPE	0.1515	-0.0246	-0.0623	-	1.0
TBME	0.4997	-0.0406	-0.0614	-	1.9
TAME	0.4129	-0.0451	-0.0254	-	2.3
tetrahydrofuran	-0.2393	-0.1003	0.0144	-	2.3
tetrahydropyran	-0.256	-0.130	0.023	-0.427	3.5
1,4-dioxane	-0.373	-0.0514	0.1021	-	2.8
di-n-propylamine					
IPE	-0.9294	0.1364	-0.0276	-0.0773	3.0
TBME	-0.1985	-0.0161	-0.0486	-	1.8
TAME	0.0193	0.0808	0.0760	-0.3323	3.7
tetrahydrofuran	-0.1146	-0.0324	-0.0294	-0.0345	1.4
tetrahydropyran	-0.1854	-0.1710	-0.0174	-0.0467	1.5
1,4-dioxane	0.645	0.060	-0.1590	-	3.2

TABLE 2.14 Coefficients A_r and standard deviations σ for [an 1-alkyne (1) + a branched chain ether (2)] at the temperature 298.15 K by equation 2.8.

Branched				$\sigma^{(a)}$
Chain ether	A_0	A_1	A_2	$cm^3 \cdot mol^{-1} \cdot 10^{-3}$
		1-hexyne		
IPE	-1.5085	-0.0489	-0.0109	2.0
TBME	-1.3295	-0.0375	-0.2178	13.6
TAME	-1.0988	0.0876	-0.0938	11.8
		1-heptyne		
IPE	-1.8311	0.0737	-0.0052	4.7
TBME	-1.4818	0.1663	-0.1249	4.4
TAME	-1.0250	0.2211	-0.2690	16.3
		1-octyne		
IPE	-2.2101	0.2603	-0.1462	5.6
TBME	-1.5743	0.3686	0.0132	2.7
TAME	-1.0780	0.1958	-0.1409	5.8

[a]In Tables 2.11 to 2.14 σ refers to

$$\sigma = \left[\sum (H^E_{m_{(expt.)}} - H^E_{m_{(calc.)}})^2 / (n-k)\right]^{1/2} \qquad (2.10)$$

where n is the number of experimental points

2.5 Discussion

2.5.1 Mixtures of (an alkanol + a branched chain ether or cyclic ether)

2.5.1.1 Previous work

It has been suggested that there exists a strong interaction between the polar alkanol and the aprotic aliphatic ether.[58,59] The degree of interaction depends on the hydrogen bonding propensity(proton donor capability) of the alkanol and the proton acceptor capability of the ether. Alcohols are known to be self associated through hydrogen bonded linear chains to variable degrees of polymerization.[60-64] The degree and strength of polymerization decrease with increasing hydrocarbon chain length and also with position of the hydroxyl group in the molecule. The addition of a non-polar compound to an alkanol generally breaks the three dimensional hydrogen bonded network of pure alkanols and give positive excess molar volumes in mixtures.[65] For the sake of comparison, the thermodynamic volumetric behaviour of (alkanols + *n*-alkanes) mixtures have been compared with that of (alkanols + ether) mixtures. Formally, ethers can be classified as homomorphic products obtained by replacing a CH_2 group in *n*-alkanes by a O (oxygen) atom. Mixtures containing short chain alkanol with n-alkane have been studied extensively.[66-74] For the thermodynamic description of alkanol + alkane systems there prevails the relatively simple picture wherein the alkanol is self associated and interacts with the alkane only by weak physical forces (London dispersive). This picture has been corroborated by spectroscopic studies.[75] Treszczanowicz and Benson[70] determined the V_m^E at 298.15 K for (methanol or ethanol or n-propanol + heptane) and found that the excess volume is positive over the whole mole fraction range. Similar results were observed for mixtures of (propan-2-ol + heptane) at 333.15 K.[76] These results were attributed to the dissociation of the hydrogen bonds in the alkanol molecule.

The branched chain mono-ethers are aprotic and are considered essentially to be weakly-polar molecules. Interactions between a polar component and an ether are proposed to occur via complex formation between the two species. Di-isopropyl ether has been known to participate in cross association effects with the hydrogen present in trichloromethane and the

excess molar volume has been reported as large and negative ($V_m^E(0.5) = -1.65$ cm^3·mol^{-1}).[77-81]
Negative excess molar volumes have also been reported for chloroform with monoethers.[82]
Treszczanowicz[83] has reported positive excess molar volumes for mixtures of (methyl butyl
ether or di-isopropyl ether + heptane) at 298.15 K with $V_m^E(0.5) = 0.24$ cm^3·mol^{-1} for the
(di-isopropylether + heptane) system . Arm and Bankay[60] have reported volume changes
upon mixing for (methanol + diethyl ether) which are negative over the whole composition
range with $V_m^E(0.5) = -0.80$ cm^3·mol^{-1}. They have discussed the results in terms of the
dominance of the association between the component molecules.

The cyclic ethers deviate somewhat in the thermochemical behaviour to branched
chain ethers because the magnitude and symmetry of the excess properties are influenced by
structural factors imposed by ring closure. Pintos et al.[84,85] have recently reported positive
excess molar volumes for the whole range of mole fraction for mixtures of (THF or THP +
hexane or heptane or octane or nonane) at 298.15 K. The magnitudes of V_m^E depended on the
size of the ring and the number of carbons in the alkane molecule and the results were
discussed in terms of interactions between components. Andrews and Morcom[86] studied the
volumetric properties of (1,4-dioxane + benzene or cyclohexane or hexane) at 298.15 K and
concluded that for there exists a specific interaction between the benzene and 1,4-dioxane
(negative V_m^E) which decreases (becomes positive) on changing to cyclohexane. This specific
interaction is stronger than might be expected from dispersion or dipole-induced dipole forces
and it is these forces that dictate the behaviour of the mixture. These workers have also
confirmed similar behaviour to 1,4-dioxane for mixtures containing THF and THP. Negative
V_m^E have been reported[87] for (1,4-dioxane or THF + carbon tetrachloride) at 303.15 K
suggesting specific solute-solvent interaction. Weak interactions between an aromatic and
substituted aromatic hydrocarbon with cyclic ethers have also been proposed by Meyer et al.[88]
to give negative V_m^E data at 298.15 K. The excess volumes for (n-alkanes (C_6 - C_9) + THF
or THP or 1,4-dioxane) were reported[89,90] to be positive. Guillen et al. [90] reported negative
V_m^E at 283.15 and 303.15 K for (tetrachloromethane + THF or THP or 1,4-dioxane) and have
concluded that the THF mixture exhibits the largest specific interaction. Solimo et al.[91]
reported negative V_m^E for (chloroform + THF) at 303.15 K and attributed this effect to two

main contributions (i) interstitial accommodation of one component within the structure of the other and (ii) the possibility of formation of a new chemical species in the solution by specific interaction.

2.5.1.2 This work

(a) Mixtures of (an alkanol + a branched chain ether)

The excess molar volumes V_m^E at the temperature 298.15 K are listed in Table 2.2 with the parameters of equation 2.8 given in Table 2.11. The experimental data points are presented in figures 2.8 to 2.11 for each of the 12 mixtures over the entire mole fraction range. All of the V_m^E curves are negative and symmetrical about x = 0.5. For each of the alkanols, the V_m^E data increase in the following order: IPE < TBME < TAME. This trend would seem to indicate (a) a more organized packing effect and (b) stronger specific interactions for systems containing IPE than TBME or TAME. This can be explained by considering the structural implications of the three branched ethers. IPE is less sterically hindered than TBME or TAME where the latter two molecules experience greater intramolecular congestion arising from the packing of three methyl groups around a common C (carbon) group. This leads to a strained structure and hence the lesser availability of the O atom in the ether to interaction with the OH group of the alkanol. This effect is enhanced as the degree of branching increases. At equimolar concentrations for each of the ethers, all of the systems exhibit a similar trend in V_m^E when increasing the chain length of the alkanol e.g., for the IPE systems, V_m^E is less negative for ethanol than methanol, -0.99 cm³·mol⁻¹ and -0.82 cm³·mol⁻¹, respectively while propan-1-ol is more negative than either ethanol or methanol i.e., -1.02 cm³·mol⁻¹. The lack of trend displayed by the V_m^E (x = 0.5) values is indicative of the significant role molecular packing effects play in determining the excess molar volume. This result is to be expected if the large differences in the molar volumes of the different components in each mixture are considered. V_m^E for the mixtures (propan-2-ol + IPE or TBME or TAME) show the least negative behaviour and this is probably attributable to the shielding effect on the alkanol hydroxy group by the two adjacent methyl groups thus

preventing any association between the alkanol and the ether species.

As far as we know, the V_m^E results for the mixtures discussed here have not been reported in the literature except for (methanol or ethanol or propan-2-ol + IPE or TBME). Blanco et al.[92] recently reported the V_m^E at 298.15 K for (methanol or ethanol or propan-2-ol + IPE or TBME) and showed that V_m^E was negative over the whole mole fraction range. Our V_m^E (x = 0.5) results for (methanol + IPE or TBME) are -0.98 and -0.64 cm³·mol⁻¹ while those reported by Blanco and co_workers are -0.99 and -0.65 cm³·mol⁻¹, respectively. Our V_m^E (x = 0.5) results for (ethanol + IPE or TBME) are -0.82 and -0.52 cm³·mol⁻¹ while those reported by Blanco and co-workers are -0.83 and -0.50 cm³·mol⁻¹, respectively. Our V_m^E (x = 0.5) results for (propan-2-ol + IPE or TBME) are -0.49 and -0.26 cm³·mol⁻¹ while those reported by Blanco and workers are -0.49 and -0.25 cm³·mol⁻¹, respectively. These authors[92] have also reported positive V_m^E for a highly branched hydrocarbon analogous to the branched chain ether with methanol or ethanol or propan-2-ol. Comparison of their results seems to indicate the negative volumetric behaviour exhibited here is most likely due to the association between the proton of the alkanol hydroxy group and the ethereal oxygen. Nakanishi et al.[93] have reported V_m^E (x = 0.5) for (methanol + IPE) at 298.15 K of -1.02 cm³·mol⁻¹. Farkova et al.[94] have recently reported V_m^E (x = 0.5) for (methanol + IPE or TBME) at 298.15 K of -0.98 and -0.65 cm³·mol⁻¹, respectively. These authors[94] have also investigated the effect on V_m^E of the degree of branching of the ether in (alkanol + ether) systems by determining V_m^E for the (alkanol + unsymmetrical straight chain ethers). They have reported an increase in V_m^E (x = 0.5) for (methanol + butyl methyl ether or butyl ethyl ether) at 298.15 K of -0.29 and -0.39 cm³·mol⁻¹, respectively as compared to the branched chain ether counterparts.
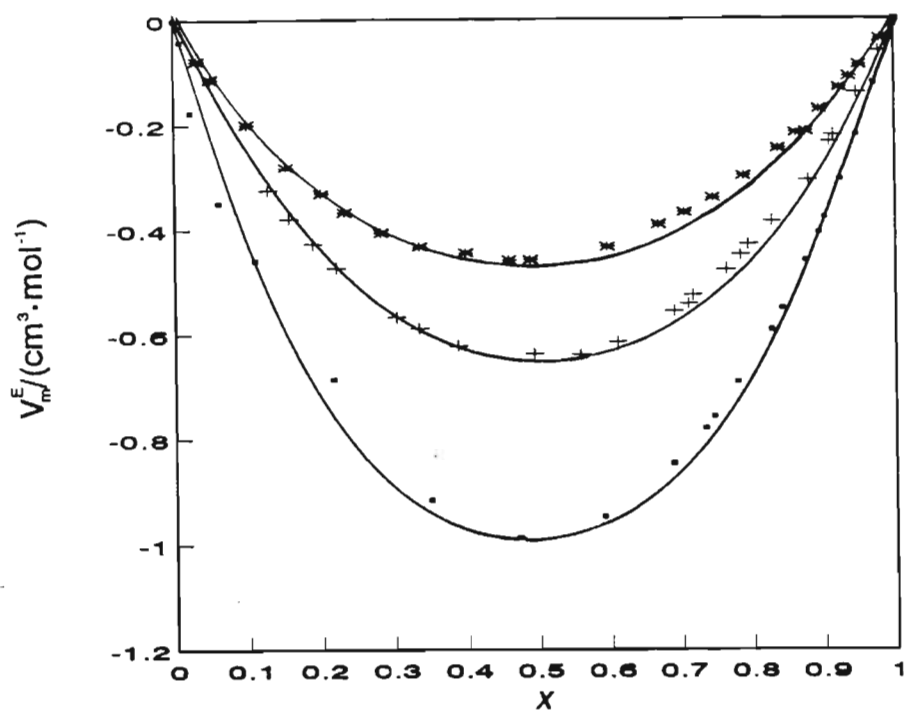
Figure 2.8 Excess molar volumes, V_m^E at 298.15 K for {x CH$_3$OH + (1-x)ROR'} where ROR' is ■, IPE or $+$, TBME or $*$, TAME
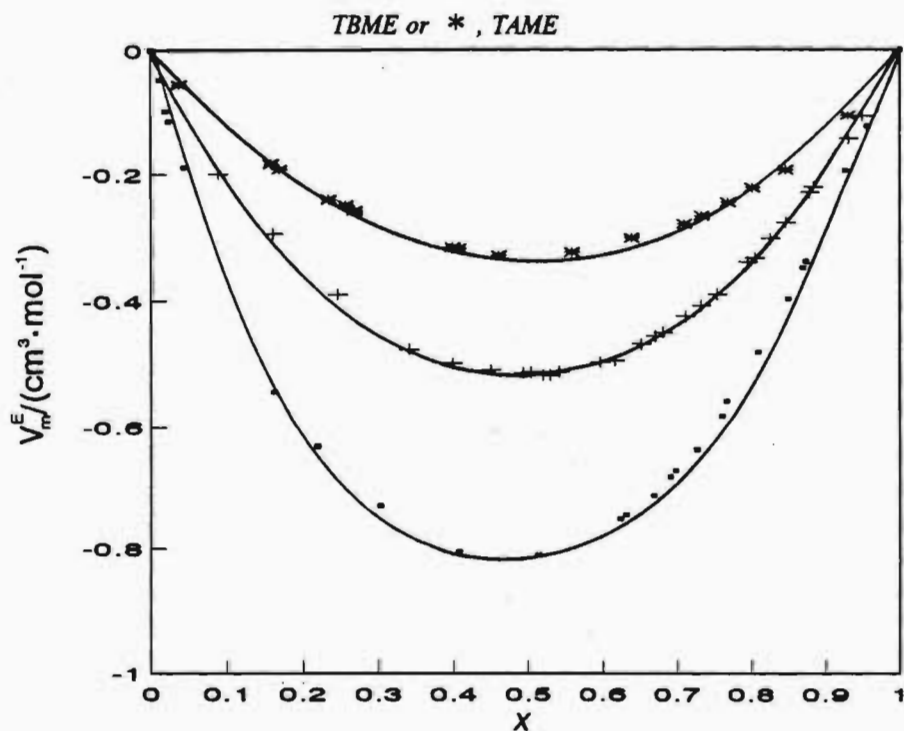
Figure 2.9 Excess molar volumes, V_m^E at 298.15 K for {x C$_2$H$_5$OH + (1-x) ROR'} where ROR' ■, IPE or $+$, TBME or $*$, TAME
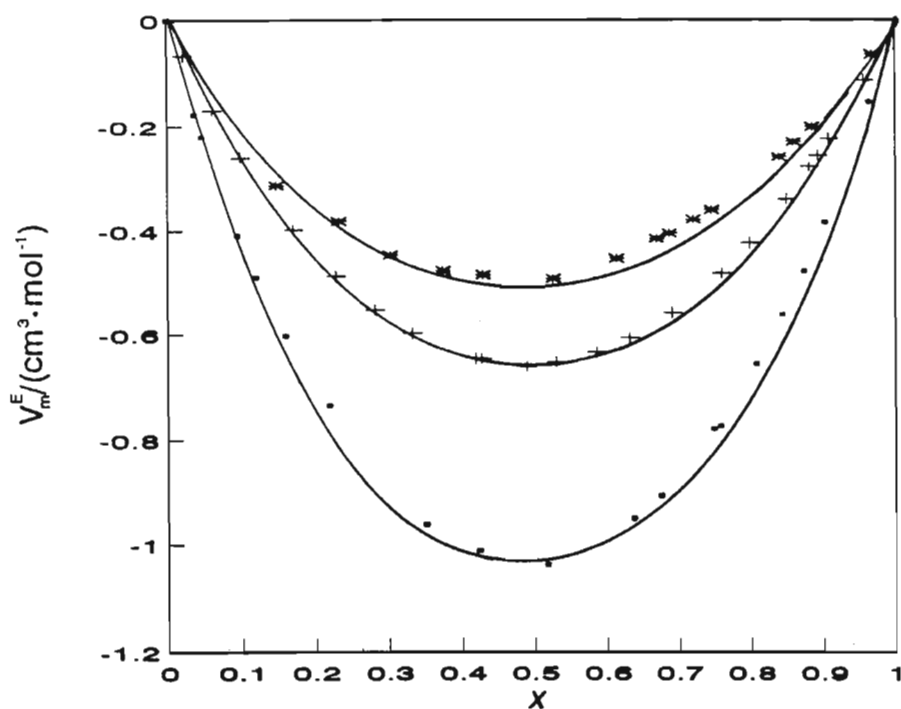
Figure 2.10 Excess molar volumes, V_m^E at 298.15 K for $\{x\ C_3H_7OH + (1-x)\ ROR'\}$ where ROR' is ■, IPE or +,
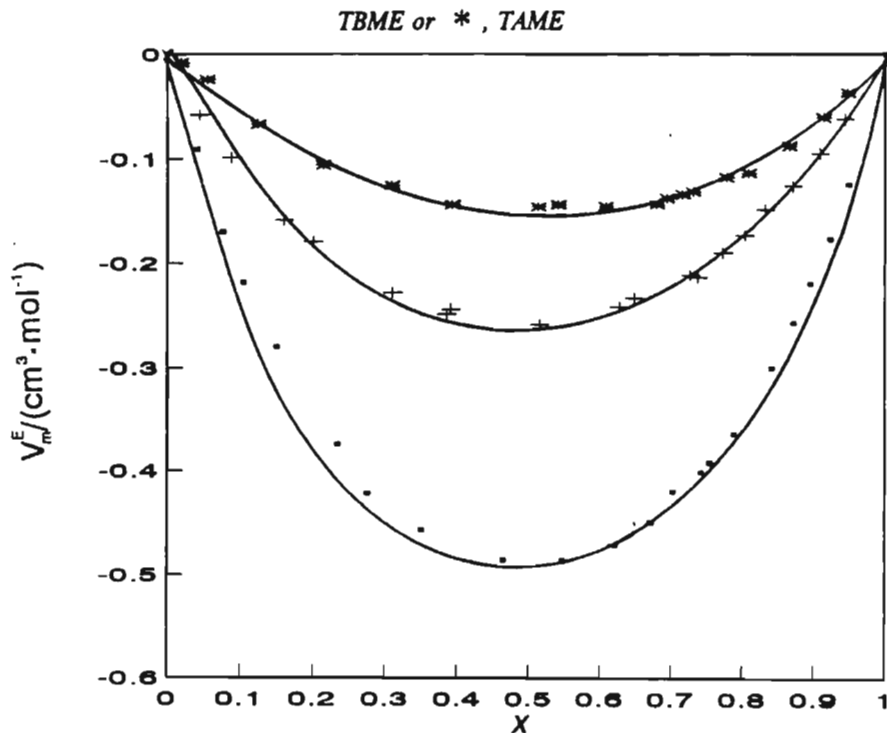
*TBME or * , TAME*

Figure 2.11 Excess molar volumes, V_m^E at 298.15 K for $\{x\ CH_3CH\ (OH)CH_3 + (1-x)\ ROR'\}$ where $ROR'$is ■, IPE

*or +, TBME or * , TAME*

(b) Mixtures of (an alkanol + a cyclic ether)

The excess molar volumes V_m^E at the temperature 298.15 K are listed in Table 2.3 with the parameters by equation 2.8 in Table 2.12 and the experimental data points are presented in figures 2.12 to 2.15 for each of the 12 mixtures over the entire mole fraction range. For the (methanol + a cyclic ether) systems all the V_m^E curves are negative and skewed towards the alkanol rich region at $x \equiv 0.6$. For the (ethanol + a cyclic ether) systems all of the V_m^E curves are sine shaped and show positive V_m^E at alkanol mole fraction less than 0.3 and negative V_m^E's at alkanol mole fraction greater than 0.6. The shapes of the V_m^E curves of the (propan-1-ol + THF or THP) systems are similar to those exhibited by the analogous ethanol systems. For the (propan-1-ol + 1,4-dioxane) and the (propan-2-ol + a cyclic ether) systems all of the V_m^E curves are positive. The large difference in the sign and shape of the volumetric behaviour of these systems can be explained in terms of the decrease in intermolecular association between the alkanol and the ether as the chain length of the alkanol increases.

It may be proposed that ring strain in the cyclic compounds is a dominant factor affecting the ability of proton donor molecules to form hydrogen bonds with these molecules. This effect seems to be enhanced in all of the systems containing 1,4-dioxane except the methanol mixture. The (methanol + 1,4-dioxane) systems exhibits the largest negative V_m^E values and is probably attributable to two factors (i) a more efficient packing of the methanol molecule in the six membered heterocyclic ring and (ii) greater interaction between the 1,4-dioxane with the methanol probably due to the presence of two ethereal oxygen atoms per 1,4-dioxane molecule. When changing from methanol to ethanol or propan-1-ol the packing and intermolecular interaction effects become dominant only in the alkanol rich region with dissociation effects taking prominence at alkanol mole fractions less than 0.4. The positive V_m^E suggest that the "structure breaking" effect of the components is dominant when the alkanol concentration is smaller than that of the cyclic ether. In the regions poor in the cyclic ether V_m^E become negative since the packing effect and intermolecular association become more significant. Values of the dipole moments[54,95] of THF and THP indicate that the O·····O

interactions within each molecule are stronger in THF than in THP.[96] Also the spatial configurations of the molecules of both these ethers imply an easier accommodation of the alkanol molecules of the mixtures with THP than in those of THF.[96] These deductions agree somewhat with the values found experimentally for all the alkanols presented here.

V_m^E's for the mixtures (propan-2-ol + THF or THP or 1,4-dioxane) are positive and is probably attributable to the shielding effect on the alkanol hydroxy group by the two adjacent methyl groups thus preventing any major association between the alkanol and the ether species. In interpreting V_m^E in terms of molecular phenomena, these positive values can be explained by the breaking of chemical and non-chemical interactions among the pure alkanol or ether molecules during the mixing process. This effect seems to be more pronounced for the (propan-2-ol + cyclic ether) mixtures than the corresponding (propan-2-ol + branched chain ether) systems.

As far as we know, the V_m^E results for the mixtures discussed here have not been reported in the literature except for (methanol or ethanol + 1,4-dioxane) and (methanol + THF) at temperatures ranging from 298.15 to 303.15 K. Nakanishi and Shirai[97] reported negative V_m^E at 298.15 K for (methanol + THF) of -0.15 cm^3·mol^{-1} while those reported here are -0.15 cm^3·mol^{-1} at equimolar concentrations. Singh et al.[98] have reported negative V_m^E at 303.15 K for (methanol + 1,4-dioxane) of -0.38 cm^3·mol^{-1} while those reported here at 298.15 K are -0.27 cm^3·mol^{-1} at equimolar concentrations. Ling and van Winkle[99] have reported negative V_m^E at 303.15 K for (ethanol + 1,4-dioxane) of -0.048 cm^3·mol^{-1} while those reported here at 298.15 K are -0.028 cm^3·mol^{-1} at equimolar concentrations.
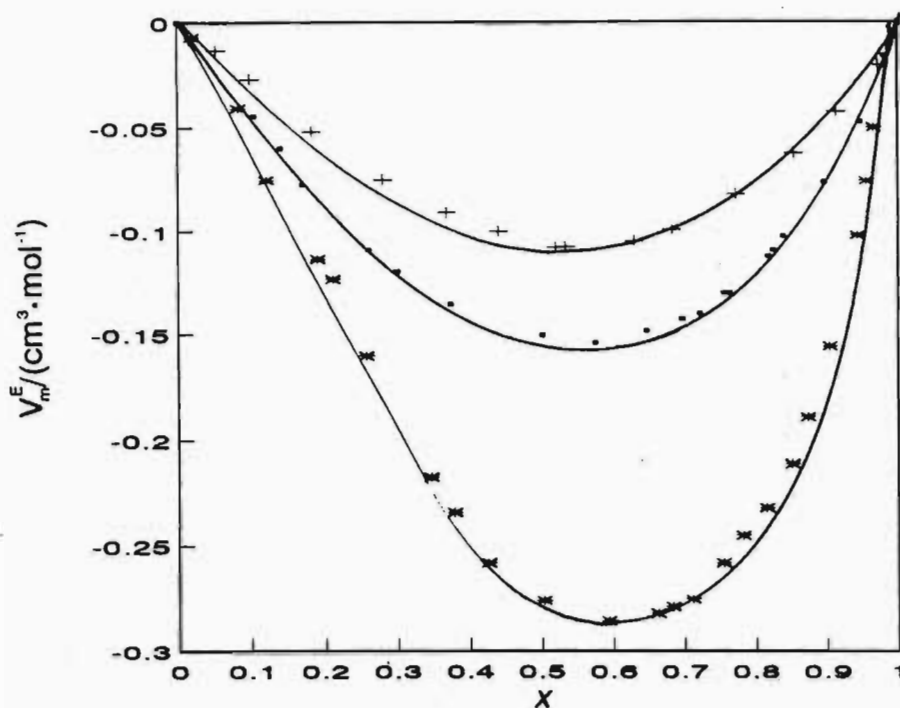
Figure 2.12 Excess molar volumes, V_m^E at 298.15 K for $\{x\ CH_3OH\ +\ (1-x)\ ROR'\}$ where ROR' is ■, THF or $+$,
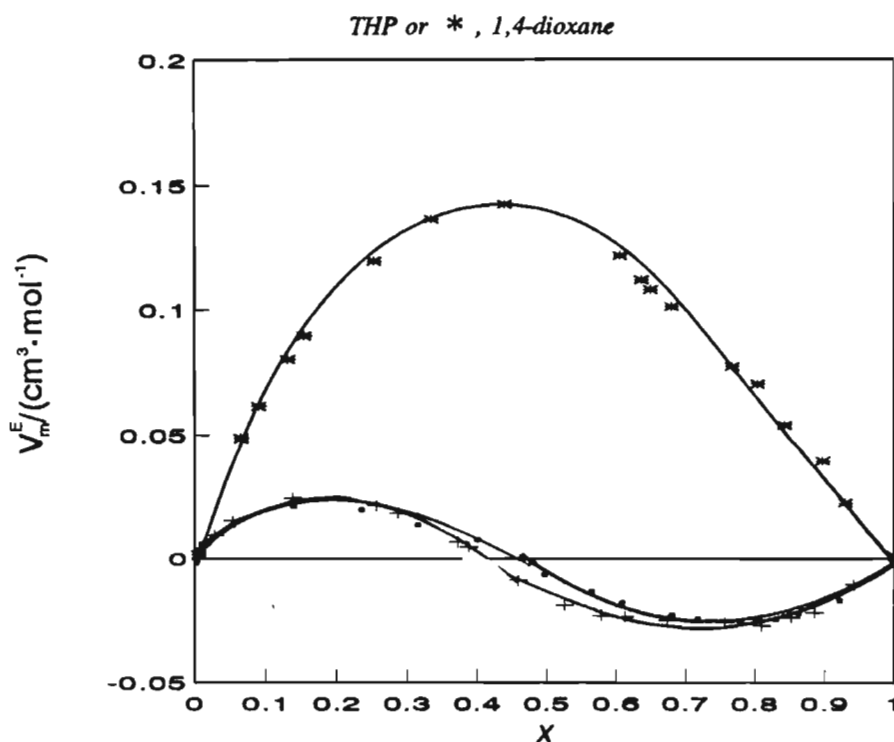
THP or $*$, 1,4-dioxane

Figure 2.13 Excess molar volumes, V_m^E at 298.15 K for $\{x\ C_2H_5OH\ +\ (1-x)\ ROR'\}$ where ROR/ is ■, THF or $+$,
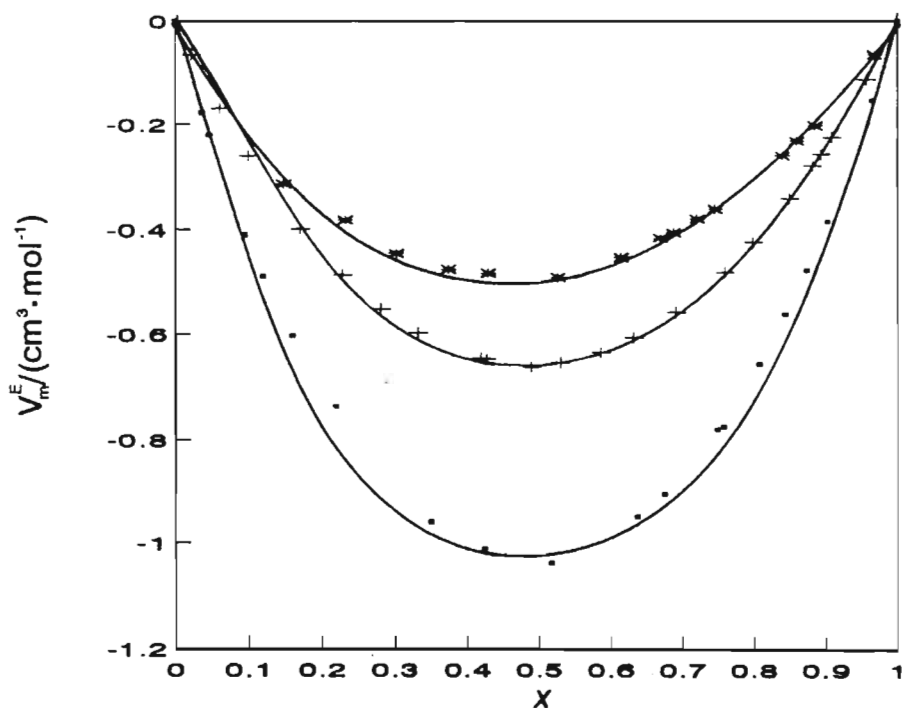
THP or $*$, 1,4-dioxane

Figure 2.14 Excess molar volumes, V_m^E at 298.15 K for $\{x\ C_3H_7OH\ +\ (1-x)\ ROR'\}$ where ROR' is ■, THF or $+$, THP or $*$, 1,4-dioxane
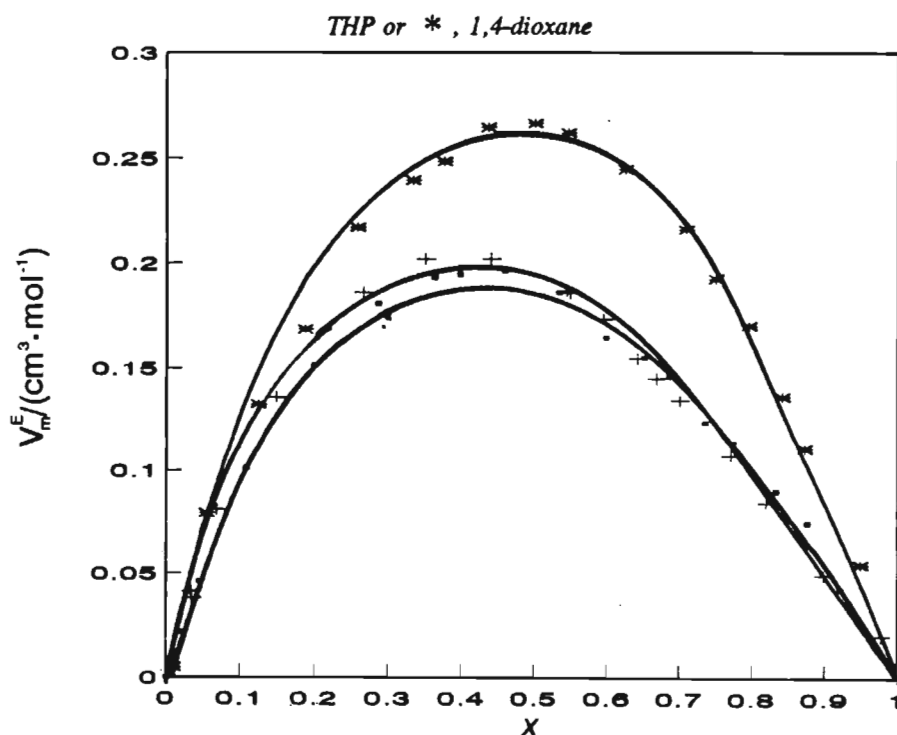
Figure 2.15 Excess molar volumes, V_m^E at 298.15 K for $\{x\ CH_3CH(OH)CH3\ +(1-x)\ ROR'\}$ where ROR' is ■, THF or $+$, THP or $*$, 1,4-dioxane

2.5.2 Mixtures of a (secondary amine + a branched chain ether or cyclic ether)

2.5.2.1 Previous work

The aliphatic amines like the alkanols are polar molecules associated in the pure state by hydrogen bonds though the extent of association is lower than that of the alkanols. The association of amines has been studied extensively by Wolff et al.[100-102], and Nagata et al.[103,104] and it has been proposed by both these research teams that a linear association is the prevailing type of association in amines. Cibulka et al.[105,106] in their work on the thermodynamics of associating components have suggested that the extent of self association in the secondary amines is less than that of the primary n-alkylamines but that this behaviour becomes insignificant in mixtures i.e. the role of the non-H bonded hydrogen atoms in -(NH)-H·····N associated chains in the pure primary amines is not a significant contributor to the observed behaviour of the related mixtures. Kehiaian[107] has established that in mixtures containing (a secondary aliphatic amine + n-alkane) specific -N-H·····N interaction is the main source of non-ideal behaviour and that the -N-H·····N interaction is relatively weak. Wolff et al[101] in their calculations have suggested that an increase in the chain length of the aliphatic chain of the secondary amine leads to decreased association between the molecules.

The V_m^E behaviour of the secondary amines in n-alkanes or cycloalkanes or aromatics has been extensively reported by Letcher[108] at 298.15 K. The V_m^E results for (diethylamine or di-n-propylamine + hexane or heptane) systems are positive over the whole mole fraction range and show fairly symmetrical V_m^E curves. The maximum value becomes more negative the larger the size of the amine molecule and this effect was attributed to the ability of the alkane molecules to fit better into the chain structure of the longer chain amines than into the less open structure of the shorter chain amines. Handa and Benson[109] have reported large negative volumetric behaviour of (diethylamine + an alkanol) at 298.15 K and Panayiotou[110] has recently suggested that in the (a dialkylamine + an alkanol) mixture homopolymer and copolymer association complex structures exist. The latter structure results

from the specific interaction between the hydroxyl group of the alkanols and the polarizable nitrogen atom of the amines.

Recently, V_m^E results have been reported at 298.15 K for (a primary, secondary and tertiary amine + a branched chain or cyclic ether) by Letcher et al.[111,112] In particular the V_m^E results for (di-n-butylamine + IPE or TBME or TAME or THP or THF or 1,4-dioxane) at 298.15 K have been reported by the present author[111] and the various trends observed for the di-n-butylamine systems have been compared to the results presented here. No other data could be found in the literature for comparison with the work presented here.

2.5.2.2 *This work*

(a) Mixtures of (diethylamine or di-n-propylamine + a branched chain ether)

The excess molar volumes V_m^E at the temperature 298.15 K are listed in Tables 2.4 and 2.6 with the parameters by equation 2.8 given in Table 2.13 and the experimental data points are presented in figures 2.16 and 2.17 for each of the amine mixtures over the entire mole fraction range. For the (diethylamine + IPE or TBME or TAME) systems all of the V_m^E curves are positive and slightly asymmetrical with the minima at x ≡ 0.45 and show increased values in the sequence IPE < TAME < TBME. In molecular terms this positive value can be interpreted as the dominance of breakdown of the self association in the amine and in the ethers. For the (di-n-propylamine + IPE or TBME) systems the V_m^E curves are small and negative while the (di-n-propylamine + TAME) are small and positive in the amine rich region and negative at the amine mole fractions less than 0.35. The magnitude of the V_m^E values of the (di-n-propylamine + TAME) are very small and never exceed $|0.028|$ cm^3·mol^{-1}. The values of V_m^E (x = 0.5) for (diethylamine or di-n-propylamine or di-n-butylamine + IPE or TBME or TAME) are listed in Table 2.15 and plotted in figure 2.18 as a function of the alkyl chain length of the secondary amine. For all the ethers the V_m^E (x = 0.5) decrease in the order diethylamine > di-n-propylamine > di-n-butylamine. These results seem to indicate that as the aliphatic chain length of the secondary amine increases, the packing and association effects

between the amine and the ether become the dominant feature.

TABLE 2.15 Equimolar V_m^E for (a secondary amine + a branched chain ether) at 298.15 K

	$V_m^E(x = 0.5)$		
	$(cm^3 \cdot mol^{-1})$		
Secondary amine	IPE	TBME	TAME
diethylamine	0.0379	0.1249	0.1032
di-n-propylamine	-0.0232	-0.0496	0.0048
di-n-butylamine	-0.3836	-0.1372	-0.0238
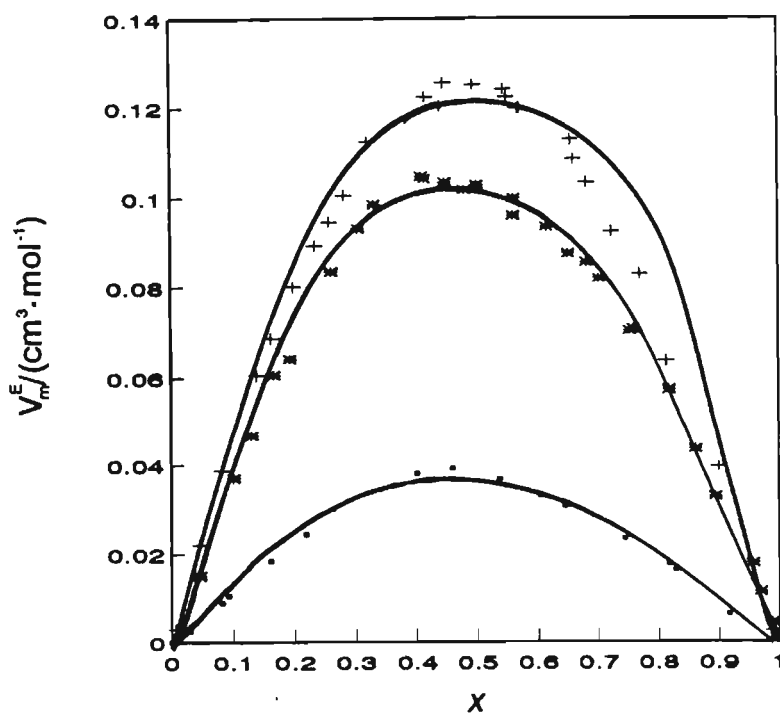
Figure 2.16 Excess molar volumes, V_m^E at 298.15 K for $\{x\ CH_3CH_2NHCH_2CH_3 + (1-x)\ ROR'\}$ where ROR' is ■, IPE or $+$, TBME or $*$, TAME
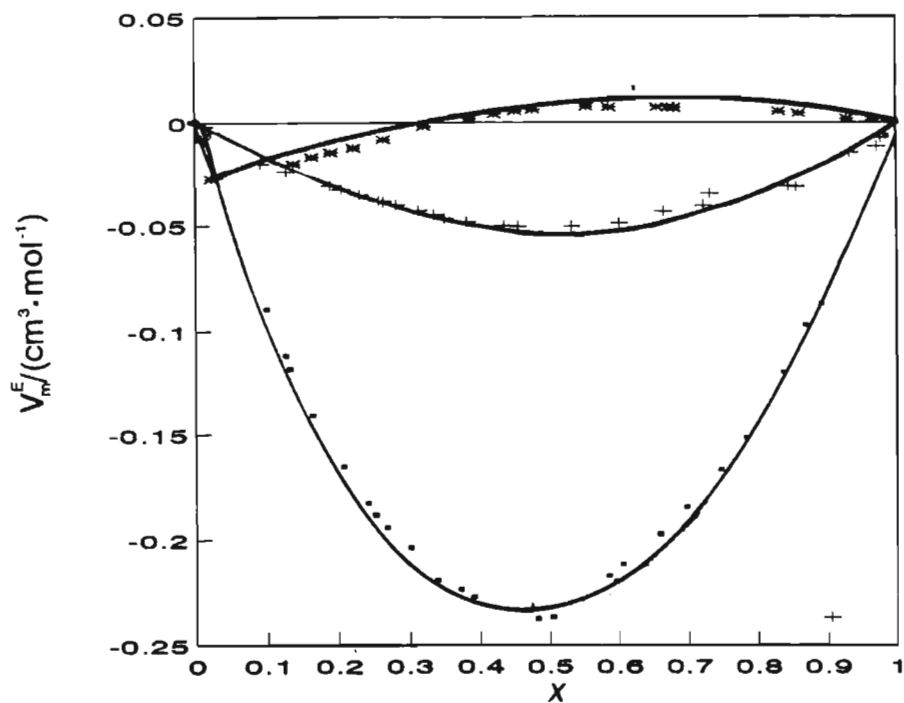
Figure 2.17 Excess molar volumes, V_m^E at 298.15 K for {x $CH_3(CH_2)_2NH(CH_2)_2CH_3$ +ROR'} where ROR' is ■*,*

IPE or +*, TBME or* * *, TAME*
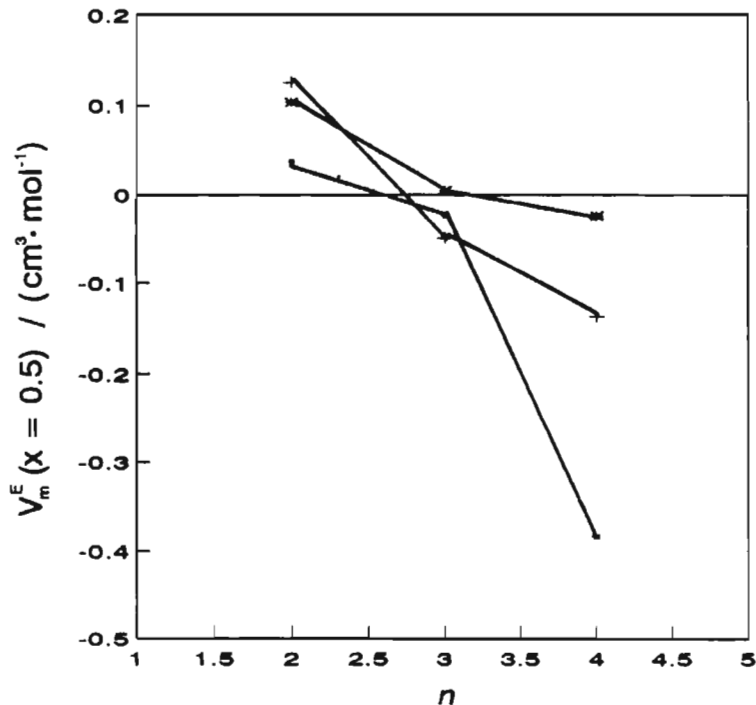
Figure 2.18 Excess molar volumes, V_m^E (x = 0.5) at 298.15 K for {x $C_nH_{(2n+1)}NHC_nH_{(2n+1)}$ + (1-x) ROR'} where n

= 2, 3 or 4 and ROR' is ■*, IPE or* +*, TBME or* * *, TAME*

(b) Mixtures of (diethylamine or di-n-propylamine + a cyclic ether)

The excess molar volumes V_m^E for {(diethylamine or di-n-propylamine) + (THF or THP or 1,4-dioxane)} at the temperature 298.15 K are listed in Tables 2.5 and 2.7 with the parameters by equation 2.8 given in Table 2.13 and the experimental data points are presented in figures 2.19 and 2.20 for each of the amine mixtures over the entire mole fraction range. For the (diethylamine + THF or 1,4-dioxane) systems the V_m^E curves are negative and skewed towards the amine rich region with the minima at $0.55 < x < 0.8$. This suggests greater association and efficient packing of the component species upon mixing. For the (diethylamine + THF) an s-shaped concentration dependence of V_m^E with a positive effect at amine mole fraction less than 0.1 is displayed. This small positive behaviour in the dilute amine region may be interpreted as the disruption of all the associated species in the amine component by the mixing process. At higher amine concentrations association effects between the amine and the ether play a major role in determining the volumetric behaviour of these systems.

The V_m^E curves for the (di-n-propylamine + THF or THP) systems are small and negative while the (di-n-propylamine + 1,4-dioxane) system is positive. The magnitude of $V_{m \ (max)}^E$ for the THP system is double that of the THF system i.e. -0.0542 and -0.0300 cm³·mol⁻¹, respectively. This can be explained by the more efficient packing of the amine molecule in the larger structured THP than THF and for the (di-n-propylamine + THP) system this effect seems to be enhanced at amine mole fractions greater than 0.6. The positive V_m^E behaviour of the di-n-propylamine + 1,4-dioxane system is probably a result of the breakdown of the self association due to the quadrupole moment of 1,4-dioxane.[54,113] This effect was also the dominant feature in determining V_m^E for the (di-n-butylamine + 1,4-dioxane) system.

A comparison of the values presented here with those of the analogous systems of di-n-butylamine are presented at V_m^E (x = 0.5) in Table 2.16 and plotted on figure 2.21 as a function of the alkyl chain length of the secondary amine. For all the (an amine + an ether) mixtures the V_m^E (x = 0.5) decreases (become more negative) in the order di-n-butylamine > di-n-propylamine > diethylamine. These results seem to indicate that as the aliphatic chain

length of the secondary amine increases, the packing effects and amine-cyclic ether interactions become relatively weaker. This implies that (a) the disruption of the self association of the amine and (b) the breaking of the ether-ether interactions, become important in the determination of V_m^E with an increase in the chain length of the alkyl moiety of the amine.

TABLE 2.16 Equimolar V_m^E for (a secondary amine + a cyclic ether) at 298.15 K

| | $V_m^E(x = 0.5)$ | | |
| | $(cm^3 \cdot mol^{-1})$ | | |
Secondary amine	THF	THP	1,4-dioxane
diethylamine	-0.0598	-0.0640	-0.0933
di-n-propylamine	-0.0287	-0.0464	0.1629
di-n-butylamine	0.0917	0.1295	0.4778
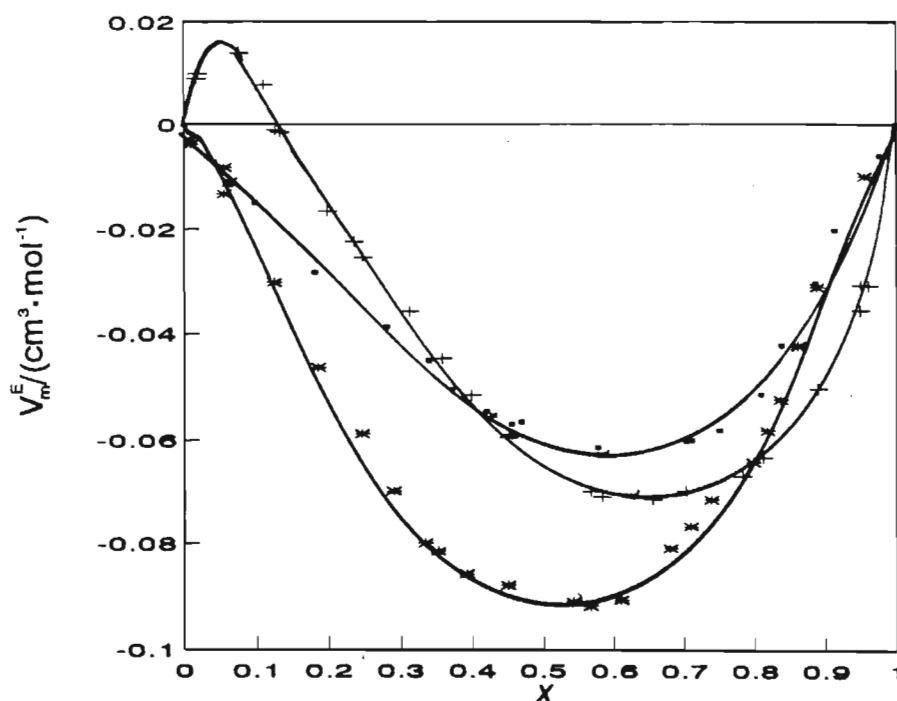
Figure 2.19 Excess molar volumes, V_m^E at 298.15 K for $\{x\ CH_3CH_2NHCH_2CH_3\ +(1-x)\ ROR'\}$ where ROR' is ■ ,

THF or ＋ , THP or ＊ , 1,4-dioxane
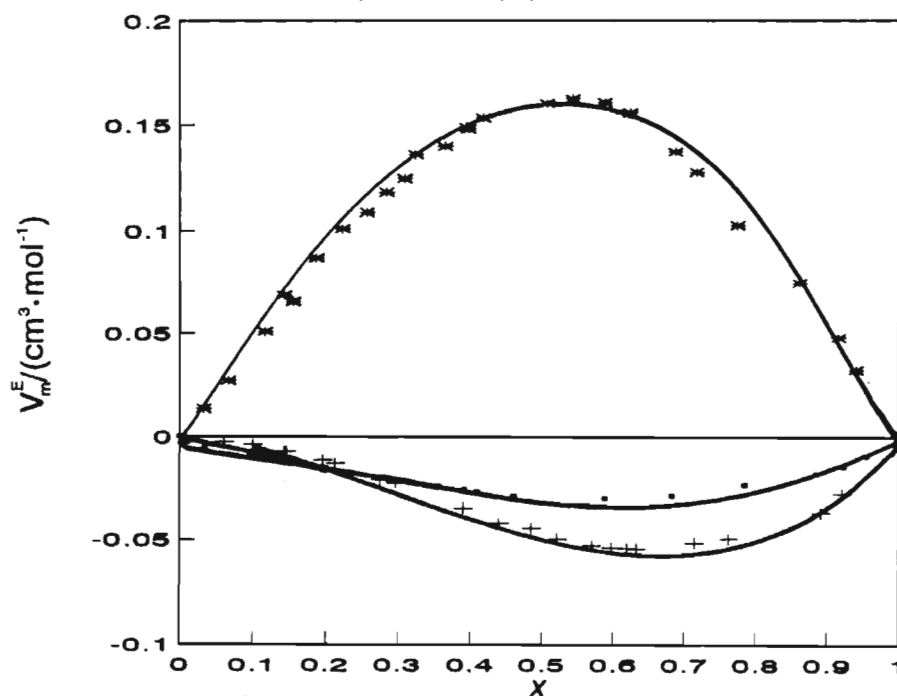
Figure 2.20 Excess molar volumes, V_m^E at 298.15 K for $\{x\ CH_3(CH_2)_2NH(CH_2)_2CH_3\ +\ (1-x)\ ROR'\}$ where ROR' is

■ , THF or ＋ , THP or ＊ , 1,4-dioxane
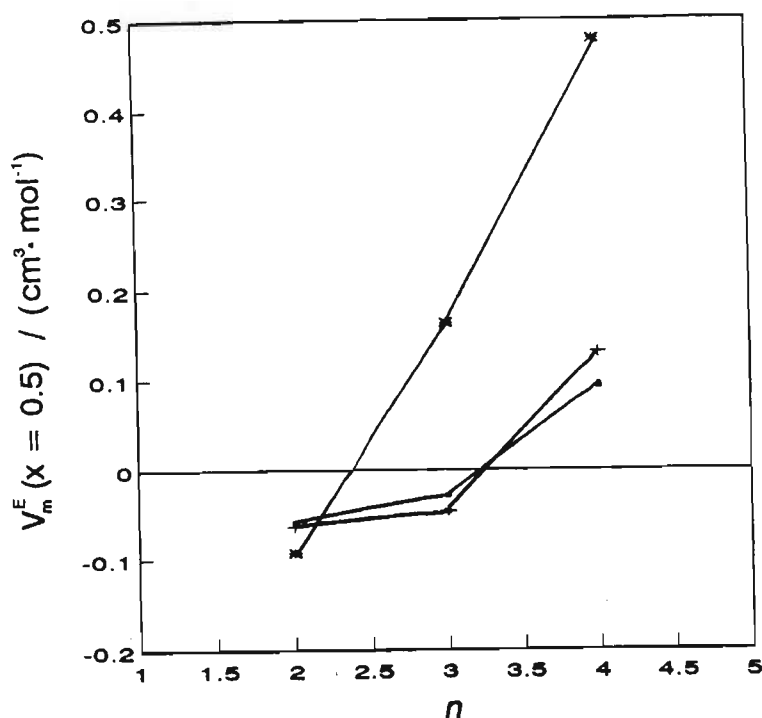
Figure 2.21 Excess molar volumes, V_m^E (x = 0.5) at 298.15 K for {x $C_nH_{(2n+1)}NHC_nH_{(2n+1)}$ + (1-x) ROR'} where n

*= 2, 3 or 4 and ROR' is ■, THF or +, THP or * , 1,4-dioxane*

2.5.3 Mixtures of a 1-alkyne + a branched chain ether

2.5.3.1 Previous work

It has been established that there exists specific interaction between 1-hexyne and di-n-dodecyl ether.[114,115] This interaction is probably due to   (a) the high electron density surrounding the triple bond of the alkyne ie., the nature of the triple bond itself and to (b) the acidic nature and hydrogen bonding tendency of the acetylenic hydrogen. Wilhelm et al.[116,117] presented thermodynamic data for binary liquid mixtures containing alkynes with heptane or cyclohexane or benzene or carbon tetrachloride or dipropyl ether or triethylamine. In their examination of mixtures containing alkynes with n-alkanes specific interaction with the acetylenic compound such as charge transfer complexes and hydrogen bonds[118] was not considered and the behaviour of the acidic hydrogen becomes discernable and responsible for

the overall thermodynamics of mixtures containing this component. Prausnitz and collaborators have studied the thermodynamics of several systems with hexyne and strongly polar solvents[119,120,121] and Desplances[122] have reported vapour liquid data of 1-hexyne or 1-heptyne with acetonitrile.

Woycicki and Rhensius[123] and Otsa et al.[124] have examined the thermodynamic behaviour of alkynes + n-alkane mixtures and have suggested relatively strong self association between the alkyne molecules. Letcher et al.[125-128] studied the V_m^E behaviour of {(1-hexyne or 1-heptyne or 1-octyne) + benzene and the methyl substituted derivatives} at 298.15 K. Their results have been discussed in terms of the association between the 1-alkyne and the aromatic compound due to $\pi \cdots \pi$ and $\pi \cdots H$ interactions. The V_m^E behaviour of {(1-hexyne or 1-heptyne or 1-octyne) + an alkanol} at 298.15 K has been studied by the Letcher et al. and the present author.[129,130] The V_m^E results ranged from positive to negative to sine shaped V_m^E curves and were interpreted as (i) positive effect due to the breakdown of the hydrogen bonds between the alkanol molecules on mixing (ii) the positive effect due to the breakdown of the $\pi \cdots \pi$ interactions between the 1-alkyne molecules and (iii) the negative effect of the association between the alkanol and the 1-alkyne molecules. In addition the packing effect due to specific interactions of the triple bonds of the 1-alkyne and the OH group of the alkanol leads to a small but significant enhancement to the V_m^E.

2.5.3.2 This work

The results of the volume change on mixing, V_m^E (1-alkyne + IPE or TBME or TAME) are presented in Tables 2.8 to 2.10 with the parameters for equation 2.8 given in Table 2.14. Figures 2.22 to 2.24 show the curves calculated from equation 2.14 and the experimental results for all the mixtures. The V_m^E curves for all the mixtures reported here are negative and symmetrical. The V_m^E results for (a 1-alkyne + IPE or TBME or TAME) seem to indicate a dependence on the carbon number of the 1-alkyne. For all the ethers the V_m^E at any particular mole fraction is more negative the greater the carbon number of the 1-alkyne. This could well be due to the fact that the addition of methylene groups to the 1-alkyne increases the electron density in the 1-alkyne and the acidity of the acetylenic hydrogen

resulting in enhanced $\pi \cdots O$ interactions. In addition, V_m^E for (a 1-alkyne + a branched chain ether) increase in the order IPE < TBME < TAME indicating that the degree of branching in the ethers diminishes the packing effect induced by specific interaction between the triple bond of the 1-alkyne and the O group of the ether. This is shown graphically in figure 2.25 where for each of the mixtures reported here, V_m^E (x=0.5) have been plotted against the carbon number of the 1-alkyne. All of the results presented here are significantly more negative than the V_m^E for n-alkane + IPE or TBME or TAME.[83,131-134] This indicates the dominance of the possibility of formation of a new chemical species in solution by specific interaction i.e., $\pi \cdots O$ interaction over any dissociation effects due to hydrogen bonding and $\pi \cdots \pi$ interactions in the 1-alkynes and dissociation of interactions between the ethers.

Comparing these V_m^E results with the (a 1-alkyne + an alkanol)[129,130] results at x = 0.5 given in Table 2.17 and figure 2.25, indicates that the association effects predominate in the (a 1-alkyne + an ether) mixtures while the volumetric behaviour of the (a 1-alkyne + an alkanol) is largely determined by the breakdown of the strong hydrogen bonds between the alkanol molecule. These results are also more negative than those reported for the (a 1-alkyne + benzene or 1,3,5 trimethylbenzene) mixtures again indicating more efficient packing of the component species in the mixture than in the pure state and greater association between the component molecules.

TABLE 2.17 Equimolar V_m^E for (1-alkyne + a branched chain ether) and (1-alkyne + an alkanol) at 298.15 K

1-alkyne	$V_m^E(x = 0.5)$		
	$(cm^3 \cdot mol^{-1})$		
	IPE	TBME	TAME
1-hexyne	-0.377	-0.332	-0.275
1-heptyne	-0.458	-0.370	-0.256
1-octyne	-0.525	-0.394	-0.270
	methanol	ethanol	propan-1-ol
1-hexyne	-0.131	-0.095	-0.085
1-heptyne	-0.029	-0.014	0.008
1-octyne	0.028	0.048	0.049
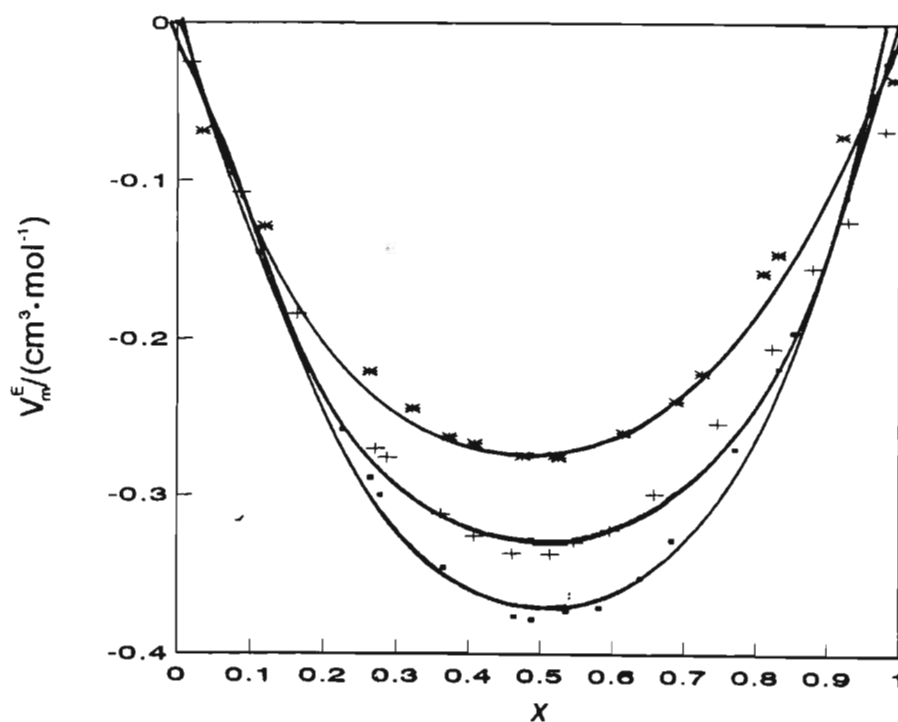
Figure 2.22 Excess molar volumes, V_m^E at 298.15 K for $\{x\ 1\text{-}C_6H_{10} + (1\text{-}x)\ ROR'\}$ where ROR' is ■, IPE or $+$, TBME or $*$, TAME
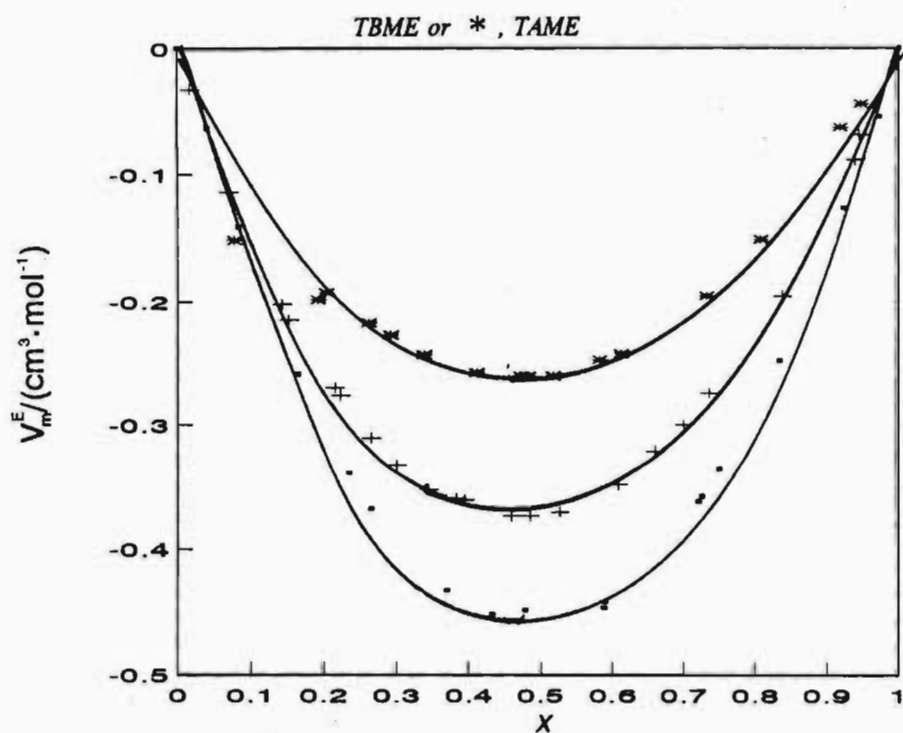
Figure 2.23 Excess molar volumes, V_m^E at 298.15 K for $\{x\ 1\text{-}C_7H_{12} + (1\text{-}x)\ ROR'\}$ where ROR' is ■, IPE or $+$, TBME or $*$, TAME
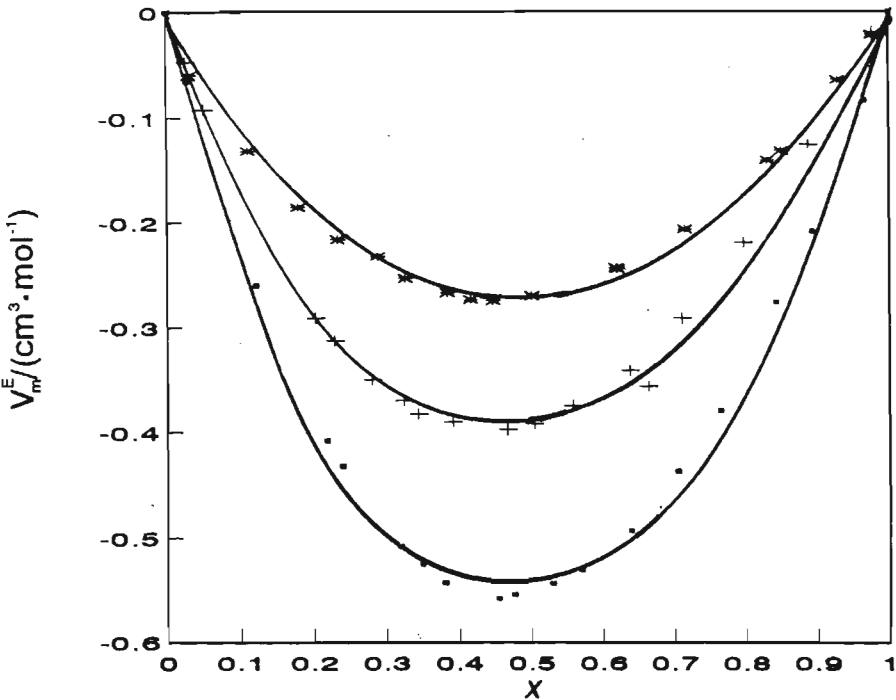
Figure 2.24 Excess molar volumes, V_m^E at 298.15 K for {x 1-C$_8$H$_{14}$ + (1-x) ROR'} where ROR' is ■, IPE or +,

TBME or ✳ , TAME
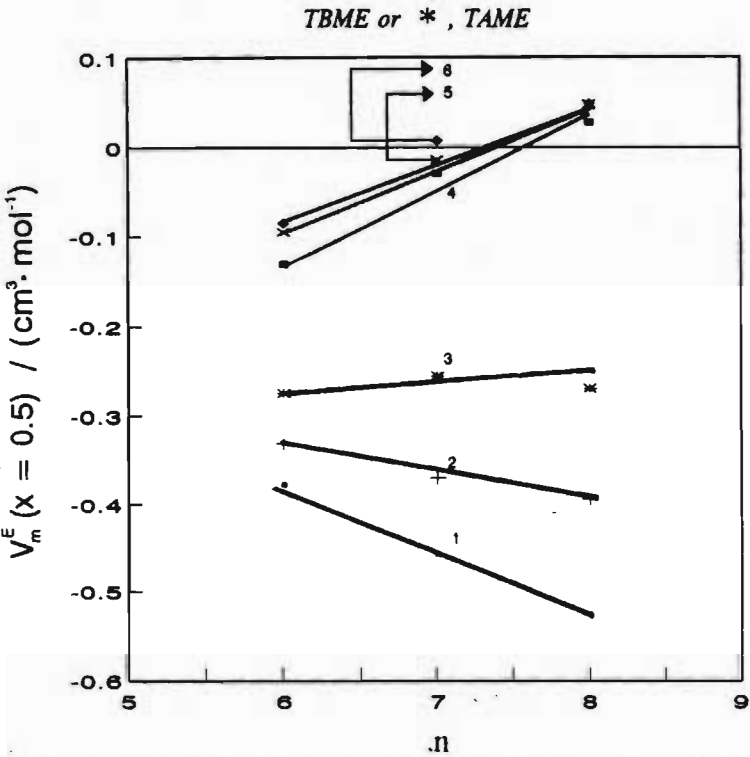
Figure 2.25 Excess molar volumes, V_m^E (x = 0.5) at 298.15 K for {x 1-C$_n$H$_{(n-2)}$ +(1-x) 1, IPE or 2, TBME or 3,

TAME or 4, methanol or 5, ethanol or 6, propan-1-ol} for n = 6 or 7 or 8

<div align="right">

Chapter Three

The Excess Molar Enthalpies of Mixing

</div>

3.1 Introduction

Chemical and physical reactions have a net heat evolution which gives basic information on the mechanism and extent of reaction, a process which often only calorimetry can detect and measure.[136] For binary liquid mixtures, the excess molar enthalpies of mixing, H_m^E, may in principle,[137] be defined by the relation

$$H_m^E = G_m^E - T \, (\partial G_m^E / \partial T)_p \tag{3.1}$$

However, the determination of H_m^E, from G_m^E and the temperature dependance is not considered a satisfactorily accurate method. It has been reported that the errors in H_m^E derived in this way are at least 15 times as large as the error in the free energies from which it is derived.[138] For this reason the most precise values of H_m^E are those measured directly by means of a calorimeter.

In principle, the direct measurement of heats of mixing is quite simple. The basic design involves a cell in which the two liquids are initially separated.[138] All that is required

is an apparatus in which known quantities of two liquids can be brought to a constant temperature, a thermometer to measure the temperature change when the two liquids are mixed and an electrical heater in which measured amounts of energy can be dissipated in order to calibrate the apparatus.[138-140] One of the earliest elementary and simple apparatus in which approximate measurements of heats of mixing were made is shown in figure 3.1.[138] Measured quantities of two liquids are placed in the vessels A and B in a thermostat bath. Mixing is brought about by forcing the liquid from A over into B and the temperature change on mixing is measured by the thermometer C. The heat capacity of the apparatus is determined for each experiment by passing a measured current through the heater D of known resistance for a measured time. The heat of mixing is then given by the relation

$$H_m^E = \Delta T_1 / \Delta T_2 \ (I^2 Rt) \tag{3.2}$$

where ΔT_1 is the temperature change on mixing, ΔT_2 is the temperature rise on calibration, R is the resistance of the heater, I is the current of the heater, and t is the time for which the current flows.[138]

Two isothermal calorimeters were used in this work. One is a commercial LKB 2107-107 flow microcalorimeter and the other is the more recent Thermometric 2277 Thermal Activity Monitor. The excess molar enthalpies, H_m^E, were determined over the whole composition range at 298.15 K for binary mixtures of a short chain alkanol (methanol, ethanol, 1-propanol, 2-propanol) or a symmetrical secondary amine (diethylamine, di-n-propylamine) or a 1-alkyne (1-hexyne, 1-heptyne, 1-octyne) with a branched chain ether (diisopropyl ether {IPE}, 1,1-dimethylethyl methyl ether{TBME}, 1,1-dimethylpropyl methyl ether{TAME})

and/or a cyclic ether (tetrahydrofuran {THF}, tetrahydropyran {THP}, 1,4-dioxane). The H_m^E

data presented here were used to test the applicability of the modified UNIFAC theory to

binary systems containing component molecules differing greatly in size, shape and chemical

behaviour. The H_m^E together with the V_m^E from Chapter 2 data has been treated in terms of the

Extended Real Associated Solution (ERAS) model. The theoretical results are reported in

Chapter 6.
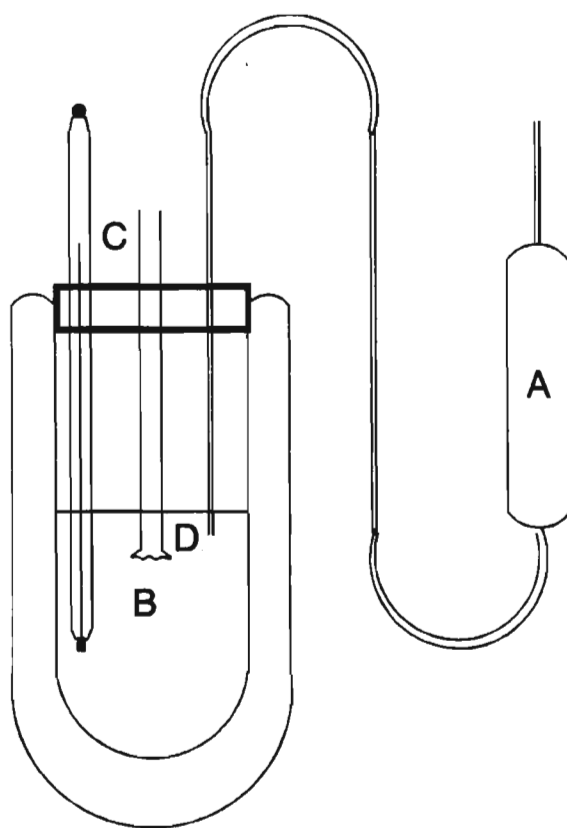
Figure 3.1 Simple apparatus for measurements of heats of mixing[138]

3.2   Calorimetric Measuring Techniques

The enthalpies of mixing are measured in calorimeters of which many types have been described.[141-143]   The most commonly used methods in calorimetry are the adiabatic and isothermal methods.   In the adiabatic experiments, the two liquids are mixed in an isolated vessel (i.e.   vacuum jacket) which is thermally insulated from its surroundings.[143]   If the excess enthalpy ,H_m^E is positive, there will be a lowering of the temperature on mixing.   This drop in temperature may be nullified by the simultaneous supply of heat.   Such a process is considered nearly isothermal and any small difference can be corrected for by observing the temperature change for a calculated supply of electrical energy.[144]   If H_m^E is negative, then the mixture warms on mixing.   Such exothermic mixing requires two experiments - one to measure the temperature rise on mixing and the other to measure the amount of electrical energy needed to produce such a rise.[144]

One of the most important points in the design of any calorimeter designed to measure heats of mixing, is the elimination of vapour space.   If the calorimeter has a vapour space[138] there will be evaporation and/or condensation of small quantities of the volatile liquids upon mixing.[25,138,143]   When the heat of mixing is small, evaporation or condensation of as little as 10^{-2} to 10^{-3} mole of liquid can produce a heat effect as large or larger than that of the heats of mixing.[145]   McGlashan[141] has reported that vapour spaces of up to 0.25 cm³ could lead to an error in H_m^E of ± 100 J·mol⁻¹.   For this reason much effort has gone into designing mixing vessels in which vapour spaces are completely eliminated.   Accounts can be found in the literature[145-151] of all kinds of mixing vessel for calorimeters.   Hirobe's mixing vessel[143] developed in 1914 was arguably the first mixing vessel which attempted to keep vapour spaces

as small as possible. Hirobe's mixing vessel is shown in figure 3.2. The liquids are initially separated by mercury, and in contact with vapour spaces which were kept at a minimum. Mixing comes about by inversion of the vessel by means of the threads, A shown in the figure.
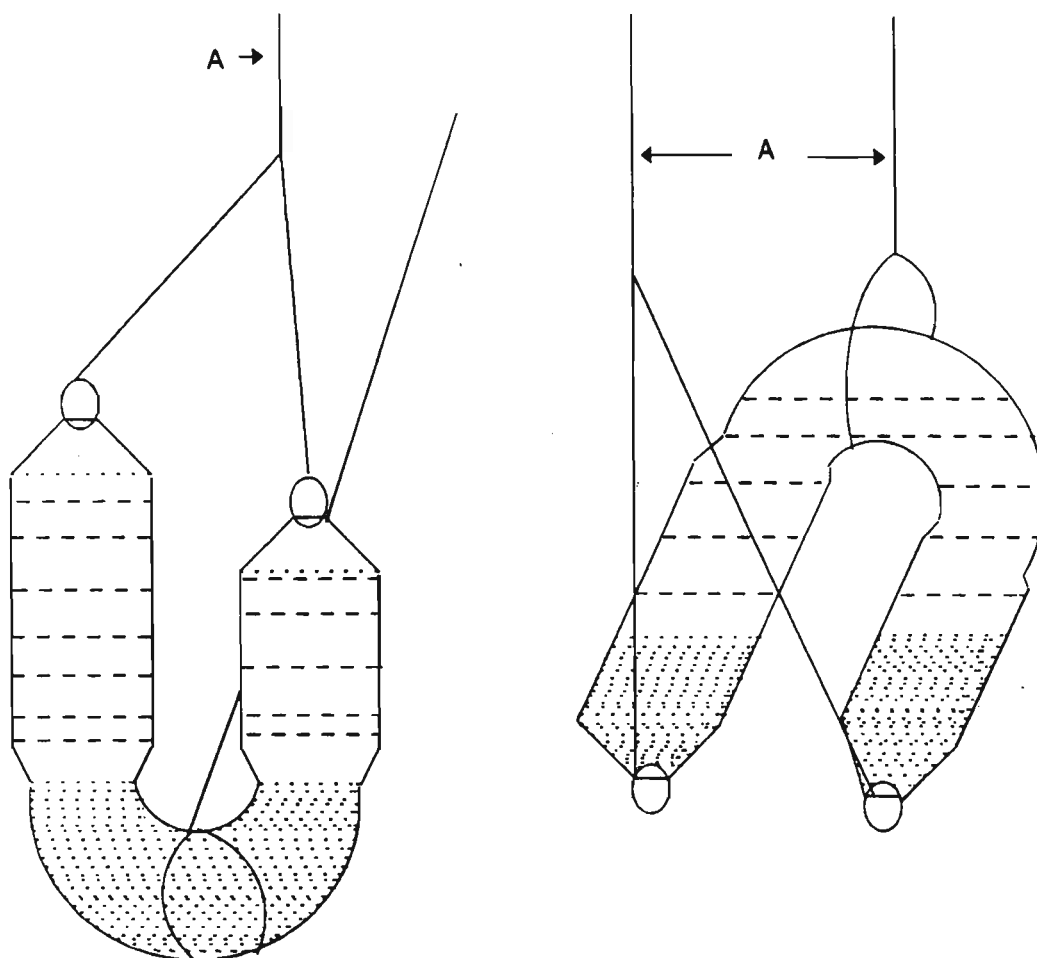
Figure 3.2 Hirobe's mixing vessel[143]

Modified designs but with more attention focused on the reduction of the effects of vapour spaces have been developed by later workers.[152,153] One of the major advancements in the development of mixing vessels was the one introduced by van der Waals in 1950[154] for heats of mixing measurements and is shown in figure 3.3. It was made of brass and the liquids were introduced into compartments A and B and isolated by means of a ground-in stopper K. The lid was screwed on against the packing L. Mixing was brought about by manipulation of nylon threads from outside the calorimeter which served to invert the vessel and displace K.

Figure 3.3 Van der Waals's mixing vessel[154]

The mixing vessel of McGlashan and Larkin[155], developed in 1961, is shown in figure 3.4. This was one of the first calorimeters suitable for the measurement of enthalpy changes as it eradicated the errors due to the presence of vapour space. It did not, unfortunately,

allow for volume changes that occurred on mixing.[138,155]   The vessel consists of two

compartments A and B in its upper half, and a capillary C with bulb D which is attached to

the vessel through the ground glass joint E and F. A heating element, H, and four thermistors

(T_1 to T_4) distributed over the surface of the mixing vessel form   part of the Wheatstone bridge

assembly. The vessel is completely filled with and immersed in a bowl of mercury. The

mercury is displaced from the upper compartments by introducing weighed quantities of the

mixture through opening A by means of a hypodermic syringe. The loaded vessel with the

capillary tube, C, half filled with mercury and attached at the ground joint, F is placed in an

evacuated enclosure within a thermostat until temperature equilibration is achieved. After

temperature equilibration, the liquids are mixed in the absence of a vapour space by rotation

of the apparatus through 180^c, the direction of rotation being such that the liquid never comes

into contact with the greased joints. The temperature change on mixing is measured by the

four thermistors.[155] The accuracy of the apparatus has been quoted at 0.7 $J.mol^{-1}$ at

$H^E_{m(max)}$.[137,155] One of the major disadvantages of this technique and the subsequent designs is

that it takes a long time to get a single measurement and the method cannot be readily

automated.
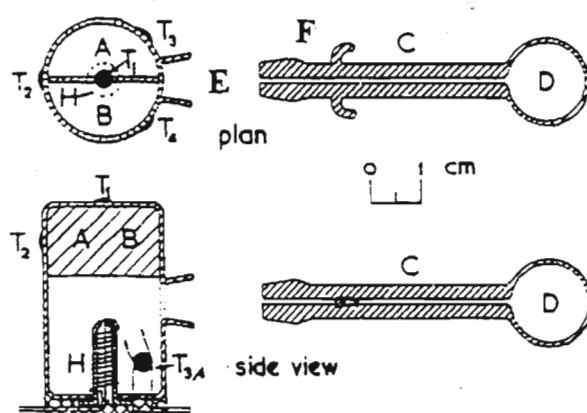
Figure 3.4 Adiabatic calorimeter of McGlashan and Larkin[155]

For the most precise measurements, in which enthalpies of mixing are determined with an accuracy of approximately 0.1 J.mol^{-1}, flow microcalorimetry was developed.[156,157] Basically, in flow microcalorimetry, two liquids are injected at a steady known rate into a mixing vessel, where complete mixing is achieved in the absence of a vapour space.[138] The measured excess enthalpy is related to the power output of the heating element and the molar flow rates of the two components[137] (refer to experimental section 3.3 for details). The major advantage flow microcalorimetry has over other techniques, is that (i) it produces rapid, sensitive results, (ii) that both endothermic and exothermic mixing reactions can be studied, and (iii) that only small quantities (often less than 50 cm^3 of each liquid) are needed for each set of experimental measurements.[25] A flow microcalorimeter can be modified to be either adiabatic or isothermal.[158,159] The adiabatic condition is achieved when the flow cell and the temperature sensitive elements are thermally insulated from their surroundings. In the isothermal mode, the heat of mixing in the reaction vessel is transferred to the heat sink.[158]

An excellent review of the history of flow microcalorimetry as well as the description and working principles of flow microcalorimeters (both isothermal and adiabatic) is given by Monk and Wadsö.[159] Amongst the earliest of these designs was that of McGlashan and Stoeckli.[160] It was reported that this type of instrument gave an error in H$_m^E$ of about 1%.[160] One major drawback in this instrument was that it required a large sample volume to cover the whole composition range. Furthermore, heat leaks inherent in the design of the instrument were not compensated for in the final calculation.[159,160]

A twin conduction calorimeter designed in the laboratory of Monk and Wadsö[159] and later commercialised by the LKB company (recently taken over by Thermometric) served to eradicate some of the uncertainties produced by the McGlashan[160] type calorimeter. Basically,

the apparatus consists of a metal block heat sink containing a centrally located heat exchanger unit, surrounded by calorimetric units in a twin arrangement. The calorimetric units comprise two flow reaction cells surrounded by surface thermopiles in contact with primary heat sinks. The heat sinks are thermally isolated and immersed in a water bath. Heat evolved or absorbed during the mixing process, is thus conducted to or from a heat sink arrangement through the semi-conductor thermopiles. Peristaltic and or piston pumps were used to introduce the liquids into the mixing cell.[159]

Work done by Hsu and Clever[161] on the instrument developed by Monk and Wadsö[159] showed that possible errors could arise from the variation of flow rate required to cover the complete mole fraction composition range. An error of about 20 J.mol^{-1} in H_m^E [161]was reported using the recommended IUPAC[162] test system (i.e cyclohexane + n-hexane). This error was not accounted for in H_m^E determinations. This error becomes more substantial and serious in the dilute mole fraction range where H_m^E is small and the sample liquid flow rates are near their limits.[161]

Further designs of flow microcalorimeters include that of Randzio and Tomaszkiewicz[163], Siddiqi and Lucas[164] and Christensen et al. [146,147]). In all of these designs frictional effects were simply neglected and these friction heating effects have been shown to produce substantial error if not carefully accounted and corrected for.[165,170]

Raal and Webley[165], recently designed a new differential microflow calorimeter. The following points were incorporated into the microcalorimeter design (in addition to the absence

of vapour space and careful composition control):

(a)   Carefully designed equilibrators preceding the mixing cell facilitating component liquids at the exact calorimeter temperature at all flow rates

(b)   accurate separation of frictional energy from the desired excess enthalpy and

(c)   the elimination of heat leaks dependent on fluid flow rates and physical properties.

Accommodating all the above points, the new differential microflow calorimeter is capable of producing H_m^E with an accuracy of 0.53 J.mol^{-1}. Raal and Webley[165] have reported results for the (cyclohexane + n-hexane) binary liquid system (the IUPAC recommended test system)[162] which are in excellent agreement with the data of Marsh and Stokes[166] and reportedly superior in precision and accuracy to those of Grolier[167] (Picker type calorimeter), and McGlashan and Stoeckli.[160]

Developments[168,163] by workers such as Randzio[163] and his research team are on instruments capable of measuring H_m^E at high temperatures and pressures as well as on instruments designed to cope with very viscous systems.

3.3   Experimental

3.3.1   Materials

A summary of the materials used in this work together with the suppliers, purity and methods of purification are given in section 2.3.1 of chapter 2.

3.3.2 Apparatus Details

The H_m^E results for the binary liquid mixtures reported in this work were determined using the LKB 2107-101 and Thermometric 2277 Thermal Activity flow-mix microcalorimeter.

3.3.2.1 The LKB 2107-101 flow-mix microcalorimeter

(i) Principle of operation

The isothermal flow-mix measuring cylinder for the LKB calorimeter used in this work is shown diagrammatically in figure 3.5. The mixing vessel, A, has two separate inlets and is comprised of a bifilar spiral-wound 24 carat gold tube of 1 mm i.d. with a volume of 0.5 cm³. The design is such that adequate mixing is achieved with no vapour space. The mixing vessel is in thermal contact with a pair of matched thermocouples in the thermopiles, B, and an aluminium heat-sink assembly, C, and with heat sink compound covering all the surfaces of these items. An exothermic reaction results in heat flow to the heat sink assembly, while the opposite effect is observed for endothermic reactions. In each case the resultant temperature difference is detected by the thermopiles positioned between the vessel and the heat sink. The output from the thermopiles is amplified and fed to a digital readout system and a Perkin-Elmer 561 chart recorder.

The aluminium block heat sink assembly is contained within an insulated housing. A heater and a temperature sensor are mounted within the main heat sink. The entire arrangement is contained within an LKB thermostat which comprises a thermostatically controlled air bath. To maintain the temperature required for this investigation, water cooled

to 287 K by a Labcon Thermostat unit was pumped through at a rate of 500 cm^3·min^{-1}. The LKB was used in conjunction with an LKB control unit. This incorporates a power supply capable of providing an adjustable current to the calibration heaters contained within the insulated mixing vessel assembly, and a facility for heating and monitoring the temperature of the calorimeter heat sink assembly. This heating facility helps to reduce the equilibration time of the apparatus during "startup" or when raising the operating temperature and was always switched off when measurements with the instrument were made.

Since liquids entering the microcalorimeter are required to be within 0.05 K of the experimental temperature, they were first routed through an external heat exchanger fitted into a recess in the bottom of the air bath of the thermostat unit and then through the internal heat exchangers, D, situated inside the insulated housing containing the mixing vessel assembly. Samples were introduced using two Jubilee peristaltic pumps, capable of stable flow rates ranging from 0.03 - 2.0 cm^3·min^{-1}. Viton tubing, 1.5 mm i.d. and teflon tubing, 1.2 mm i.d. were used in the pumps and flow lines respectively. The temperature inside the microcalorimeter was monitored by a Hewlett Packard 2804A quartz thermometer and was found to be constant to within 2 x 10^{-4} K.
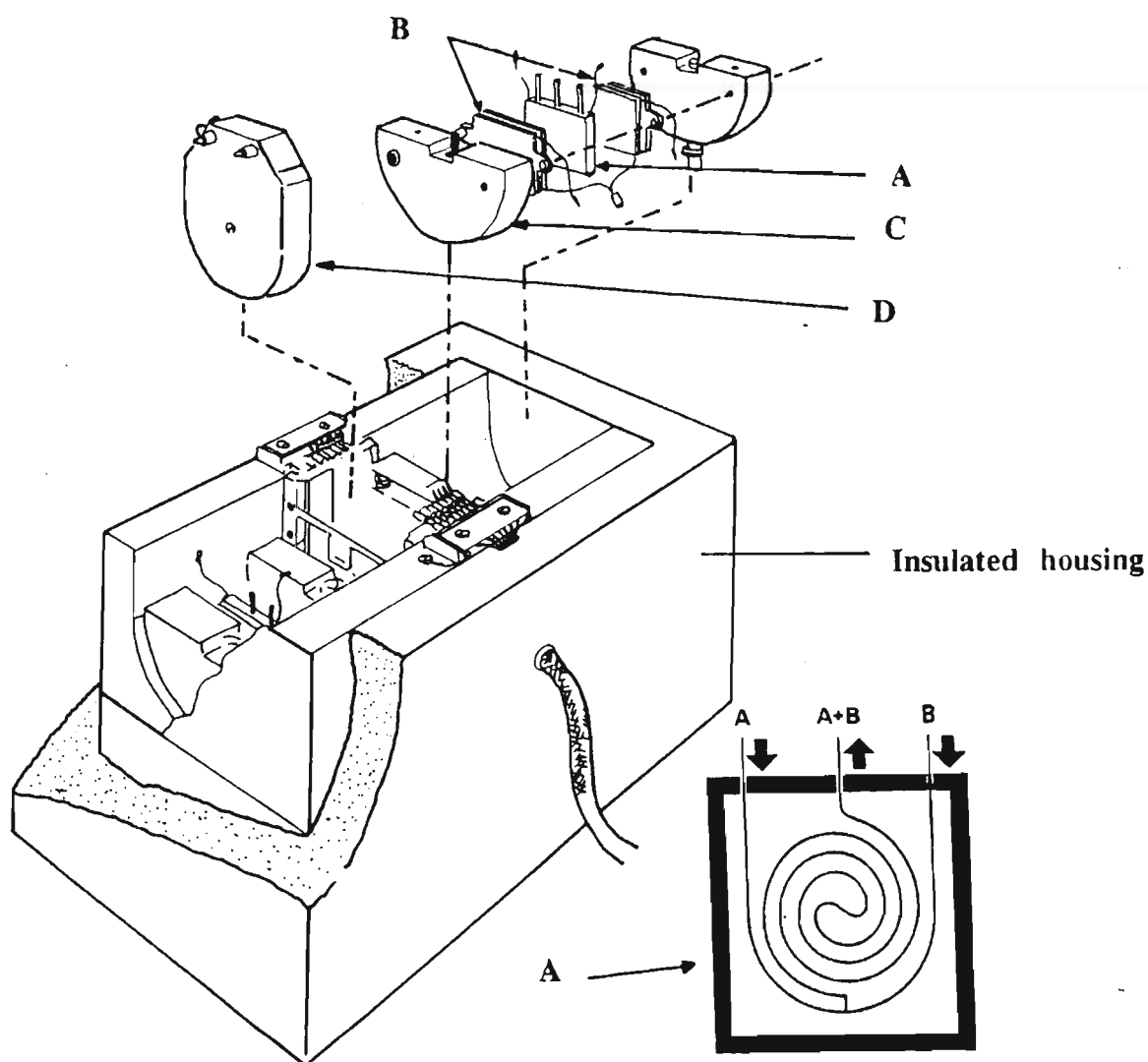
Figure 3.5 Representation of the LKB microcalorimeter and the exploded view of the flow cell taken from LKB manual

3.3.2.2 The 2277 Thermal Activity Monitor (TAM)

(i) Principle of operation

The 2277 Thermal Activity Monitor equipped with an external thermostatic water circulator (Thermometric 2219 Multi-temp II) and a pair of Eldex variable speed piston pumps capable of stable flow rates ranging from 0.05 to 3 $cm^3 \cdot min^{-1}$ was used in conjunction with the LKB microcalorimeter for the (secondary amine + ether) work. The Viton tubing necessary for the operation of the peristaltic pumps was not suitable as it was not sufficiently resistant to some of the solvents, particularly THF and the secondary amine. In addition the LKB microcalorimeter was considered not sufficiently accurate for precise excess enthalpy determinations in the $|1 - 50$ $J \cdot mol^{-1}|$ (microwatt power) range.

The Thermal Activity Monitor (TAM), utilises the heat flow or heat leakage principle where heat produced in a thermally defined vessel flows away in an effort to establish thermal equilibrium with its surroundings (figure 3.6(a)). The calorimetric mixing device used in the TAM (figure 3.6(b)), has a 24 carat gold flow-mix cell, A, where two different liquids can be mixed. The flow mix cell has a small bore T-piece at the base of the measuring cup where the two incoming flows are mixed. After mixing, the reaction takes place as the mixed flow passes up the spiral, B, around the measuring cup and out to waste.

The measuring cup is sandwiched between a pair of Peltier thermopile heat sensors. These sensors are in contact with a metal heat sink. The system is designed so that the main path for the flow of heat to or from the measuring cup is through the Peltier elements. The Peltier elements act as thermoelectric generators capable of responding to temperature gradients of less than one millionth of a degree kelvin. These highly sensitive detectors convert the
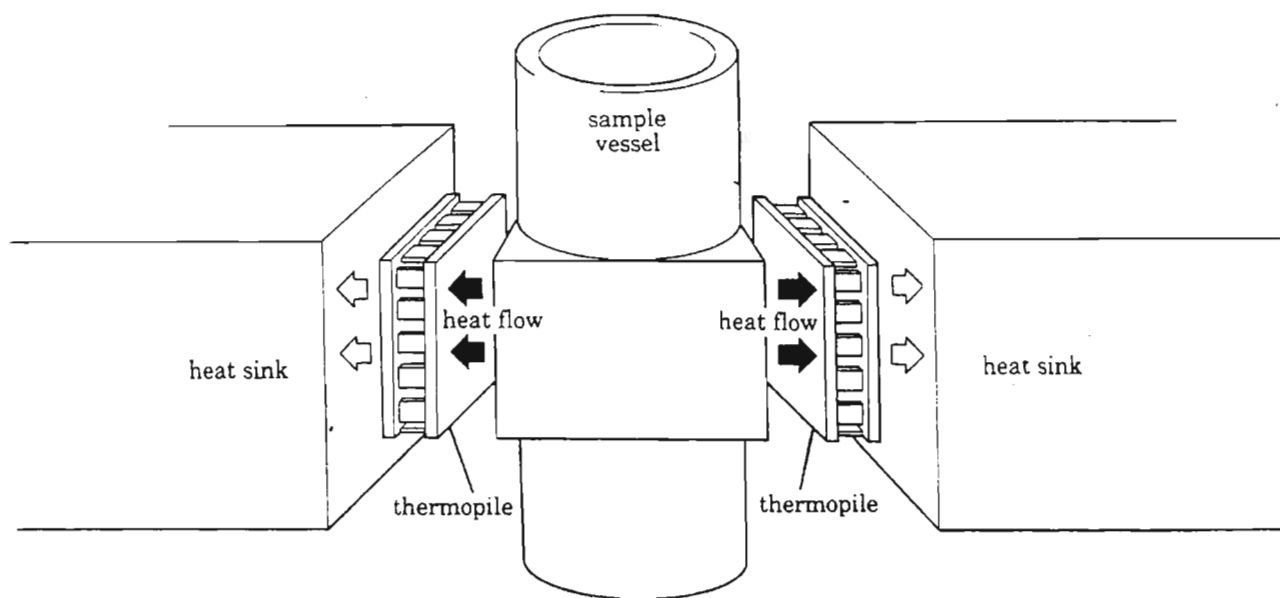
(a)
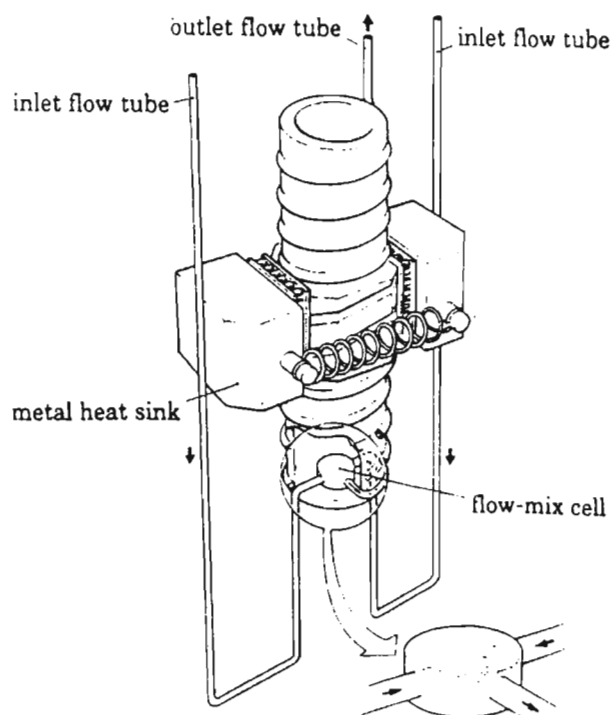
(b)

Figure 3.6 (a) Representation of the heat flow principle used in the TAM and (b) the flow-mix measuring cup in the TAM taken from TAM manual

heat energy into a voltage signal proportional to the heat flow. Results are presented as a measure of the thermal energy produced by the sample per unit time.

The calorimeter was calibrated by passing a measured amount of power through built in precision resistors. Precision wire wound resistors (C in figure 3.6(b)) are located within each measuring cup to represent a reaction during electrical calibration. The calibration resistors is integral with the measuring cup, to simulate as near as possible, the position of the reaction. This ensures that the output from the detector will be, as near as possible, identical to the output when the same power is dissipated from the resistor as from the sample. During calibration, a known current is passed through the appropriate channel heater resistor, and because the resistor value is known, a specific thermal power gives a calibration level which may then be used to determine quantitative experimental results. A typical calibration (A) and experimental (B) recorder output is shown in figure 3.7.

This entire assembly is located in a stainless steel cylinder. Each cylinder has two measuring cup assemblies as described; the Peltier elements in each measuring cup are connected in series but in opposition so that the resultant signal represents the difference in the heat flow from the two measuring cups. This design allows one measurement cup assembly to be used for the sample and the other to be used as the reference.

This instrument is suitable for the solvents used in this investigation as outside the calorimeter unit the liquids are in contact with the teflon (all the flow lines and the tips of the pistons) and glass only. The inside contacts are the gold tube of the heat exchanger, the mixing cell and the teflon tubes. Samples were introduced into the cell using two Eltron piston pumps capable of producing flow rates between 0.5 and 3.0 $cm^3 \cdot min^{-1}$.

The sensitivity and high level of precision of the TAM is largely due to the stability of the infinite heat sink which surrounds the measuring cylinders. This heat sink is formed by

a closed 25 litre thermostatted water bath, maintained to approximately 2×10^{-4} K within the experimental range. Water is continuously circulated by pumping upwards into a cylindrical stainless steel tank, where it overflows into a similar but larger outer tank. The pump then re-circulates the water from the outer tank back into the inner tank. Several interactive controlling systems work together to maintain the water at a constant temperature. Two thermistors monitor the water temperature whose signals are fed to an electronic temperature regulator unit. The 25 litre thermostat is filled with deionised water and a corrosion inhibitor containing sodium nitrate, sodium metasilicate and benzotriazole.

3.3.2.3 Operation procedure and actual sample measurement

For both instruments, an initial equilibration time of at least three days was required. Power to the equipment was left on continuously for the duration of the experimental determinations to ensure that thermal equilibrium was maintained in the temperature control units. The flow lines were filled with water after use. Before measurements absolute ethanol was pumped through each flow line to flush out the water at a rate of 5 $cm^3 min^{-1}$ for 15 minutes before introduction of the component liquids.

For the LKB microcalorimeter, the two inlets were separately flushed and primed with the two degassed sample components. A typical recorder output as a function of time for a steady state H_m^E measurement is represented in figure 3.8. Section A represents the steady state baseline obtained without any fluid flowing through the mixing vessel. This was always recorded before commencing a set of experimental measurements. Since accurate time lapse values were required for the determination of sample flow rates, the pumps and the stopwatch were activated simultaneously. Pumping of the samples was continued until a new steady state

was reached, depicted by the baseline deflection B in figure 3.8. Thereafter a calibration current to the calibration heater was applied in order to nullify this deflection, in the case of an endothermic reaction restoring the original baseline. In the case of an exothermic reaction, enough current was applied to reproduce this baseline deflection B. In practice, noise and non-uniform flow rates resulting from the peristaltic pumps operating at low speeds produced regular baseline deflections on the recorder. The current was thus always adjusted to a point where the spread about the mean value on the deflected baseline was reproduced about the zero flow-baseline.
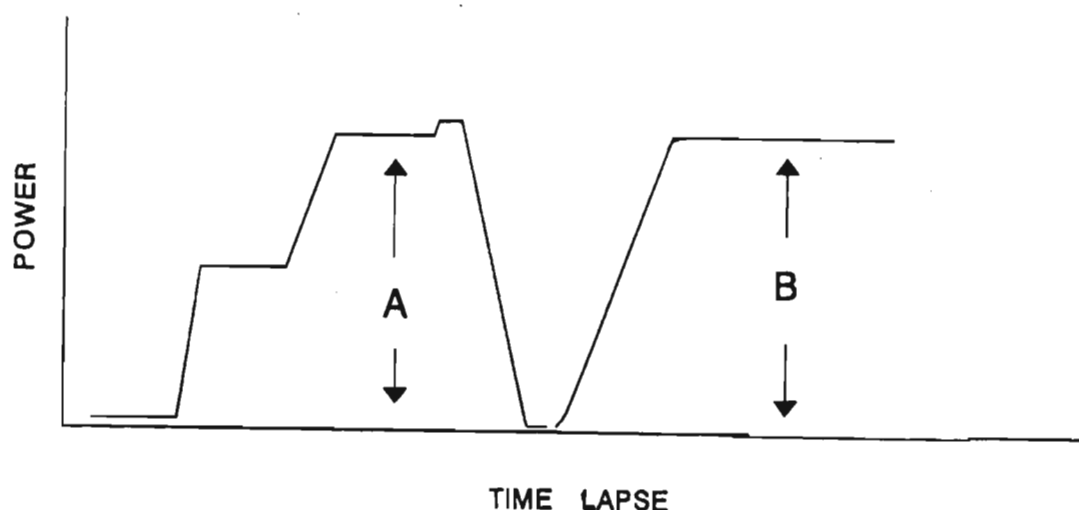
Figure 3.7 A typical calibration and experimental recorder output for the TAM

Once the original baseline had been regained , both pumps were switched off. The molar flow rates f_1 and f_2 were determined by weighing the two component flasks before and after each experimental run. From these masses and the time elapsed for the experiment, the molar flow rates were determined. A Mettler AE240 electronic balance, accurate to 0.0005 g was used for the mass determinations.

For the TAM, due to the sensitivity of the instrument and the absence of a control unit containing an inbuilt current supply, calibration of the individual flow rates was necessary. This involved flushing one of the component solvents through both the inlet tubings at a flow rate similar to that for the actual experimental determination. A known current, I, from an external power source is simultaneously passed through the inbuilt resistor and because R for the resistor is known, the expected thermal power ,P, can be obtained from the equation

$$P = I^2 R \qquad (3.3)$$

and the calorimeter power reading is adjusted accordingly. Both the pumps, the external power supply were then switched off, the baseline was allowed to return to zero and flow of the second sample component in one of the lines was initiated for sufficient time to coat the tubing. Experiments were then carried out according to a method similar to that of the LKB microcalorimeter with the flow-rates identical to those used in the calibration.

3.3.2.4 Preparation of Mixtures

The sample liquids were prepared in 25 cm³ Quickfit conical flasks fitted with modified B 14 stoppers - which had one 1.8 mm i.d. inlet connected by teflon tubing to the pump. This

design was efficient in reducing evaporation of the component samples hence reducing the problem of co-existing liquid and gaseous phases. The masses of the effluent collected after each run were compared to the amounts of pure component consumed, thus serving as a constant check against liquid leaks in the system. For each new run, a new pumping rate was set and the process carried out as described.

During initial experiments air bubbles were seen in the outlet tube and were disclosed on the recorder as sudden decreases or increases in the steady state line. This is most likely due to dissolved gases in the sample components. Hence degassing of all solvents prior to an experimental run was imperative.

3.3.2.5 Friction Effects and Flow rate determinations

The friction effects due to flow of the solvents and the characteristics of the sample components towards the teflon tubing have to be corrected for in the LKB 2107 microcalorimeter. This correction was not necessary in the TAM as the calibration process incorporated these factors. For an experimental run done on the LKB microcalorimeter the values of the baseline deflections ,B, and the corresponding currents ,I, required to nullify these deflections were plotted for each system (cf. figure 3.8). In each case the resulting graph together with the graph for the mixture from each run were employed to adjust the experimental readings for the frictional effects.
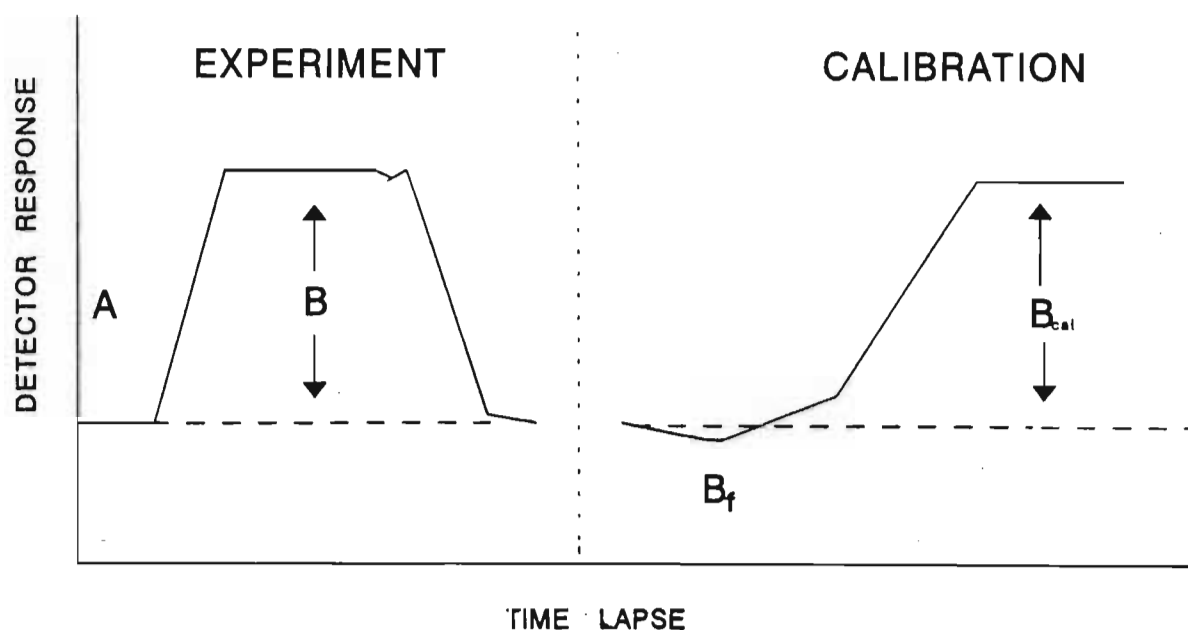
Figure 3.8 A typical calibration and experimental recorder output for the LKB microcalorimeter

These calibrations were carried out collectively at the end of a series of experimental runs for a system. Each calibration involved purging the mixing vessel with the effluent from a particular run. With the same pumping parameters as were employed for that particular run, any heating effect due to friction exhibited a deflection, B_f, in figure 3.8. The experimental detector voltage shift was thus corrected to

$$B_o = B - B_f \qquad\qquad (3.4)$$

The indicated calibration current, I_{cal}, corresponding to B_o, was then interpolated from the experimentally determined graph and was passed through the calorimeter heater, thereby producing a baseline deflection corresponding to B_{cal} in figure 3.8. The excess molar enthalpy was thus calculated from

$$H_m^E = [\{B_o(I_{cal})^2 R\}/B_{cal}]/(f_1 + f_2) \qquad (3.5)$$

where R is the heater resistance. It was however, observed that $B_o \approx B_{cal}$ for flow rates less than 0.80 cm^3·min^{-1}. Since the majority of the experimental runs were carried out at flow rates less than this, the above calibration procedure became unnecessary in many cases and H_m^E was then determined by

$$H_m^E = (I_{cal}^2 R) / (f_1 + f_2) \qquad (3.6)$$

For exothermic reactions, the steady state deflection, B, was noted and a current, I, was applied to double this deflection. Heating due to frictional effects would once again produce a deflection, B_f, and hence equation 3.4 becomes

$$B_o = B + B_f \qquad (3.7)$$

The TAM was, however, found to give more precise results for small endothermic and exothermic reactions and hence for most of the systems discussed in this work it was the instrument of choice.

3.3.2.6 Test systems

The excess enthalpies of the nonviscous system (cyclohexane + n-hexane) has recently been recommended by the IUPAC[162] Commission on Thermodynamics and Thermochemistry for checking calorimeter accuracy and data, since results for this system obtained in five different laboratories with three types of isothermal calorimeters showed no systematic discrepancies. The recommended equation at 298.15 K is

$$H_m^E(J\,mol^{-1}) = x_1(1-x_1)[866.1 - 249.4(1-2x_1) + 97.0(1-2x_1)^2 - 31.8(1-2x_1)^3] \qquad (3.8)$$

where x_1 is the mole fraction of cyclohexane. Marsh and Stokes[166] reported very accurate and precise results using an isothermal batch calorimeter with a standard deviation of 0.09 J·mol^{-1}; Grolier et al.[167] obtained data with a Picker flow calorimeter with a standard deviation of 0.35 J·mol^{-1}; McGlashan and Stoeckli,[160] and Siddiqi and Lucas[164] used an isothermal flow calorimeter and obtained a standard deviation of 1.1 J·mol^{-1} and 0.78 J·mol^{-1}, respectively. The accuracy and precision for this work were estimated from the data sets obtained for the (cyclohexane + benzene) system and the standard deviation for these results and those interpolated from the IUPAC equation was 1.0 J·mol^{-1}. The data presented here show equal precision to those of McGlashan and Stoeckli.[160]

3.4 Results

The measured excess molar enthalpies, H_m^E , are given in Tables 3.1 to 3.9, together with the deviations, δH_m^E calculated from the smoothing equation

$$\delta H_m^E (J\,mol^{-1}) = H_m^E(J\,mol^{-1}) - x(1-x)\sum_{r=0}^{n} A_r(1-2x)^r \qquad (3.9)$$

by the method of unweighted least squares. The coefficients A_r are given in Tables 3.10 to 3.14.

TABLE 3.1 Experimental excess molar enthalpies H_m^E for binary mixtures of $\{x\ C_jH_{2j+1}OH + (1-x)\ ROR'\}$ for $j = 1, 2$ or 3 and the deviations, δH_m^E at the temperature 298.15 K. ROR' is a branched chain ether.

x	H_m^E	δH_m^E	x	H_m^E	δH_m^E	x	H_m^E	δH_m^E
	$J \cdot mol^{-1}$	$J \cdot mol^{-1}$		$J \cdot mol^{-1}$	$J \cdot mol^{-1}$		$J \cdot mol^{-1}$	$J \cdot mol^{-1}$

$$x CH_3OH + (1-x)\{CH_3CH(CH_3)\}_2O$$

x	H_m^E	δH_m^E	x	H_m^E	δH_m^E	x	H_m^E	δH_m^E
0.088	150.4	-2.2	0.605	103.3	-0.1	0.846	-25.5	2.2
0.132	189.6	0.2	0.606	101.4	-1.6	0.874	-34.8	2.0
0.227	218.6	2.0	0.702	53.2	3.0	0.928	-37.9	2.7
0.276	215.6	1.6	0.708	43.3	-3.4	0.963	-35.5	-6.5
0.340	202.0	-0.0	0.716	39.2	-3.0	0.976	-26.1	-5.0
0.404	179.4	-4.9	0.756	20.0	1.5	0.986	-12.7	1.0
0.532	142.6	5.2	0.775	6.4	-0.9	0.993	-6.1	0.9

$$x CH_3OH + (1-x)CH_3C(CH_3)_2OCH_3$$

x	H_m^E	δH_m^E	x	H_m^E	δH_m^E	x	H_m^E	δH_m^E
0.095	205.9	9.4	0.377	310.7	2.1	0.884	16.1	-3.8
0.132	249.6	9.4	0.493	282.3	2.2	0.910	9.4	3.1
0.141	242.2	-6.8	0.494	280.0	0.1	0.921	0.4	-1.2
0.187	271.2	-10.1	0.592	225.2	-9.9	0.922	0.7	-0.7
0.202	280.2	-9.2	0.745	133.1	5.5	0.936	-5.6	-2.4
0.265	313.5	5.3	0.820	68.8	2.5	0.936	-6.1	1.0
0.347	316.9	5.4						

$$x CH_3OH + (1-x)CH_3CH_2C(CH_3)_2OCH_3$$

x	H_m^E	δH_m^E	x	H_m^E	δH_m^E	x	H_m^E	δH_m^E
0.185	300.5	-9.9	0.386	382.0	-2.9	0.856	87.7	4.6
0.236	359.4	10.4	0.422	374.7	-5.1	0.929	31.4	0.4
0.350	390.1	4.8	0.644	261.6	-1.7	0.978	-6.2	-12.7
0.372	386.9	-1.3	0.772	156.7	1.6	0.987	-4.3	-7.9

TABLE 3.1 Continued

x	H_m^E	δH_m^E	x	H_m^E	δH_m^E	x	H_m^E	δH_m^E
	$J \cdot mol^{-1}$	$J \cdot mol^{-1}$		$J \cdot mol^{-1}$	$J \cdot mol^{-1}$		$J \cdot mol^{-1}$	$J \cdot mol^{-1}$

$$xC_2H_5OH \ + \ (1-x)\{CH_3CH(CH_3)\}_2O$$

x	H_m^E	δH_m^E	x	H_m^E	δH_m^E	x	H_m^E	δH_m^E
0.080	240.4	14.5	0.459	402.1	3.7	0.871	74.1	2.3
0.106	295.9	10.2	0.564	348.5	-0.2	0.882	59.1	-3.1
0.215	402.8	-10.6	0.641	289.9	1.7	0.934	28.7	4.0
0.299	442.6	-0.6	0.694	233.2	-7.9	0.935	25.7	1.9
0.366	448.2	7.8	0.789	150.0	0.7	0.985	3.4	0.8

$$xC_2H_5OH \ + \ (1-x)CH_3C(CH_3)_2OCH_3$$

x	H_m^E	δH_m^E	x	H_m^E	δH_m^E	x	H_m^E	δH_m^E
0.077	214.9	-0.6	0.526	470.1	-5.5	0.766	266.1	1.5
0.120	300.8	-5.8	0.581	448.7	2.6	0.825	198.9	2.6
0.222	460.1	7.9	0.591	440.6	2.4	0.830	183.0	-7.2
0.359	525.6	-1.0	0.678	361.0	1.0	0.881	135.5	4.8
0.451	515.8	-2.0	0.686	350.4	-1.5	0.923	79.4	-2.1
0.525	478.1	-5.5	0.732	304.0	2.2	0.982	14.0	-4.4

$$xC_2H_5OH \ + \ (1-x)CH_3CH_2C(CH_3)_2OCH_3$$

x	H_m^E	δH_m^E	x	H_m^E	δH_m^E	x	H_m^E	δH_m^E
0.075	263.0	3.3	0.551	492.7	-4.6	0.871	160.2	-4.2
0.190	465.6	-9.3	0.643	428.5	1.9	0.923	107.6	-2.1
0.253	536.7	6.4	0.680	380.0	-11.2	0.934	77.2	-3.6
0.341	561.6	0.6	0.778	300.5	17.0	0.984	17.8	-0.8

TABLE 3.1 Continued

x	H_m^E	δH_m^E	x	H_m^E	δH_m^E	x	H_m^E	δH_m^E
	$J \cdot mol^{-1}$	$J \cdot mol^{-1}$		$J \cdot mol^{-1}$	$J \cdot mol^{-1}$		$J \cdot mol^{-1}$	$J \cdot mol^{-1}$

$$x C_3H_7OH \ + \ (1-x)\{CH_3CH(CH_3)\}_2O$$

x	H_m^E	δH_m^E	x	H_m^E	δH_m^E	x	H_m^E	δH_m^E
0.059	182.6	9.9	0.291	453.8	-2.7	0.635	297.7	-7.2
0.081	225.6	2.5	0.334	460.6	-1.5	0.699	246.1	-2.0
0.116	295.7	3.3	0.376	468.4	10.1	0.767	188.2	1.7
0.139	320.9	-10.2	0.461	428.0	-0.4	0.856	107.2	1.4
0.165	369.7	2.7	0.540	386.9	6.8	0.915	60.6	3.4
0.207	408.4	-1.9	0.590	340.2	-2.0	0.979	6.9	-5.6
0.252	435.6	-5.6						

$$x C_3H_7OH \ + \ (1-x)CH_3C(CH_3)_2OCH_3$$

x	H_m^E	δH_m^E	x	H_m^E	δH_m^E	x	H_m^E	δH_m^E
0.098	322.9	7.7	0.464	562.6	1.9	0.765	314.2	0.3
0.176	460.3	2.2	0.566	518.2	10.2	0.797	270.4	-3.2
0.248	523.6	-9.3	0.612	464.9	-8.1	0.869	172.7	-3.3
0.315	559.8	-7.5	0.639	455.9	6.0	0.925	110.2	12.5
0.386	583.4	7.4	0.696	385.1	-8.8	0.992	7.0	-3.3

$$x C_3H_7OH \ + \ (1-x)CH_3CH_2C(CH_3)_2OCH_3$$

x	H_m^E	δH_m^E	x	H_m^E	δH_m^E	x	H_m^E	δH_m^E
0.073	220.8	-5.1	0.361	592.2	-2.0	0.787	306.1	-0.3
0.110	320.5	1.2	0.462	577.8	0.5	0.828	261.7	3.2
0.136	380.9	6.1	0.523	552.7	6.1	0.890	179.1	1.0
0.193	473.9	2.6	0.620	472.0	-2.1	0.937	112.8	4.1
0.235	515.9	-7.8	0.677	420.9	-0.6	0.978	30.1	-11.1
0.282	566.2	2.2	0.735	359.1	-3.9			

TABLE 3.1 Continued

x	H_m^E	δH_m^E	x	H_m^E	δH_m^E	x	H_m^E	δH_m^E
	$J \cdot mol^{-1}$	$J \cdot mol^{-1}$		$J \cdot mol^{-1}$	$J \cdot mol^{-1}$		$J \cdot mol^{-1}$	$J \cdot mol^{-1}$

$$xCH_3CH(CH_3)OH + (1-x)\{CH_3CH(CH_3)\}_2O$$

x	H_m^E	δH_m^E	x	H_m^E	δH_m^E	x	H_m^E	δH_m^E
0.087	379.4	12.4	0.348	688.3	0.5	0.748	386.3	-9.9
0.131	479.0	-3.1	0.452	672.1	2.7	0.787	326.4	-11.6
0.149	520.2	-0.4	0.540	626.2	5.4	0.837	257.6	0.3
0.232	628.7	-7.5	0.626	547.6	1.1	0.879	192.4	4.6
0.287	670.7	-2.3	0.709	456.3	6.9	0.926	120.6	10.2

$$xCH_3CH(CH_3)OH + (1-x)CH_3C(CH_3)_2OCH_3$$

x	H_m^E	δH_m^E	x	H_m^E	δH_m^E	x	H_m^E	δH_m^E
0.063	298.6	5.3	0.393	742.3	-6.4	0.631	682.8	-3.3
0.126	471.8	-3.6	0.417	747.4	-4.8	0.645	679.4	-6.2
0.168	547.6	-7.8	0.445	747.0	-0.6	0.684	625.7	-2.2
0.227	640.5	7.2	0.515	739.9	-6.9	0.866	270.2	-5.7
0.343	712.8	-3.5	0.614	692.1	-9.0	0.871	259.5	-4.2

$$xCH_3CH(CH_3)OH + (1-x)CH_3CH_2C(CH_3)_2OCH_3$$

x	H_m^E	δH_m^E	x	H_m^E	δH_m^E	x	H_m^E	δH_m^E
0.095	400.1	13.1	0.358	738.3	2.2	0.678	577.4	-6.4
0.117	453.1	5.2	0.410	753.4	6.7	0.680	587.2	4.3
0.174	565.5	-2.2	0.460	754.2	-9.4	0.755	458.7	-5.7
0.206	603.4	-13.8	0.566	700.0	0.0	0.819	351.0	9.3
0.274	681.3	-8.2	0.640	625.8	-6.4	0.878	220.7	0.2

TABLE 3.2 Experimental excess molar enthalpies, H_m^E for binary mixtures of $\{x\ C_jH_{2j+1}OH\ +\ (1\text{-}x)\ ROR_j\}$ and the deviations, δH_m^E at the temperature 298.15 K. ROR_j is a cyclic ether.

x	H_m^E J·mol^{-1}	δH_m^E J·mol^{-1}	x	H_m^E J·mol^{-1}	δH_m^E J·mol^{-1}	x	H_m^E J·mol^{-1}	δH_m^E J·mol^{-1}
				xCH$_3$OH + (1-x) c-(CH$_2$)$_4$O				
0.073	200.5	-9.9	0.310	540.4	4.9	0.788	265.7	2.1
0.098	271.0	1.9	0.330	548.4	4.3	0.858	184.0	10.5
0.136	340.6	-3.6	0.418	544.3	-11.0	0.910	99.7	-7.6
0.178	415.9	3.3	0.587	473.1	-3.5	0.933	70.7	-7.3
0.218	463.9	0.3	0.664	404.6	-1.9	0.951	51.0	-5.0
0.255	503.8	4.2	0.730	340.6	6.2			
				xCH$_3$OH + (1-x) c-(CH$_2$)$_5$O				
0.081	302.5	4.0	0.295	671.3	-4.4	0.625	589.2	5.7
0.123	423.3	7.3	0.315	685.7	-1.9	0.699	493.7	-11.8
0.169	510.9	-4.3	0.376	703.9	-2.4	0.778	399.9	-5.6
0.206	571.0	-8.9	0.431	706.5	3.3	0.846	309.9	4.8
0.248	641.1	7.7	0.556	649.0	7.0	0.922	175.6	5.2
				xCH$_3$OH + (1-x) c-(CH$_2$)$_2$O(CH$_2$)$_2$O				
0.082	370.1	-4.3	0.301	1018.9	-9.8	0.693	904.1	3.8
0.129	560.2	-4.1	0.323	1061.6	0.1	0.748	800.0	12.1
0.159	668.6	-4.7	0.360	1107.8	2.1	0.848	549.9	12.6
0.198	795.7	3.6	0.435	1130.8	-13.8	0.890	409.2	-2.9
0.203	816.7	9.5	0.586	1039.6	-23.4	0.924	292.9	-5.2
0.259	948.0	-0.5	0.672	939.7	-1.4	0.951	179.6	-20.7

TABLE 3.2 Continued

x	H_m^E	δH_m^E	x	H_m^E	δH_m^E	x	H_m^E	δH_m^E
	$J \cdot mol^{-1}$	$J \cdot mol^{-1}$		$J \cdot mol^{-1}$	$J \cdot mol^{-1}$		$J \cdot mol^{-1}$	$J \cdot mol^{-1}$

$$xC_2H_5OH + (1-x)\ c\text{-}(CH_2)_4O$$

x	H_m^E	δH_m^E	x	H_m^E	δH_m^E	x	H_m^E	δH_m^E
0.060	220.0	-5.5	0.377	809.0	5.1	0.774	475.5	1.3
0.102	366.6	5.9	0.401	808.9	-0.9	0.823	393.1	3.1
0.148	490.9	1.9	0.523	777.1	-0.6	0.865	317.7	9.5
0.195	600.0	4.6	0.629	680.3	-0.1	0.892	251.9	-3.2
0.229	646.4	-12.8	0.666	630.9	-4.8	0.912	202.8	-9.1
0.328	780.0	2.8						

$$xC_2H_5OH + (1-x)\ c\text{-}(CH_2)_5O$$

x	H_m^E	δH_m^E	x	H_m^E	δH_m^E	x	H_m^E	δH_m^E
0.078	360.3	-9.4	0.321	822.0	-1.1	0.667	706.8	0.5
0.122	520.9	7.2	0.374	849.2	1.0	0.694	659.1	-9.2
0.165	626.0	4.8	0.462	853.2	-2.8	0.750	572.0	-0.3
0.179	651.2	2.0	0.481	855.2	2.9	0.787	494.6	-3.1
0.219	717.3	-0.0	0.521	837.0	-0.9	0.842	360.5	7.0
0.261	763.5	-7.3	0.601	791.6	9.4	0.905	223.0	-1.6

$$xC_2H_5OH + (1-x)\ c\text{-}(CH_2)_2O(CH_2)_2O$$

x	H_m^E	δH_m^E	x	H_m^E	δH_m^E	x	H_m^E	δH_m^E
0.073	462.8	3.6	0.336	1407.6	-3.5	0.759	1130.1	7.2
0.101	600.0	-11.9	0.427	1525.2	7.5	0.783	1045.8	0.2
0.146	830.7	2.3	0.508	1530.2	-1.4	0.832	864.0	-6.4
0.149	850.9	8.8	0.582	1471.1	-10.0	0.868	721.9	1.4
0.197	1029.9	-7.2	0.646	1395.9	4.7	0.898	581.5	1.0
0.221	1115.8	-4.6	0.683	1310.0	-8.6	0.936	383.7	-3.9
0.230	1160.5	9.2	0.729	1215.6	9.1	0.937	376.4	-1.1

TABLE 3.2 Continued

x	H_m^E	δH_m^E	x	H_m^E	δH_m^E	x	H_m^E	δH_m^E
	$J \cdot mol^{-1}$	$J \cdot mol^{-1}$		$J \cdot mol^{-1}$	$J \cdot mol^{-1}$		$J \cdot mol^{-1}$	$J \cdot mol^{-1}$

$$x C_3H_7OH \ + \ (1\text{-}x) \ c\text{-}(CH_2)_4O$$

x	H_m^E	δH_m^E	x	H_m^E	δH_m^E	x	H_m^E	δH_m^E
0.074	309.8	17.8	0.370	916.3	-2.1	0.580	874.4	-5.3
0.113	415.4	-7.3	0.434	940.8	-1.7	0.665	784.2	3.1
0.151	540.6	1.1	0.450	952.4	9.1	0.734	665.8	-6.7
0.217	693.2	-11.3	0.476	951.5	11.3	0.789	571.5	2.6
0.261	791.2	0.6	0.508	922.8	-6.8	0.840	456.8	-1.4
0.330	885.2	0.9	0.525	920.1	-0.6	0.939	204.1	5.7

$$x C_3H_7OH \ + \ (1\text{-}x) \ c\text{-}(CH_2)_5O$$

x	H_m^E	δH_m^E	x	H_m^E	δH_m^E	x	H_m^E	δH_m^E
0.050	200.9	-8.9	0.269	800.1	-2.6	0.779	552.5	6.3
0.080	336.2	14.3	0.355	902.5	8.4	0.849	400.0	9.3
0.096	374.4	-4.4	0.447	929.1	-5.1	0.874	324.6	-5.0
0.158	564.8	-0.8	0.549	898.8	7.8	0.906	243.6	-5.0
0.191	651.5	1.8	0.615	815.7	-8.4	0.952	128.6	-1.9
0.217	701.9	-5.4	0.711	674.9	-3.9			

$$x C_3H_7OH \ + \ (1\text{-}x) \ c\text{-}(CH_2)_2O(CH_2)_2O$$

x	H_m^E	δH_m^E	x	H_m^E	δH_m^E	x	H_m^E	δH_m^E
0.055	405.9	6.2	0.388	1800.0	0.9	0.733	1407.9	-6.2
0.077	555.9	8.0	0.446	1851.8	0.1	0.818	1097.4	11.5
0.114	783.2	-0.8	0.466	1852.9	-4.7	0.871	821.0	-9.5
0.159	1025.1	-13.8	0.547	1820.3	-1.6	0.900	675.1	5.5
0.192	1209.0	4.0	0.586	1772.2	-1.1	0.927	518.3	8.6
0.254	1451.6	-11.9	0.672	1598.1	2.8	0.940	415.9	-13.3
0.322	1690.2	17.9						

TABLE 3.2 Continued

x	H_m^E	δH_m^E	x	H_m^E	δH_m^E	x	H_m^E	δH_m^E
	$J \cdot mol^{-1}$	$J \cdot mol^{-1}$		$J \cdot mol^{-1}$	$J \cdot mol^{-1}$		$J \cdot mol^{-1}$	$J \cdot mol^{-1}$

$$x\text{CH}_3\text{CH(CH}_3)\text{OH} + (1\text{-}x)\ c\text{-}(\text{CH}_2)_4\text{O}$$

x	H_m^E	δH_m^E	x	H_m^E	δH_m^E	x	H_m^E	δH_m^E
0.023	150.1	32.3	0.331	1061.0	-2.9	0.756	815.7	0.8
0.087	400.0	-19.0	0.405	1121.5	3.6	0.821	676.5	1.7
0.131	600.1	8.0	0.494	1120.1	3.6	0.855	575.4	-8.2
0.188	790.9	9.4	0.604	1040.8	3.6	0.882	499.5	-3.7
0.223	870.5	-4.7	0.691	922.8	-4.2	0.981	140.7	38.2
0.257	942.1	-8.2						

$$x\text{CH}_3\text{CH(CH}_3)\text{OH} + (1\text{-}x)\ c\text{-}(\text{CH}_2)_5\text{O}$$

x	H_m^E	δH_m^E	x	H_m^E	δH_m^E	x	H_m^E	δH_m^E
0.051	265.0	-12.7	0.301	1040.6	4.3	0.641	975.9	-4.0
0.090	451.2	-9.4	0.400	1120.1	-2.0	0.680	914.4	-3.3
0.103	519.5	4.2	0.448	1124.6	-5.7	0.757	778.7	13.2
0.151	700.3	9.5	0.501	1112.7	-4.4	0.836	571.0	5.2
0.307	862.9	7.6	0.544	1098.9	9.1	0.863	479.0	-8.1
0.228	899.3	-6.4	0.623	1003.0	-3.0	0.937	236.6	-6.5

$$x\text{CH}_3\text{CH(CH}_3)\text{OH} + (1\text{-}x)\ c\text{-}(\text{CH}_2)_2\text{O(CH}_2)_2\text{O}$$

x	H_m^E	δH_m^E	x	H_m^E	δH_m^E	x	H_m^E	δH_m^E
0.046	375.1	4.2	0.391	2000.7	31.9	0.780	1520.3	9.2
0.072	561.9	-0.7	0.451	2053.5	9.0	0.816	1352.2	6.9
0.111	835.1	2.9	0.535	2045.7	-14.5	0.852	1164.3	9.2
0.153	1092.8	-1.5	0.579	2020.4	-7.5	0.901	839.1	-4.5
0.226	1467.9	3.0	0.673	1845.3	-19.2	0.943	515.4	-10.8
0.253	1566.0	-12.3	0.741	1676.1	12.5	0.964	326.0	-17.8
0.323	1802.3	-14.6						

TABLE 3.3 Experimental excess molar enthalpies, H_m^E for binary mixtures of $\{x$ CH$_3$CH$_2$NHCH$_2$CH$_3$ + $(1-x)$ ROR$'\}$ and the deviations, δH_m^E at the temperature 298.15 K. ROR$_\prime$ is a branched chain ether.

x	H_m^E	δH_m^E	x	H_m^E	δH_m^E	x	H_m^E	δH_m^E
	J·mol⁻¹	J·mol⁻¹		J·mol⁻¹	J·mol⁻¹		J·mol⁻¹	J·mol⁻¹

x(C$_2$H$_5$)$_2$NH + $(1-x)\{$CH$_3$CH(CH$_3$)$\}_2$O

x	H_m^E	δH_m^E	x	H_m^E	δH_m^E	x	H_m^E	δH_m^E
0.048	31.0	-0.9	0.351	159.9	-0.2	0.784	123.5	-0.4
0.082	53.5	0.4	0.408	169.2	-1.0	0.848	91.8	-3.5
0.114	74.9	4.0	0.474	174.5	-1.8	0.918	59.6	3.2
0.198	109.9	-1.3	0.569	176.0	1.2	0.933	45.0	-1.8
0.247	129.7	-0.9	0.663	163.0	2.3	0.962	25.3	-2.4
0.282	142.3	0.2	0.719	148.4	1.8			

x(C$_2$H$_5$)$_2$NH + $(1-x)$CH$_3$C(CH$_3$)$_2$OCH$_3$

x	H_m^E	δH_m^E	x	H_m^E	δH_m^E	x	H_m^E	δH_m^E
0.036	16.0	-0.1	0.413	109.2	0.1	0.820	55.6	-2.1
0.050	20.9	1.1	0.429	111.2	1.4	0.871	42.8	0.1
0.110	45.2	-0.6	0.520	109.2	-0.3	0.885	40.7	2.2
0.160	63.2	0.5	0.592	103.0	-0.7	0.901	34.2	0.7
0.239	86.1	1.8	0.651	95.1	-0.4	0.935	20.1	-2.1
0.271	90.8	-0.3	0.692	88.9	0.7			
0.340	100.5	-2.0	0.759	74.6	1.0			

x(C$_2$H$_5$)$_2$NH + $(1-x)$CH$_3$CH$_2$C(CH$_3$)$_2$OCH$_3$

x	H_m^E	δH_m^E	x	H_m^E	δH_m^E	x	H_m^E	δH_m^E
0.018	4.13	-2.4	0.333	94.5	0.7	0.714	82.0	-4.6
0.037	10.3	-3.1	0.363	99.2	0.9	0.811	64.3	1.0
0.099	30.0	-4.5	0.452	108.0	1.4	0.831	59.4	1.9
0.148	47.8	-2.3	0.459	109.5	2.6	0.865	59.3	3.9
0.182	60.7	0.9	0.543	107.6	0.5	0.900	39.0	2.9
0.201	66.2	1.0	0.549	106.9	-0.0	0.932	25.6	0.6
0.227	73.7	1.8	0.604	100.1	-2.9			
0.281	84.8	0.7	0.701	84.6	-4.4			

TABLE 3.4 Experimental excess molar enthalpies, H_m^E for binary mixtures of $\{x\ CH_3CH_2NHCH_2CH_3 +$ $(1-x)\ ROR'\}$ + and the deviations, δH_m^E at the temperature 298.15 K. ROR' is a cyclic ether.

x	H_m^E	δH_m^E	x	H_m^E	δH_m^E	x	H_m^E	δH_m^E
	$J \cdot mol^{-1}$	$J \cdot mol^{-1}$		$J \cdot mol^{-1}$	$J \cdot mol^{-1}$		$J \cdot mol^{-1}$	$J \cdot mol^{-1}$
			$x(C_2H_5)_2NH + (1-x)c\text{-}(CH_2)_4O$					
0.045	13.7	2.2	0.306	51.8	-1.3	0.746	22.2	0.7
0.052	16.3	3.2	0.339	54.6	-0.2	0.769	18.7	0.4
0.053	14.1	0.8	0.352	55.6	0.4	0.815	11.9	-0.4
0.063	16.5	0.7	0.434	57.7	2.9	0.856	7.92	0.2
0.099	23.9	0.1	0.439	57.6	3.0	0.925	2.75	0.9
0.159	34.1	-1.5	0.506	52.3	1.5	0.947	1.46	0.7
0.222	43.8	-1.3	0.540	46.6	-1.3	0.966	0.29	0.2
0.227	44.3	-1.4	0.607	39.0	-1.5			
0.267	48.6	-1.4	0.659	30.9	-2.7			
			$x(C_2H_5)_2NH + (1-x)c\text{-}(CH_2)_5O$					
0.037	1.13	-0.4	0.328	34.0	0.2	0.773	2.10	0.1
0.095	9.64	-3.1	0.333	33.8	-0.1	0.824	-1.21	-0.5
0.148	19.6	-0.4	0.369	33.9	-1.0	0.846	-1.83	-0.3
0.163	21.4	-0.4	0.445	29.7	-1.5	0.849	-1.95	-0.4
0.202	27.5	1.3	0.496	25.4	-2.2	0.899	-2.45	-0.2
0.218	30.1	2.3	0.577	20.0	-0.2	0.934	-2.30	-0.3
0.299	33.9	0.9	0.637	15.4	1.4	0.971	-1.60	-0.5
0.314	34.5	1.0	0.698	10.1	2.0			
			$x(C_2H_5)_2NH + (1-x)c\text{-}(CH_2)_2O(CH_2)_2O$					
0.040	77.7	-11.8	0.223	457.0	2.4	0.634	551.3	1.6
0.061	106.3	-28.5	0.275	522.1	-5.4	0.734	451.8	7.2
0.083	187.1	2.9	0.307	565.1	2.4	0.795	376.7	12.0
0.097	207.1	-9.0	0.376	620.0	5.3	0.806	353.0	3.6
0.145	334.4	19.0	0.421	629.0	-1.9	0.865	260.1	0.4
0.147	356.3	6.1	0.437	627.0	-6.7	0.899	190.4	-12.7
0.174	378.8	6.8	0.542	601.0	-12.0	0.939	118.1	-11.6

TABLE 3.5 Experimental excess molar enthalpies, H_m^E for binary mixtures of $\{x$ $CH_3(CH_2)_2NH(CH_2)_2CH_3 +$ $(1-x)$ $ROR'\}$ and the deviations, δH_m^E at the temperature 298.15 K. ROR' is a branched chain ether.

x	H_m^E	δH_m^E	x	H_m^E	δH_m^E	x	H_m^E	δH_m^E
	$J \cdot mol^{-1}$	$J \cdot mol^{-1}$		$J \cdot mol^{-1}$	$J \cdot mol^{-1}$		$J \cdot mol^{-1}$	$J \cdot mol^{-1}$

$$x(C_3H_7)_2NH + (1-x)\{CH_3CH(CH_3)\}_2O$$

x	H_m^E	δH_m^E	x	H_m^E	δH_m^E	x	H_m^E	δH_m^E
0.062	3.75	-0.3	0.374	24.0	0.3	0.715	22.0	0.0
0.124	7.78	-0.7	0.437	25.8	0.1	0.773	18.3	-0.3
0.160	11.7	0.6	0.494	26.2	-0.4	0.834	14.8	0.5
0.185	12.8	-0.0	0.619	25.5	-0.2	0.853	13.2	-0.3
0.238	16.7	0.4	0.679	23.8	0.2	0.944	4.38	-0.8
0.330	21.3	-0.6						

$$x(C_3H_7)_2NH + (1-x)CH_3C(CH_3)_2OCH_3$$

x	H_m^E	δH_m^E	x	H_m^E	δH_m^E	x	H_m^E	δH_m^E
0.050	5.48	-0.5	0.265	27.2	0.7	0.593	24.3	0.1
0.062	6.76	-0.4	0.322	25.2	0.1	0.628	22.8	-0.2
0.100	9.98	-0.8	0.384	27.0	-0.7	0.709	18.9	-0.3
0.153	16.2	0.6	0.453	26.6	-1.6	0.773	16.1	0.5
0.157	16.1	0.0	0.525	26.1	-1.4	0.827	12.5	0.3
0.183	18.5	0.5	0.528	25.6	-1.5	0.919	5.39	-0.4
0.184	18.3	0.2						

$$x(C_3H_7)_2NH + (1-x)CH_3CH_2C(CH_3)_2OCH_3$$

x	H_m^E	δH_m^E	x	H_m^E	δH_m^E	x	H_m^E	δH_m^E
0.080	5.88	-0.3	0.294	17.5	0.8	0.598	12.5	-0.0
0.140	10.1	-0.3	0.360	17.2	-0.1	0.670	10.6	0.5
0.181	12.5	-0.2	0.390	16.7	-0.5	0.751	7.63	-0.0
0.230	15.2	0.3	0.479	15.2	-0.8	0.856	4.70	-0.2
0.268	16.5	0.4	0.594	12.9	0.3	0.922	2.95	-0.1

TABLE 3.6 Experimental excess molar enthalpies, H_m^E for binary mixtures of $\{x\ CH_3(CH_2)_2NH(CH_2)_2CH_3 + (1-x)\ ROR'\}$ and the deviations, δH_m^E at the temperature 298.15 K. ROR' is a cyclic ether.

| x | H_m^E | δH_m^E | x | H_m^E | δH_m^E | x | H_m^E | δH_m^E |
	$J \cdot mol^{-1}$	$J \cdot mol^{-1}$		$J \cdot mol^{-1}$	$J \cdot mol^{-1}$		$J \cdot mol^{-1}$	$J \cdot mol^{-1}$

$x(C_3H_7)_2NH\ +\ (1-x)c\text{-}(CH_2)_4O$

x	H_m^E	δH_m^E	x	H_m^E	δH_m^E	x	H_m^E	δH_m^E
0.040	7.01	-1.6	0.366	23.1	-0.7	0.753	-4.90	0.6
0.066	11.2	-2.0	0.473	15.3	-0.9	0.863	-6.50	1.2
0.105	19.9	1.3	0.549	9.39	-0.2	0.932	-6.84	-1.3
0.157	25.4	1.7	0.654	1.47	0.8	0.938	-7.03	-1.9
0.224	27.3	0.5	0.752	-5.14	0.3	0.961	-4.20	-0.6
0.296	26.2	-0.4						

$x(C_3H_7)_2NH\ +\ (1-x)c\text{-}(CH_2)_5O$

x	H_m^E	δH_m^E	x	H_m^E	δH_m^E	x	H_m^E	δH_m^E
0.030	3.68	-0.3	0.442	57.4	1.8	0.722	50.9	-1.0
0.097	13.7	0.2	0.497	59.8	1.4	0.775	45.3	-0.6
0.126	17.8	-0.1	0.523	60.0	0.7	0.846	36.0	1.2
0.145	20.5	-0.1	0.600	58.5	-0.8	0.893	26.9	1.3
0.257	35.4	-1.2	0.607	58.3	-0.8	0.961	11.0	0.9
0.353	47.9	-0.1	0.651	56.0	-1.4			

$x(C_3H_7)_2NH\ +\ (1-x)c\text{-}(CH_2)_2O(CH_2)_2O$

x	H_m^E	δH_m^E	x	H_m^E	δH_m^E	x	H_m^E	δH_m^E
0.053	134.5	-17.9	0.258	595.0	8.6	0.636	633.7	7.4
0.088	252.4	7.0	0.319	649.7	-8.4	0.709	538.3	-7.8
0.123	342.3	9.5	0.410	713.9	1.1	0.773	455.0	-1.7
0.153	402.8	2.8	0.413	716.6	2.9	0.836	361.5	6.8
0.192	468.4	-10.0	0.492	711.5	-3.2	0.936	150.4	4.3

TABLE 3.7 Experimental excess molar enthalpies, H_m^E for binary mixtures of $\{x\ 1\text{-}C_6H_{10} +$ $(1\text{-}x)\ ROR'\}$ and the deviations, δH_m^E at the temperature 298.15 K. ROR' is a branched chain ether.

x	H_m^E $J \cdot mol^{-1}$	δH_m^E $J \cdot mol^{-1}$	x	H_m^E $J \cdot mol^{-1}$	δH_m^E $J \cdot mol^{-1}$	x	H_m^E $J \cdot mol^{-1}$	δH_m^E $J \cdot mol^{-1}$

$x1\text{-}C_6H_{10} + (1\text{-}x)\{CH_3CH(CH_3)\}_2O$

x	H_m^E	δH_m^E	x	H_m^E	δH_m^E	x	H_m^E	δH_m^E
0.069	-51.2	6.4	0.486	-258.2	-1.0	0.807	-183.1	-1.6
0.153	-113.3	6.1	0.557	-260.9	-0.1	0.850	-150.9	0.1
0.207	-157.1	-2.8	0.633	-249.2	3.4	0.910	-100.1	-1.1
0.251	-183.0	-4.4	0.705	-229.4	3.1	0.945	-72.1	-8.2
0.345	-222.1	-0.7	0.756	-207.6	2.7	0.977	-31.8	-4.2
0.391	-239.6	-2.4						

$x1\text{-}C_6H_{10} + (1\text{-}x)CH_3C(CH_3)_2OCH_3$

x	H_m^E	δH_m^E	x	H_m^E	δH_m^E	x	H_m^E	δH_m^E
0.070	-101.9	2.3	0.360	-397.6	-0.6	0.661	-375.6	7.0
0.122	-176.4	3.8	0.466	-436.6	-7.0	0.749	-314.1	3.3
0.162	-232.7	-2.8	0.505	-435.3	-4.1	0.825	-251.4	-10.7
0.203	-282.7	-7.7	0.570	-420.3	1.2	0.912	-131.0	1.0
0.287	-340.5	10.6	0.609	-405.9	2.6	0.954	-67.3	4.0

$x1\text{-}C_6H_{10} + (1\text{-}x)CH_3CH_2C(CH_3)_2OCH_3$

x	H_m^E	δH_m^E	x	H_m^E	δH_m^E	x	H_m^E	δH_m^E
0.030	-30.1	11.1	0.365	-302.8	0.3	0.835	-203.2	-2.0
0.086	-105.9	3.0	0.450	-321.0	3.0	0.869	-163.8	5.0
0.150	-173.9	-1.0	0.515	-331.6	-2.5	0.907	-125.8	1.5
0.200	-222.6	-8.2	0.584	-326.4	-2.4	0.955	-74.9	-8.2
0.251	-249.7	-0.7	0.693	-293.7	-1.2	0.979	-41.0	-8.6
0.321	-281.1	4.9	0.768	-248.0	4.1			

TABLE 3.8 Experimental excess molar enthalpies, H_m^E for binary mixtures of $\{x$ 1-C_7H_{12} + (1-x) ROR$'\}$ and the deviations, δH_m^E at the temperature 298.15 K. ROR$'$ is a branched chain ether.

x	H_m^E $J \cdot mol^{-1}$	δH_m^E $J \cdot mol^{-1}$	x	H_m^E $J \cdot mol^{-1}$	δH_m^E $J \cdot mol^{-1}$	x	H_m^E $J \cdot mol^{-1}$	δH_m^E $J \cdot mol^{-1}$

x1-C_7H_{12} + (1-x)$\{CH_3CH(CH_3)\}_2O$

x	H_m^E	δH_m^E	x	H_m^E	δH_m^E	x	H_m^E	δH_m^E
0.040	-22.7	9.2	0.311	-209.0	-1.6	0.678	-215.5	4.2
0.070	-60.0	4.2	0.339	-220.9	-3.8	0.744	-187.3	6.8
0.131	-110.2	0.5	0.392	-233.0	-1.4	0.846	-137.1	-1.3
0.190	-149.9	-0.9	0.514	-248.0	-2.5	0.918	-88.9	-9.0
0.250	-180.1	1.1	0.614	-234.5	1.5	0.972	-38.1	-9.4

x1-C_7H_{12} + (1-x)$CH_3C(CH_3)_2OCH_3$

x	H_m^E	δH_m^E	x	H_m^E	δH_m^E	x	H_m^E	δH_m^E
0.020	-20.3	13.6	0.375	-387.0	-5.2	0.761	-275.1	-0.3
0.044	-70.2	3.5	0.476	-387.6	10.5	0.816	-228.1	-3.1
0.092	-150.2	-5.5	0.478	-392.8	5.3	0.820	-226.3	-5.3
0.112	-175.2	-4.0	0.517	-400.2	-4.8	0.906	-112.3	13.0
0.171	-240.8	1.1	0.638	-362.5	-5.4	0.962	-51.5	1.6
0.310	-352.7	0.7						

x1-C_7H_{12} + (1-x)$CH_3CH_2C(CH_3)_2OCH_3$

x	H_m^E	δH_m^E	x	H_m^E	δH_m^E	x	H_m^E	δH_m^E
0.044	-58.6	-3.3	0.336	-303.8	-6.1	0.726	-249.0	5.7
0.089	-104.0	3.1	0.420	-320.1	3.8	0.801	-202.3	-1.8
0.110	-127.7	1.7	0.498	-329.3	1.3	0.871	-145.9	-7.2
0.155	-172.7	1.3	0.511	-331.2	-1.2	0.916	-90.1	3.5
0.191	-206.2	-0.6	0.622	-309.9	-3.5	0.981	-20.0	2.7
0.250	-249.9	-0.0	0.660	-288.2	2.2			

TABLE 3.9 Experimental excess molar enthalpies, H_m^E for binary mixtures of $\{x\ 1\text{-}C_8H_{14}\ +$ $(1\text{-}x)\ ROR'\}$ and the deviations, δH_m^E at the temperature 298.15 K. ROR' is a branched chain ether.

x	H_m^E	δH_m^E	x	H_m^E	δH_m^E	x	H_m^E	δH_m^E
	$J \cdot mol^{-1}$	$J \cdot mol^{-1}$		$J \cdot mol^{-1}$	$J \cdot mol^{-1}$		$J \cdot mol^{-1}$	$J \cdot mol^{-1}$

$$x1\text{-}C_8H_{14}\ +\ (1\text{-}x)\{CH_3CH(CH_3)\}_2O$$

x	H_m^E	δH_m^E	x	H_m^E	δH_m^E	x	H_m^E	δH_m^E
0.068	-62.3	3.1	0.326	-232.6	2.5	0.655	-225.2	8.7
0.120	-111.0	-0.3	0.374	-254.9	-4.4	0.739	-194.3	1.5
0.173	-150.1	1.1	0.386	-259.2	-5.7	0.799	-160.0	-0.2
0.201	-169.5	0.7	0.484	-271.8	-6.1	0.885	-105.3	-7.4
0.271	-207.6	3.6	0.593	-248.9	4.1	0.949	-48.6	-3.4

$$x1\text{-}C_8H_{14}\ +\ (1\text{-}x)CH_3C(CH_3)_2OCH_3$$

x	H_m^E	δH_m^E	x	H_m^E	δH_m^E	x	H_m^E	δH_m^E
0.040	-57.5	4.2	0.274	-313.0	10.7	0.801	-210.3	0.6
0.073	-128.4	-19.5	0.356	-359.6	10.3	0.814	-193.5	5.3
0.121	-180.3	-8.6	0.466	-393.1	-0.8	0.853	-155.6	3.8
0.166	-225.1	-0.5	0.557	-379.4	-2.4	0.898	-102.9	8.1
0.210	-270.0	-0.0	0.683	-323.6	-12.6	0.944	-50.1	10.8
0.246	-301.1	1.2	0.752	-265.3	-9.4			

$$x1\text{-}C_8H_{14}\ +\ (1\text{-}x)CH_3CH_2C(CH_3)_2OCH_3$$

x	H_m^E	δH_m^E	x	H_m^E	δH_m^E	x	H_m^E	δH_m^E
0.040	-51.6	1.1	0.362	-310.4	3.0	0.742	-239.0	2.4
0.077	-98.8	-0.5	0.370	-317.2	-1.3	0.812	-185.3	2.8
0.121	-150.2	-3.9	0.479	-334.6	-1.2	0.835	-167.4	1.6
0.163	-190.5	-2.8	0.599	-316.1	-2.6	0.891	-120.0	-3.1
0.189	-211.0	-0.3	0.646	-299.4	-3.7	0.946	-59.3	1.1
0.286	-272.5	6.5						

TABLE 3.10 Coefficients A_r and standard deviations σ for [an alkanol (1) + a branched chain ether (2)] at the temperature 298.15 K by equation 3.9.

Branched Chain ether	A_0	A_1	A_2	A_3	$\sigma^{(a)}$ $J \cdot mol^{-1}$
			methanol		
IPE	602.4	785.4	129.6	1009.7	3.3
TBME	1110.4	736.3	129.4	938.0	6.5
TAME	1414.8	901.5	6.1	288.3	8.0
			ethanol		
IPE	1556.5	1123.1	374.7	711.6	8.3
TBME	1992.4	998.7	137.5	157.5	4.5
TAME	1977.8	998.2	147.4	131.7	12.4
			propan-1-ol		
IPE	1625.4	1225.2	347.2	190.8	5.9
TBME	2183.7	935.7	511.5	566.5	8.2
TAME	2240.0	1091.5	490.7	-284.6	5.2
			propan-2-ol		
IPE	2585.6	1137.6	803.2	951.5	7.8
TBME	2995.4	198.5	599.7	2008.0	7.8
TAME	2938.3	706.9	419.1	1339.5	8.7

TABLE 3.11 Coefficients A_r and standard deviations σ for [an alkanol (1) + a cyclic ether (2)] at the temperature 298.15 K by equation 3.9.

Cyclic ether	A_0	A_1	A_2	A_3	$\sigma^{(a)}$
					J·mol^{-1}
			methanol		
tetrahydrofuran	2126.6	932.9	82.5	208.5	6.9
tetrahydropyran	2709.4	1051.7	676.8	-93.5	7.2
1,4-dioxane	4538.0	951.2	112.0	-705.8	11.3
			ethanol		
tetrahydrofuran	3163.1	1024.6	207.2	-313.0	6.5
tetrahydropyran	3386.6	701.9	648.8	1181.5	5.8
1,4-dioxane	6133.9	387.9	640.7	-209.6	7.1
			propan-1-ol		
tetrahydrofuran	3731.5	784.9	166.3	-445.1	8.0
tetrahydropyran	3686.7	882.4	-68.7	-11.7	7.7
1,4-dioxane	7416.0	700.4	271.3	-808.3	9.5
			propan-2-ol		
tetrahydrofuran	4456.4	813.1	975.0	-934.7	16.5
tetrahydropyran	4469.7	908.0	590.0	23.4	8.3
1,4-dioxane	8263.7	-169.3	1060.0	-678.6	14.1

TABLE 3.12 Coefficients A_r and standard deviations σ for [a secondary amine (1) + a branched chain or cyclic ether (2)] at the temperature 298.15 K by equation 3.9.

Branched chain or cyclic ether	A_0	A_1	A_2	A_3	$\sigma^{(a)}$ $J \cdot mol^{-1}$
			diethylamine		
IPE	708.5	26.7	24.9	-	2.2
TBME	440.8	-58.2	-30.3	-	1.3
TAME	431.6	7.2	-60.3	-	2.7
tetrahydrofuran	204.9	-148.8	-80.4	10.5	1.7
tetrahydropyran	109.3	-164.2	-74.6	86.2	1.3
1,4-dioxane	2514.2	-522.0	-254.8	591.9	11.5
			di-n-propylamine		
IPE	106.7	15.4	-30.2	-	0.4
TBME	105.7	-27.1	-6.9	-	0.5
TAME	61.6	-51.3	2.2	37.2	0.5
tetrahydrofuran	55.5	-173.1	10.2	-	1.3
tetrahydropyran	234.3	70.9	-34.2	-	1.1
1,4-dioxane	2850.8	-547.2	-28.6	370.7	9.1

TABLE 3.13 Coefficients A_r and standard deviations σ for [an 1-alkyne (1) + a branched chain ether (2)] at the temperature 298.15 K by equation 3.9.

Branched Chain ether	A_0	A_1	A_2	$\sigma^{(a)}$ $J \cdot mol^{-1}$
		1-hexyne		
IPE	-1035.1	-186.4	-36.8	4.2
TBME	-1725.1	24.4	102.7	6.2
TAME	-1315.0	-79.9	-199.4	5.6
		1-heptyne		
IPE	-981.2	-52.8	-47.0	5.5
TBME	-1588.4	158.7	-23.8	7.2
TAME	-1322.0	60.1	76.3	3.8
		1-octyne		
IPE	-1062.0	55.7	94.2	4.8
TBME	-1560.1	253.5	229.6	9.2
TAME	-1331.3	113.5	68.8	3.1

[a]In Tables 3.10 to 3.13 σ refers to

$$\sigma = \left[\sum (H^E_{m_{(expt.)}} - H^E_{m_{(calc.)}})^2 / (n-k) \right]^{1/2} \tag{3.10}$$

where n is the number of experimental points

3.5 Discussion

3.5.1 Mixtures of (an alkanol + a branched chain ether)

3.5.1.1 Previous work

Calorimetric investigations involving (an alkanols + a mono- or poly-ether) have been extensively reported by Villamanan et al.[59,171,172]. Kehiahian et al. and Tresczanowicz et al. [173-179] have also investigated the thermodynamics of (a n-mono or poly ether or branched mono or poly ether + an n-alkane or cyclohexane or aromatic compound) at 298.15 K. In recent years the technological use of the alkanols and ethers(TAME and TBME) as "blending agents" for gasoline has provided an incentive for studying the thermodynamic properties of these liquids with hydrocarbons.[180-189] Zhu et al.[180-182] recently reported H_m^E for (TAME + an n-alkane) at 298.15 K. The values of the H_m^E for all the systems were positive at all mole fractions and with increased chain length of the alkane the maxima of the curves shift towards the ether rich region. These authors have also determined H_m^E for (TBME + an n-alkane) solutions.[182-186] Tusel Langer et al.[188] have reported endothermic behaviour for (TBME + an n-alkane) of 385 J·mol⁻¹ at equimolar concentrations at 298.15 K. Nagata[187] reported H_m^E for (TBME + benzene) at 298.15 K of 127.4 J·mol⁻¹ at equimolar fractions. Oba et al.[189] have investigated the (IPE + heptane) system and have reported H_m^E at 298.15 K of 243 J·mol⁻¹ at x = 0.5.

3.5.1.2 This work

The H_m^E results for {(methanol or ethanol or propan-1-ol or propan-2-ol) + IPE or TAME or TAME)} are presented in Table 3.1 with the parameters by equation 3.9 given in Table 3.10. Figures 3.9 to 3.12 show the curves calculated from equation 3.9 and the experimental results for all the mixtures. H_m^E for the mixtures of ethanol or propan-1-ol or propan-2-ol + IPE or TBME or TAME are positive over the whole alkanol mole fraction range with H_m^E(maximum) decreasing with increased symmetry of the ether side chains in the order TAME > TBME > IPE. For methanol + IPE or TBME or TAME, H_m^E is positive

over most of the mole fraction range with the H_m^E(maximum) decreasing in the same order as those for the other alkanols. In the methanol rich region, a small exothermic effect is found and this is probably due to the breakdown of self association of methanol.

For all the mixtures reported here, H_m^E(maximum) lies between 0.28 and 0.40 mole fraction of the alkanol. The skewness reflects the strong self association of the alkanol. The skewing becomes less prominent in the order methanol > ethanol > propan-1-ol > propan-2-ol for each of the ethers investigated.

Of the 12 mixtures reported here, four have been reported elsewhere. Our H_m^E(maximum) results for [x(methanol) + (1 - x)TBME] of 282.3 $J \cdot mol^{-1}$ at x = 0.49 is 1.3 $J \cdot mol^{-1}$ less than those reported by Tusel Langer et al.[188]. Our results of [x(ethanol) or x(propan-1-ol) + (1 - x) TBME] at x = 0.4 (approximate maximum values) are 520 and 580 $J \cdot mol^{-1}$, respectively, while the results reported by Zhu et al.[182-184] are 514 and 553 $J \cdot mol^{-1}$, respectively. Our H_m^E(maximum) results for [x (propan-2-ol) + (1 - x)IPE] at x = 0.35 is 688 $J \cdot mol^{-1}$ while that of Blanks and Prausnitz[190] is 682 $J \cdot mol^{-1}$ at x = 0.46. To confirm our technique and methods, we have repeated H_m^E for a number of reliable [x(benzene) + (1 - x)cyclohexane] results in the literature[191] and in all cases our results are within 5 $J \cdot mol^{-1}$ (or 2%) of those reported. We have also repeated the four systems done by other workers at least twice.

The values of H_m^E(maximum) are less positive than those for the corresponding n-alkane mixtures for all the alkanols investigated in this work[186,188,192]. For example H_m^E(maximum) for [x(methanol) + (1 - x)heptane] is 454 $J \cdot mol^{-1}$ at x = 0.29 while for [x(methanol) + (1 - x)IPE] it is 219 $J \cdot mol^{-1}$ at x = 0.23. This suggests that the H_m^E reported here depends on the the balance between two opposing contributions: (i) a positive term from the rupture of alkanol-alkanol hydrogen bonds and (ii) a negative term from the formation of $-OH \cdots O\{CH(CH_3)_2\}_2$ or $-OH \cdots O(CH_3)C(CH_3)_3$ or $-OH \cdots O(CH_3)C(CH_3)_2C_2H_5$ hydrogen bonded complexes. These contributions can be semiquantitatively analyzed for H_m^E for each mixture by use of the following expression:[193,194]

$$h_{int} = A - B - C \qquad\qquad (3.11)$$

where A = H_m^E(max)($C_jH_{2j+1}OH$ + ROR'); B = H_m^E(max)($C_jH_{2j+1}OH$ + C_6H_{12} or C_7H_{14}) for j = 1,2, or 3 ; C = H_m^E(max)(ROR' + C_7H_{16}) and H_{int} = (A - B - C), respectively. B, C and H_{int} are, respectively, hydrogen bonds between alcohol molecules, the enthalpic contributions from ether-ether interactions, and hydrogen bonds between alcohol-ether molecules. The values of A, B, C and H_{int} for the different mixtures are shown in Table 3.14. For a given alcohol (j = 1, 2 or 3), H_{int} decreases in the sequence TAME < IPE < TBME. The negative value indicates a reasonably strong association between the alkanol and the ether.
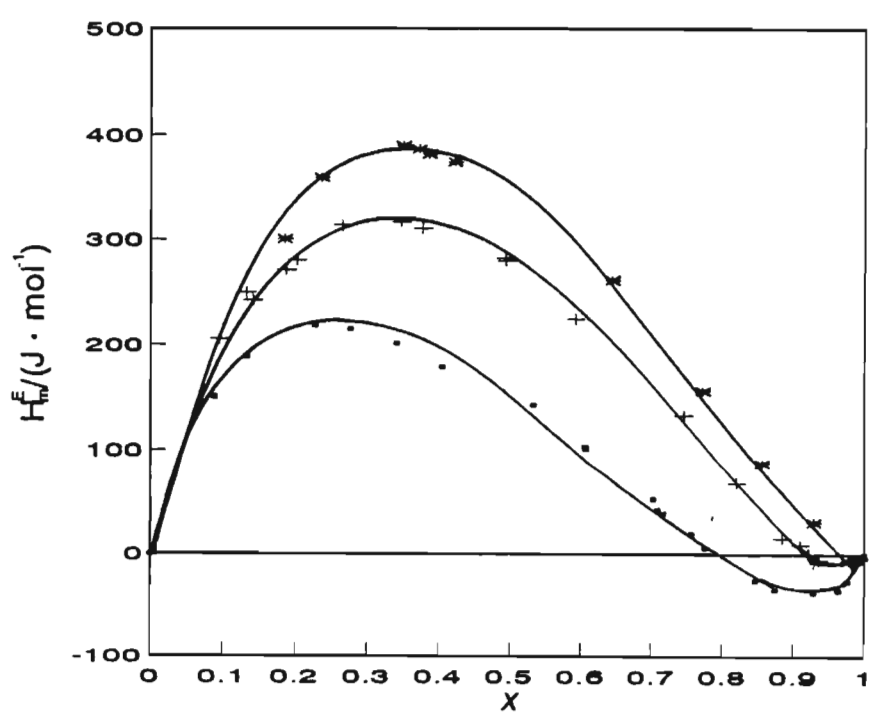
Figure 3.9 Excess molar enthalpies, H_m^E at 298.15 K for {x CH_3OH + (1-x) ROR'} where ROR' is ■, IPE or +,

TBME or *, TAME)}

TABLE 3.14 Excess molar enthalpies: $A = H_m^E(max)(C_jH_{2j+1}OH + ROR')$; $B = H_m^E(max)(C_jH_{2j+1}OH + C_6H_{12}$ or $C_7H_{14})$ for $j = 1, 2$, or 3 ; $C = H_m^E(max)(ROR' + C_6H_{14})$ and $H_{int} = (A - B - C)$. ROR' is a branched chain ether

| ROR' | $H_m^E(max)/(J \cdot mol^{-1})$ | | | | | |
	A[a]	B	ref[b]	C	ref[b]	H_{int}
	CH_3OH					
$\{CH_3CH(CH_3)\}_2O$	219	454	188	240	196	-475
$CH_3C(CH_3)_2OCH_3$	250	454	188	383	188	-587
$CH_3CH_2C(CH_3)_2OCH_3H_3$	390	454	188	268	182	-332
	C_2H_5OH					
$\{CH_3CH(CH_3)\}_2O$	448	610	192	240	196	-402
$CH_3C(CH_3)_2OCH_3$	526	610	192	383	188	-467
$CH_3CH_2C(CH_3)_2OCH_3$	562	610	192	268	182	-316
	C_3H_7OH					
$\{CH_3CH(CH_3)\}_2O$	468	580	195	240	196	-352
$CH_3C(CH_3)_2OCH_3$	583	580	195	383	188	-380
$CH_3CH_2C(CH_3)_2OCH_3$	592	580	195	268	182	-256
	$CH_3CH(OH)CH_3$					
$\{CH_3CH(CH_3)\}_2O$	688	587	192	240	196	-139
$CH_3C(CH_3)_2OCH_3$	747	587	192	383	188	-223
$CH_3CH_2C(CH_3)_2OCH_3$	754	587	192	268	182	-101

[a] this work

[b] data taken from literature as given by reference numbers
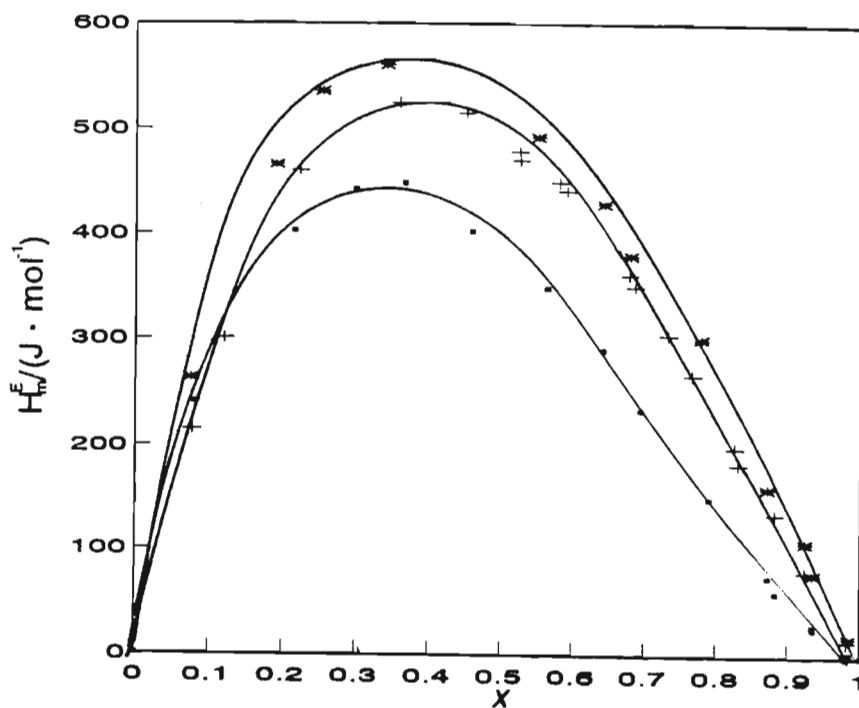
*Figure 3.10 Excess molar enthalpies, H_m^E at 298.15 K for $\{x\ C_2H_5OH + (1-x)\ ROR'\}$ where ROR' is ■, IPE or +, TBME or *, TAME*
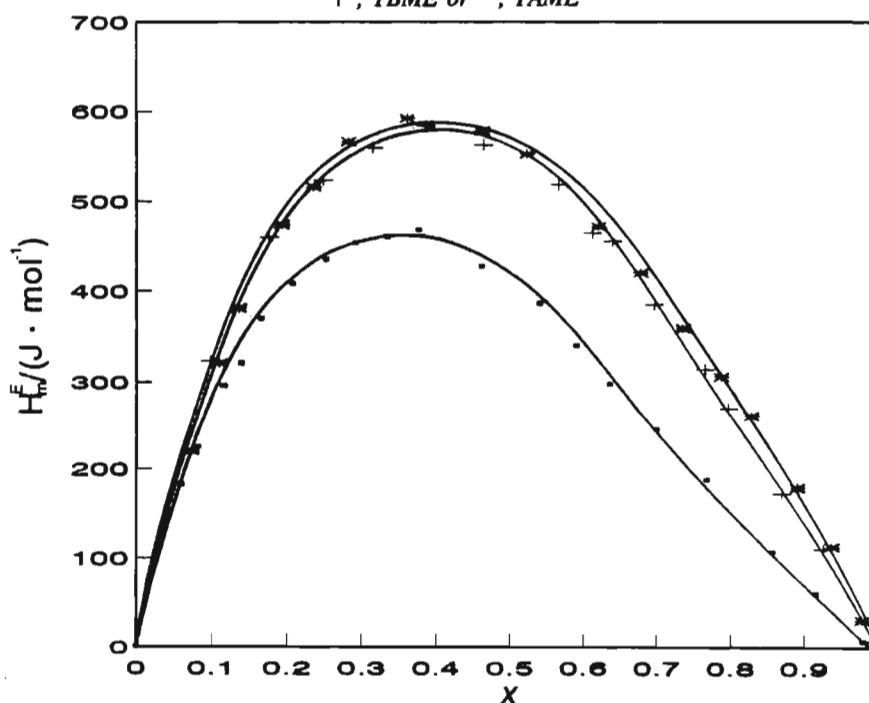
*Figure 3.11 Excess molar enthalpies, H_m^E at 298.15 K for $\{x\ C_3H_7OH + (1-x)\ ROR'\}$ where ROR' is ■, IPE or +, TBME or *, TAME*
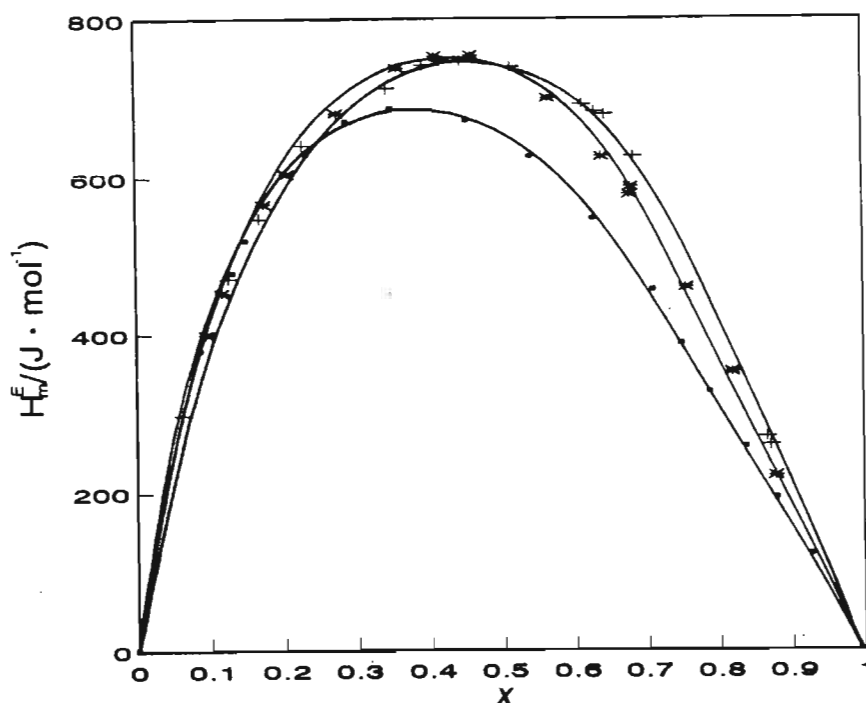
*Figure 3.12 Excess molar enthalpies, H_m^E at 298.15 K for $\{x\ CH_3CH(OH)CH_3 + (1-x)\ ROR'\}$ where ROR' is ■, IPE or +, TBME or *, TAME*

3.5.2 Mixtures of (an alkanol + a cyclic ether)

3.5.2.1 Previous work

The excess thermodynamic functions and relative strengths of interactions between a polar component and cyclic mono or di-ethers have been studied extensively.[59,88,91,113,176,179,197,198] Inglese et al.[113] determined the H_m^E for (1,1,1-trichloroethane + THF or THP or 1,4-dioxane) systems to determine the nature and/or strength of interaction between the component species. The results for these systems were negative (-100 to -500 J·mol^{-1}) whose magnitude depended on both the size of the cyclic ether, and the number and relative position of oxygen atoms in the cycloether molecules. Solimo et al.[91] measured small exothermic H_m^E behaviour for the (chloroform + THF) binary system and concluded that new bonds were formed between the unlike molecules and that this was the primary contributor to the observed H_m^E. For the binary system (1,4-dioxane + an alkanoic acid), Wilhelm et

al.[199] found negative H_m^E at 298.15 K indicating association between the cyclic diether and the acid. Sharma et al.[200] measured H_m^E for (a chloroalkane + THF or THP) at 299.6 K. The results were exothermic over the entire composition range and were explained on the basis of the strong O$\cdots$H-C and weak Cl$\cdots$O specific interactions.

3.5.2.2 *This work*

The H_m^E results for {(methanol or ethanol or propan-1-ol or propan-2-ol) + IPE or TAME or TAME)} are presented in Table 3.2 with the parameters for equation 3.9 given in Table 3.11. Figures 3.13 to 3.16 show the curves calculated from equation 3.9 and the experimental results for all the mixtures. H_m^E for the mixtures of {(ethanol or propan-1-ol or propan-2-ol) + (THF or THP or 1,4-dioxane)} are positive over the whole alkanol mole fraction range with H_m^E(maximum) decreasing in the order 1,4-dioxane > > > THP $\geq$ THF. For each of the ethers investigated in this work, H_m^E(maximum) increases with increased chain length of the alkanol.

H_m^E for six of the twelve mixtures presented here have been reported previously. We have repeated the measurements reported in the literature because some of the results are very different to ours. The H_m^E (x = 0.5) smoothed results reported here for (methanol or ethanol or propan-1-ol + THF) are 532, 791 and 933 J$\cdot$mol^{-1}, respectively, while those of Chao and Dai[201] are 531, 826, 946 J$\cdot$mol^{-1}, respectively. Our H_m^E (x = 0.5) smoothed result for the (methanol + THF) binary system is 532 J$\cdot$mol^{-1} while the results of Matous et al.[202] is 529 J$\cdot$mol^{-1}, of Arm et al.[205] is 462 J$\cdot$mol^{-1} and of Keller et al.[204] is 479 J$\cdot$mol^{-1}.

The H_m^E (x = 0.5) smoothed results presented here for (methanol or ethanol or propan-1-ol + 1,4-dioxane) are 1135, 1534 and 1854 J$\cdot$mol^{-1}, respectively, while those of Dai and Chao[205] at 298.15 K are 955, 1201 and 1435 J$\cdot$mol^{-1}, respectively. Our H_m^E (x = 0.5) result for the (methanol + 1,4-dioxane) mixture is 1135 J$\cdot$mol^{-1} is greater than the result of Singh et al.[206] at 303.15 K and Kortum and Valent[207] of 1040 J$\cdot$mol^{-1} at 298.15 K. Our H_m^E (x = 0.5) result for the (ethanol + 1,4-dioxane) is 1534 J$\cdot$mol^{-1} while those of Belousov et al.[208] is 1456 J$\cdot$mol^{-1}. To confirm our technique and methods we have repeated the present

work a number of times. In addition the purities of all the solvents were constantly checked and cleaned if necessary and the alkanols were specifically checked for the presence of water.

From Table 3.15, it can be seen that the result of H_m^E (x = 0.5) for (an alkanol + a cycloether) is less endothermic than the sum of the corresponding H_m^E (x = 0.5) or(a cycloether + heptane) mixtures[209-212]. This suggests that the H_m^E reported here depend oħ three effects i.e.,the endothermic contributions from the disruption of alkanol-alkanol hydrogen bonds and ether-ether interactions and aмexothermic contribution from the

ether-alkanol interaction. The semiquantitative magnitude of the latter enthalpic contribution is obtained in a similar manner to that for (an alkanol + a branched chain ether) systems done in section 3.5.1.2. The values of A, B, C and H_{int} are shown in Table 3.15. The negative value of H_{int} indicates an association between the alkanol and the cyclic ether. By comparing H_{int} for (an alkanol + a branched chain ether) with the H_{int} in Table 3.15 we conclude that the interaction between an alkanol and a cycloether is generally greater than that between an alkanol and a branched chain ether. This is no doubt a result of a higher degree of exposure of the oxygen atom/s in the cycloether molecule as opposed to the branched ether molecule in which the oxygen atom is shielded by hydrocarbon groups.
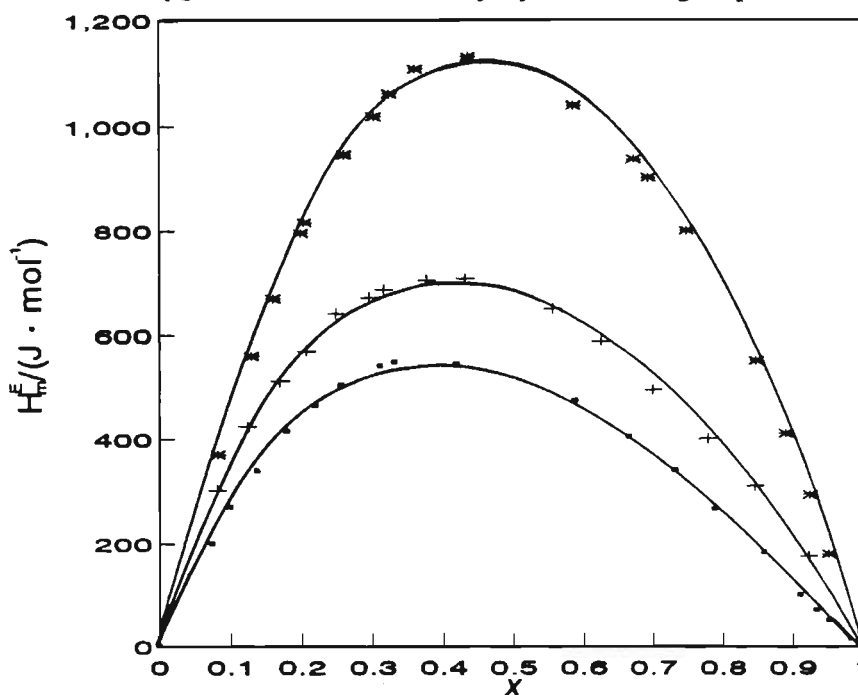
Figure 3.13 Excess molar enthalpies, H_m^E at 298.15 K for {x CH$_3$OH + (1-x) ROR'} where ROR' is ■, *THF or*

+, *THP or* *,*1,4-dioxane*

TABLE 3.15 Excess molar enthalpies: $A = H_m^E$ $(0.5C_jH_{2j+1}OH + 0.5ROR')$; $B = H_m^E(0.5C_jH_{2j+1}OH + 0.5$ c-$C_6H_{12})$ for $j = 1,2,$ or 3 ; $C = H_m^E(0.5ROR' + 0.5C_7H_{16})$ and $H_{int} = (A - B - C)$

ROR'	$H_m^E(0.5)/(J \cdot mol^{-1})$						
	$A^{(a)}$	B	ref[b]	C	ref[b]	H_{int}
			CH$_3$OH			
C_4H_8O	532	449	212	791	209	-708
$C_5H_{10}O$	677	449	212	598	209	-370
$C_4H_8O_2$	1135	449	212	1642	209	-956
			C$_2$H$_5$OH			
C_4H_8O	791	622	210	791	209	-622
$C_5H_{10}O$	847	622	210	598	209	-373
$C_4H_8O_2$	1534	622	210	1642	209	-730
			C$_3$H$_7$OH			
C_4H_8O	933	565	210	791	209	-423
$C_5H_{10}O$	922	565	210	598	209	-241
$C_4H_8O_2$	1854	565	210	1642	209	-353
			CH$_3$CH(OH)CH$_3$			
C_4H_8O	1141	767	211	791	209	-417
$C_5H_{10}O$	1117	767	211	598	209	-248
$C_4H_8O_2$	2066	767	211	1642	209	-343

[a] this work

[b] data taken from literature as given by reference numbers
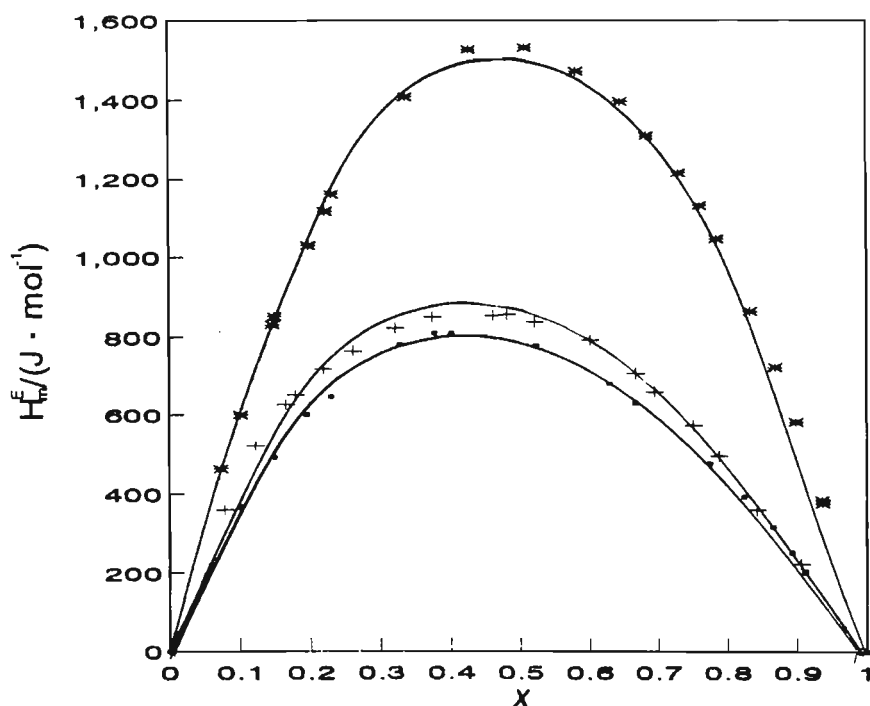
Figure 3.14 Excess molar enthalpies, H_m^E at 298.15 K for {x C_2H_5OH + (1-x) ROR'} where ROR' is ▪, THF or
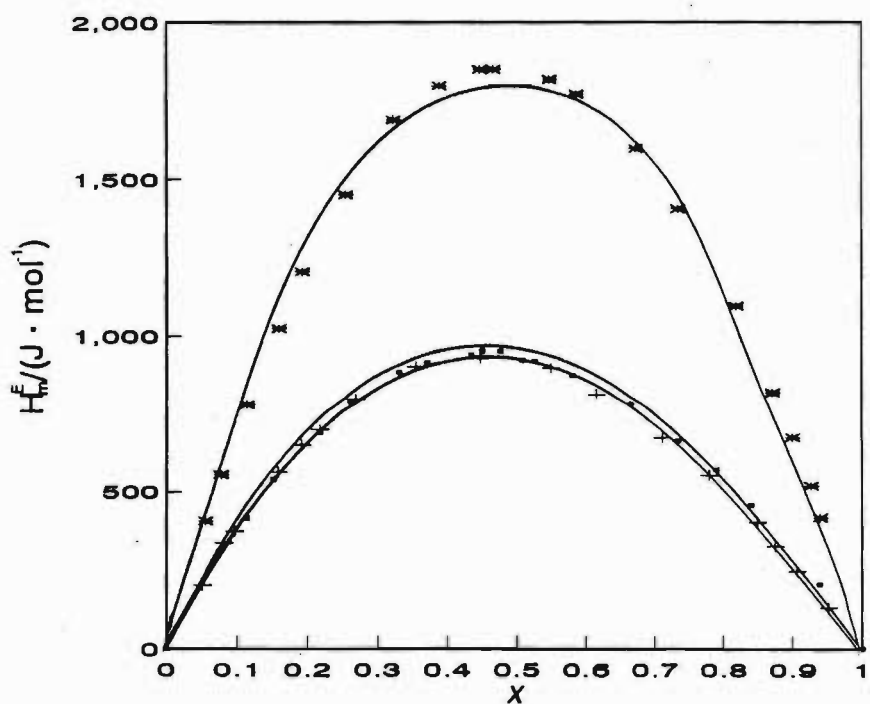
+ , THP or *,1,4-dioxane

Figure 3.15 Excess molar enthalpies, H_m^E at 298.15 K for {x C_3H_7OH + (1-x) ROR'} where ROR' is + ▪, THF or
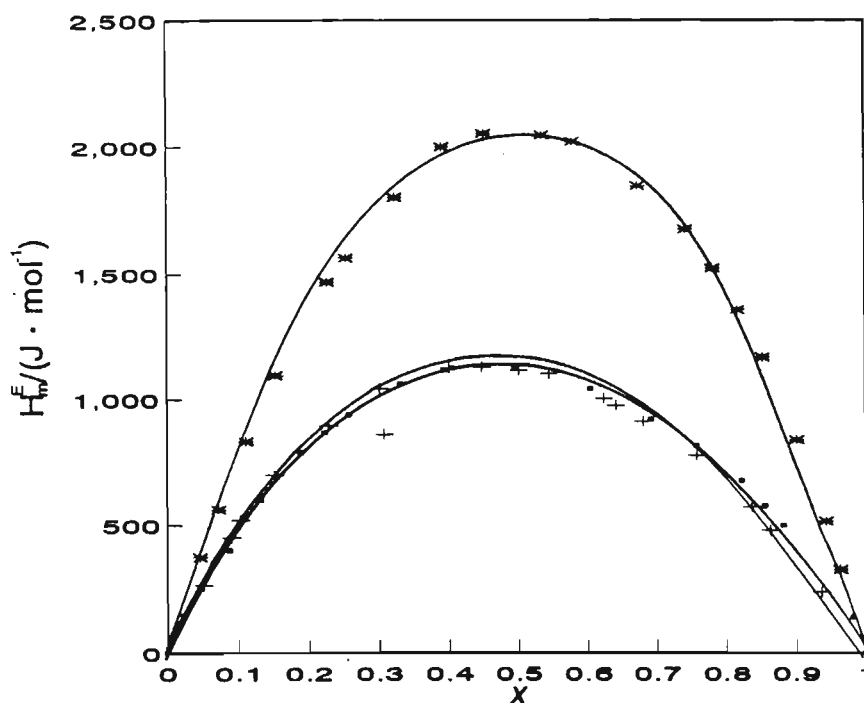
or + , THP or *,1,4-dioxane

Figure 3.16 Excess molar enthalpies, H_m^E at 298.15 K for {CH₃CH(OH)CH₃ + (1-x) ROR'} where ROR' is ■,

*THF or +, THP or *,1,4-dioxane*

3.5.3 Mixtures of (a secondary amine + a branched chain or cyclic ether)

3.5.3.1 Previous work

H_m^E values have been reported for many binary systems containing secondary amines. Direct calorimetric H_m^E data have been reported by Sosnkowska Kehiaian et al.[213] for (diethylamine + *n*-pentane) at 298.15 K and for (diethylamine + *n*-hexane) by Velasco et al.[214] at 303.15 K. The endothermic effects exhibited by the (a secondary amine + a hydrocarbon) mixture were reported to be smaller than the corresponding primary amine counterpart. This led to the conclusion that the association energy in primary amines is larger than in the corresponding secondary amine and the the association energy in aliphatic amines decreases with increasing length of the hydrocarbon chain.[214] Letcher and Bayles[139] have also reported H_m^E data at 298.15 and 318.15 K for (diethylamine + benzene or chlorobenzene). These authors reported endothermic behaviour for the (diethylamine + benzene) system

(332 J·mol^{-1} at 298.15 K and 315 J·mol^{-1} at 318.15 K) while exothermic behaviour was reported for the (diethylamine + chlorobenzene) system (-125 J·mol^{-1} at 298.15 K and -114 J·mol^{-1} at 318.15 K). Sarmiento et al.[215] have reported endothermic behaviour for (di-n-propylamine + an n-alkane) systems at 298.15 K. The results were interpreted as the dominance of the rupture of hydrogen bonds formed by the amine group over the formation of other interactions in the mixture. The maxima of all the curves reported by Sarmiento et al.[215] lie toward the lower amine concentration which was explained by supposing that the addition of a small quantity of di-n-propylamine to an inert liquid breaks all hydrogen bonds whereas unbroken bonds remain in mixtures rich in amine.[215,216] Positive H$_m^E$ values, which are symmetrical about mole fraction x = 0.52 were observed for (ethyl-acetate or ethyl-propionate + di-n-propylamine) at 298.15 K by Nunez et. al.[217,218]

Excess enthalpies measured on mixtures of (an amine + an alkanol) show some of the strongest negative values, found for organic mixtures in the literature.[82,110,219] The reason is the existence of strong intermolecular interactions between the NH group of the amine molecule(A) and the oxygen atom of the alcohol molecule. In contrast to that, the H$_m^E$ for (an amine + an ester or an ether)[220] were found to be positive. H$_m^E$ data have been reported by the present author[221] for the same ethers investigated here with di-n-butylamine. The results indicated a strong interaction between the secondary amine + an ether which increased in the following order: IPE > TAME > TBME for the branched chain ethers and THP > THF > 1,4-dioxane for the cyclic ethers. These results together with the results presented here, have been used to obtain a discernable trend displayed by the (symmetrical secondary amine + ethers) systems upon increasing the alkyl chain length of the amine.

3.5.3.2 *This work*

The H$_m^E$ results for {(diethylamine or di-n-propylamine) + IPE or TBME or TAME or THF or THP or 1,4-dioxane)} are presented in Table 3.3 to 3.6 with the parameters by equation 3.9 given in Table 3.12. Figures 3.17 to 3.20 show the curves calculated from equation 3.9 and the experimental results for all the mixtures. H$_m^E$ for the (a secondary amine + a branched chain ether) are small and positive over the whole mole fraction range with

H_m^E(maximum) decreasing marginally in the order IPE > TBME $\approx$ TAME for diethylamine and IPE $\approx$ TBME $\geq$ TAME for di-n-propylamine. The H_m^E curves for the (a secondary amine + a branched chain ether) are all symmetrical around equimolar concentrations with the exception of (di-n-propylamine + TAME) system. For the latter mixture the H_m^E curves are skewed towards x = 0.3 amine mole fraction. H_m^E curves for the (diethylamine + THF) and (di-n-propylamine + THP) mixtures are small and positive over the entire composition range while the H_m^E curves for the (diethylamine + THP) and (di-n-propylamine + THF) mixtures are S-shaped with positive effects at mole fraction x < 0.6 and negative effects in the amine rich region. The H_m^E curves for the (diethylamine + 1,4-dioxane) and (di-n-propylamine + 1,4-dioxane) mixtures are substantially more positive than the other amine + cycloether binary systems. This could be due to the larger more positive effect of the breakdown of the self association of the dioxane ring ether molecules which in turn is due to the large quadrupole moment.[221]

H_m^E (x = 0.5) for (a secondary amine + branched chain ether) are more positive than H_m^E (x = 0.5) for (a secondary amine + a cyclic ether) mixtures. This indicated that the inductive effect of the methyl groups in the branched chain ethers appears to increase the electron density at the oxygen atom resulting in enhanced self association. This result is similar to that obtained in our previous work with di-n-butylamine. It can be concluded from the relatively small H_m^E (x = 0.5) results for all the systems investigated here (14 < H_m^E(x = 0.5)/(J·mol^{-1}) < 177) except the (diethylamine or di-n-propylamine + 1,4-dioxane) system, that the overall magnitude of H_m^E is due to two almost equivalent effects (a) the positive effect due to the combined breakdown of the diethylamine or di-n-propylamine and ether self association and (b) the negative effect of the (amine -ether) association. The small positive results are direct evidence of the presence of amine-ether interactions.

If we compare the H_m^E (x = 0.5) results for (di-butylamine + IPE or TBME or TAME)[221] with those presented here, no trend relating the increase in alkyl chain length of the amine to the H_m^E behaviour for all of the ethers could be elucidated except for 1,4-dioxane. These results are presented in Table 3.16 and for (diethylamine or di-n-propylamine or di-n-butylamine + 1,4-dioxane) systems the increase in alkyl chain length of the amine results in

a much more positive H_m^E (x = 0.5) value. This effect indicates that with the addition of -CH_2 groups to the amine molecule, the association effects between the two oxygen atoms in the ring ether and the -NH group in the amine become weaker and the breakdown of the self association effects in both the amine and the ether takes prominence and dictates the behaviour of the system. The fact that no trend could be established for H_m^E for the three amines (diethylamine or di-n-propylamine or di-n-butylamine) with all the ethers except 1,4-dioxane is quite surprising as the three amines have similar dipole moments.[108] Consequently, we can deduce that structural effects are significant and play an important role in describing H_m^E results.

TABLE 3.16 Excess molar enthalpies: H_m^E (0.5 $CH_3(CH_2)_nNH(CH_2)_nCH_3$ + 0.5ROR') for n = 1, 2 or 3 at 298.15 K. ROR' is a branched chain or cyclic ether.

ROR'	$H_m^E(0.5)/(J \cdot mol^{-1})$		
	n=1[a]	n=2[a]	n=3[b]
$\{CH_3CH(CH_3)\}_2O$	177.1	26.7	31.9
$CH_3C(CH_3)_2OCH_3$	110.2	26.4	80.4
$CH_3CH_2C(CH_3)_2OCH_3$	107.9	15.4	45.2
C_4H_8O	51.2	13.9	104.1
$C_5H_{10}O$	27.3	58.6	62.9
$C_4H_8O_2$	628.6	712.7	980.7

[a] this work

[b] data taken from reference 221
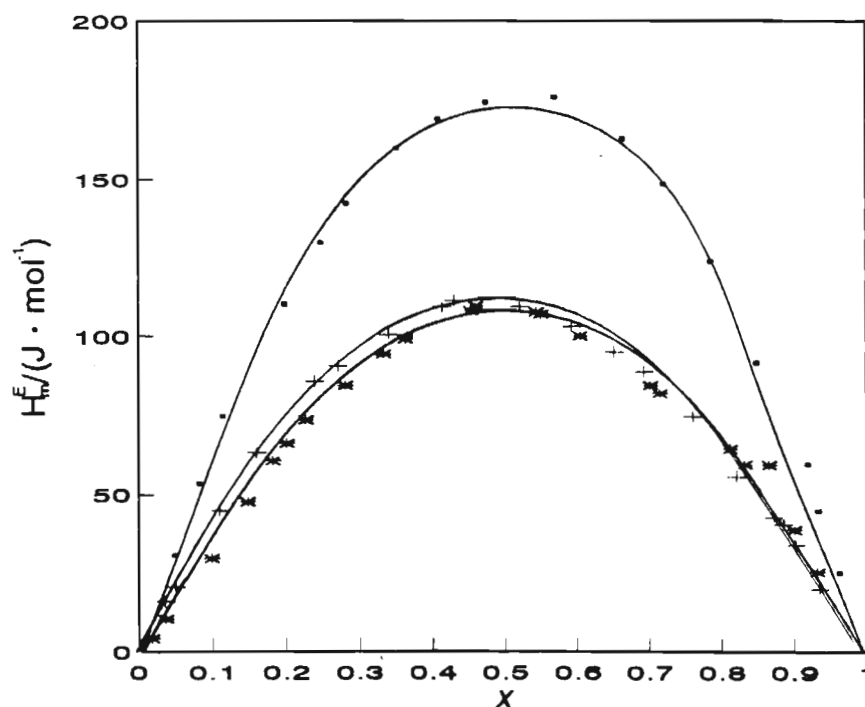
Figure 3.17 Excess molar enthalpies, H_m^E at 298.15 K for {x $CH_3CH_2NHCH_2CH_3$ + (1-x) ROR'} where ROR' is ■,
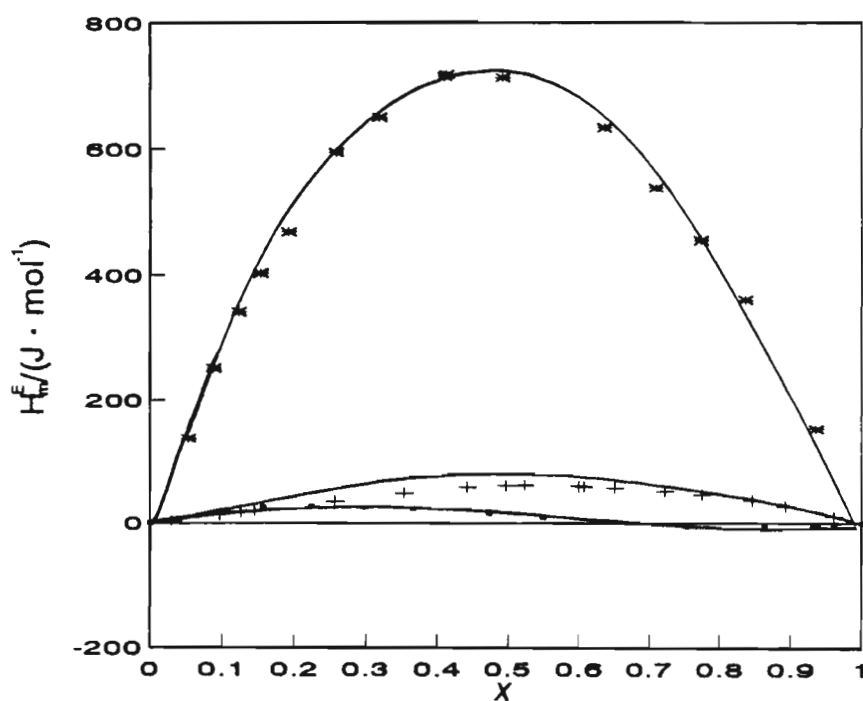
*IPE or +, TBME or *,TAME*

Figure 3.18 Excess molar enthalpies, H_m^E at 298.15 K for {x $CH_3CH_2NHCH_2CH_3$ + (1-x)ROR/} where ROR/ is

*■, THF or +, THP or *,1,4-dioxane*
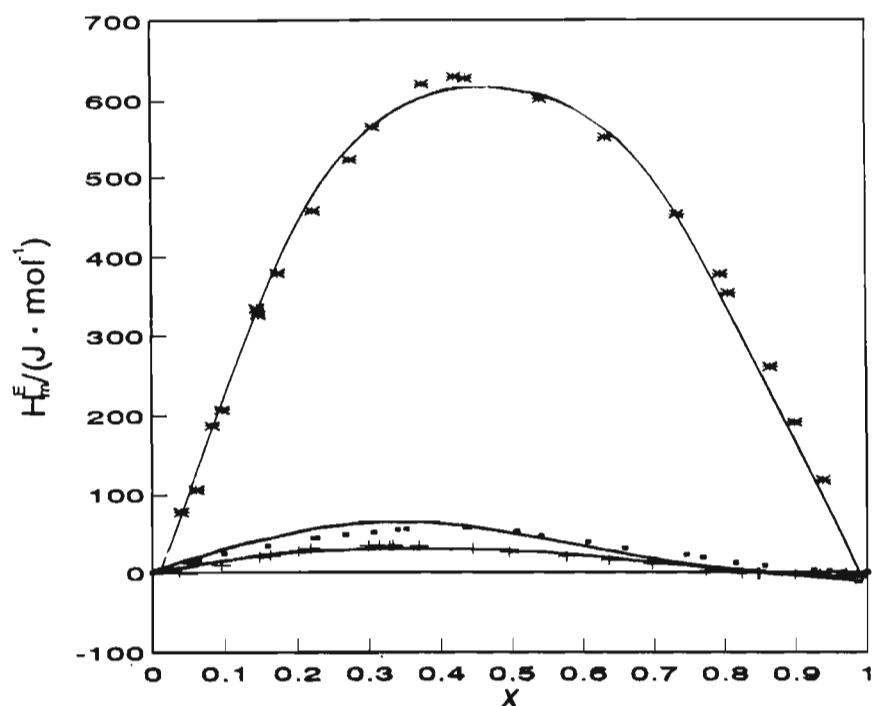
*Figure 3.19 Excess molar enthalpies, H_m^E at 298.15 K for {x $CH_3(CH_2)_2NH(CH_2)_2CH_3$ + (1-x) ROR'} where ROR' is + ■, IPE or +, TBME or *,TAME*
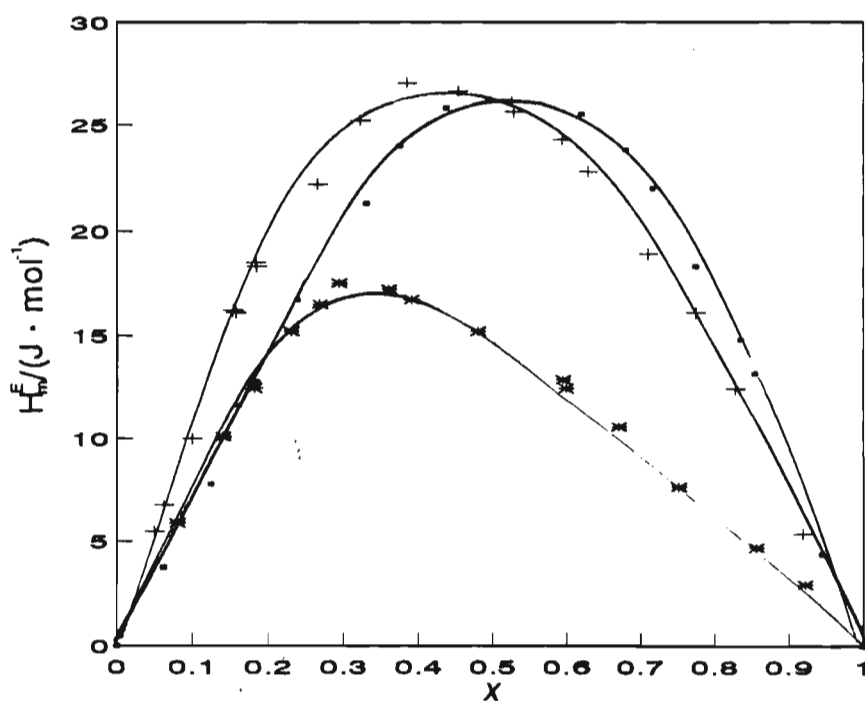
*Figure 3.20 Excess molar enthalpies, H_m^E at 298.15 K for {x $CH_3(CH_2)_2NH(CH_2)_2CH_3$ + (1-x) ROR'} where ROR' is ■, THF or +, THP or *,1,4-dioxane)}*

3.5.4 <u>Mixtures of (1-alkyne + a branched chain ether)</u>

3.5.4.1 Previous work

There is a scarcity of available literature data on systems containing alkynes and polar or nonpolar components. Woycicki and Rhensius[123] have reported endothermic H_m^E curves for the (an alkane + a 1-alkyne) system which are nearly symmetrical. These authors compared H_m^E(maximum) for 1-alkene + alkane with the corresponding (a 1-alkyne + an alkane) system and concluded that the triple bonds in the 1-alkyne molecules are disproportionably stronger than the double bond between the 1-alkene molecules. Small positive or negative H_m^E results for the system (1-hexyne or 1-heptyne + tetrachloromethane) were indicative of the n-π type interaction between the 1-alkyne and the chlorinated compound.[123,222]

Otsa et al.[124] reported $H_m^E(x=0.5)$ data for (1-octyne + *n*-octane) at 298.15 and 318.15 K of 518.5 and 479.2 J·mol^{-1}, respectively. Wilhelm et al.[116] have reported exothermic behaviour for $H_m^E(x=0.5)$ = 300.1 J·mol^{-1} of (1-hexyne + triethylamine) and the results were interpreted in terms of association between the acidic hydrogen of the terminal alkyne and the lone pair electrons of the nitrogen. Letcher et al.[125-128], have reported small positive H_m^E results for (1-hexyne + benzene and the methyl substituted derivatives) while exothermic H_m^E behaviour was observed for the (1-heptyne or 1-octyne + benzene and the methyl substituted derivatives) systems at 298.15 K. These authors interpreted the results in terms of increased association between the aromatic ring and the acidic hydrogen of the 1-alkyne with an increase in chain length of the 1-alkyne. The H_m^E behaviour of {(1-hexyne or 1-heptyne or 1-octyne) + an alkanol} at 298.15 K has been studied by Letcher et al. and the present author.[129,130] The H_m^E results were all positive with the H_m^E curves skewed towards the alkyne rich region and dissociation effects of the component molecules were considered to be the dominating factor in determining H_m^E.

3.5.4.2 This work

The H_m^E results for {(1-hexyne or 1-heptyne or 1-octyne) + IPE or TBME or

TAME)} are presented in Table 3.7 to 3.9 with the parameters by equation 3.9 given in Table 3.13. Figures 3.21 to 3.23 show the curves calculated from equation 3.9 and the experimental results for all the mixtures. H_m^E for the (an 1-alkyne + a branched chain ether) are all exothermic with no significant change in H_m^E(maximum) on increasing the carbon number of the 1-alkyne. For each of the 1-alkynes, the IPE system exhibits the largest negative H_m^E(maximum) value compared with almost equivalent H_m^E(maximum) values for TBME or TAME. All the H_m^E curves presented here are symmetrical as seen in figures 3.21 to 3.23. The negative H_m^E values obtained in this work for all the systems is most likely a superimposition of two effects (i) the hydrogen bond capability between the acidic terminal hydrogen in the 1-alkyne and the oxygen in the ether and (ii) the π-n interactions between the carbon-carbon triple bond in the 1-alkyne and the lone pair electrons of the oxygen in the ether. Similar behaviour has been reported by other workers.[116,123,222,223]

No H_m^E results have been reported in the literature for comparison with the data presented here. However, H_m^E results at 298.15 K for the (1-hexyne + di-n-propyl ether) system have been reported by Wilhelm et al.[116] Our H_m^E (x=0.5) result for (1-hexyne + IPE) is -259 J·mol^{-1} while the result of Wilhelm et al.[116] for (1-hexyne + di-n-propyl ether) is reported as -185.5 J·mol^{-1}.

Comparing the H_m^E results presented here with the (a 1-alkyne + an alkanol) system[129,130] at x = 0.5 as shown in Table 3.17 shows that dissociation effects are prominent in the alkanol mixtures while for the ether mixtures dissociation effects become negligible and the behaviour of the system is determined by cross association between the component molecules.

TABLE 3.17 Equimolar H_m^E for (1-alkyne + a branched chain ether) and (1-alkyne + an alkanol) at 298.15 K

1-alkyne	$H_m^E(x = 0.5)$			
	$(J \cdot mol^{-1})$			
	IPE	TBME	TAME	-
1-hexyne	-259	-431	-329	-
1-heptyne	-245	-397	-331	-
1-octyne	-266	-390	-333	-
	methanol	ethanol	propan-1-ol	propan-2-ol
1-hexyne	521	622	806	1097
1-heptyne	579	723	836	1126
1-octyne	611	676	860	1154
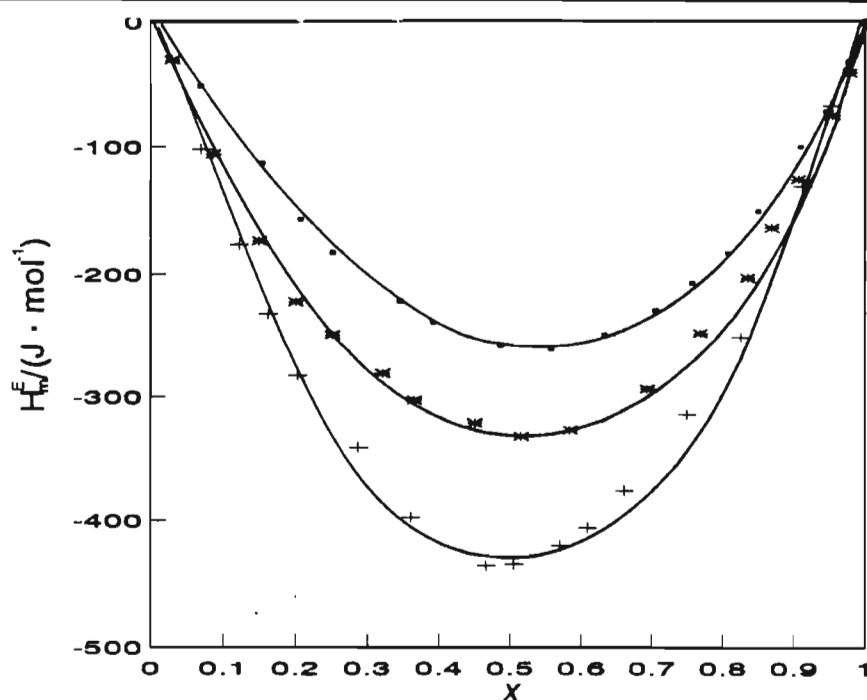
*Figure 3.21 Excess molar enthalpies, H_m^E at 298.15 K for {x 1-C_6H_{10} + (1-x) ROR'} where ROR' is (■, IPE or +, TBME or *,TAME*
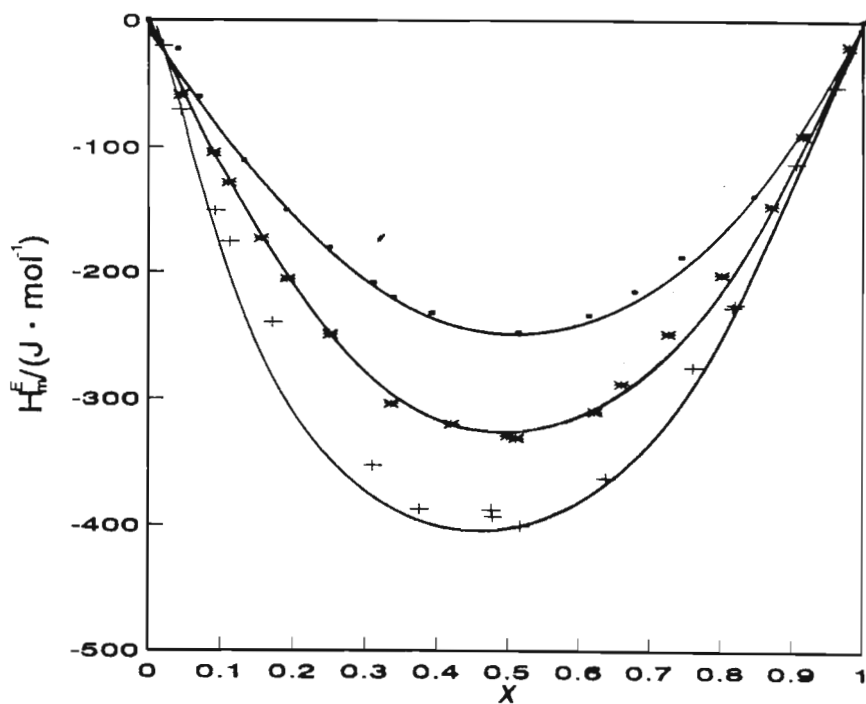
Figure 3.22 Excess molar enthalpies, H_m^E at 298.15 K for {x 1-C_7H_{12} + (1-x) ROR'} where ROR' is ■, *IPE or* +,
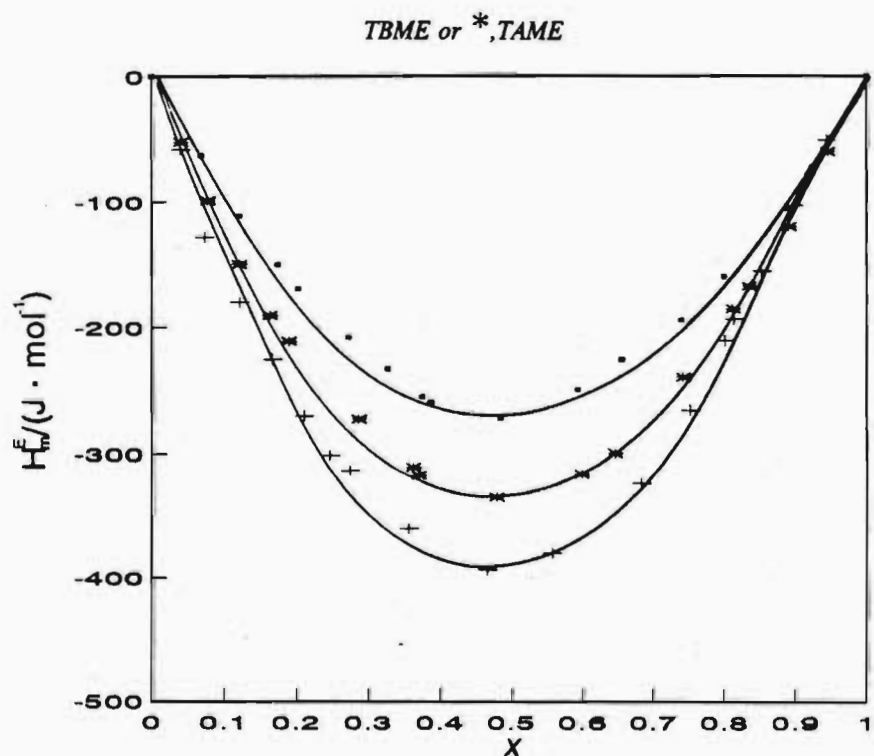
TBME or *,*TAME*

Figure 3.23 Excess molar enthalpies, H_m^E at 298.15 K for {x 1-C_8H_{14} + (1-x) ROR'} where ROR' is ■, *IPE or* +,

TBME or *,*TAME*

3.6   Application of NRTL. UNIQUAC and UNIQUAC ASM Theories

3.6.1 Introduction

The experimental H_m^E results have been correlated using the NRTL equation,[14,224] the simple UNIQUAC equation[15] and UNIQUAC ASM model.[16] The equations related to the models are given in chapter 5, section 5.3.2 and the exact mathematical forms of the pure components structural parameter r (volume parameter) and q (surface parameter) have been presented by Domanska et al.[225]. All the results of the calculations are shown in Tables 3.18 to 3.20, where the binary parameters and absolute arithmetic mean deviations are obtained by minimizing the sum of the deviations between the experimental and calculated H_m^E values using the Marquardt's maximum likelihood method for minimization.[226] The molar enthalpies of formation for all the associating species (h_A) were assumed to be independent of temperature and the temperature dependence of the equilibrium constant was calculated by the van't Hoff relation. The molar volume for all the pure components were calculated from the experimental density values given in Table 2.1.

3.6.2 Results and Discussion

3.6.2.1 Mixtures of (an alkanol + a branched chain or cyclic ether)

The calculations with the NRTL, UNIQUAC and UNIQUAC ASM (Mecke Kempter model of association for all the methanol systems and the Krestchmer Wiebe model of association for all the other systems) are listed in Table 3.18 for all the alkanols investigated here. The UNIQUAC ASM calculations were carried out with the association equilibrium constants and molar enthalpy of formation for the pure alkanols ($h_A = -25.0$ kJ·mol^{-1}) obtained from the literature.[227-231] Figure 3.24 shows the comparison of the experimental and calculated H_m^E values using the NRTL equation for (propan-1-ol + IPE) as an example.

The results of the correlation of experimental points with the two parameters NRTL and UNIQUAC equations are fairly high as judged by the values of the average standard deviation $<\sigma^b>$. From Table 3.18 it can be seen that for all the mixtures, $<\sigma>$ improves slightly for the NRTL and UNIQUAC models as the chain length of the alkanol increases however that the opposite trend is observed for the UNIQUAC ASM model i.e.,the $<\sigma>$ is larger for the propan-1-ol systems than the methanol systems. The description obtained by means of the NRTL, UNIQUAC and UNIQUAC ASM models with two-and three-adjustable parameter is larger than that obtained by the three-or four-parameter Redlich-Kister equation.
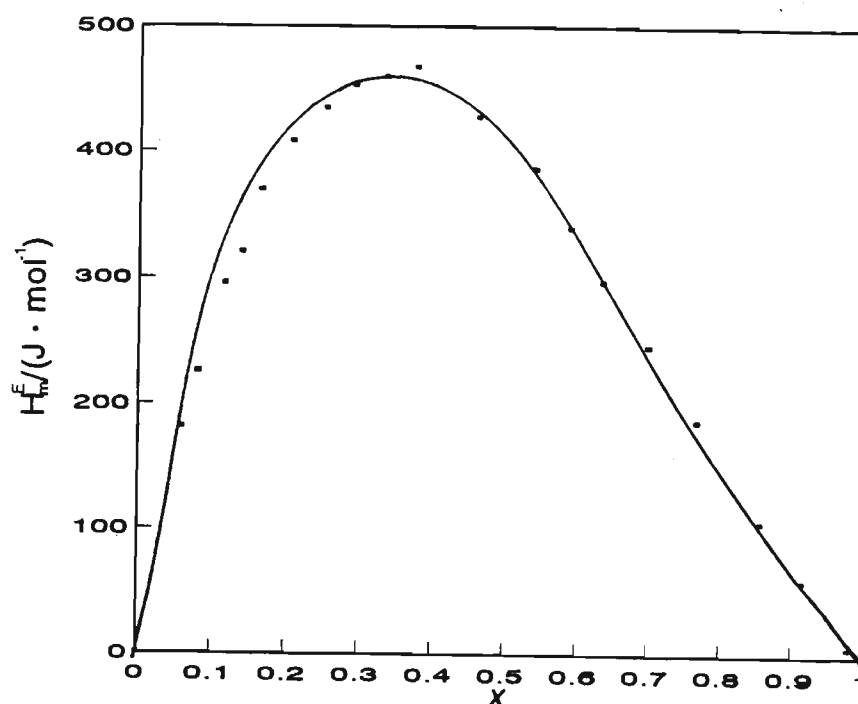
Figure 3.24 Excess molar enthalpies, H_m^E at 298.15 K for {x CH₃(CH₂)₂OH + (1-x) ■, IPE } Experimental points are matched by the curve calculated by the NRTL equation

TABLE 3.18 Correlation of the excess molar enthalpies for $\{x\ C_jH_{2j+1}OH\ +\ (1\text{-}x)\ ROR'\}$ for j = 1, 2 or 3 by means of the NRTL, UNIQUAC and UNIQUAC ASM equations: values of parameters, where u^o = 1 J·mol⁻¹, and measures of deviations. ROR′ is a branched chain or cyclic ether.

ROR′	Parameters			Deviations		
	NRTL[a]	UNIQUAC	UNIQUAC ASM	NRTL	UNIQUAC	UNIQUAC ASM
	$g_{12}\text{-}g_{11}/u^o$	$\Delta u_{12}/u^o$	$\Delta u_{12}/u^o$		σ^b	
	$g_{12}\text{-}g_{22}/u^o$	$\Delta u_{21}/u^o$	$\Delta u_{12}/u^o$	σ^c	σ_r^d	σ_r^d
			CH₃OH			
$\{CH_3CH(CH_3)\}_2O$	-2156.1	-1112.1	-595.5	17.5	16.1	29.5
	5230.3	3087.2	-665.7	62.0	36.3	47.5
$CH_3C(CH_3)_2OCH_3$	-1732.7	-919.5	915.0	18.8	14.9	30.9
	4913.1	3281.5	1662.2	1765.2	425.6	1865.2
$CH_3CH_2C(CH_3)_2OCH_3$	-1370.4	-828.8	-847.7	11.9	9.2	22.9
	4445.7	3115.3	1725.1	138.4	81.5	127.9
$c\text{-}(CH_2)_4O$	-601.0	-180.6	-255.7	66.7	66.8	66.7
	4004.3	3184.0	1779.9	27.3	27.7	27.3
$c\text{-}(CH_2)_5O$	-32.1	72.4	-110.1	14.5	10.1	24.1
	4207.0	3767.1	2136.2	5.4	4.0	6.9
$c\text{-}(CH_2)_2O(CH_2)_2O$	2106.2	2233.7	1403.5	15.0	82.4	50.0
	4044.3	4246.7	2896.3	3.0	15.2	11.4

[a]: calculated for α_{12} = 0.2 taken from reference 188

[b]: given by eqn. $\sigma = [\Sigma(H^E_{m(exp)} - H^E_{m(calc)})^2/ (n - k)]^{1/2}$.

[c]: given by eqn. $\sigma = (\delta H^E_m / H^E_m)$

[d]: given by eqn. $\sigma_r = 100\ [\Sigma(H^E_{m(exp)} - H^E_{m(calc)})^2/(H^E_{m(exp)})^2 (n - k)]^{1/2}$.

TABLE 3.18 Continued

ROR′	Parameters			Deviations		
	NRTL[a]	UNIQUAC	UNIQUAC ASM	NRTL	UNIQUAC	UNIQUAC ASM
	$g_{12}\text{-}g_{11}/u^\circ$	$\Delta u_{12}/u^\circ$	$\Delta u_{12}/u^\circ$		σ^b	
	$g_{12}\text{-}g_{22}/u^\circ$	$\Delta u_{21}/u^\circ$	$\Delta u_{12}/u^\circ$	σ^c	σ_r^d	σ_r^d
			C_2H_5OH			
$\{CH_3CH(CH_3)\}_2O$	-1409.9	-821.1	-820.9	12.3	14.9	50.7
	5326.6	3143.2	726.1	48.2	8.3	58.9
$CH_3C(CH_3)_2OCH_3$	-815.1	-567.1	-220.7	6.9	5.6	54.5
	4294.2	2745.4	211.8	13.3	8.6	27.2
$CH_3CH_2C(CH_3)_2OCH_3$	-732.4	-578.9	-269.3	13.0	18.8	45.2
	4591.3	2979.7	256.0	7.1	8.3	17.9
$c\text{-}(CH_2)_4O$	509.9	450.1	719.5	8.3	12.9	53.7
	3852.2	2535.5	325.9	2.2	3.6	81.7
$c\text{-}(CH_2)_5O$	548.8	290.8	293.9	20.9	15.6	29.7
	4506.2	3151.0	680.3	3.7	3.2	8.0
$c\text{-}(CH_2)_2O(CH_2)_2O$	4703.9	3168.7	2431.7	11.8	182.9	57.8
	5345.2	3640.9	1738.9	1.5	14.5	8.9

[a]: calculated for $\alpha_{12} = 0.2$ taken from reference 188

[b]: given by eqn. $\sigma = [\Sigma(H_{m(exp)}^E - H_{m(calc)}^E)^2/(n - k)]^{1/2}$.

[c]: given by eqn. $\sigma = (\delta H_m^E / H_m^E)$

[d]: given by eqn. $\sigma_r = 100 [\Sigma(H_{m(exp)}^E - H_{m(calc)}^E)^2/(H_{m(exp)}^E)^2 (n - k)]^{1/2}$.

TABLE 3.18 Continued

ROR$'$	Parameters			Deviations		
	NRTL[a]	UNIQUAC	UNIQUAC ASM	NRTL	UNIQUAC	UNIQUAC ASM
	$g_{12}\text{-}g_{11}/u^\circ$	$\Delta u_{12}/u^\circ$	$\Delta u_{12}/u^\circ$		σ^b	
	$g_{12}\text{-}g_{22}/u^\circ$	$\Delta u_{21}/u^\circ$	$\Delta u_{12}/u^\circ$	σ^c	σ_r^d	σ_r^d
			C_3H_7OH			
$\{CH_3CH(CH_3)\}_2O$	-1286.9	-770.4	-795.5	6.2	7.7	79.7
	4991.8	2696.0	695.6	28.9	15.1	39.1
$CH_3C(CH_3)_2OCH_3$	-629.2	-478.5	1222.6	11.5	12.6	41.4
	4420.2	2457.9	-760.4	15.8	14.3	34.0
$CH_3CH_2C(CH_3)_2OCH_3$	-473.2	-492.9	-217.8	10.3	13.6	80.9
	4107.9	2381.2	208.8	6.1	7.2	28.9
$c\text{-}(CH_2)_4O$	1370.1	911.9	1536.0	10.0	13.3	57.8
	3474.3	1805.3	33.5	2.5	2.4	13.9
$c\text{-}(CH_2)_5O$	1032.7	435.3	1112.0	12.6	16.7	75.6
	3869.7	2121.5	-50.3	4.2	5.2	25.9
$c\text{-}(CH_2)_2O(CH_2)_2O$	6762.1	3253.5	3119.6	139.2	316.9	118.5
	7223.0	3423.2	2256.9	8.6	19.4	16.3

[a]: calculated for $\alpha_{12} = 0.2$ taken from reference 188

[b]: given by eqn. $\sigma = [\Sigma(H^E_{m(exp)} - H^E_{m(calc)})^2/ (n - k)]^{1/2}$.

[c]: given by eqn. $\sigma = (\delta H^E_m / H^E_m)$

[d]: given by eqn. $\sigma_r = 100 [\Sigma(H^E_{m(exp)} - H^E_{m(calc)})^2/(H^E_{m(exp)})^2 (n - k)]^{1/2}$.

TABLE 3.18 Continued

ROR'	Parameters			Deviations		
	NRTL[a]	UNIQUAC	UNIQUAC ASM	NRTL	UNIQUAC	UNIQUAC ASM
	$g_{12}\text{-}g_{11}/u^o$	$\Delta u_{12}/u^o$	$\Delta u_{12}/u^o$		σ^b	
	$g_{12}\text{-}g_{22}/u^o$	$\Delta u_{21}/u^o$	$\Delta u_{12}/u^o$	σ^c	σ_r^d	σ_r^d

$CH_3CH(OH)CH_3$

ROR'	NRTL	UNIQUAC	UNIQUAC ASM	NRTL	UNIQUAC	UNIQUAC ASM
$\{CH_3CH(CH_3)\}_2O$	-427.3	-497.7	-384.2	18.0	22.2	63.9
	5228.3	2923.5	357.7	4.2	5.8	14.3
$CH_3C(CH_3)_2OCH_3$	354.1	-151.8	1681.0	34.4	34.6	68.8
	3913.9	2284.7	-760.7	7.7	7.6	18.9
$CH_3CH_2C(CH_3)_2OCH_3$	87.7	-310.6	1714.8	21.6	22.7	69.5
	4433.8	2580.0	-875.6	4.9	5.0	16.7
$c\text{-}(CH_2)_4O$	2415.2	1519.8	2130.0	30.2	23.9	59.1
	3792.7	2078.1	59.5	13.0	11.5	22.2
$c\text{-}(CH_2)_5O$	1886.5	865.9	1430.2	10.9	8.8	67.9
	4506.2	2479.1	64.3	1.7	2.1	18.5
$c\text{-}(CH_2)_2O(CH_2)_2O$	7486.8	3722.2	3478.1	289.9	192.6	460.9
	7142.1	2565.1	3363.8	17.0	20.5	27.8

[a]: calculated for $\alpha_{12} = 0.2$ taken from reference 188

[b]: given by eqn. $\sigma = [\Sigma(H^E_{m(exp)} - H^E_{m(calc)})^2/ (n - k)]^{1/2}$.

[c]: given by eqn. $\sigma = (\delta H^E_m / H^E_m)$

[d]: given by eqn. $\sigma_r = 100 \,[\Sigma(H^E_{m(exp)} - H^E_{m(calc)})^2/(H^E_{m(exp)})^2 (n - k)]^{1/2}$.

3.6.2.2 Mixtures of a secondary amine + a branched chain or cyclic ether

The calculations with the NRTL, UNIQUAC and UNIQUAC ASM (Krestchmer Wiebe model of association) equations are listed in Table 3.19 for all the (a secondary amine + an ether) systems investigated here. The UNIQUAC ASM calculations were carried out with the association equilibrium constants and molar enthalpies of formation for the pure amines (h_A = -8.5 and -7.5 kJ·mol^{-1} for diethylamime and di-n-propylamine, respectively) obtained from the literature.[104,133,232] The enthalpy of formation was assumed to be independent of temperature and the equilibrium constant was calculated by the van't Hoff relation. Figure 3.25 shows the comparison of the experimental and calculated H_m^E values using the UNIQUAC equation for (di-n-propylamine + TBME) as an example.

The results of the correlation of experimental points with the two-parameter NRTL and UNIQUAC equations are in the same range as the three- or four- parameter Redlich-Kister equation. For the all the systems presented here, the description of the excess molar enthalpies were given by the NRTL model with average standard deviations $<\sigma>$ = 2.9 and 1.2 J·mol^{-1} for the diethylamine and di-n-propylamine systems (with the exception of 1,4-dioxane) respectively. The description of excess molar enthalpy given by the UNIQUAC model with average standard deviations $<\sigma>$ = 3.3 and 1.7 J·mol^{-1} for the diethylamine and di-n-propylamine systems,(with the exception of 1,4-dioxane) respectively. The correlation of experimental points in binary mixtures with the results, obtained by means of the UNIQUAC ASM model are not as good as those obtained by simple NRTL and UNIQUAC models($<\sigma>$ = 15.2 and 8.4 J·mol^{-1} for diethylamine and di-n-propylamine systems). The description obtained by means of the UNIQUAC ASM model with the association constant as the third adjustable parameter are worse than that observed experimentally.
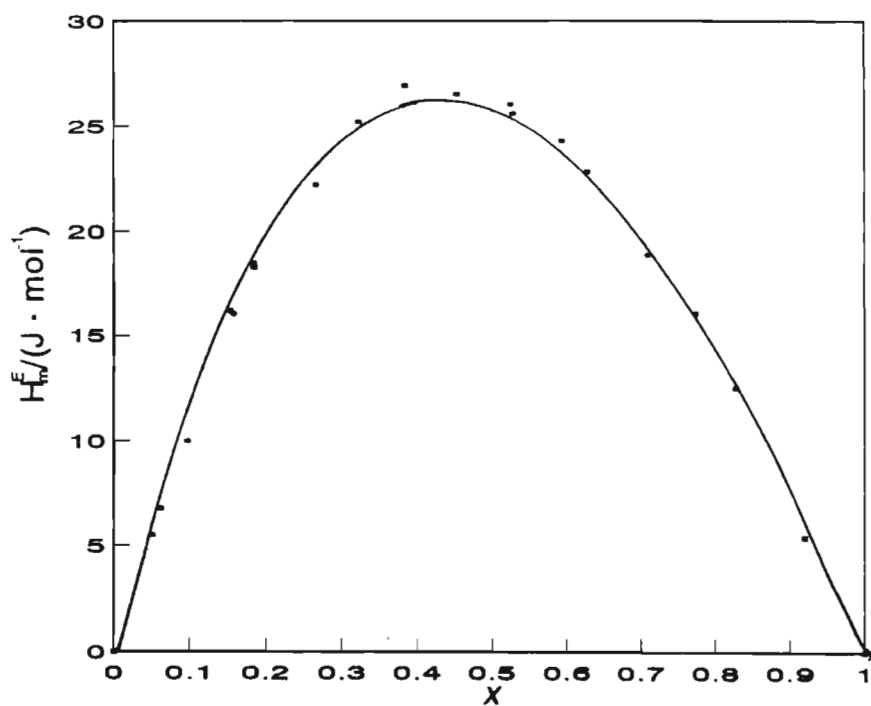
Figure 3.25 Excess molar enthalpies, H_m^E at 298.15 K for $\{x\ CH_3(CH_2)_2NH(CH_2)_2CH_3 + (1-x)$ ■, TBME$\}$ Experimental points are matched by the curve calculated by the UNIQUAC equation

TABLE 3.19 Correlation of the excess molar enthalpies for $\{x\ CH_3(CH_2)_nNH(CH_2)_nCH_3 + (1-x)\ ROR'\}$ for n = 1 or 2 by means of the NRTL, UNIQUAC and UNIQUAC ASM equations: values of parameters, where $u^\circ = 1\ J\cdot mol^{-1}$, and measures of deviations

ROR'	Parameters				Deviations		
	NRTL[a]	UNIQUAC	UNIQUAC	ASM	NRTL	UNIQUAC	UNIQUAC
			$\Delta u_{12}/u^\circ$				ASM
	$g_{12}\text{-}g_{11}/u^\circ$	$\Delta u_{12}/u^\circ$	$\Delta u_{12}/u^\circ$			σ^b	
	$g_{12}\text{-}g_{22}/u^\circ$	$\Delta u_{21}/u^\circ$			σ^c	σ_r^d	σ_r^d

$$CH_3CH_2NHCH_2CH_3$$

ROR'	NRTL	UNIQUAC	UNIQUAC ASM		NRTL	UNIQUAC	UNIQUAC ASM
$\{CH_3CH(CH_3)\}_2O$	533.9	-121.3	-1016.5		2.2	2.3	24.9
	218.8	386.6	845.8		3.4	4.0	30.9
$CH_3C(CH_3)_2OCH_3$	-259.8	-301.2	-1079.8		1.7	1.7	16.1
	775.8	528.4	888.9		5.5	5.3	38.5
$CH_3CH_2C(CH_3)_2OCH_3$	288.5	-149.3	-1102.4		3.3	3.3	20.2
	146.2	315.6	906.8		21.0	21.0	77.6
$c\text{-}(CH_2)_4O$	-983.1	-506.0	-1198.6		3.8	4.8	7.3
	1594.7	765.3	1027.6		188.9	256.5	309.1
$c\text{-}(CH_2)_5O$	-1112.0	-635.0	-1001.9		3.7	4.5	7.6
	1702.7	927.4	545.5		119.8	158.2	270.5
$c\text{-}(CH_2)_2O(CH_2)_2O$	1084.8	695.2	1522.4		19.9	19.5	32.2
	1985.4	532.7	-680.7		15.1	14.8	22.8

[a]: calculated for $\alpha_{12} = 0.2$ taken from reference 188

[b]: given by eqn. $\sigma = [\Sigma(H^E_{m(exp)} - H^E_{m(calc)})^2/ (n - k)]^{1/2}$.

[c]: given by eqn. $\sigma = (\delta H^E_m / H^E_m)$

[d]: given by eqn. $\sigma_r = 100\ [\Sigma(H^E_{m(exp)} - H^E_{m(calc)})^2/(H^E_{m(exp)})^2\ (n - k)]^{1/2}$.

TABLE 3.19 Continued

ROR'	Parameters				Deviations		
	NRTL[a]	UNIQUAC	UNIQUAC	ASM	NRTL	UNIQUAC	UNIQUAC
			$\Delta u_{12}/u^o$				ASM
	$g_{12}\text{-}g_{11}/u^o$	$\Delta u_{12}/u^o$	$\Delta u_{12}/u^o$			σ^b	
	$g_{12}\text{-}g_{22}/u^o$	$\Delta u_{21}/u^o$			σ^c	σ^d_r	σ^d_r

$$CH_3(CH_2)_2NH(CH_2)_2CH_3$$

ROR'	NRTL	UNIQUAC	UNIQUAC		NRTL	UNIQUAC	UNIQUAC ASM
$\{CH_3CH(CH_3)\}_2O$	545.9	264.8	-896.4		1.1	1.2	10.9
	-390.1	-212.5	760.2		16.9	17.1	115.6
$CH_3C(CH_3)_2OCH_3$	-534.1	-251.4	-889.3		0.5	0.6	8.5
	738.9	317.2	756.4		6.4	7.0	1.1
$CH_3CH_2C(CH_3)_2OCH_3$	-764.3	-408.5	-628.4		0.7	0.8	1.3
	1022.2	513.3	347.7		9.9	9.7	16.4
$c\text{-}(CH_2)_4O$	-1260.0	-686.4	-502.9		1.7	4.6	5.5
	1962.4	1017.5	135.0		29.7	64.5	71.8
$c\text{-}(CH_2)_5O$	1066.4	773.4	-840.8		1.8	1.3	15.9
	-649.5	-523.2	716.6		10.8	6.4	99.9
$c\text{-}(CH_2)_2O(CH_2)_2O$	1287.5	978.2	1307.5		13.1	12.0	17.3
	2450.2	312.5	-329.3		6.6	6.2	8.5

[a]: calculated for $\alpha_{12} = 0.2$ taken from reference 188

[b]: given by eqn. $\sigma = [\Sigma(H^E_{m(exp)} - H^E_{m(calc)})^2/ (n - k)]^{1/2}$.

[c]: given by eqn. $\sigma = (\delta H^E_m / H^E_m)$

[d]: given by eqn. $\sigma_r = 100 [\Sigma(H^E_{m(exp)} - H^E_{m(calc)})^2/(H^E_{m(exp)})^2 (n - k)]^{1/2}$.

3.6.2.3 Mixtures of 1-alkyne + a branched chain ether

The calculations with the NRTL and UNIQUAC are listed in Table 3.20 for all (a 1-alkyne + a branched chain ether) systems investigated here. Figure 3.26 shows the comparison of the experimental and calculated H_m^E values using the UNIQUAC equation for (1-octyne + TAME) as an example.

The results of the correlation of experimental points with the two-parameter NRTL and UNIQUAC equations are in the same range and in some cases better than those obtained for the three-or four- parameter Redlich-Kister equation. For the all the systems presented here, the descriptions of excess molar enthalpy were given by the NRTL and UNIQUAC models with average standard deviations $<\sigma>$ = 6.6 J·mol^{-1} and $<\sigma>$ = 6.6 J·mol^{-1}, respectively. The correlation of the experimental points in the binary mixtures with the UNIQUAC ASM model was not possible as the application of the model required an association constant as the third-adjustable parameter. The 1-alkynes are not known to be associated in the pure state.
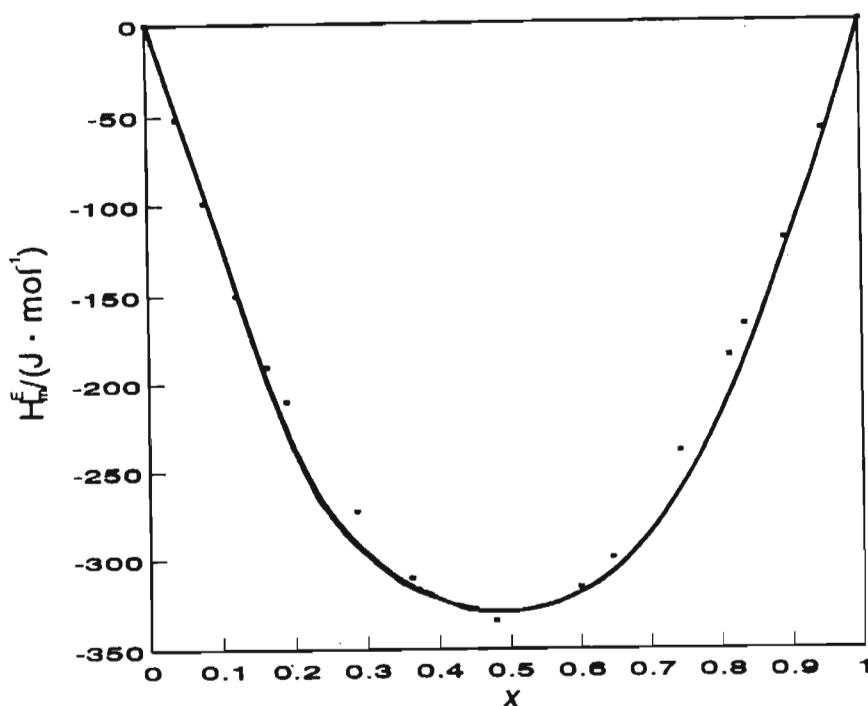
Figure 3.26 Excess molar enthalpies, H_m^E at 298.15 K for {x 1-C_8H_{14} + (1-x) ■, *TAME} Experimental points are matched by the curve calculated by the UNIQUAC equation*

TABLE 3.20 Correlation of the excess molar enthalpies for $\{xCH_3(CH_2)_nC \equiv CH + (1-x)\ ROR'\}$ for $n = 3$, 4 or 5 by means of the NRTL and UNIQUAC equations: values of parameters, where $u^o = 1\ J \cdot mol^{-1}$, and measures of deviations

ROR'	Parameters		Deviations	
	NRTL[a]	UNIQUAC	NRTL	UNIQUAC
	$g_{12}\text{-}g_{11}/u^o$	$\Delta u_{12}/u^o$		
	$g_{12}\text{-}g_{22}/u^o$	$\Delta u_{21}/u^o$	σ^b	
			σ^c	σ_r^d
$CH_3(CH_2)_3C \equiv CH$				
$\{CH_3CH(CH_3)\}_2O$	-231.2	59.3	4.0	4.0
	-602.8	-360.0	5.8	5.9
$CH_3C(CH_3)_2OCH_3$	-818.0	-338.0	7.3	7.0
	-743.0	-208.4	4.4	4.3
$CH_3CH_2C(CH_3)_2OCH_3$	-420.4	219.8	9.2	9.3
	-794.6	-196.5	51.1	51.0
$CH_3(CH_2)_4C \equiv CH$				
$\{CH_3CH(CH_3)\}_2O$	-294.6	101.0	5.5	5.5
	-617.8	-180.9	13.2	13.1
$CH_3C(CH_3)_2OCH_3$	-1009.4	-375.5	6.9	6.9
	-390.8	-101.4	18.4	18.3
$CH_3CH_2C(CH_3)_2OCH_3$	-719.7	-303.8	4.7	4.6
	-469.7	-72.8	6.1	6.0
$CH_3(CH_2)_5C \equiv CH$				
$\{CH_3CH(CH_3)\}_2O$	-633.1	-216.6	5.7	5.6
	-331.0	-64.6	3.9	3.9
$CH_3CH_2C(CH_3)_2OCH_3$	-1170.2	-376.2	12.4	12.5
	-111.9	-52.9	12.6	12.8
$CH_3CH_2C(CH_3)_2OCH_3$	-853.3	-270.2	4.1	4.1
	-328.5	-92.1	3.0	2.9

[a]: calculated for $\alpha_{12} = 0.4$

[b]: given by eqn. $\sigma = [\Sigma(H^E_{m(exp)} - H^E_{m(calc)})^2/\ (n - k)]^{1/2}$.

[c]: given by eqn. $\sigma = (\delta H^E_m / H^E_m)$

[d]: given by eqn. $\sigma_r = 100\ [\Sigma(H^E_{m(exp)} - H^E_{m(calc)})^2/(H^E_{m(exp)})^2\ (n - k)]^{1/2}$.

Chapter Four

Density, Cubical Expansion Coefficient and Isothermal Compressibility of Ethers from 288.15 K to 328.15 K and 0.1 to 10 MPa

4.1 Introduction

The second-order molar volume thermodynamic quantities of pure components; the thermal expansion coefficient, α, and the isothermal compressibilities, κ_T, are necessary parameters used in the prediction of the excess thermodynamic quantities of liquid mixtures from theoretical models[20,233] These models utilize an equation of state whose characteristic parameters for the pure liquids are obtained directly from α, κ_T and V_m (molar volume). Reliable values of α and κ_T have been determined either experimentally or through derivation for only a few liquids and in some instances are not known to sufficient accuracy.[234] One of the aims of this thesis was to test the various theories of liquid mixtures as applied to associating mixtures and for the pure liquids used in this work there existed little or no data for α and κ_T. As the equipment required to measure these pure component properties was unavailable in South Africa this work was then undertaken at the Thermodynamics Laboratory of the Indian Institute of Technology, India, New Delhi under the guidance of Professor Ahluwahlia. In this chapter the density ρ, molar volumes V_m, cubic expansion coefficients α,

and the isothermal compressibilities κ_T are determined for diisopropylether (IPE), 1,1-dimethylethyl methyl ether (tert-butyl methyl ether, TBME), 1,1-dimethylpropyl methyl ether (tert-amyl methyl ether, TAME), tetrahydrofuran (THF), tetrahydropyran (THP), and 1,4-dioxane. The data presented here have been used in chapters 5 and 6 to test the application of the Extended Real Associated Solution (ERAS) and the simple Flory and the Prigogine-Flory-Patterson(PFP) theoretical models to the H_m^E and V_m^E data for the mixtures used in this work.

4.2   Experimental

4.2.1 Materials

A summary of all the ethers used in this investigation together with the purity, density and methods of purification are given in section 2.3.1 of chapter 2.

4.2.2 Apparatus Details

Densities ρ were measured with an Anton Paar DMA 60/512 vibrating tube densimeter. All the data and results presented in this chapter have been experimentally determined at the Thermodynamics Laboratory of the Indian Institute of Technology, New Delhi, India.

4.2.2.1 The Anton Paar DMA 60/512 Densimeter

(i) Principle of operation

The density measurement of liquids is based on the electronic measurement of

frequency or period of the instrument. The mathematical derivation and the principle of operation of the Anton Paar DMA 60/512 instrument are identical to that of the Anton Paar DMA 601 used for excess molar volume determination as presented in chapter 2, sections 2.2.2 and 2.3.2. A schematic diagram of the digital densimeter DMA 60/512 is given in figure 4.1.

(ii) DMA 60 Electronic Processing Unit

The DMA 60 electronic processing unit in combination with the DMA 512 cell, offers a system for liquid density measurements of the highest accuracy for temperatures ranging from 283.15 to 313.25 K and pressure ranges up to 40 MPa. The remote cell generates a frequency analog square wave signal in synchronism with the zero amplitude position of the oscillation sample tube. These signals are transmitted into the DMA 60 electronics processing unit. The signal is fed through an optical isolator for the purpose of electrical separation and then through a noise filter. The signal is amplified and displayed digitally through the light emitting diodes.

(iii) DMA 512 Density Measuring Cell

This measuring cell is contained in its own separate housing complete with oscillator counter mass and thermostat connectors. The sample tube is made of stainless steel with a wall thickness of 0.3 mm and an internal diameter of 2.4 mm; the tube is in a brass housing which is thermostatted by the thermostat liquid. The system is excited by two magnetic dynamic invertors in connection with an electronic control and amplifier circuit, which guarantees a constant amplitude of the oscillator tube even at pressures as high as 40 MPa and temperatures as high as 423.15 K. Exit ports to and from the remote cell are fitted with stainless steel nut and swagelok fittings, which ensure tight connection for the sample transfer. A built in air pump for drying the sample tube is provided.
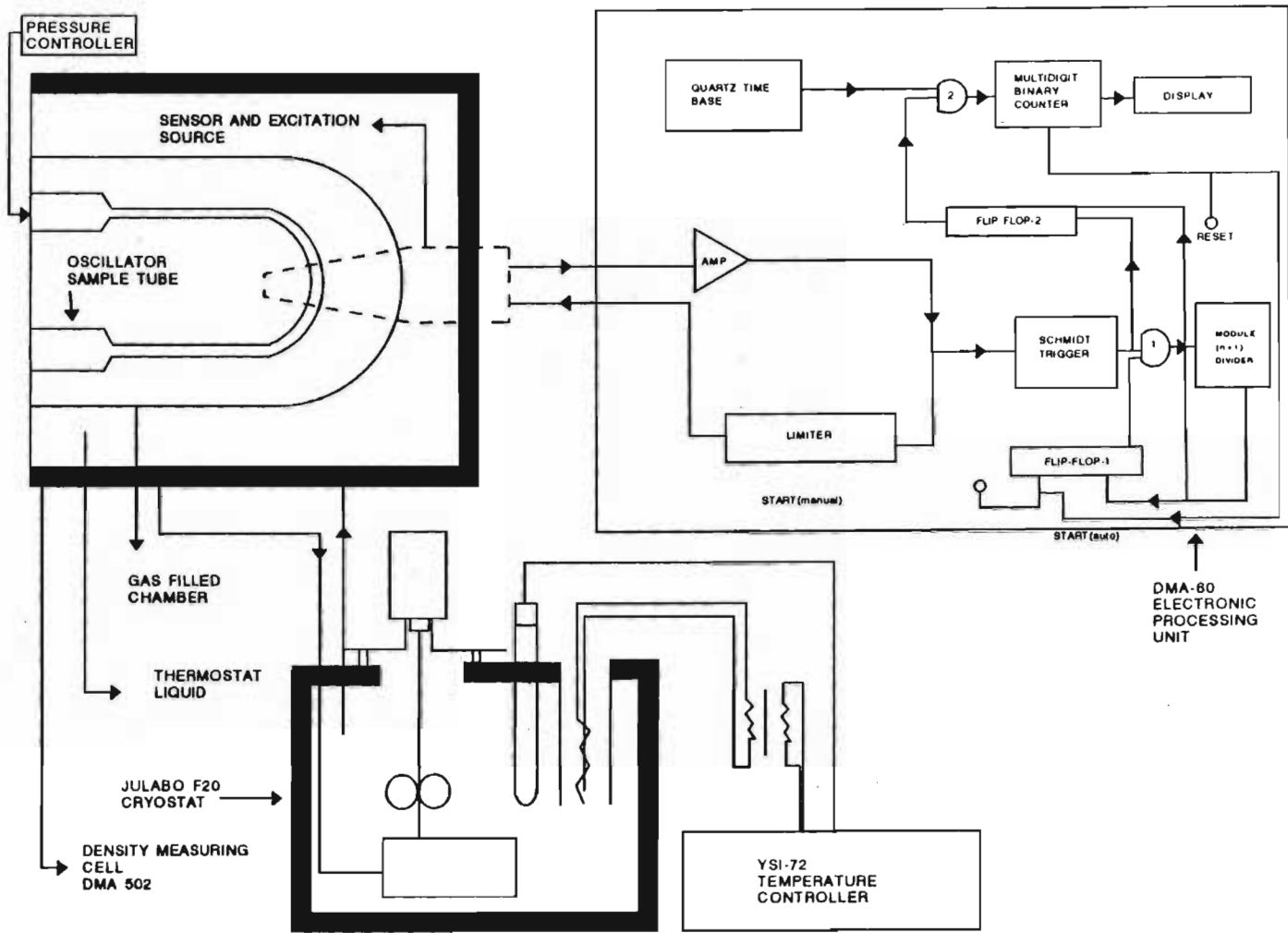
Figure 4.1 Schematic diagram of Laboratory arrangement of DMA 60/512 digital densimeter

4.2.2.2 Thermostat

The Julabo F20 cryostat was used as a thermostat bath the temperature of which was controlled by using proportional temperature controller (YSI Model 72). The temperature of the bath was measured with a Leeds and Northrup four-lead platinum resistance thermometer accurate to about 0.03 K on IPTS-68.[235] The thermal stability of the bath was better than approximately 0.01 K below 343.15 K and approximately 0.02 K above that temperature.

4.2.2.3 Pressure Measurement

Pressure was measured with a static high pressure unit (Setaram) accurate to 0.01 MPa. The unit was calibrated by the National Physical Laboratory, New Delhi, against its transfer standard gauges.[236] The reference pressure was taken as 1×10^5 Pa.

4.2.2.4 Operation Procedure for instrument and actual density sample measurement

Liquid sample was introduced into the lower part of the U-tube slowly enough to enable the liquid properly to wet the walls of the sample tube. To avoid trapping of microbubbles on the walls of the sample tube, the liquid was injected slowly. Care was also taken to ensure no air bubbles were trapped in the disposable syringes used for the introduction of the samples to the U-tube. Disposable polyethylene syringes(2.5 cm^3 volume) were used for all the measurements. The sample tube (A) was completely filled and the upper tube opening was closed off with a stainless steel nut fitted with a teflon stopper. The lower

U-tube was connected to the pressure tubing and the power was turned on. After observing a few period cycles, a constant period value (T value) was manually recorded.

The constant of the instrument k was calculated after measuring T values for dry air and doubly distilled degassed water in the U-tube, which were taken as the standards. The density of air-free water was taken from the literature[237] and the density of the dry air was calculated using the following equation

$$d_{t,p} = \frac{0.0012930}{1 + 0.00367 \cdot t} \cdot \frac{p}{760} \qquad (4.1)$$

where $d_{t,p}$ is the density in units of $g \cdot cm^{-3}$ at a given temperature t (°C) and atmospheric pressure p (torr). k, the instrument constant was checked from time to time. The densimeter was tested by measuring the densities of ethylbenzene and n-heptane at 298.15 K. The results are listed in Table 4.1 and the difference between our values and the literature values is $<$ $|0.0005\rho|$.[238,239] The accuracy of the density measurements was estimated at approximately 0.03 $kg \cdot m^{-3}$. The accuracy of the applied method of determination of α and κ_T was checked by comparing our experimental κ_T results for hexadecane at 0.1 MPa along the 318.15 and 333.15 K isotherms with those of Diaz Pena and Tardajos[240]. Our results are within 0.024 GPa^{-1} of those reported and the results are listed in Table 4.2.

TABLE 4.1 Densities ρ of pure compounds to check accuracy of densitometer

			$\rho/(kg \cdot m^{-3})$	
			---	---
Compound	T/K	Purity(%)	this work	lit.
ethylbenzene	298.15	> 99.5	862.25	862.46[a]
heptane	298.15	> 99.9	679.26	679.53[b]

[a]: taken from reference 239

[b]: taken from reference 238

TABLE 4.2 Comparison of κ_T results for hexadecane with literature values

T/K	κ_T/TPa^{-1}	
	exptl.	lit.[a]
318.15	975	978
333.15	1080	1066

[a]: taken from reference 240

4.3 Results

The measured densities for each of the six ethers at temperatures ranging from 288.15 K to 328.15 K and pressures up to 8 MPa are summarized in Table 4.3. The density values of water, which was used as a reference was taken from the NBS Steam Tables[237]. Polynomials of different degrees and with different numbers of terms were fitted as a function of temperature and pressure by the method of least squares and the molar volumes, V_m (molar mass / ρ) were fitted to the following best fit polynomial in T and P :

$$V_m(T,P)/(cm^3 \cdot mol^{-1}) = v_0 + v_1(T/K) + v_2(T/K)(P/MPa) + v_3(P/MPa) \qquad (4.2)$$

The parameters v_0, v_1, v_2 and v_3, estimated by the method of unweighed least squares are given in Table 4.4, together with the standard deviations. The cubic expansion coefficients α and isothermal compressibilities κ_T were derived from the molar volumes using the following relations :

$$\alpha V = (\partial V/\partial T)_P \qquad (4.3)$$

$$-\kappa_T V = (\partial V/\partial P)_T \qquad (4.4)$$

α and κ_T were fitted to the following power series in T and P :

$$\alpha (T,P)/(kK^{-1}) = v_0' + v_1'(T/K) + v_2' (T/K)(P/MPa) + v_3' (P/MPa) \qquad (4.5)$$

$$\kappa_T (T,P)/(GPa^{-1}) = v_0'' + v_1'' (T/K) + v_2'' (T/K)(P/MPa) + v_3'' (P/MPa) \qquad (4.6)$$

The constants of equations 4.5 and 4.6 are given in Tables 4.5 and 4.6 together with their standard deviations, respectively. For all the ethers studied in this work, plots of ρ, α and κ_T as functions of temperature (at 0.1 MPa) and pressure (at 298.15 K) are given in figures 4.2 - 4.7.

TABLE 4.3 Experimental densities, ρ for branched and cyclic ethers at different temperatures and pressures

$$\rho/(\text{kg} \cdot \text{m}^{-3})$$

P/MPa	T/K:	288.15	298.15	308.15	318.15	328.15
			Diisopropyl Ether			
0.1		726.44	717.81	708.28	701.56	693.66
0.5		726.91	718.27	710.57	702.29	694.66
1.0		727.50	719.18	711.41	703.15	695.63
2.0		728.64	720.28	712.92	704.83	697.50
3.0		729.77	721.57	714.36	706.41	699.22
4.0		730.93	722.76	715.71	707.81	700.78
5.0		732.03	724.00	716.93	709.25	702.45
6.0		733.10	725.12	718.21	710.58	703.98
7.0		734.17	726.45	719.39	711.87	705.75
8.0		735.21	727.59	720.56	713.19	707.29
			tert-Butyl Methyl Ether			
0.1		743.39	734.80	727.20	718.75	715.18
0.5		743.86	735.33	727.81	719.49	715.92
1.0		744.55	735.95	728.54	720.31	716.75
2.0		745.57	737.15	729.52	721.90	718.24
3.0		746.70	738.35	731.03	723.35	719.63
4.0		747.69	739.47	732.32	724.78	721.11
5.0		748.68	740.59	733.53	726.11	722.52
6.0		749.65	741.64	734.76	727.34	723.96
7.0		750.63	742.90	735.92	728.58	725.36
8.0		751.49	743.94	737.00	729.71	726.69
			tert-Amyl Methyl Ether			
0.1		773.29	765.71	758.83	752.10	746.63
0.5		773.72	766.13	759.28	752.61	747.19
1.0		774.20	766.68	759.86	753.22	747.90
2.0		775.17	767.70	761.00	754.45	749.28
3.0		776.04	768.69	762.12	755.64	750.55
4.0		776.96	769.84	763.16	756.81	751.72
5.0		777.79	770.63	764.17	757.93	752.95
6.0		778.59	771.54	765.15	759.07	754.11
7.0		779.45	772.64	766.16	760.13	755.21
8.0		780.23	773.56	767.14	761.13	756.34

TABLE 4.3 Continued

P/MPa		$\rho/(kg \cdot m^{-3})$				
	T/K:	288.15	298.15	308.15	318.15	328.15

			Tetrahydrofuran			
0.1		889.44	881.42	873.78	865.89	859.04
0.5		889.81	881.78	874.20	866.35	859.51
1.0		890.26	882.26	874.71	866.95	860.10
2.0		891.05	883.15	875.70	868.08	861.35
3.0		891.76	884.04	876.66	869.14	862.49
4.0		892.57	884.84	877.61	870.17	863.50
5.0		893.31	885.68	878.47	871.16	864.52
6.0		894.02	886.47	879.33	872.10	865.51
7.0		894.80	887.46	880.19	873.04	866.47
8.0		895.51	888.26	881.07	873.83	867.42

			Tetrahydropyran			
0.1		885.39	878.54	871.20	864.04	858.70
0.5		885.61	878.85	871.54	864.42	859.20
1.0		885.73	879.46	872.04	864.92	859.77
2.0		886.65	880.15	873.02	865.95	860.89
3.0		887.43	881.00	873.95	866.92	861.97
4.0		888.26	881.78	874.85	867.90	862.94
5.0		889.01	882.72	875.73	868.85	863.95
6.0		889.81	883.33	876.57	869.75	864.92
7.0		890.61	884.29	877.44	870.71	865.85
8.0		891.41	885.05	878.23	871.64	866.79

			1,4-Dioxane			
0.1		1034.65	1026.66	1019.71	1011.68	1005.57
0.5		1034.95	1027.25	1020.11	1012.04	1005.95
1.0		1035.29	1027.73	1020.55	1012.51	1006.49
2.0		1035.93	1028.06	1021.41	1013.43	1007.52
3.0		1036.62	1028.82	1022.28	1014.32	1008.43
4.0		1037.40	1029.54	1023.07	1015.19	1009.26
5.0		1038.14	1030.30	1023.86	1016.06	1010.19
6.0		1038.87	1031.39	1024.66	1016.85	1011.11
7.0		1039.62	1031.90	1025.40	1017.70	1011.96
8.0		1040.31	1032.66	1026.11	1018.51	1012.85

TABLE 4.4 Parameters v_i and standard deviations, σ calculated by equation 4.2

$v_o \cdot 10^{-1}$	$v_1 \cdot 10$	$v_2 \cdot 10^3$	$v_3 \cdot 10$	$\sigma \cdot 10$
	Diisopropyl Ether			
9.3332	1.6434	-3.4028	7.6991	0.73
	tert-Butyl Methyl Ether			
8.0136	1.3342	-2.4150	5.3549	0.38
	tert-Amyl Methyl Ether			
9.4729	1.2971	-3.8330	9.7449	2.7
	Tetrahydrofuran			
6.0397	0.71809	-0.83637	1.7080	0.19
	Tetrahydropyran			
7.5381	7.6166	-0.83465	1.5608	0.56
	1,4-Dioxane			
6.7441	0.61589	-0.48950	0.82509	0.36

TABLE 4.5 Parameters v_i' and standard deviations, σ calculated by equation 4.5

$v_o' \cdot 10^3$	$v_1' \cdot 10^6$	$v_2' \cdot 10^8$	$v_3' \cdot 10^5$	$\sigma \cdot 10^6$
		Diisopropyl Ether		
1.54	-1.31	4.69	-3.62	0.794
		tert-Butyl Methyl Ether		
1.33	-1.10	3.46	-2.70	0.453
		tert-Amyl Methyl Ether		
1.25	-0.927	4.78	-4.21	1.920
		Tetrahydrofuran		
1.10	-0.759	1.59	-1.42	0.298
		Tetrahydropyran		
0.954	-0.596	1.18	-1.14	0.468
		1,4-Dioxane		
0.870	-0.511	0.775	-0.752	0.323

TABLE 4.6 Parameters v_i'' and standard deviations, σ calculated by equation 4.6

$v_0'' \cdot 10^3$	$v_1'' \cdot 10^5$	$v_2'' \cdot 10^8$	$v_3'' \cdot 10^5$	$\sigma \cdot 10^6$
		Diisopropyl Ether		
-4.68	2.15	8.26	-2.16	3.84
		tert-Butyl Methyl Ether		
-3.87	1.81	5.85	-1.50	2.40
		tert-Amyl Methyl Ether		
-6.79	2.70	8.35	-2.32	5.52
		Tetrahydrofuran		
-1.79	0.923	1.86	-0.46	1.20
		Tetrahydropyran		
-1.34	0.766	1.51	-0.36	0.793
		1,4-Dioxane		
-0.782	0.510	0.813	-0.187	0.520

4.4 Discussion

A regular linear variation of density with either pressure or temperature over the ranges used in this work is a feature common to all the ethers used in this work as seen in figures 4.2 and 4.3. For all the ethers, the coefficients of cubic expansion decrease with an increase of temperature or pressure while the isothermal compressibilities increase with an increase in temperature or pressure over the temperature and pressure ranges used in this work. Like the density isotherms, those of α and κ_T exhibit complete linearity at the pressures used in this work. This linear behaviour is expected within the pressure ranges used in this work and is in agreement with the characteristic behaviour previously observed for most liquids in the similar range of pressures.[241-243] At higher pressures (20-100 MPa), it has been observed that curvilinear forms of α and κ_T are characteristic with the temperature dependence of α, changing sign at some intermediate pressure.[241] In general, an increase in density implies a decrease in the molar volume, V_m, with a corresponding decrease in the free intermolecular space. As a result, the ability of the liquid to expand or compress, decreases as well. This opposite trend of compressibility / expansivity as a function of temperature to that observed of density as a function of temperature or pressure has been shown to be true for the n-alkanes[240] and the methyl substituted benzenes.[240,242,246] In this work, however, as the density decreases the corresponding increase in the molar volume is observed but this is accompanied by a slight decrease in the cubic expansion coefficient, α (figure 4.4). This deviation from the expected behaviour is unusual and could be attributed to the presence of differing functional groups e.g. the OCH_3 group present in the molecule.

For IPE and TBME, Obama et al.[244] have reported α results at 298.15 K and atmospheric pressure, of 1.45 and 1.42 kK^{-1}, respectively while those reported here are 1.15

and 1.11 kK⁻¹, respectively. For the cyclic ethers, our α results at 298.15 K and 0.1 MPa for THF, THP and 1,4-dioxane are 0.8767, 0.7760 and 0.7171 kK⁻¹, respectively while those reported by Spanedda et al.[245] are 1.24, 1.14 and 1.09 kK⁻¹, respectively.

Our κ_T results at 298.15 K and 0.1 MPa for THF, THP and 1,4-dioxane are 0.9603, 0.9462 and 0.7392 GPa⁻¹, respectively while those reported by Spanedda et al.[245] and Berti et al.[220] are 1.00, 0.99 and 0.72 GPa⁻¹, respectively. This discrepancy between our results with those reported previously could possibly be due to the method of estimation of α and κ_T. The data reported here involve density measurements made as functions of temperature and pressure. Spanneda and co-workers have obtained their data from previously reported density values from many laboratories with possible differences in purity, technique and precision. No other results detailing the changes in α or κ_T with temperature and pressure could be found in the literature for the liquids involved in this work.
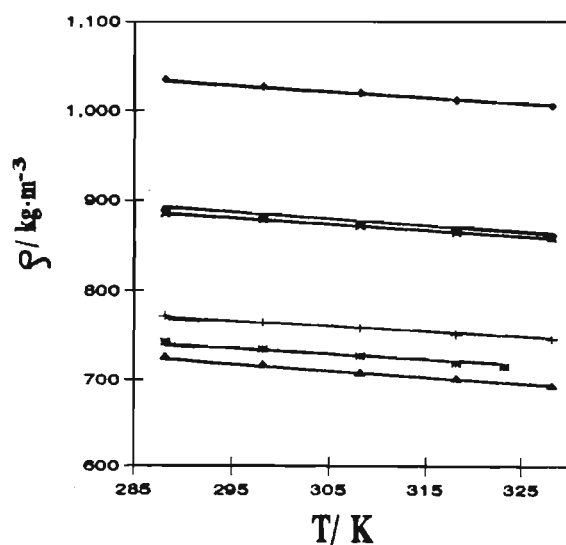
Figure 4.2 Density against temperature at 0.1 MPa for ▲ *IPE,* ✦ *TBME,* + *TAME,* ■ *THF,* × *THP,* ◆ *1,4-dioxane*
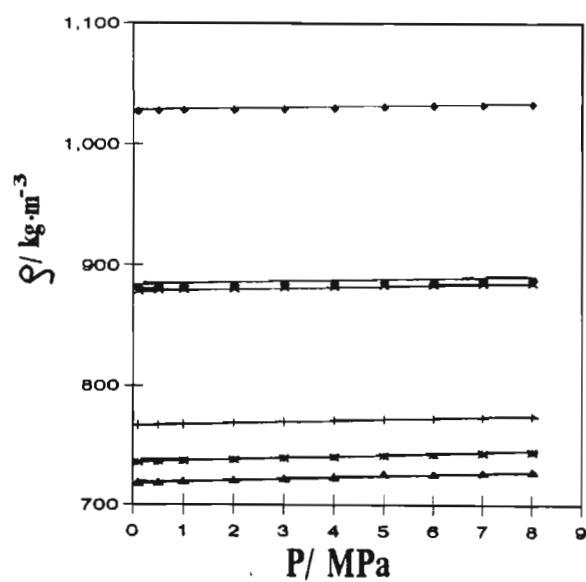
Figure 4.3 Density against pressure at 298.15 K for ▲ *IPE,* ✱ *TBME,* + *TAME,* ■ *THF,* × *THP,* ◆ *1,4-dioxane*
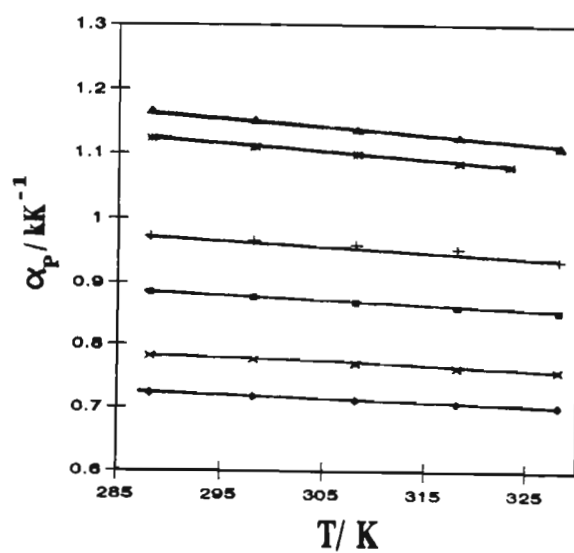
Figure 4.4 Cubic expansion coefficient against temperature at 0.1 MPa for ▲ *IPE,* ✱ *TBME,* + *TAME,* ■ *THF,*
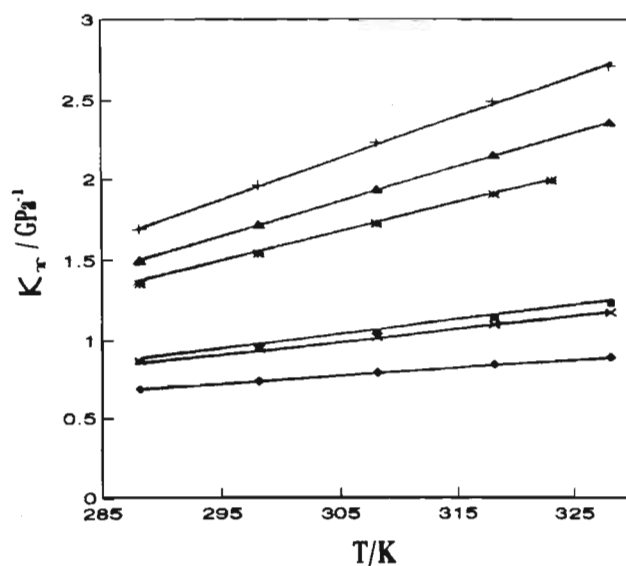
× *THP,* ◆ *1,4-dioxane*

*Figure 4.5 Isothermal compressibility against temperature at 298.15 K for ▲ IPE, * TBME, + TAME, ■ THF,*
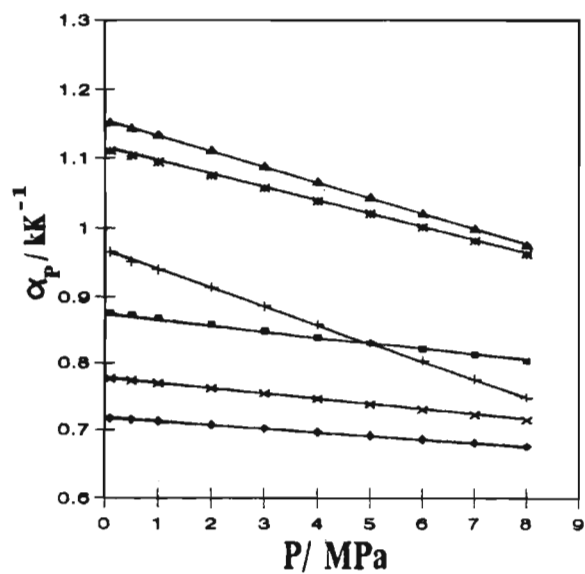
× THP, ♦ 1,4-dioxane

*Figure 4.6 Cubic expansion coefficient against pressure at 298.15 K for ▲ IPE, * TBME, + TAME, ■ THF, ×*
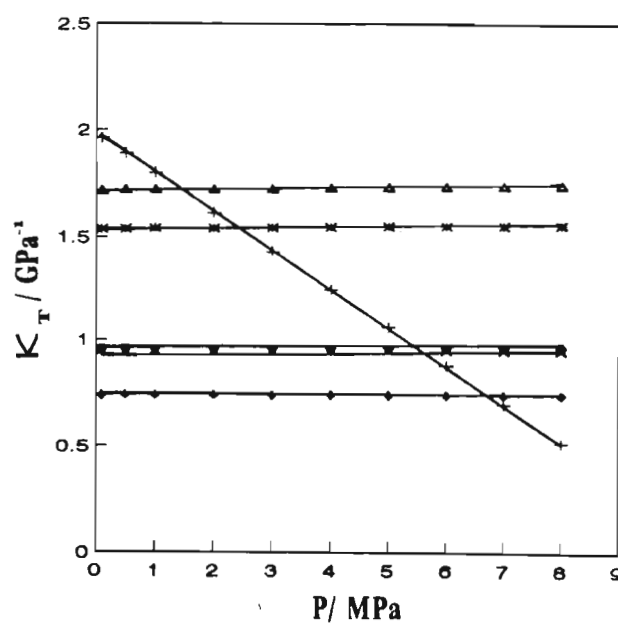
THP, ♦ 1,4-dioxane

*Figure 4.7 Isothermal compressibility against pressure at 298.15 K for ▲ IPE, * TBME, + TAME, ■ THF, ×*

THP, ♦ 1,4-dioxane

Thermodynamic Models of Liquid Mixtures

5.1   Introduction

In the design of many chemical engineering operations precise knowledge of thermophysical properties viz. Gibbs energy, phase equilibria etc., of liquid mixtures of a system to be separated is essential. Furthermore, experimental data are not always available and as a result solution thermodynamics has become increasingly important in predicting these properties. Predictive solution thermodynamics relates the nature of a given system to its thermodynamic properties, by necessarily postulating a "molecular model" for the system, i.e. concise definition of the structure of the molecules and the molecular interactions.[247] The thermodynamic properties are then derived from the molecular model either by computer simulation or by means of a theoretical model, based on statistical thermodynamics. In recent years the behaviour of real solutions can be calculated with the help of G^E models[248-251] and equations of state using pure component data and fitting parameters obtained for the related systems. More recently the group contribution methods have proven to be a fast and reliable tool for predicting the excess thermodynamic functions.[17,252] The success of the group

contribution models lies in the fact that the thermodynamic properties can be predicted from very limited experimental data of reference systems.[17,248-250,252]

In this chapter a brief overview of some of the theories of liquid mixtures developed in the last thirty years will be given. The fundamental equations of the NRTL(Non-Random Two Liquid)[14,224] model, the UNIQUAC (Universal Quasichemical)[15] model, the UNIQUAC ASM (Universal Quasichemical Association),[16] Modified-UNIFAC(UNIQUAC Functional Group Activity Coefficient)[17,18], the Prigogine-Flory-Patterson (PFP)[11,12] and the ERAS (Extended Real Associated Solution)[20,21] models will be discussed as these models have been applied to all the H_m^E and V_m^E experimental data reported in this work. These results are listed and analyzed in Chapter 6.

5.2   Brief History

5.2.1   __Before 1965__

Over 100 years ago van der Waals introduced a systematic approach to describe the properties of fluid mixtures. He proposed corrections to the ideal gas equation of state to account for the attractions and repulsions between molecules in the liquid state[11,253]. In 1910 Van Laar[254] and Margules[41] incorporated the Van der Waals equation of state and were one of the earliest recorded workers to treat the changes in the entropy or enthalpy of a mixture of two liquids. Van Laar[254] proposed an equation (the well known Van Laar equation) which relates the activity coefficient to the temperature, composition and pure component properties. These equations were useful empirical relations which were successful in correlating experimental activity coefficients for many binary systems[260]. However the success of these

early treatments of liquid solutions was limited to mixtures of molecules equivalent in size and shape. During the 1940's, Scatchard and Hildebrand[255-257,259] introduced the regular solution equation which described a solution in which the components mix with no excess entropy and no volume change. For many solutions of nonpolar liquids, the regular solution equations provide reasonable approximations and give good quantitative representation of activity coefficients but when used to calculate excess enthalpy the results are poor[253]. Flory and Huggins[258,261,262] proposed a modified regular solution model to account for mixtures differing in size and shape and the results showed an improvement in the calculated excess functions (excess Gibbs energy and excess enthalpy).[253,258]. The Van Laar, Margules, Scatchard-Hildebrand and Flory-Huggins equations of state were constructed on the premise that a liquid is a dense, highly non-ideal fluid and limited to mixtures of spherical molecules. in the 1950's Guggenheim[263] abandoned the equation of state approach and introduced the so called "lattice model" involving molecules of equal size forming mixtures that are not necessarily random. The model usually referred to as the "Guggenheim Quasichemical Lattice" model is based on the concept that in the condensed state, molecules arrange themselves in a lattice-like structure where each molecule occupies one lattice point. This model, in its simplest form, assumes that the motions of the molecules reduce to oscillations about their equilibrium positions and that the changes in any thermodynamic property on mixing may be expressed in terms of a lattice partition function. Further assumptions in this model include *(i)* the molecules of both the pure components and the mixture are regarded as being arranged on a regular lattice with a well defined coordination number (z). This implies that *(ii)* the molecules have to be sufficiently similar in size and shape to fit on the same lattice and *(iii)* for a fixed temperature the lattice spacings for the two pure liquids and for the mixture are the same, independent of composition (i.e. $V^E = 0$)[263,265]. Attempts to extend the model to larger molecules were

performed by Barker and co-workers[266]. These models, however, involve the use of an excessive number of adjustable parameters required to reduce the theory to practice. Further extensions by Flory[19,279,280] and Huggins[13,253] developed a quasichemical model which were successfully applied to liquid mixtures with molecules of one component which are very much larger but chemically similar (athermal solutions) to those of the other component (e.g. polymer solutions). The work of Flory[19,258,279,280] and Huggins[261] has been used as a basis for the derivation of the well documented UNIQUAC[15] model.

Wilson[267] derived an analytical expression which applied to mixtures of components differing in molecular size and intermolecular forces and by doing so established the pioneering concept of local compositions. The central idea of this concept is that a liquid mixture, when viewed microscopically, is not homogenous: the composition at one point in the mixture is not necessarily the same as that at another point. Wilson conceived that the interactions between molecules depend primarily on these local concentrations which are defined in probabilistic terms i.e. the Boltzmann distribution of energies. The inception and success of the semi-emperical Wilson equation and introduction of the nonrandomness parameter in the equation of state represented a major analytical advance in the theories of mixtures containing one or more polar components.

5.2.2 From 1965 to 1995

Initiated by the success of the Wilson equation[267] in 1964, numerous local composition equations and subsequent modified versions e.g. the NRTL model of Renon and Prausnitz[14] and the UNIQUAC model of Abrams and Prausnitz[15], have been proposed for solutions containing one or more polar components. The UNIQUAC model is a two parameter model

formulated by the combination of the local composition concept and quasichemical model of Guggenheim[263,265]. This model was extended and improved upon to introduce the concept of group contribution[18]. Although the estimation of thermodynamic properties of liquid mixtures from group contributions was first suggested by Langmuir[268] in 1925 it received very little attention until 1959. The "analytical solution of groups" method (ASOG) was first proposed by Derr and Deals[269-273] and then further enhanced by Ratcliff and co-workers[274].

Their success prompted Fredenslund and co-workers[18] in 1975 to combine the solution of groups theory with the UNIQUAC model to arrive at the popular UNIFAC (UNIQUAC Functional Group Activity Coefficient) model. Briefly, in group contribution methods it is assumed that the mixture does not consist of molecules but of functional groups as shown in figure 5.1. In recent publications(1991 to 1995), Gmehling et al.[248,250,252] have extended the original UNIFAC to propose the MODIFIED UNIFAC model in which modifications to the UNIFAC equation are made to account for the temperature dependence of excess thermodynamic functions. Success of the group contribution methods with the UNIQUAC model prompted development of models which combine group contribution methods with equations of state. Different methods (eg., THE PSRK, MHV2 etc.)[275,276] have been suggested and have shown to be successful in applications containing highly polar systems.[250,275]

Kehiaian et al.[249] in 1983, extended the classical pseudo-lattice quasichemical theory of Guggenheim[263-265] and proposed the DISQUAC (Dispersive Quasichemical) model[247,249]. In this model, the excess thermodynamic function equations is made up of a quasichemical term and a dispersive term which are calculated independently (DISQUAC can also be classified as the so-called pseudo-lattice group contribution method). The DISQUAC model was proposed to alleviate the following shortcomings of the classical quasichemical approach:

(i) the entire interchange energy of any given contact is assumed to generate non-randomness expressed in terms of the coordination number z and (ii) z is assumed to be the same for all the contacts. DISQUAC has proved successful when applied to many binary systems containing one or two polar components.[277,278]
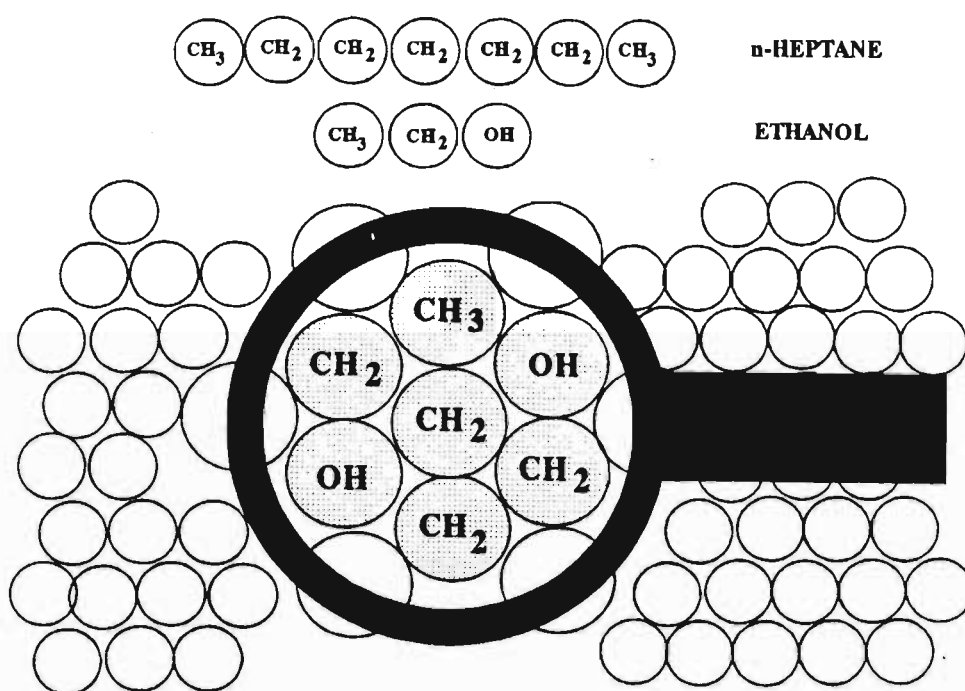
Figure 5.1 Illustration of the group contribution approach for the ethanol + n-heptane mixture[250]

In 1965 another successful theory and subsequent equation of state, was that proposed by Flory[19,279,280,] in which liquid mixtures were treated on the basis of a simple partition function affording an approximate but satisfactory representation of liquid state properties. The Flory theory showed applicability to mixtures of molecules differing in size.[281] Patterson et

al.[11,12] extended the theory of Abe and Flory[280] to include associated and strongly polar components in liquid mixtures. In the last decade Heintz et al.[20,21] have combined the Flory equation of state with the Real Associated Solution model of Renon and Prausnitz[282] and Kehiahian et al.[283,285] to propose the Extended Real Associated Solution (ERAS) model applicable primarily to associated solutions (mixtures containing one or more polar species).

5.3   Models used in this work

5.3.1 Introduction

The fundamental equations of the following theories will be detailed in this section as these theories have been applied to the experimental binary data reported here:

NRTL

UNIQUAC and UNIQUAC ASM (Associated Solution Model)

Modified UNIFAC

Simple Flory and Prigogine-Flory-Patterson

ERAS

5.3.2 The NRTL, UNIQUAC, UNIFAC and MODIFIED UNIFAC MODELS

5.3.2.1 Introduction

The Wilson[267], NRTL[14] and UNIQUAC[15] models have as their basis the concept of

local composition. The central idea of this concept is that when viewed microscopically, a liquid mixture is not homogeneous: the composition at one point in the mixture is not necessarily the same as that at another point (cf. figure 5.2). The Wilson equation for excess Gibbs energy for athermal mixtures contains terms expressing local volume fractions and has two adjustable parameters per binary mixture. Renon and Prausnitz[14] incorporated Scott's[284] two liquid model and derived a new equation based on Wilson's local composition concept to account for non-randomness of mixing (cf. figure 5.2). The NRTL equation is defined as :

$$\frac{g^E}{RT} = x_1 x_2 \left[\frac{\tau_{21} G_{21}}{x_1 + x_2 G_{21}} + \frac{\tau_{12} G_{12}}{x_2 + x_1 G_{12}} \right] \tag{5.1}$$

where

$$\tau_{12} = \frac{g_{12} - g_{22}}{RT} \quad ; \quad \tau_{21} = \frac{g_{21} - g_{11}}{RT} \tag{5.2}$$

and

$$G_{12} = \exp(-\alpha_{12}\tau_{12}) \quad ; \quad G_{21} = \exp(-\alpha_{21}\tau_{21}) \tag{5.3}$$

The two adjustable parameters are g_{12} and g_{21}. The third parameter α_{12} provides the flexibility required for representing the shape of the excess functions and is selected according to the chemical characteristics of the components of the mixture. The two adjustable terms, $(g_{12} - g_{22})$ and $(g_{21} - g_{11})$ in equation 5.2 are reflective of the energies of interaction between the molecules and are considered dependent on temperature. The NRTL equation has been shown to be successful in fitting excess enthalpy data.[286]

Both the quasi-chemical lattice model of Guggenheim[263-265] extended to mixtures containing molecules of different size and shape, and the Wilsons[267] local composition concept were adopted by Abrams and Prausnitz[15] in the development of the semi-theoretical

UNIQUAC equation. The UNIQUAC model expresses the excess Gibbs energy by the addition of two parts: (i) a contribution due to differences in sizes and shapes of the molecules (the configurational or combinatorial part) and (ii) a contribution due to differences in energy of molecular interactions between them (residual part).
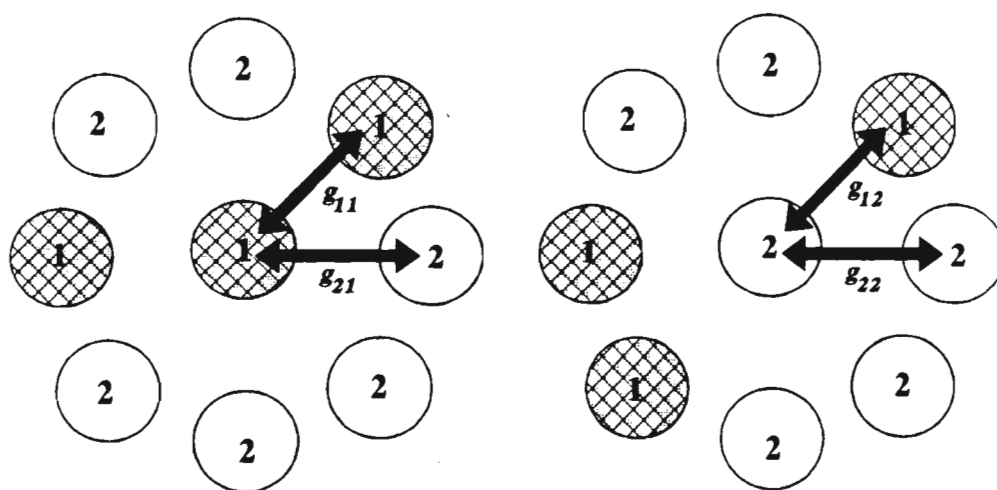
Figure 5.2 A diagrammatic reprsentation of the interactions occuring in a binary liquid mixture by Scotts Two Liquid Theory[11,284]

The major characteristics of the UNIQUAC equation are (i) the superior representations of liquid mixtures with the pure components differing largely in molecular sizes, (ii) the ability to represent multicomponent mixtures using only two adjustable parameters per binary and (iii)

it is the basis of a group contribution method (the UNIFAC model) for obtaining excess functions from properties of pure components.[15] It is perhaps the latter point which has accelerated the number of publications focused on the application of the original UNIQUAC model and subsequent modifications to multicomponent mixtures. Anderson and Prausnitz [287,288] modified the UNIQUAC equation, to make it applicable to associating species in solution, by using different values for the pure component area parameter q for water and alcohols in the combinatorial and residual parts. To account for association effects, Nagata and co-workers[16] proposed a modified UNIQUAC equation, the so-called UNIQUAC ASM (ASM = Associating model), to represent the properties of liquid mixtures containing one associating component. This latter model combines the continuous association models of Kretschmer Wiebe[289,290] (and the modified version of Kehiahian et al.[291,295]) or Mecke Kempter[292,293] (and the modified version of Keiahian et al.[295] and Tresczezenowicz et al.)[294] with the original UNIQUAC equation. This theory has been successfully applied to the correlation of the excess thermodynamic functions of (a cycloalkanol + a cycloalkane systems.[16]

The UNIFAC and subsequent Modified UNIFAC[17,18] models are the most well established and successful of the group contribution methods. Such models treat liquid mixtures as mixtures of the functional groups making up the molecular species present. Interactions between molecules are interpreted as interactions between functional groups, and these interactions are assumed to be independent of how the functional groups are joined together in the molecule (as shown in figure 5.1). This basic assumption permits the properties of a mixture to be related to those of other different molecular mixtures provided that the same groups are present. The great advantage of the group contribution concept is

that the number of functional groups is much smaller than the number of possible compounds. This means that the behaviour of a large number of systems of interest can be predicted with a limited number of group interaction parameters. For example the interaction parameters between an alkanol and an alkane group derived from data for a single binary system (methanol + heptane) can be used to predict the real behaviour of all other alkanol-alkane systems.[248,253]

Both the UNIFAC and Modified UNIFAC models are based on the UNIQUAC equation with two additive terms namely the (a) configurational (C) (size contribution) and (b) residual (R)(group contribution). These models introduce the concepts of group interaction parameters, a_{mn} and a_{nm} ; group volume parameters, R_k and group surface parameters, Q_k.[18]

5.3.2.2   *The UNIQUAC and UNIQUAC ASM Models*

Abrams and Prausnitz[15] expressed the UNIQUAC equation for a two component system as

$$g_m^E = g_m^E \ (combinatorial) + g_m^E \ (residual) \qquad (5.4)$$

where

$$\frac{g_m^E \ (combinatorial)}{RT} = \sum_{i=1}^{2} x_i \ln\left(\frac{\Phi_i}{x_i}\right) + \left(\frac{Z}{2}\right)\sum_{i=1}^{2} q_i x_i \ln\left(\frac{\theta_i}{\Phi_i}\right) \qquad (5.5)$$

and

$$\frac{g_m^E \ (residual)}{RT} = - q_1 x_1 \ln (\theta_1 + \theta_2 \tau_{21}) - q_2 x_2 \ln (\theta_2 + \theta_1 \tau_{12}) \tag{5.6}$$

where

$$\tau_{21} \equiv \exp (-[\frac{u_{21} - u_{11}}{RT}]) \qquad \tau_{12} \equiv \exp (-[\frac{u_{12} - u_{22}}{RT}]) \tag{5.7}$$

In equation 5.5, Φ is the average segment fraction and θ is the average area fraction given as:

$$\Phi_1 = 1 - \Phi_2 = \frac{x_1 r_1}{x_1 r_1 + x_2 r_2} \tag{5.8}$$

$$\theta_1 = 1 - \theta_2 = \frac{q_1 x_1}{q_1 x_1 + q_2 x_2} \tag{5.9}$$

In equations 5.4 to 5.9, r and q are the pure component structural parameters and are defined as the van der Waals volume and area of the molecule relative to those of a standard segment, respectively. These parameters are evaluated from bond angles and bond distances.[296] Z in equation 5.5 is the coordination number and ranges from $6 \leq Z \leq 12$ but is consistently taken as 10. Equations 5.5 to 5.7 gives the excess Gibbs energy for a binary mixture in terms of two adjustable parameters $(u_{21} - u_{11})$ and $(u_{12} - u_{22})$. From the derivation of the equations it follows that $u_{21} = u_{12}$. When correlating excess enthalpy data with the UNIQUAC equation, the combinatorial part falls away and the Gibbs Helmholtz relation($H^E = \{\partial G^E / T\} / \{\partial 1/T\}$) is applied to the residual part.

In the UNIQUAC ASM model, Nagata et al.[16,297] used an association model with the

UNIQUAC equation. The association model considers that, in a mixture of (associating species + a non-polar component), the hydrogen bonding of associating species is the main cause of large deviations from an ideal solution behaviour. These approaches are broadly classified as the chemical solution theories whose characteristic is to use several equilibrium constants to fit experimental data.[253] The fundamental assumptions of continuously associated solution models are : (Let A denote the pure associating liquid eg. alcohol, amine etc. and B the solvent eg. unsaturated hydrocarbons, esters, ketones, ethers etc.).

(i) The associating liquid forms linear hydrogen bonded polymers by consecutive chemical reactions to form chemical complexes A_i and A_iB of the type

$$A_1 + A_{i-1} = A_i \tag{5.10}$$

(ii) The association constant K_A for the above reaction is independent of i. They are expressed by two possible equations

$$K_A = \frac{\phi_{A_i}}{\phi_{A_1}\phi_{A_{i-1}}} \cdot \frac{i-1}{i} \tag{5.11}$$

$$K_A = \frac{\phi_{A_i}}{\phi_{A_1}\phi_{A_{i-1}}} \tag{5.12}$$

(iii) The volume change on mixing is zero, i.e. the molar volume of the i-mer, V_i is given by $V_i = iV_i$, where V_i is the molar volume of the monomer

(iv) The temperature dependence of the association constant K_A is such that the heat of formation of a hydrogen bond is independent of the temperature and the degree of association

and

(v) both chemical and physical contributions are responsible for deviations from an ideal solution of (associating species + saturated hydrocarbons), i.e. the excess Gibbs energy and excess enthalpy are expressed as the sum of two contributions, one chemical and the other physical:

$$g^E = g_c^E + g_p^E$$
$$H^E = H_c^E + H_p^E$$

(5.13)

Nagata et al.[16] proposed that the chemical contribution be expressed by two associating models, the Kretschmer-Wiebe[290] and the Mecke-Kempter[292,293,294] models. The two models differ from each other in simple definition of the chemical equilibrium constant K_A. For the Kretschmer-Wiebe model K_A is given as

$$K_A = \frac{\phi_{A_i}}{\phi_{A_1} \phi_{A_{i-1}}} \cdot \frac{i-1}{i}$$

(5.14)

and for the Mecke-Kempter model

$$K_A = \frac{\phi_{A_i}}{\phi_{A_1} \phi_{A_{i-1}}}$$

(5.15)

The derived excess function equations for the Kretschmer-Wiebe and Mecke-Kempeter models are :

KRETSCHMER − WIEBE

$$H_m^E = h_A x_1 K_A (\phi_{A_1} - \phi_{A_1}^o)$$ (5.16)

where $\phi_{A_1}^0$ is the volume fraction of the pure associating species and is determined by

$$\phi_{A_1}^o = \frac{[2 K_A + 1 - (1 + 4 K_A)^{\frac{1}{2}}]}{2 K_A^2}$$ (5.17)

and ϕ_{A_1} is the overall volume fraction of the associating species

$$\phi_{A_1} = \frac{[2 K_A \phi_1 + 1 - (1 + 4 K_A \phi_1)^{\frac{1}{2}}]}{2 K_A^2 \phi_1}$$ (5.18)

h_A is the molar enthalpy of hydrogen bond formation and K_A is given as in equation 5.14.

MECKE KEMPTER

$$H_m^E = h_A x_1 \left[\ln \frac{(1 + K_A)}{K_A} - \ln \frac{(1 + K_A \phi_1)}{K_A \phi_1} \right]$$ (5.19)

where

$$\phi_{A_1}^0 = \frac{1}{1 + K_A}$$ (5.20)

and

$$\phi_{A_1} = \frac{\phi_1}{(1 + K_A \phi_1)}$$ (5.21)

h_A is the molar enthalpy of hydrogen bond formation and K_A is given as in equation 5.15.

In the UNIQUAC ASM model the excess enthalpy is given as the sum of two contributory terms: (i) a chemical term and (ii) a physical (residual) term. The chemical contribution to the excess enthalpy used in the UNIQUAC ASM model can be taken as that defined in equations 5.16 or 5.19 given in the preceding paragraph. The physical contribution is given by

$$H_{physical}^E = \frac{\partial[\frac{G_{(physical)}^E}{T}]}{\partial(\frac{1}{T})} = -R \sum_i^2 q_i x_i \frac{\sum_j^3 \theta_j \frac{\partial \tau_{ji}}{\partial(\frac{1}{T})}}{\sum_j^3 \theta_j \tau_{ji}} \qquad (5.22)$$

where

$$\tau_{ji} = \exp[\frac{-(u_{ji} - u_{ii})}{RT}] \qquad (5.23)$$

The constants in equations1 5.14 to 5.23 are defined as those in the UNIQUAC equation 5.4 to 5.9.

Alcohols are known to self-associate and to form associated complexes in solution and many experimental data for the excess thermodynamic properties of solutions of alcohols in nonpolar or polar solvents have been published to develop the theory of associated solutions.[298-301]

5.3.2.3 The UNIFAC and Modified UNIFAC Models

Group contribution models have been shown to be useful for the prediction of both activity coefficient and excess enthalpy thermodynamic properties of liquid mixtures.[18,249,250]

UNIFAC and the Analytical Solution of Groups (ASOG)[302,303] models are examples of group contribution methods for the prediction of liquid phase activity coefficients and excess enthalpies of mixing. Like the UNIQUAC equation[15], the UNIFAC activity coefficient equation and excess Gibbs energy equation consist of two parts:

$$\ln \gamma_i = \ln \gamma_i^C + \ln \gamma_i^R$$

or

$$\frac{g^E}{RT} = \sum_i x_i (\ln \gamma_i^C + \ln \gamma_i^R) \tag{5.24}$$

The combinatorial(C) part is identical to the combinatorial part of the UNIQUAC equation i.e. (cf. equations 5.4-5.6)

$$\ln \gamma_i^C = \ln \frac{\Phi_i}{x_i} + \frac{Z}{2} q_i \ln \frac{\theta_i}{\Phi_i} + l_i - \frac{\Phi_i}{x_i} \sum_j x_j l_j$$

$$\frac{g_m^{E(C)}}{RT} = \sum_i x_i \ln (\frac{\Phi_i}{x_i}) + (\frac{Z}{2}) \sum_i q_i x_i \ln (\frac{\theta_i}{\Phi_i}) \tag{5.25}$$

where

$$l_i = \frac{Z}{2}(r_i - q_i) - (r_i - 1) \quad ; Z = 10 \tag{5.26}$$

Parameters r_i and q_i are calculated as the sum of the group volume and area parameters, R_k and Q_k, respectively as

$$r_i = \sum_k v_k^{(i)} R_k \quad ; \quad q_i = \sum_k v_k^{(i)} Q_k \tag{5.27}$$

$v_k^{(i)}$ is the number of groups of type k in molecule i. R_k and Q_k are the group parameters obtained from the van der Waals group volume and surface areas V_{wk} and A_{wk}, respectively,

given by Bondi[296] as $R_k = V_{wk} / 15.17$ and $Q_k = A_{wk} / (2.5 \cdot 10^9)$. The values 15.17 and $2.5 \cdot 10^9$ are normalization factors given by Abrams and Prausnitz.[15]

The residual part of equation 5.24 is a term formulated by the solution of groups concept[302] given as

$$\ln\gamma_i^R = \sum_k v_k^{(i)} [\ln\Gamma_k - \ln\Gamma_k^{(i)}] \qquad (5.28)$$

where Γ_k is the group residual activity coefficient, and $\Gamma_k^{(i)}$ is the residual activity coefficient of group k in a reference solution containing only molecules of type i. The activity coefficient for group k in molecule i depends on the molecule i in which k is situated. The group activity coefficient Γ_k is found by

$$\ln\Gamma_k = Q_k [1 - \ln(\sum_m \Theta_m \Psi_{mk}) - \sum_m (\frac{\Theta_m \Psi_{km}}{\sum_n \Theta_n \Psi_{nm}})] \qquad (5.29)$$

Equation 5.29 also holds for $\Gamma_k^{(i)}$. $\Theta_{m\ or\ n}$ is the area fraction of group m or n and is calculated as:

$$\Theta_m = \frac{Q_m X_m}{\sum_n Q_n X_n} \qquad (5.30)$$

where X_m is the mole fraction of group m in the mixture. The group interaction parameter Ψ_{mn} is given by

$$\Psi_{mn} = \exp -[\frac{U_{mn} - U_{nn}}{RT}] = \exp -(\frac{a_{mn}}{T}) \qquad (5.31)$$

where U_{mn} is a measure of the energy of interaction between groups m and n. The group

interaction parameters a_{mn} (two parameters per binary mixture of groups) are parameters which must be evaluated from experimental phase equilibrium data. a_{mn} (units are K) is not equal to a_{nm} and both have to be obtained from a data base using a wide range of experimental data. Nagata and Ohta[304] applied the following equations 5.32 to 5.34 to predict the excess enthalpies of mixing of mixtures of alkanes with n-alcohols, esters, ethers and ketones with satisfactory accuracy. They obtained a relationship between the group excess enthalpies and the group activity coefficient by using the Gibbs Helmholtz relation:

$$\frac{\partial}{\partial T}(\Gamma_k)_{P,k} = -\frac{H_k}{RT^2} \tag{5.32}$$

where H_k is the group excess enthalpy of group k and is a function of the group fraction, temperature and pressure. Analytical expressions for H_k in binary group mixtures are given by

$$\frac{H_1}{RT^2} = Q_1\Theta_2 \left[\frac{\Psi_{21}'}{\Theta_1 + \Theta_2\Psi_{21}} + \frac{\Theta_2\Psi_{12}'}{(\Theta_1\Psi_{12} + \Theta_2)^2} - \frac{\Theta_1\Psi_{21}'}{(\Theta_1 + \Theta_2\Psi_{21})^2} \right] \tag{5.33}$$

and

$$\frac{H_2}{RT^2} = Q_2\Theta_1 \left[\frac{\Psi_{12}'}{\Theta_2 + \Theta_1\Psi_{12}} + \frac{\Theta_1\Psi_{21}'}{(\Theta_2\Psi_{21} + \Theta_1)^2} - \frac{\Theta_2\Psi_{12}'}{(\Theta_2 + \Theta_1\Psi_{12})^2} \right] \tag{5.34}$$

where $\Psi_{12}' = \partial(\Psi_{12}) / \partial T$ and $\Psi_{21}' = \partial(\Psi_{21}) / \partial T$ and all the other parameters are defined as in the UNIFAC model.

Many comparisons, using experimental data for various combinations of pure components, have shown that the UNIFAC model is particularly well suited for calculating vapour-liquid and liquid-liquid equilibria.[305-307] However, various publications by Kikic et

al.[308,309] and Thomas et al.[310] have concluded that the results obtained for the calculation of activity coefficients at infinite dilution are in most cases unsatisfactory especially when systems with molecules very different in size and shape are considered. Gmehling and Weidlich[17] modified the UNIFAC equation with respect to the form and size of the molecules in the combinatorial part of the original UNIFAC. They then modified the residual part of the original UNIFAC by incorporating a description of the temperature dependence of the activity coefficients. Equations 5.36 to 5.47 below show the original UNIFAC and Modified UNIFAC for the combinatorial and residual parts, respectively.

ORIGINAL UNIFAC - COMBINATORIAL

$$\ln\gamma_i^C = 1 - \phi_i + \ln\phi_i - \frac{Z}{2} q_i [\, 1 - \frac{\phi_i}{\theta_i} + \ln\frac{\phi_i}{\theta_i} \,]; \quad \phi_i = \frac{r_i}{\sum_j r_j x_j}; \quad \theta_i = \frac{q_i}{\sum_j q_j x_j} \quad (5.35)$$

MODIFIED UNIFAC - COMBINATORIAL

$$\ln\gamma_i^C = 1 - \phi_i' + \ln\phi_i' - \frac{Z}{2} q_i [\, 1 - \frac{\phi_i}{\theta_i} + \ln\frac{\phi_i}{\theta_i} \,]; \quad \phi_i = \frac{r_i}{\sum_j r_j x_j}; \quad \theta_i = \frac{q_i}{\sum_j q_j x_j}$$

$$\phi_i' = \frac{r_i^{\frac{3}{4}}}{\sum_j r_j^{\frac{3}{4}} x_j} \quad (5.36)$$

Temperature dependent interaction parameters were introduced into the residual part. This inclusion affected the group interaction parameter in the original UNIFAC as is given by :

ORIGINAL UNIFAC - RESIDUAL

$$\Psi_{nm} = \exp-(\frac{a_{nm}}{T}) \qquad (5.37)$$

MODIFIED UNIFAC - RESIDUAL

$$\Psi_{nm} = \exp-(\frac{a_{nm} + b_{nm}T + c_{nm}T^2}{T}) \qquad (5.38)$$

where the relative van der Waals volumes and surfaces of the structural groups (R_k and Q_k values) were not calculated from molecular parameters like the original UNIFAC but were fitted together with the interaction parameters a_{nm}, b_{nm}, c_{nm} to the experimental values.

The thermodynamic relationships for the determination of excess enthalpies using both the original UNIFAC and the Modified UNIFAC are given in equations 5.39 to 5.46.

From the Gibbs-Helmholtz equation

$$(\frac{\partial \frac{G^E}{RT}}{\partial T}) = -\frac{H^E}{RT^2} \qquad (5.39)$$

we can calculate the excess molar enthalpy. Since the combinatorial part is temperature-independent, only the residual part is used for calculating the excess enthalpy:

Γ_k is the group activity coefficient of group k in the mixture and $\Gamma_k^{(i)}$ is the group activity

$$H^E = -RT \sum_i \sum_k x_i v_k^{(i)} [\; T(\frac{\partial \ln\Gamma_k}{\partial T})_{P,x} - T(\frac{\partial \ln\Gamma_k^{(i)}}{\partial T})_{P,x}\;] \tag{5.40}$$

coefficient of group k in the pure substance. For the original and modified UNIFAC the following relations apply as:

ORIGINAL UNIFAC

$$T(\frac{\partial \ln\Gamma_k}{\partial T})_{P,x} = Q_k \sum_m \theta_m [\frac{\Psi_{mk} \ln\Psi_{mk}}{\sum_n \theta_n \Psi_{nk}} + \frac{\Psi_{km} \sum_n \theta_n \Psi_{nm} \ln(\frac{\Psi_{km}}{\Psi_{nm}})}{(\sum_n \theta_n \Psi_{nm})^2}] \tag{5.41}$$

where

$$\Psi_{nm} = \exp-(\frac{a_{nm}}{T}) \tag{5.42}$$

MODIFIED UNIFAC

$$T(\frac{\partial \ln\Gamma_k}{\partial T})_{P,x} = Q_k \sum_m \theta_m [\frac{(b_{mk} + \ln\Psi_{mk} + 2c_{mk}\,T)\Psi_{mk}}{\sum_n \theta_n \Psi_{nk}} +$$

$$\frac{\Psi_{km} \sum_n \theta_n \Psi_{nm}}{(\sum_n \theta_n \Psi_{nm})^2} (b_{km} - b_{nm} + \ln(\frac{\Psi_{km}}{\Psi_{nm}}) + \frac{(c_{km} - c_{nm})}{2T})] \tag{5.43}$$

where

$$\Psi_{nm} = \exp-(\frac{a_{nm} + b_{nm}T + c_{nm}T^2}{T}) \tag{5.44}$$

Similar expressions to equations 5.41 to 5.44 apply to the term $T(\partial \ln \Gamma_k^{(i)} / \partial T)_{P,x}$ where the parameters in the equations refer to the pure substance.

In this work the Modified UNIFAC equation is tested for the experimental excess enthalpy data presented. The most recent parameter tables of Gmehling et al. published in 1993[248,311] have been used in all our calculations.

5.3.3 The Flory Theory

5.3.3.1 *Introduction*

Flory and co-workers[19,279,280,312] developed a statistical theory which relates thermodynamic excess properties of liquid mixtures to the measurable macroscopic properties of the pure components. They introduced a partition function which (i) was modelled on that introduced for simple liquids by Eyring and Hirschfelder[313,314] and (ii) included the concepts of degrees of freedom of the component molecules and the *r-meric* structural representation of linear molecules proposed by Prigogine and co-workers.[262,315,316,317,330] In its original form the theory was developed specifically for application to the properties of chain molecule liquids and their mixtures.[279] The success of the theory as applied to chain-like molecules subsequently initiated the extension of the theory to mixtures of small non-polar molecules differing in size and shape.[280,281] Although the theory did not give good quantitative agreement for the latter mixtures, it did give a good qualitative correlation of the systems. Since its inception in 1964, the Flory theory has been applied with general success to systems of simple liquids involving mixtures of benzene, a cycloalkane, and *n*-alkane with an *n*-alkane,[318-321] and to methyl substituted benzenes with carbon tetrachloride.[322] However, the theory when applied to mixtures containing strongly polar components(e.g. alcohols)fails.[323,324]

This is not surprising considering the fact that the theory specifically excludes hydrogen bonding and all other strong dipolar interactions. Consequently Patterson et al.[11,12,325] improved on the original Flory theory by proposing that the properties of binary mixtures comprised the sum of three contributions: (i) a combinatorial term, (ii) an interactional term arising from the chemical nature of the two components and (iii) a free volume contribution. Patterson et al.,[11,12] proposed approximate equations which le. d to the separation of these three contributions. They concluded that the excess enthalpies mainly reflect the interactional contribution while the excess molar volume is mostly determined by three components:(a) an interactional term which is proportional to the Flory parameter X_{12}, (b) a free volume contribution which originates from a difference in the degrees of thermal expansion of the two components and (c) a P^* contribution which arises from the differences in internal pressures and reduced volumes of the pure components. This modified theory has been applied successfully to predict excess thermodynamic properties for mixtures of *n*-alkane with a linear siloxane or decamethyltetrasiloxane or benzene or carbon tertrachloride[11,12] and for 1-alkynes with benzene or cyclohexane or hexane.[326]

5.3.3.2 *The Flory Equations*

One of the basic ideas of the Flory model of *r*-mer liquids involves the assumption that the component molecules may be divisible into *r* segments of equal so-called "hard-core" volumes. The introduction of the reduced variables rests on the theoretical expectation that a mixture of chemically related components made up of similar structural elements should at constant composition follow an equation of state of the same mathematical form as that for the pure liquids if its variables are expressed as reduced quantities. The Flory generalized form of the reduced partition function is:

$$Q = Q_{comb}(gV^*)^{rNC}(\tilde{V}^{\frac{1}{3}}-1)^{3rNC}e^{\frac{rNC}{\tilde{V}\tilde{T}}} \qquad (5.45)$$

where Q_{comb} is the combinatorial factor including the communal entropy factor taking into account the number of possible ways of disposing the molecular segments among one another in space, g is a constant geometric parameter, $\tilde{V}$ and V^* are the reduced volume, and hard core volume of one single segment, respectively. The term 3c is the number of external degrees of freedom per segment, C characterizes the number of intermolecular degrees of freedom and r is the number of segments in r-mer chain molecule and N is the number of molecules.

The equation of state in reduced form has been derived as

$$\frac{\tilde{P}\cdot\tilde{V}}{\tilde{T}} = \frac{\tilde{V}^{\frac{1}{3}}}{\tilde{V}^{\frac{1}{3}}-1} - \frac{1}{\tilde{V}\cdot\tilde{T}} \qquad (5.46)$$

where $\tilde{P}, \tilde{V}$ and $\tilde{T}$ without subscripts, are the reduced variables of pressure, volume and temperature for the mixture, respectively. The reduced temperature and volume for the mixture are defined as

$$\tilde{T} = \frac{(\phi_1 P_1^* \tilde{T}_1)+(\phi_2 P_2^* \tilde{T}_2)}{(\phi_1 P_1^*)+(\phi_2 P_2^*)-(\phi_1\theta_2 X_{12})} \qquad (5.47)$$

$$\tilde{T}\tilde{V}^{\frac{4}{3}} - \tilde{V}^{\frac{1}{3}} + 1 = 0 \qquad (5.48)$$

The excess molar volume of a binary mixture is given by

$$V_m^E = (x_1 V_1^* + x_2 V_2^*)(\tilde{V} - \phi_1 \tilde{V}_1 - \phi_2 \tilde{V}_2) \tag{5.49}$$

and the excess molar enthalpy as

$$H_m^E = \sum_{i=1}^{2} x_i p_i^* V_i^* (\frac{1}{\tilde{V}_i} - \frac{1}{\tilde{V}}) + x_1 \theta_2 (\frac{V_1^*}{\tilde{V}}) X_{12} \tag{5.50}$$

The excess molar volume is related to the reduced and characteristic volume while the excess enthalpy contains the characteristic pressures and the adjustable interaction parameter X_{12}. X_{12} is an empirical parameter and its value is usually adjusted to give the best fit between theoretical and experimental values of the excess functions.

At zero pressure and temperature T, the reduced volume of a pure substance i is defined in terms of the thermal expansion coefficient α_i

$$\tilde{V}_i = [\frac{(1 + \frac{4}{3} \alpha_i T)}{(1 + \alpha_i T)}]^3 \tag{5.51}$$

and the reduced temperature is

$$\tilde{T}_i = \frac{(\tilde{V}_i^{\frac{1}{3}} - 1)}{\tilde{V}_i^{\frac{4}{3}}} \tag{5.52}$$

At low temperature the characteristic pressure for pure substance i is defined as

$$P_i^* = (\frac{\alpha_i}{\kappa_i}) \tilde{V}_i^2 T \tag{5.53}$$

By hypothesis each molecule consists of a number of segments and each segment carries a number of sites which may interact with sites on adjacent molecules. The segment or hard core volume fraction ϕ_i and the contact site/surface fractions θ_i are defined as

$$\phi_1 = 1 - \phi_2 = \frac{x_1 \cdot V_1^*}{x_1 \cdot V_1^* + x_2 \cdot V_2^*} \tag{5.54}$$

$$\theta_2 = 1 - \theta_1 = \frac{s_2 \phi_2}{s_1 \phi_1 + s_2 \phi_2} \tag{5.55}$$

The ratio of the intermolecular surface contact sites per segment for the respective components s_1/s_2 has been calculated from the approximation by Abe and Flory[280,312] on the assumption that the number of sites on each molecule is proportional to the surface area of a sphere having a volume equal to the characteristic volume i.e.

$$\frac{s_1}{s_2} = \left(\frac{V_2^*}{V_1^*}\right)^{\frac{1}{3}} \tag{5.56}$$

The Flory-Prigogine theory was examined and extended by Patterson and co-workers[11,12] to derive an approximate equation of V_m^E in terms of three contributions:

$$\frac{V^E}{x_1 V_1^* + x_2 V_2^*} = \frac{(\tilde{V}^{\frac{1}{3}} - 1)\tilde{V}^{\frac{2}{3}}}{(\frac{4}{3}\tilde{V}^{-\frac{1}{3}} - 1)} \psi_1 \theta_2 \frac{X_{12}}{P_1^*} \quad \textit{(interactional)}$$

$$- \frac{(\tilde{V}_1 - \tilde{V}_2)^2 (\frac{14}{9}\tilde{V}^{-\frac{1}{3}} - 1)}{(\frac{4}{3}\tilde{V}^{-\frac{1}{3}} - 1)\tilde{V}} \psi_1 \psi_2 \quad \textit{($\tilde{V}$ curvature)} \tag{5.57}$$

$$+ \frac{(\tilde{V}_1 - \tilde{V}_2)(P_1^* - P_2^*)}{P_2^* \psi_1 + P_1^* \psi_2} \psi_1 \psi_2 \quad \textit{(P^* effect)}$$

and the corresponding equation for the excess enthalpies, H_m^E can be separated into an interactional contribution and a free volume contribution:

$$\frac{H_m^E}{(x_1 U_1^* + x_2 U_2^*)} = (-\tilde{U} + \tilde{T}\tilde{C}_P)\psi_1\theta_1\frac{X_{12}}{P_1^*} \qquad \text{(interactional)}$$

$$-\frac{1}{2}[\frac{(\tilde{V}_1 - \tilde{V}_2)^2}{(\frac{\partial \tilde{U}}{\partial \tilde{T}})}]\frac{\partial^2 \tilde{U}}{\partial \tilde{T}^2}\psi_1\psi_2 \qquad (\tilde{U} \, \textit{curvature})$$

(5.58)

The reduced configurational energy, $\tilde{U}_i$,and the reduced heat capacity, $\tilde{C}_P$, of the mixture are related to the reduced volume of the mixture and to the macroscopic quantities of the pure components by the following equations

$$-\tilde{U} = \frac{1}{\tilde{V}}$$

(5.59)

$$\tilde{C}_P = \frac{\alpha}{\tilde{V}} = \frac{4}{3}(\tilde{V})^{-\frac{1}{3}} - 1$$

(5.60)

$$U_i^* = P_i^* V_i^*$$

(5.61)

In equations 5.57 to 5.61, $\tilde{V}$ and $\tilde{T}$ without subscripts, are the reduced volume and temperature of the mixture and $\tilde{V}$ is given by

$$\tilde{V} = \psi_1\tilde{V}_1 + \psi_2\tilde{V}_2$$

(5.62)

ψ, the parameter introduced initially by Prigogine and used by Patterson is termed the contact energy fraction and only for $P_1^* = P_2^*$ will $\psi_i = \phi_i$. ψ_i is evaluated by the equation

$$\psi_1 = 1 - \psi_2 = \frac{\phi_1 P_1^*}{(\phi_1 P_1^* + \phi_2 P_2^*)}$$

(5.63)

The remaining parameters in equation 5.57 and 5.58 are identical to those given by Flory.[19,279,280,312]

5.3.4   The Extended Real Associated Solution (ERAS) Model

5.3.4.1   Introduction

For highly associating binary organic liquids (alcohols etc.), a molecular model which accounts for the self association of either one of the components in the pure and mixed state is necessary.   Two independent research groups, Renon and Pruasnitz,[282] and Kehiahian and Treszczanowicz,[283] developed the Real Associated Solution model based on Guggenheims' rigid lattice approach.[263,265] This model proved satisfactory when tested for excess energy and enthalpy functions for alcohol + alkane mixtures.[283,327,328] However, due to this model being based on the rigid lattice model it was not able to describe and predict V_m^E and its related properties.   As a result an extended version of this association theory was developed by Heintz[20] called the Extended Real Associated Solution (ERAS) model. This model combines the associated solution model with an equation of state developed by Flory. In its original form, any excess property(F^E) of a binary mixture containing a self associating component A and an inert component B is expressed as the sum of a physical and chemical contribution i.e.

$$F^E = F_{phys}^E + F_{chem}^E \tag{5.64}$$

The physical part arises from the van der Waals interactions and the chemical part from hydrogen bonding. In this section the equations of the ERAS model will be detailed as applied to the binary solutions containing self associating liquids used in this work i.e. the short chain alcohols and the secondary amines.

5.3.4.2   The Associated Solution Model - The Chemical Contribution - F_{chem}^E

The ERAS model uses the associated solution model of Kretschmer and Wiebe[290] to account for association effects arising from hydrogen bonding. This is described by a chemical

equilibrium constant K_A. K_A is independent of the chain length i of the associated species A_i:

$$A_1 + A_{i-1} \overset{K_A}{\rightleftharpoons} A_i \qquad (5.65)$$

This association model has proved to be a good approach for the mechanism occurring in pure alcohols or amines. K_A, the association constant, is a true constant with the temperature dependence given by the following relation:

$$K_A = \frac{c_{A_i}}{c_{A_{i-1}} \cdot c_{A_1}} \cdot \frac{1}{V_{A_1}^*} = K_{A_0} \cdot \exp\{\frac{-\Delta h_A^*}{R} \cdot [\frac{1}{T} - \frac{1}{T_0}]\} \qquad (5.66)$$

where c_{Ai}, c_{Ai+1} and c_{A1} are the molar concentrations of A_i, A_{i+1} and A_1 respectively. V_{A1}^* is the hard core volume and Δh_A^* is the hydrogen bonding energy of the monomeric associating species. A corresponding expression has been applied by Nath and Bender[227] to mixtures containing two associating species and a second equilibrium association constant K_B can be defined. K_B is assumed to be independent of chain length i and cross association is accounted for by the following equilibrium:

$$A_j + B_i \overset{K_{AB}}{\rightleftharpoons} A_j B_i \qquad (5.67)$$

The number of distinguishable associated species is restricted by formulation of equation 5.67 since only one contact between A and B is considered in each $A_j B_i$ species for all combinations of i and j. The equilibrium constant of equation 5.67 is also assumed to be independent of i and j and is defined by

$$K_{AB} = \frac{c_{A_j B_i}}{c_{A_j} \cdot c_{B_i}} \cdot \frac{1}{V_A^*} \qquad (5.68)$$

In this work the cross association between the self associating species and an ether has been restricted since only one contact between A and B is considered in each A_iB_j species for all combinations of i and j. Possible species with more than one A-B bonding are not considered.

5.3.6.3   *The Flory Model as used in ERAS - The Physical Contribution - F^E_{phys}*

The ERAS model incorporates the equation of state accounting for the effects of free volume in liquids and liquid mixtures as used by Flory[279] and given previously in equation 5.46. For the sake of completeness it is rewritten:

$$\frac{\tilde{P} \cdot \tilde{V}}{\tilde{T}} = \frac{\tilde{V}^{\frac{1}{3}}}{\tilde{V}^{\frac{1}{3}} - 1} - \frac{1}{\tilde{V} \cdot \tilde{T}} \tag{5.69}$$

This equation holds not only for the pure components(A and B) but also for the mixture (M). $\tilde{P}$, $\tilde{V}$ and $\tilde{T}$ are the reduced quantities of pressure P, the molar volume V and the temperature T, respectively. P^*, V^* and T^* are the corresponding reduction parameters and are defined as:

$$P^* = \frac{P}{\tilde{P}} , V^* = \frac{V}{\tilde{V}} , T^* = \frac{T}{\tilde{T}} \tag{5.70}$$

The reduction parameters for the pure components are obtained from the experimental data of the thermal expansion coefficient $\alpha = (d\ln V/dT)_P$, the compressibility $\kappa_T = -(d\ln V/dP)_T$ and V the molar volume for the pure components. The Flory equation of state yields the following expressions for the excess properties as:

$$V_{phys,Flory}^{E} = (V_A^* x_A + V_B^* x_B) \cdot [\tilde{V}_M - \Phi_A \cdot \tilde{V}_A - \Phi_B \cdot \tilde{V}_B] \qquad (5.71)$$

and

$$H_{phys,Flory}^{E} = (V_A^* x_A + V_B^* x_B) \cdot [\Phi_A \frac{P_A^*}{\tilde{V}_A} + \Phi_B \frac{P_B^*}{\tilde{V}_B} - \frac{P_M^*}{\tilde{V}_M}] \qquad (5.72)$$

where

$$P_M^* = \Phi_A \cdot P_A^* + \Phi_B \cdot P_B^* - \Phi_A \theta_B \cdot X_{AB} \qquad (5.73)$$

Φ_A and Φ_B in equations 5.71 to 5.73 are the so called hard core volume fractions

$$\Phi_A = 1 - \Phi_B = \frac{x_A \cdot V_A^*}{x_A \cdot V_A^* + h_B \cdot V_B^*} \qquad (5.74)$$

and θ_B and θ_A are the surface fractions defined as

$$\theta_B = 1 - \theta_A = \frac{s_B \cdot \Phi_B}{s_A \cdot \Phi_A + s_B \cdot \Phi_B} \qquad (5.75)$$

where s_A and s_B are the surface to volume ratios of molecules which can be calculated from molecular geometry using Bondi's[296] method. X_{AB} is the adjustable parameter which has the definition of the interaction energy parameter characterizing the differences in dispersive intermolecular interactions of molecules A and B in the mixture and the pure components.

5.3.4.4   *The ERAS equations i.e.* $F_{chem}^{E} + F_{phys}^{E}$

The derivation of the ERAS model starts with the partition function Z, of a mixture of self-associating (A) and inert molecules (B) written in the following way:

$$Z = C_{mix(T)} \cdot \exp[- \frac{\Delta h^* \cdot x_A \cdot K \cdot \phi_A}{kT}] \{(v^{\frac{1}{3}} - v^{*\frac{1}{3}})^{3N\tilde{r}\tilde{c}} \cdot \exp[\frac{P_M^* \cdot V_M^*}{\tilde{V}_M \cdot RT}] \qquad (5.76)$$

The first factor C_{Mix} in equation 5.76 is a combinatorial term and represents the number of distinguishable arrangements of associated and non-associated species in the liquid mixture at temperature T. The second factor, $\exp[-\{\Delta h^* x_A K \phi_A / kT\}]$, contains the total hydrogen bonding energy of the associating species in the liquid mixture. The term $(\Delta h^* \cdot x_A \cdot K \cdot \phi_A)$ in equation 5.76 represents the summation over the hydrogen bonding energies of all the associating multimer species in the partition function. The third factor, $(v^{\frac{1}{3}} - v^{*\frac{1}{3}})^{3N\tilde{r}\tilde{c}}$ arises from Flory's theory and represents the free volume effect due to segmental movements of the molecules in the mixture. V^* is the average hard core volume of the molecular segment $(V_M^*/\tilde{r}$) and V is the corresponding segmental molar volume. $\tilde{r}$ is the average number of segments per molecule in the mixture and is an arbitrary constant involved in the reduction parameters defined by equation 5.69. Both r and c do-not appear directly in the theoretical expressions of the thermodynamic functions and c has a value between 0 and 1 characterizing the chain-like flexibility of the associating component. The fourth factor in equation 5.76 contains the intermolecular van der Waals energy $(P_M^* \cdot V_M^* / \tilde{V}_M$) of all the molecules in the mixture. P_M^* and T_M^*, the reduction parameters for the mixture is defined as in the Flory theory by equation 5.73 and by the following, respectively

$$T_M^* = \frac{P_M^*}{\frac{P_A^* \Phi_A}{T_A^*} + \frac{P_B^* \Phi_B}{T_B^*}} \qquad (5.77)$$

V_M^* can then be obtained from equations 5.69 and 5.70 following the mixing equations of

P_M^* and T_M^*.

The equations of state derived from the partition function (equation 5.76) for the excess functions H_m^E, V_m^E are:

EXCESS ENTHALPY

$$H_{ERAS}^E = H_{chem}^E + H_{phys}^E \qquad (5.78)$$

with

$$H_{chem}^E = x_A \cdot K_A \cdot \Delta h_A^* \cdot (\varphi_{A_1} - \varphi_{A_1}^0) - \frac{P_M^* V_{chem}^E}{\tilde{V}_M^2} \qquad (5.79)$$

and

$$H_{phys}^E = (V_A^* \cdot x_A + V_B^* \cdot x_B) \cdot \left[\frac{\Phi_A \cdot P_A^*}{\tilde{V}_A} + \frac{\Phi_B \cdot P_B^*}{\tilde{V}_B} - \frac{P_M^*}{\tilde{V}_M} \right] \qquad (5.80)$$

EXCESS VOLUME

$$V_{ERAS}^E = V_{chem}^E + V_{phys}^E \qquad (5.81)$$

with

$$V_{chem}^E = x_A \cdot \tilde{V}_M \cdot \Delta V_A^* \cdot K_A \cdot (\varphi_{A_1} - \varphi_{A_1}^0) \qquad (5.82)$$

and

$$V_{phys}^E = (V_A^* \cdot x_A + V_B^* \cdot x_B) \cdot (\tilde{V}_M - \Phi_A \cdot \tilde{V}_A - \Phi_B \cdot \tilde{V}_B) \qquad (5.83)$$

The reaction volume in equation 5.82 Δv_A^* is related to the formation of hydrogen bonds. In equations 5.79 and 5.82, φ_{A_1} and $\varphi_{A_1}^0$ are the hard core volume fractions of the monomeric species in the mixture and in the pure components, respectively. These volume fractions are related to the hard core volume fractions Φ_A and K_A by

$$\varphi_{A_1} = \frac{2K_A\Phi_A + 1 - \sqrt{4K_A\Phi_A + 1}}{2K^2\Phi_A} \tag{5.84}$$

with φ_{A_1} becoming $\varphi_{A_1}^0$ if $\Phi_A = 1$.

It is important to note that the procedure to obtain the reduction parameters of the physical contribution ie. V_i^*, P_i^* and T_i^* (i = pure components) in equations 5.80 and 5.83 are different from the original one of Flory. In ERAS the hard core volumes can be calculated by introducing the thermal expansion coefficient $\alpha_i = (\partial \ln V_i \,/\, \partial T)_P$ for the pure fluids by solving the following equations:

$$V_i^* = V_i \left[\frac{1 + (\alpha_i - \alpha_i^*)T}{1 + \dfrac{4}{3}(\alpha_i - \alpha_i^*)T} \right]^3 \qquad\qquad i = A,B \tag{5.85}$$

with

$$\alpha_i^* = \Delta V_i^*\Delta h_i^* \left[\frac{(4K_i + 1)^{\frac{1}{2}} - 2K_i(4K_i + 1)^{-\frac{1}{2}} - 1}{2K_iV_{i1}^*R\,T^2} \right] \tag{5.86}$$

and

$$V_{i1}^* = V_i^* - K_i \Delta V_i^* \varphi_{i1} \qquad (5.87)$$

The reduction parameter for pressure, P_i^* for the pure components is obtained from

$$P_i^* = (\alpha_i - \alpha_i^*) T \tilde{V}_i^2 [\kappa_i - \alpha_i^* T \frac{\Delta V_i^*}{\Delta h_i^*}]^{-1} \qquad (5.88)$$

$\kappa_i = (\partial \ln V_i / \partial P)_T$ is the isothermal compressibility of the pure liquids. If component B is non-associating then Δv_B^*, Δh_B^*, K_B and α_B^* are zero and equations 5.85 and 5.88 simplify.

The equations used to calculate the excess properties of binary mixtures containing two associating components differ from equations 5.79 and 5.82. The expressions for contributions by the H_{phys}^E and V_{phys}^E terms are as in equations 5.80 and 5.83 and the contributions by H_{chem}^E and V_{chem}^E are given by the following expressions:

$$H_{chem}^E = x_A K_A \Delta h_A^* (\varphi_{A1} - \varphi_{A1}^0) + x_B K_B \Delta h_B^* (\varphi_{B1} - \varphi_{B1}^*)$$

$$+ x_A K_{AB} \Delta h_{AB}^* [\frac{\varphi_{B1}(1 - K_A \varphi_{A1})}{(\frac{V_B^*}{V_A^*})(1 - K_B \varphi_{B1}) + K_{AB} \varphi_{B1}}] \qquad (5.89)$$

$$- \frac{P_M^* V_{chem}^E}{\tilde{V}_M}$$

and

$$V_{chem}^{E} = \bar{V}_{M}[x_{A}K_{A}\Delta v_{A}^{\bullet}(\varphi_{A_{1}} - \varphi_{A_{1}}^{0}) + x_{B}K_{B}\Delta v_{B}^{\bullet}(\varphi_{B_{1}} - \varphi_{B_{1}}^{0})$$

$$+ x_{A}K_{AB}\Delta v_{AB}^{\bullet} \cdot \frac{\varphi_{B_{1}}(1 - K_{A}\varphi_{A_{1}})}{(\frac{V_{B}^{\bullet}}{V_{A}^{\bullet}})(1 - K_{B}\varphi_{B_{1}}) + K_{AB}\varphi_{B_{1}}}] \qquad (5.90)$$

For all of the equations given in this section, x_{A} is the mole fraction of the associating species A in a binary mixture and $x_{B} = 1 - x_{A}$. The parameters required for the calculation of the excess properties for the cross associating liquid mixtures are evaluated in the following way: the adjustable parameters K_{AB}, $\Delta h_{AB}^{\bullet}$, $\Delta v_{AB}^{\bullet}$ and X_{AB} have to be obtained from simultaneous adjustment to experimental data of H_{m}^{E} and V_{m}^{E}.

The success of the ERAS theory lies in the ability of the model to predict V_{m}^{E} of associating mixtures which are in good agreement with experimental data and the ability of the ERAS model to account for S-shaped curves results from the counteracting contributions of V_{c}^{E} and V_{p}^{E} to V_{m}^{E}. This model was originally developed for alcohol-alkane mixtures but has been extended to binary mixtures composed of strong and a weakly associating component, such as alcohol-amine mixtures.[20,21,227-230,329]

Application of the Thermodynamic Theories of Liquid Mixtures

6.1 Introduction

The NRTL[14], UNIQUAC[15] and UNIQUAC ASM[16] theories have been discussed in detail in the preceding chapter. In this chapter these theories are tested using measurments on the binary mixtures {(an alkanol or a secondary amine or a 1-alkyne) + (a branched chain or a cyclic ether)}. The experimental H_m^E and V_m^E results relating to these mixtures are presented in Chapter 2.

The Modified UNIFAC[17,18] theory has been tested by fitting the main group R_k and Q_k parameters and the group interaction parameters (a_{nm}, b_{nm} and c_{nm}) to the experimental H_m^E data for binary mixtures of {(an alkanol + a branched chain or a cyclic ether) or (a secondary amine + a cyclic ether)}. The group interaction parameters were obtained from the latest parameter matrix of Gmehling et al.[17,248,252,311] consisting of 45 main groups and 530 group combinations. Selected group combinations for the {(secondary amine or 1-alkyne) + a branched chain ether) systems were not available and as a result the Modified UNIFAC model could not be applied to those systems.

The Flory theory[19,279,280] has been tested by fitting the various parameters to the experimental H_m^E and V_m^E results for the binary mixtures {a 1-alkyne + a branched chain ether}.

The original Flory theory was not expected to work for any of the other systems due to the limitations of the Flory model when applied to binary mixtures containing associating components. The approximate modifications to the Flory theory by Patterson et al. ie. the Prigogine Flory Patterson theory[11,12] has been fitted to the V_m^E experimental data of {(an alkanol or a secondary amine) + (a branched chain or a cyclic ether)}. The Flory interaction parameter, X_{12}, was derived from H_m^E and V_m^E and used, in turn, to predict the same and/or another excess thermodynamic property. Similar predictions have been carried out by other workers.[331,332-335]

The ERAS model[20,21], which accounts for self and cross association effects and the free volume effects between component molecules in a mixture has been fitted to both H_m^E and V_m^E experimental data for binary mixtures of {(an alkanol or a secondary amine) + (a branched chain or a cyclic ether)}. For both the alkanol and the amine, association effects arise from the chain association of the molecules and the cross association of the alkanol or amine with the lone pair on the oxygen of the ether. The parameters adjusted to the mixture properties are two cross association parameters (X_{AB}, K_{AB}) and the interaction parameters responsible for the exchange energy of the van der Waals interactions (h_{AB}^*, v_{AB}^*).

6.2   The Modified UNIFAC Model

6.2.1   <u>Mixtures of (an alkanol + a branched chain ether)</u>

The Modified UNIFAC[17,18,311] model has been tested by fitting the group volumes(R_k), group surface areas (Q_k) and the group interaction parameters to the experimental H_m^E for the binary systems {(methanol or ethanol or propan-1-ol or propan-2-ol) + (diisopropyl ether(IPE) or tert-butyl methyl ether(TBME) or tert-amyl methyl ether(TAME))}

The group volumes R_k, the group surface areas Q_k and the group interaction parameters, a_{nm} are listed in Appendix 4 and Table 4.1 for all the {alkanols + a branched chain ether} systems investigated in this work.   The calculated H_m^E results together with the deviations δH_m^E, where $\delta H_m^E = H_{m,expt}^E - H_{m,calc}^E$, are given in Table 6.1 for selected experimental data points.   The values of the standard deviations are given in Table 6.2.

TABLE 6.1 Predicted excess molar enthalpies, H_m^E for $\{ x \, C_jH_{2j+1}OH + (1-x) \, ROR' \}$ where ROR' is a branched chain ether and the deviations, δH_m^E at the temperature 298.15 K

x	H_m^E $J \cdot mol^{-1}$	δH_m^E $J \cdot mol^{-1}$	x	H_m^E $J \cdot mol^{-1}$	δH_m^E $J \cdot mol^{-1}$	x	H_m^E $J \cdot mol^{-1}$	δH_m^E $J \cdot mol^{-1}$
			$xCH_3OH + (1-x)\{CH_3CH(CH_3)\}_2O$					
0.132	116.9	72.7	0.404	275.2	-95.8	0.846	227.2	-252.7
0.276	214.9	0.7	0.606	312.8	-211.4	0.986	32.8	-45.5
			$xCH_3OH + (1-x)CH_3C(CH_3)_2OCH_3$					
0.132	288.6	-38.8	0.377	316.6	-5.9	0.884	66.6	-50.5
0.202	337.5	-57.3	0.592	196.2	29.0	0.936	43.8	-49.9
			$xCH_3OH + (1-x)CH_3CH_2C(CH_3)_2OCH_3$					
0.185	377.8	-77.3	0.422	360.2	14.5	0.856	109.7	-22.0
0.350	392.1	-41.7	0.644	222.7	38.9	0.978	26.5	-32.7
			$xC_2H_5OH + (1-x)\{CH_3CH(CH_3)\}_2O$					
0.080	381.2	-140.8	0.459	677.5	-263.5	0.871	-215.6	-141.5
0.215	653.7	-250.9	0.641	523.9	-234.0	0.985	26.5	-23.1
			$xC_2H_5OH + (1-x)\{CH_3C(CH_3)_2OCH_3$					
0.120	462.2	-161.4	0.451	729.0	-213.2	0.825	273.5	-74.6
0.222	661.7	-201.6	0.591	610.5	-169.9	0.982	25.5	-11.5
			$xC_2H_5OH + (1-x)\{CH_3CH_2C(CH_3)_2OCH_3$					
0.075	334.9	-71.9	0.341	784.2	-222.6	0.871	221.4	-61.2
0.253	727.3	-190.6	0.643	588.7	-160.2	0.934	110.5	-33.3

TABLE 6.1   *Continued*

x	H_m^E	δH_m^E	x	H_m^E	δH_m^E	x	H_m^E	δH_m^E
	$J \cdot mol^{-1}$	$J \cdot mol^{-1}$		$J \cdot mol^{-1}$	$J \cdot mol^{-1}$		$J \cdot mol^{-1}$	$J \cdot mol^{-1}$

$$xC_3H_7OH + (1-x)\{CH_3CH(CH_3)\}_2O$$

x	H_m^E	δH_m^E	x	H_m^E	δH_m^E	x	H_m^E	δH_m^E
0.081	367.3	-141.7	0.461	612.0	-184.0	0.856	-196.1	-88.9
0.207	606.8	198.4	0.590	508.6	-168.4	0.979	-29.0	-22.1

$$xC_3H_7OH + (1-x)CH_3C(CH_3)_2OCH_3$$

x	H_m^E	δH_m^E	x	H_m^E	δH_m^E	x	H_m^E	δH_m^E
0.098	388.6	-65.7	0.464	695.7	-133.1	0.797	312.2	-41.8
0.248	670.6	-147.0	0.612	564.8	-99.9	0.992	11.8	-4.8

$$xC_3H_7OH + (1-x)CH_3CH_2C(CH_3)_2OCH_3$$

x	H_m^E	δH_m^E	x	H_m^E	δH_m^E	x	H_m^E	δH_m^E
0.110	435.3	-114.8	0.462	726.1	-148.3	0.828	280.2	-18.5
0.235	678.8	-162.9	0.620	582.9	-110.9	0.978	34.8	-4.7

$$xCH_3CH(OH)CH_3 + (1-x)\{CH_3CH(CH_3)\}_2O$$

x	H_m^E	δH_m^E	x	H_m^E	δH_m^E	x	H_m^E	δH_m^E
0.131	485.4	-6.4	0.452	616.8	55.4	0.787	286.9	39.5
0.232	620.4	8.3	0.626	473.9	73.7	0.879	166.3	26.1

$$xCH_3CH(OH)CH_3 + (1-x)\{CH_3C(CH_3)_2OCH_3$$

x	H_m^E	δH_m^E	x	H_m^E	δH_m^E	x	H_m^E	δH_m^E
0.120	205.9	9.4	0.451	310.7	2.1	0.825	16.1	-3.8
0.222	249.6	9.4	0.591	282.3	2.2	0.982	9.4	3.1

$$xCH_3CH(OH)CH_3 + (1-x)\{CH_3CH_2C(CH_3)_2OCH_3$$

x	H_m^E	δH_m^E	x	H_m^E	δH_m^E	x	H_m^E	δH_m^E
0.095	370.3	29.8	0.410	710.7	42.7	0.755	375.0	83.8
0.206	608.6	-5.2	0.640	529.5	96.3	0.878	187.9	32.8

TABLE 6.2   Standard Deviations of Modified UNIFAC predicted results for H_m^E at 298.15K.

System	No. of Data Points	Deviations	
		ASD*	ARD**
		$J \cdot mol^{-1}$	%
$x CH_3OH + (1-x)[CH_3CH(CH_3)_2]O$	20	175.1	1031.7
$x CH_3OH + (1-x)CH_3C(CH_3)_2OCH_3$	18	40.8	3350.1
$x CH_3OH + (1-x)[CH_3CH_2C(CH_3)_2OCH_3$	11	32.7	209.0
$x C_2H_5OH + (1-x)[CH_3CH(CH_3)_2]O$	14	196.3	232.7
$x C_2H_5OH + (1-x)CH_3C(CH_3)_2OCH_3$	17	148.1	45.5
$x C_2H_5OH + (1-x)[CH_3CH_2C(CH_3)_2OCH_3$	11	136.9	36.8
$x C_3H_7OH + (1-x)[CH_3CH(CH_3)_2]O$	18	160.5	92.2
$x C_3H_7OH + (1-x)CH_3C(CH_3)_2OCH_3$	14	94.9	26.7
$x C_3H_7OH + (1-x)[CH_3CH_2C(CH_3)_2OCH_3$	16	108.8	25.2
$x CH_3CH(OH)CH_3 + (1-x)[CH_3CH(CH_3)_2]O$	14	42.7	10.4
$x CH_3CH(OH)CH_3 + (1-x)CH_3C(CH_3)_2OCH_3$	14	62.8	12.1
$x CH_3CH(OH)CH_3 + (1-x)[CH_3CH_2C(CH_3)_2OCH_3$	14	46.3	9.0

* Absolute Standard Deviation

** Absolute Relative Deviation $= |(H_{m(expt)}^E - H_{m(calc)}^E)/H_{m(expt,max)}^E| \times 100$ (%)

Figures 6.1(a) and 6.1(b) show selected experimental H_m^E results together with the fitted curves. For all the binary systems except the methanol systems, the Modified UNIFAC method correctly predicts the increase in excess enthalpy curves which are of the same general shape as the experimental curves. The ASD and ARD improve considerably as the chain length of the alkanol increases for each of the ethers. For {methanol + IPE or TAME or TBME} the model fails to predict the small exothermic behaviour at the methanol rich region and the largest ARD's are obtained for these systems. This could probably be due to groupings of methanol in the Modified UNIFAC model. Methanol is a compact and complex polar group which for proximity reasons is treated as a single group i.e. no distinction is made for the CH_3 and OH groups, and all interactions are considered to occur with the CH_3OH. The {propan-2-ol + IPE or TAME or TBME} calculated results show the best fit to the experimental data. The improved results are probably due to the introduction of a special sub-group for the secondary alcohol which differs in the R_k and Q_k parameters from the primary or tertiary alcohols.
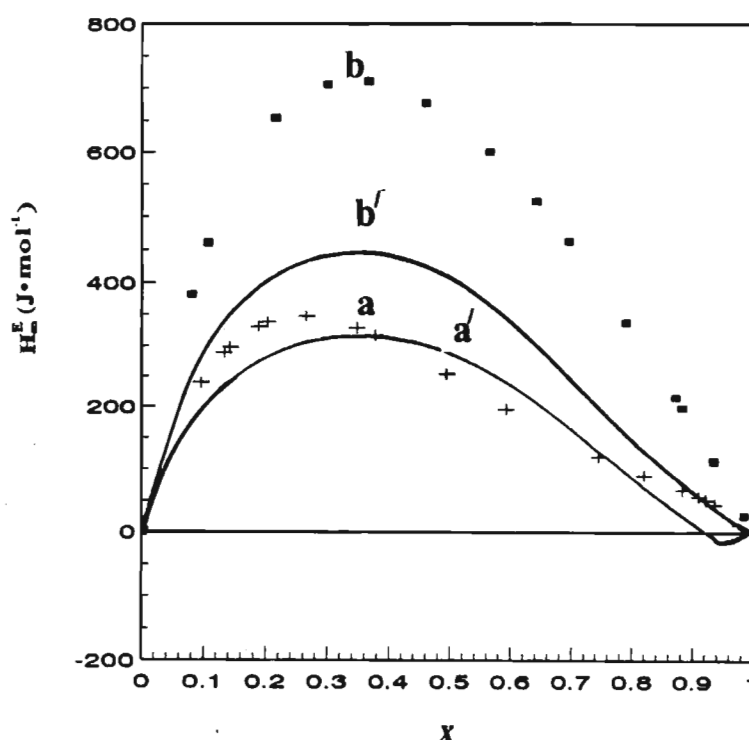
Figure 6.1(a) Experimental(a and b) and Predicted(a′ and b′) H_m^E data using Modified UNIFAC for (a and a′)
$xCH_3OH + (1-x)TBME$; (b and b′) $xC_2H_5OH + (1-x)IPE$
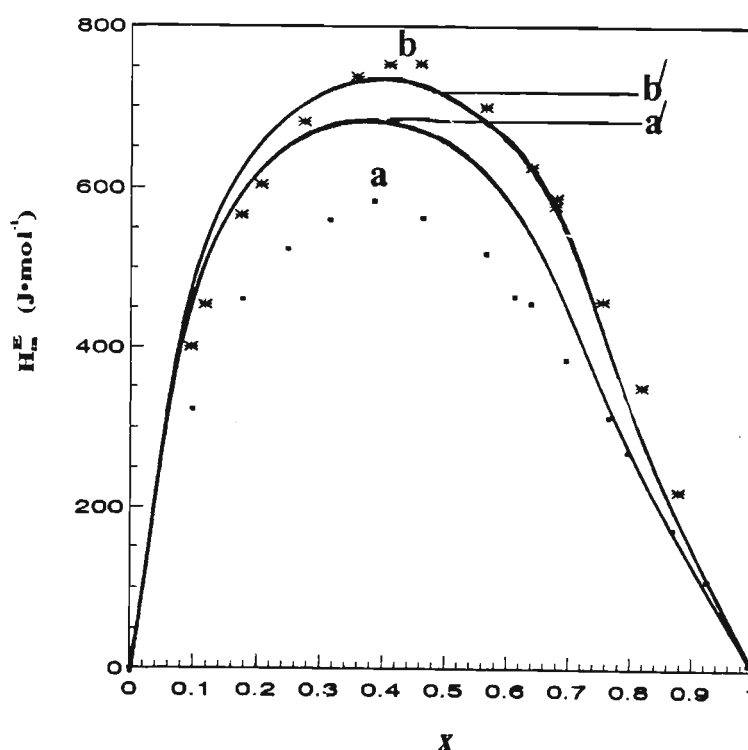
Figure 6.1(b) Experimental (a and b) and Predicted (a′ and b′) H_m^E data using Modified UNIFAC for (a and a′)
xC_3H_7OH + (1-x)TBME; (b and b′) $xCH_3CH(OH)CH_3$ + (1-x)TAME

6.2.2 Mixtures of (an alkanol + a cyclic ether)

The Modified UNIFAC model has been applied to the experimental H_m^E binary

mixtures of {(methanol or ethanol or propan-1-ol or propan-2-ol) + (tetrahydrofuran (THF)

or tetrahydropyran (THP) or 1,4 dioxane)}. The group volumes R_k, the group surface areas

Q_k and the group interaction parameters, a_{nm} are given in Appendix 4 and Table 4.2 for all

the {an alkanol + a cyclic ether} systems investigated in this work. The calculated H_m^E

results together with the deviations δH_m^E, where $\delta H_m^E = H_{mexpt}^E - H_{mcalc}^E$, are given in Table

6.3 for selected experimental data points. The values of the standard deviations are given

in Table 6.4.

Figures 6.2(a) and 6.2(b) show selected experimental H_m^E results together with the fitted

curves. For all the cyclic ethers the predictions become less successful in the order 1,4-

dioxane < < < THP < THF for each of the alkanols. The methanol + THF system

shows the largest ARD of 77.1 % and the UNIFAC model over-predicts the experimental

results over the entire composition range. For the methanol + THP system the situation

improves slightly with predicted results becoming closer to experimental results in the low and high alkanol mole fraction ranges. For methanol + 1,4-dioxane the calculated results are far lower than the experimental results by 262 $J \cdot mol^{-1}$ in the worst case; the poor results are probably due to (a) the lack of distinction between the CH_3 and OH main groups for the methanol component in the model and (b) the lack of flexibility of the model to account for the large differences in the size and shape of the two component molecules. In general, for all cyclic ethers, as the chain length of the alkanol increases the ARD improves in the order THF > THP > 1,4-dioxane. For the (an alkanol + a cyclic ether) system the theory reproduces the main features of the experimental data although quantitative agreement is not achieved. These results are in contrast to the success of the Modified UNIFAC model in correctly predicting the H_m^E for (THF or 1,4-dioxane + an alkane)[336] and (an alkanol + an alkane)[337] with a special main group for the cyclic ethers. No trend relating the accuracy of predictions and the chemical nature of the system components can be established.

TABLE 6.3 Predicted excess molar enthalpies, H_m^E for $\{x\ C_jH_{2j+1}OH + (1-x)\ ROR'\}$ where ROR' is cyclic ether and the deviations, δH_m^E at the temperature 298.15 K

x	H_m^E	δH_m^E	x	H_m^E	δH_m^E	x	H_m^E	δH_m^E
	$J \cdot mol^{-1}$	$J \cdot mol^{-1}$		$J \cdot mol^{-1}$	$J \cdot mol^{-1}$		$J \cdot mol^{-1}$	$J \cdot mol^{-1}$
			$xCH_3OH + (1-x)c\text{-}(CH_2)_4)O$					
0.098	371.3	-100.3	0.418	794.5	-250.2	0.858	337.0	-153.0
0.218	642.8	-179.0	0.664	646.3	-241.7	0.933	172.9	-102.2
			$xCH_3OH + (1-x)c\text{-}(CH_2)_5O$					
0.123	474.1	-50.8	0.315	817.2	-131.6	0.699	676.4	-182.7
0.206	670.1	-99.1	0.431	867.8	-161.2	0.846	418.1	-108.3
			$xCH_3OH + (1-x)c\text{-}(CH_2)_2O(CH_2)_2O$					
0.129	419.5	140.7	0.435	868.6	262.2	0.848	417.7	132.24
0.203	595.1	221.6	0.672	744.4	195.3	0.924	147.0	69.96
			$xC_2H_5OH + (1-x)c\text{-}(CH_2)_4)O$					
0.102	418.2	-51.6	0.401	941.0	-132.0	0.823	588.8	-195.8
0.229	740.9	-94.8	0.629	899.2	-218.9	0.892	401.6	-149.8
			$xC_2H_5OH + (1-x)c\text{-}(CH_2)_5O$					
0.123	495.0	25.9	0.462	991.5	-138.3	0.787	709.4	-214.8
0.219	739.6	-22.4	0.620	899.4	-192.6	0.842	581.3	-220.8
			$xC_2H_5OH + (1-x)\{CH_3CH(CH_3)\}_2O$					
0.101	464.4	135.7	0.427	1285.6	239.7	0.832	839.8	24.1
0.221	883.0	232.9	0.626	1270.1	125.8	0.936	384.5	-0.8

TABLE 6.3   *Continued*

x	H_m^E J·mol^{-1}	δH_m^E J·mol^{-1}	x	H_m^E J·mol^{-1}	δH_m^E J·mol^{-1}	x	H_m^E J·mol^{-1}	δH_m^E J·mol^{-1}
			$xC_3H_7OH + (1-x)c\text{-}(CH_2)_4O$					
0.113	475.4	-59.8	0.434	1017.8	-77.0	0.789	693.3	-121.8
0.217	757.2	-64.0	0.580	995.7	-121.4	0.939	247.0	-42.9
			$xC_3H_7OH + (1-x)c\text{-}(CH_2)_5O$					
0.096	422.8	-48.4	0.447	1029.2	-100.1	0.849	569.2	-169.2
0.217	761.5	-59.6	0.615	984.9	-169.2	0.906	386.1	-142.6
			$xC_3H_7OH + (1-x)c\text{-}(CH_2)_2O(CH_2)_2O$					
0.114	589.0	194.2	0.446	1497.9	353.9	0.818	1003.1	94.3
0.254	1114.4	337.2	0.672	1412.3	185.8	0.927	476.7	41.6
			$xCH_3CH(OH)CH_3 + (1-x)c\text{-}(CH_2)_4O$					
0.131	524.8	75.3	0.405	996.1	125.4	0.821	617.1	59.4
0.223	760.8	109.8	0.604	1040.8	67.2	0.882	444.1	55.4
			$xCH_3CH(OH)CH_3 + (1-x)c\text{-}(CH_2)_5O$					
0.103	437.6	81.9	0.400	996.8	123.3	0.757	785.8	-7.2
0.207	728.2	134.7	0.623	972.0	31.0	0.863	526.6	-47.6
			$xCH_3CH(OH)CH_3 + (1-x)c\text{-}(CH_2)_2O(CH_2)_2O$					
0.111	565.7	269.4	0.391	1421.9	578.8	0.816	1013.6	338.6
0.226	1017.1	450.8	0.579	1521.6	498.8	0.943	386.5	128.9

TABLE 6.4 Standard Deviations of Modified UNIFAC predicted results for H_m^E at 298.15 K for (an alkanol + a cyclic ether)

System	No. of Data Points	Deviations	
		AAD[*]	ARD[**]
		J·mol⁻¹	%
$x\mathrm{CH_3OH} + (1\text{-}x)c\text{-}(\mathrm{CH_2})_4\mathrm{O}$	15	178.9	77.8
$x\mathrm{CH_3OH} + (1\text{-}x)c\text{-}(\mathrm{CH_2})_5\mathrm{O}$	14	128.2	25.3
$x\mathrm{CH_3OH} + (1\text{-}x)c\text{-}(\mathrm{CH_2})_2\mathrm{O}(\mathrm{CH_2})_2\mathrm{O}$	17	194.6	23.9
$x\mathrm{C_2H_5OH} + (1\text{-}x)c\text{-}(\mathrm{CH_2})_4\mathrm{O}$	15	148.3	35.2
$x\mathrm{C_2H_5OH} + (1\text{-}x)c\text{-}(\mathrm{CH_2})_5\mathrm{O}$	16	139.4	30.3
$x\mathrm{C_2H_5OH} + (1\text{-}x)c\text{-}(\mathrm{CH_2})_2\mathrm{O}(\mathrm{CH_2})_2\mathrm{O}$	20	153.6	15.0
$x\mathrm{C_3H_7OH} + (1\text{-}x)c\text{-}(\mathrm{CH_2})_4\mathrm{O}$	17	87.6	13.7
$x\mathrm{C_3H_7OH} + (1\text{-}x)c\text{-}(\mathrm{CH_2})_5\mathrm{O}$	16	117.3	30.7
$x\mathrm{C_3H_7OH} + (1\text{-}x)c\text{-}(\mathrm{CH_2})_2\mathrm{O}(\mathrm{CH_2})_2\mathrm{O}$	18	238.7	18.1
$x\mathrm{CH_3C(OH)CH_3} + (1\text{-}x)c\text{-}(\mathrm{CH_2})_4\mathrm{O}$	15	82.7	15.7
$x\mathrm{CH_3C(OH)CH_3} + (1\text{-}x)c\text{-}(\mathrm{CH_2})_5\mathrm{O}$	17	83.3	10.9
$x\mathrm{CH_3C(OH)CH_3} + (1\text{-}x)c\text{-}(\mathrm{CH_2})_2\mathrm{O}(\mathrm{CH_2})_2\mathrm{O}$	18	387.1	27.6

[*] Absolute Standard Deviation

[**] Absolute Relative Deviation $= \left| (H_{m(expt)}^E - H_{m(calc)}^E)/H_{m(expt,max)}^E \right| \times 100$ (%)

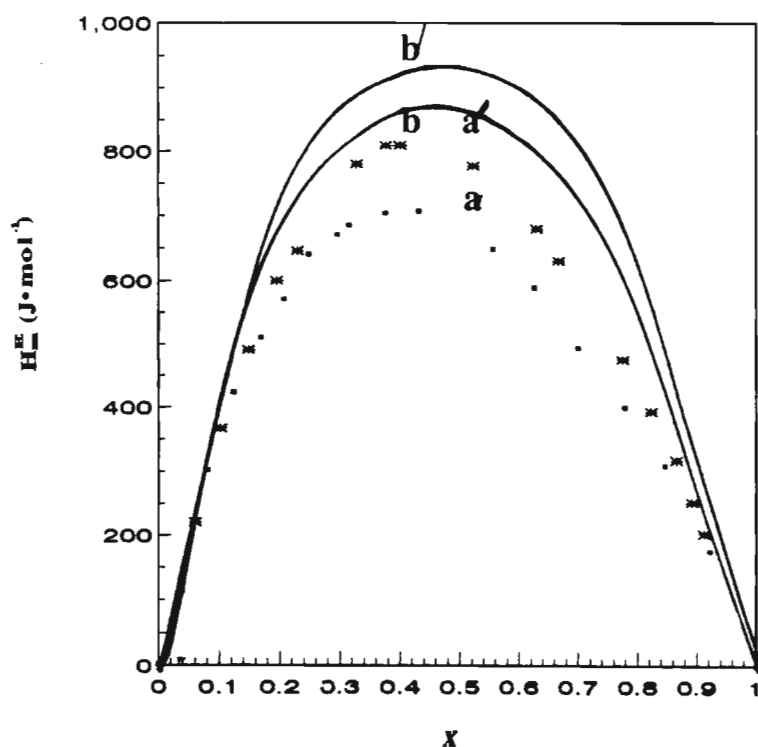*Figure 6.2 (a) Experimental (a and b) and Predicted (a′ and b′) H_m^E data using Modified UNIFAC for (a and a′)*

xCH_3OH + (1-x)THP; (b and b′) xC_2H_5OH + (1-x)THF

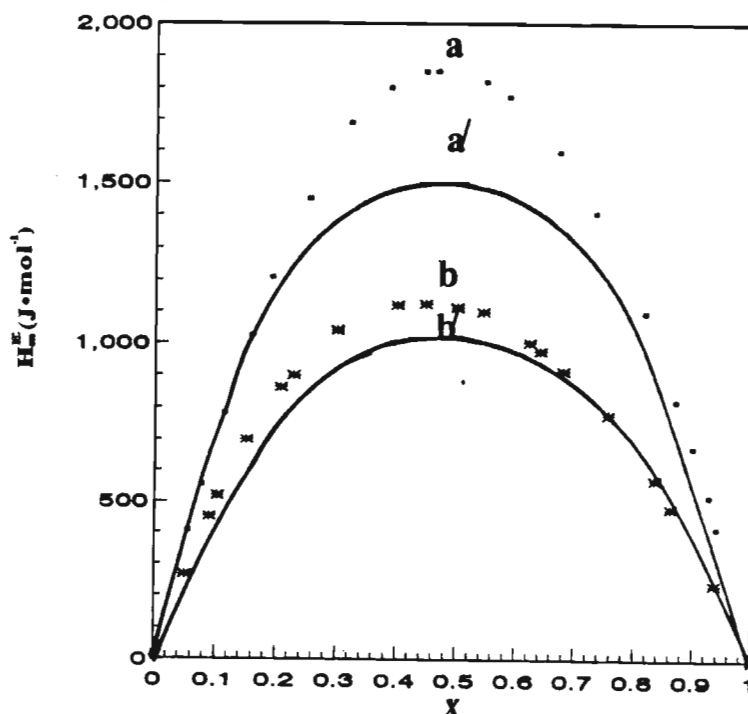*Figure 6.2(b) Experimental (a and b) and Predicted (a′ and b′) H_m^E data using Modified UNIFAC for (a and a′)*

xC_3H_7OH + (1-x)1,4-dioxane; (b and b′) $xCH_3CH(OH)CH_3$ + (1-x)THP

6.2.3 Mixtures of (diethylamine or di-n-propylamine + a cyclic ether)

Tables 6.5 and 6.6 show the calculated excess molar enthalpies together with the deviations δH_m^E and the AAD and ARD deviations for the systems {(diethylamine or di-n-propylamine) + (THF or THP or 1,4-dioxane)}. The R_k and Q_k and the group interaction parameters are listed in Appendix 4 and Table 4.3. For all the systems investigated the Modified UNIFAC model fails correctly to reproduce the experimental H_m^E data and gives large AAD deviations. Figures 6.3 and 6.4 show selected experimental H_m^E results together with the fitted curves.

For the {(diethylamine or di-n-propylamine + THF or THP)} the experimental H_m^E(max) results are small and positive (approximately 50 J·mol⁻¹) while the calculated H_m^E(max) values are fairly large and positive (300 J·mol⁻¹). The maximum H_m^E values in the Modified UNIFAC model are dependent on the R_k and Q_k parameters[252] (van der Waals properties) and the poor representation for (a secondary amine + a cyclic ether) could be due to the inability of the group parameter data to represent certain cyclic compounds correctly. In addition the model is especially suited to represent non cross-associating solutions and the small endothermic behaviour observed for these solutions is indicative of association between the NH group in the secondary amine and the O group in the ether i.e. the NH····O interaction (c.f. chapter 2 and 3) . It is probably necessary to include a special chemical term in the model properly to describe systems with association. The small exothermic behaviour observed for (diethylamine + THP) and (di-n-propylamine + THF) in the amine rich region was totally unaccounted for by the model. It is surprising that the model predicts far smaller H_m^E(max) results for the {(diethylamine or di-n-propylamine) + 1,4 dioxane} systems than the experimental H_m^E(max) data as the same main and sub-groups were used for 1,4-dioxane as THF or THP. The large endothermic behaviour of the systems {(diethylamine or di-n-propylamine) + 1,4 dioxane} is a result of the dominance of the breaking of the self association between the amine molecules over any cross association between amine and 1,4-dioxane molecules. Hence a better fit of the

Modified UNIFAC to these systems was expected. The differences in size and shape of the amine[107] and cyclic ether[335] molecules could possibly account for the poor representation by the Modified UNIFAC model.

TABLE 6.5 Predicted excess molar enthalpies, H_m^E for (x $CH_3(CH_2)_nNH(CH_2)_nCH_3$ + (1-x) ROR′) where n = 1 or 2 and ROR′ is a cyclic ether and the deviations, δH_m^E at the temperature 298.15 K

x	H_m^E	δH_m^E	x	H_m^E	δH_m^E	x	H_m^E	δH_m^E
	$J \cdot mol^{-1}$	$J \cdot mol^{-1}$		$J \cdot mol^{-1}$	$J \cdot mol^{-1}$		$J \cdot mol^{-1}$	$J \cdot mol^{-1}$
			$xC_2H_5NHC_2H_5$ + (1-x)c-$(CH_2)_4$O					
0.100	137.0	-113.1	0.434	320.0	-262.2	0.815	169.8	-157.9
0.222	248.4	-204.6	0.607	289.7	-250.7	0.966	35.7	-35.5
			$xC_2H_5NHC_2H_5$ + (1-x)c-$(CH_2)_5$O					
0.095	169.7	-160.0	0.445	439.1	-409.3	0.824	236.2	-237.4
0.202	307.1	-279.6	0.637	391.9	-376.5	0.934	95.3	-100.6
			$xC_2H_5NHC_2H_5$ + (1-x)c-$(CH_2)_2O(CH_2)_2$O					
0.097	13.1	194.0	0.421	28.0	601.0	0.806	14.0	339.0
0.223	23.2	433.8	0.634	23.0	528.3	0.939	4.8	113.3
			$xC_3H_7NHC_3H_7$ + (1-x)c-$(CH_2)_4$O					
0.105	180.8	-160.8	0.473	409.7	-394.4	0.863	169.5	-176.0
0.224	315.7	-288.5	0.654	348.1	-346.6	0.961	51.9	-56.1
			$xC_3H_7NHC_3H_7$ + (1-x)c-$(CH_2)_5$O					
0.097	191.6	-177.9	0.442	487.8	-430.3	0.846	234.6	-198.6
0.247	397.0	-261.6	0.600	456.2	-397.7	0.961	65.9	-54.9
			$xC_3H_7NHC_3H_7$ + (1-x){$CH_3CH(CH_3)$}$_2$O					
0.088	117.9	134.6	0.410	339.7	374.2	0.773	231.8	223.1
0.192	225.0	243.4	0.636	313.0	320.7	0.936	76.6	73.8

TABLE 6.6 Standard Deviations of Modified UNIFAC predicted results for H_m^E at 298.15 K for $(x\ CH_3(CH_2)_nNH(CH_2)_nCH_3 + (1-x)\ ROR')$ where n = 1 or 2 and ROR' is a cyclic ether

System	No. of Data Points	Deviations	
		AAD*	ARD**
		$J \cdot mol^{-1}$	%
$xC_2H_5NHC_2H_5 + (1-x)c\text{-}(CH_2)_4O$	24	189.3	2684.9
$xC_2H_5NHC_2H_5 + (1-x)c\text{-}(CH_2)_5O$	22	295.1	6359.9
$xC_2H_5NHC_2H_5 + (1-x)c\text{-}(CH_2)_2O(CH_2)_2O$	20	399.7	95.0
$xC_3H_7NHC_3H_7 + (1-x)c\text{-}(CH_2)_4O$	15	258.3	6443.3
$xC_3H_7NHC_3H_7 + (1-x)c\text{-}(CH_2)_5O$	16	315.0	899.2
$xC_3H_7NHC_3H_7 + (1-x)c\text{-}(CH_2)_2O(CH_2)_2O$	14	265.0	51.2

* Absolute Standard Deviation

** Absolute Relative Deviation = $\left| (H_{m(expt)}^E - H_{m(calc)}^E)/H_{m(expt,max)}^E \right| \times 100$ (%)
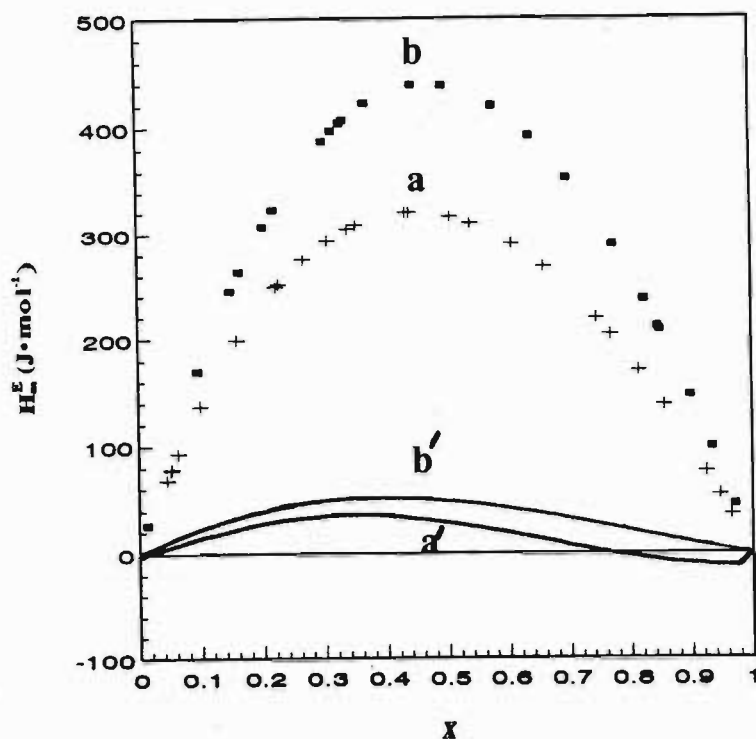
Figure 6.3 Experimental(a and b) and Predicted(a′ and b′) H_m^E data using Modified UNIFAC for {x CH$_3$CH$_2$NHCH$_2$CH$_3$ + (1-x) (a and a′) THF; (b and b′) THP}
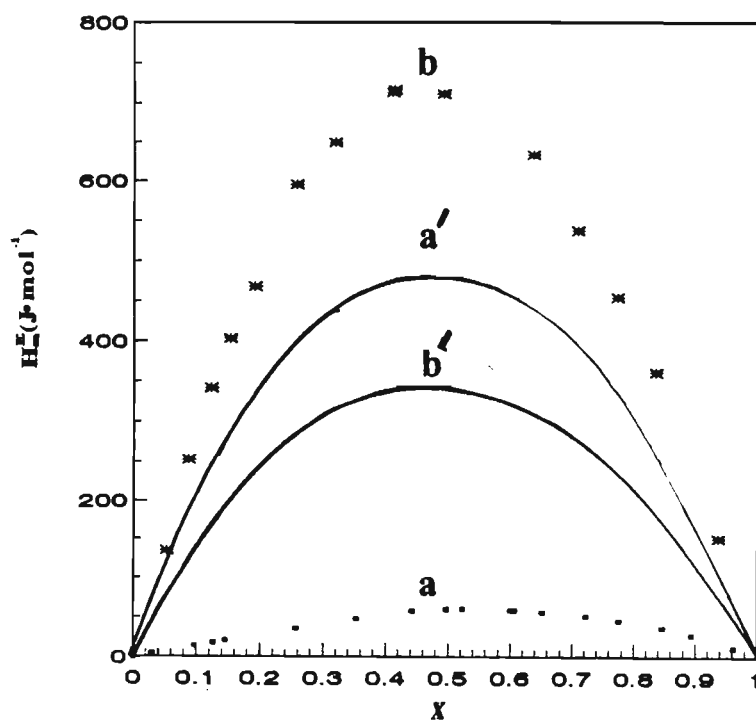
Figure 6.4 Experimental (a and b) and Predicted (a′ and b′) H_m^E data using Modified UNIFAC for {x CH$_3$(CH$_2$)$_2$NH(CH$_2$)$_2$CH$_3$ + (1-x) (a and a′) THP; (b and b′) 1,4-dioxane}

6.3   The Flory Theory and The Prigogine Flory Patterson (PFP) Theory

6.3.1   <u>Introduction</u>

The Flory theory has been tested by fitting the various parameters to the experimental H_m^E and V_m^E results for the binary mixtures {(an alk-1-yne + a branched chain ether)}. Due to the self-associating nature of the alkanols and the amines and the cross association exhibited by the alkanol/amine with a branched chain and cyclic ether, the simple Flory theory was not expected to work and therefore not tested for these systems. The Prigogine Flory Patterson(PFP) theory was, however, fitted and tested to the V_m^E data for these associating systems {(an alkanol or secondary amine) + (a branched chain ether or cyclic ether)}. For both the Flory and PFP theories an interaction parameter, X_{12}, was derived from the experimental excess molar properties presented here. The only data requirements for the application of both the Flory and PFP theories are the densities ρ, the thermal expansion coefficients α, and the isothermal compressibilities κ_T, for the two pure components, and the experimental H_m^E and V_m^E. The values of the pure component properties, together with the literature references are given in Table 6.7. The ρ for all the pure components and the α and κ_T for the branched chain and cyclic ethers were measured in this work. (c.f. Chapter 4)

TABLE 6.7 Physical properties at 298.15 K for thermal expansion coefficients α, isothermal compressibilities κ_T and densities ρ for the pure compounds used in this study

Compound	$\alpha \cdot 10^4$ —— K^{-1}	Ref.	$\kappa_T \cdot 10^4$ —— MPa^{-1}	Ref.	ρ ———— $kg \cdot m^{-3}$
methanol	11.89	231	12.48	225	786.52
ethanol	10.93	338	11.49	365	785.12
propan-1-ol	9.95	338	10.26	365	799.74
propan-2-ol	10.64	339	11.42	365	780.93
diethylamine	15.30	230	14.71	230	699.69
di-n-propylamine	13.10	232	12.20	232	733.35
hex-1-yne	13.71	340	14.04	340	711.11
hept-1-yne	12.49	340	12.56	340	730.53
oct-1-yne	11.62	340	11.46	340	746.57
IPE	14.50[†]	245	17.19	this work	718.39[*]
TBME	14.20[†]	245	15.39	this work	735.43[*]
TAME	9.66	this work	19.58	this work	765.99[*]
THF	8.77	this work	9.60	this work	882.07[*]
THP	7.76	this work	9.46	this work	879.01[*]
1,4-dioxane	7.17	this work	7.39	this work	1028.00[*]

[†] α value used from literature as Flory and ERAS models gives a better fit than measured value

[*] measured at IIT, New Delhi, India (cf. Table 2.1)

6.3.2   The Flory Theory

The approach of Benson and co-workers[331] and Diaz Pena et al.[333] has been followed in this work. Adjustable interaction parameters for each of the systems were calculated to fit the experimental excess molar enthalpy and experimental molar volume results. These X_{12} (H_m^E) and X_{12} (V_m^E) parameters were then used to check whether the Flory equations were capable of reproducing the experimental H_m^E and V_m^E curves over the entire composition range. Finally the ability of the theory to predict the excess molar volumes from excess molar enthalpy data, and conversely excess molar enthalpies from excess molar data, was examined. Equations 5.46 to 5.56 were used to fit V_m^E and H_m^E data for (a 1-alkyne + a branched chain ether) over the entire composition range at 0.01 mole fraction intervals. These predicted values were compared with the experimental V_m^E determined at the same mole fractions from the coefficients of the Redlich-Kister[342] smoothing curve, and the standard deviations $\sigma(V_m^E$ or H_m^E) over all the mole fractions were calculated according to the general expression:

$$\sigma^2 = \frac{[\sum\limits_{i=1}^{99} [X_{m(expt,x_i)}^E - X_{(calc,x_i)}^E]^2}{98}$$

(6.1)

where X_m^E is the excess thermodynamic property.

6.3.3.1   *Mixtures of (an 1-alkyne + a branched chain ether)*

For the systems {(1-hexyne or 1-heptyne or 1-octyne) + (IPE or TBME or TAME)} the best fit $X_{12}(V_m^E)$ and $X_{12}(H_m^E)$ values are given in Table 6.8 along with the values for $\sigma(V_m^E)$ and $\sigma(H_m^E)$. The values of the experimental $V_m^E(x = 0.5)$ and $H_m^E(x = 0.5)$ together with the calculated V_m^E and H_m^E at equimolar concentrations are given in Table 6.8 and figures 6.5 to 6.10   show experimental V_m^E and H_m^E results together with the fitted curves.

The Flory one-parameter equation provides a good fit of the experimental

H_m^E and V_m^E results for all the systems tested here. The theory adequately predicts the H_m^E exothermic behaviour and the general shapes of the experimental curves for all the systems tested. For the systems (1-hexyne + IPE or TBME or TAME) the value of $\sigma(H_m^E)$ does not exceed 20.7 J·mol^{-1} in the worst case. The predicted $H_m^E(x=0.5)$ for the systems (1-heptyne + IPE or TBME or TAME) show the best prediction with the standard deviation $\sigma(H_m^E)$ never exceeding 6.8 J·mol^{-1} of the experimental $H_m^E(x = 0.5)$. The theory also offers good fits for the systems (1-octyne + IPE or TBME or TAME) with standard deviations $\sigma(H_m^E)$ never greater than 25.7 J·mol^{-1}. The X_{12} values adequately reproduce the general shapes of the experimental curves for all the (1-hexyne or 1-heptyne or 1-octyne + IPE or TAME or TBME) systems. The standard deviation for these systems never exceed 0.05 cm^3·mol^{-1} in all cases except one.

The Flory theory fails in the quantitative prediction of V_m^E from X_{12} (H_m^E) and vice versa. The correct sign for both V_m^E and H_m^E was predicted but the magnitude of the calculated curves were incorrectly reproduced. The standard deviations $\sigma(V_m^{E*})$ and $\sigma(H_m^{E*})$ are as large as 40 cm^3·mol^{-1} for V_m^E and 200 J·mol^{-1} for H_m^E as listed in Table 6.9. The capability of the Flory theory can therefore only be judged on the results of fitting $X_{12}(V_m^E)$ to V_m^E and vice versa. Despite the inadequacy of the Flory theory in its prediction of V_m^E from $X_{12}(H_m^E)$ and vice versa, the simple one parameter Flory theory is remarkable in fitting to the V_m^E and H_m^E data of (a 1-alkyne + a branched chain ether) mixture for which the molecules of the two species differ appreciably in size, shape and chemical nature. Letcher and Baxter[343] have also shown that the theory also offers good H_m^E fits for the systems {(benzene or cyclohexane or *n*-hexane) + a 1-alkyne} with a standard deviation σ, never exceeding 5 % of $H_m^E(x = 0.5)$.

TABLE 6.8 Predicted and Experimental excess molar volumes and excess molar enthalpies at equimolar concentration together with the interaction parameter X_{12} and the standard deviations given by equation 6.1 for mixtures (a 1-alkyne + a branched chain ether) at 298.15 K

Mixture	$X_{12}(V_m^E)$ $J \cdot cm^{-3}$	V_m^E (0.5) Calc $cm^3 \cdot mol^{-1}$	Expt	$\sigma(V_m^E)$ $\cdot 10^2$ $cm^3 \cdot mol^{-1}$	$X_{12}(H_m^E)$ $J \cdot cm^{-3}$	H_m^E (0.5) Calc $J \cdot mol^{-1}$	Expt	$\sigma(H_m^E)$ $J \cdot mol^{-1}$
1-hexyne								
+ IPE	-0.027	-0.38	-0.38	0.3	-9.3	-260	-259	20.6
+ TBME	-0.027	-0.34	-0.33	0.9	-15.9	-429	-431	5.3
+ TAME	-0.054	-0.28	-0.28	2.6	-12.3	-335	-329	17.4
1-heptyne								
+ IPE	-0.022	-0.46	-0.46	2.1	-8.1	-248	-245	6.8
+ TBME	-0.022	-0.37	-0.37	2.2	-8.6	-400	-397	12.7
+ TAME	-0.042	-0.27	-0.26	0.8	-11.0	-329	-331	1.4
1-octyne								
+ IPE	-0.019	-0.55	-0.55	5.1	-8.0	-263	-266	5.4
+ TBME	-0.018	-0.38	-0.39	4.8	-12.2	-383	-390	25.5
+ TAME	-0.033	-0.27	-0.27	1.7	-10.3	-332	-333	8.9

TABLE 6.9 Predicted and experimental excess molar volumes and excess molar enthalpies at equimolar concentration together with the interaction parameter X_{12} and the standard deviations given by equation 6.1 for mixtures (a 1-alkyne + a branched chain ether) at 298.15 K

Mixture	$X_{12}(H_m^E)$	V_m^E (0.5) Calc	Expt	$\sigma(V_m^{E*})$	$X_{12}(V_m^E)$	H_m^E (0.5) Calc	Expt	$\sigma(H_m^{E*})$
	$J \cdot cm^{-3}$	$cm^3 \cdot mol^{-1}$		$cm^3 \cdot mol^{-1}$	$J \cdot cm^{-3}$	$J \cdot mol^{-1}$		$J \cdot mol$
1-hexyne								
+ IPE	-9.3	-40	-0.38	36	-0.027	-0.7	-259	192
+ TBME	-15.9	-39	-0.33	36	-0.027	-0.7	-431	315
+ TAME	-12.3	-38	-0.28	35	-0.054	-1.4	-329	247
1-heptyne								
+ IPE	-8.1	-41	-0.46	36	-0.022	-0.6	-245	182
+ TBME	-8.6	-37	-0.37	36	-0.022	-0.6	-245	293
+ TAME	-11.0	-38	-0.26	35	-0.042	-1.2	-331	241
1-octyne								
+ IPE	-8.0	-42	-0.55	37	-0.019	-0.6	-266	193
+ TBME	-12.2	-40	-0.39	36	-0.018	-0.5	-390	282
+ TAME	-10.3	-39	-0.27	35	-0.033	-1.0	-333	243
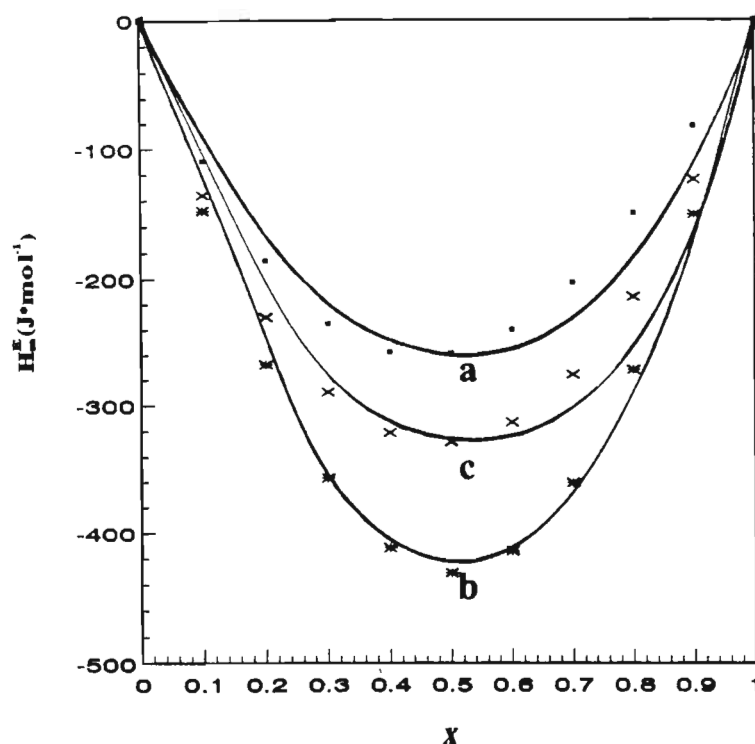
Figure 6.5 The predicted and experimental H_m^E for $\{x\ 1\text{-}C_6H_{10} + (1\text{-}x)(a)$ IPE or (b) TBME or (c) TAME$\}$. Experimental points are fitted by the curve predicted by the Flory equation
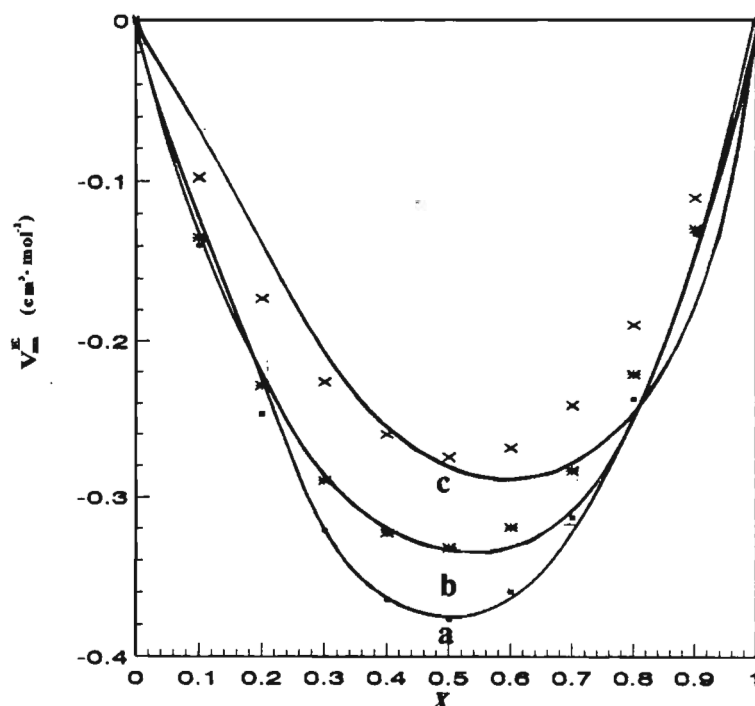
Figure 6.6 The predicted and experimental V_m^E for $\{x\ 1\text{-}C_6H_{10} + (1\text{-}x)(a)$ IPE or (b) TBME or (c) TAME$\}$.

Experimental points are fitted by the curve predicted by the Flory equation
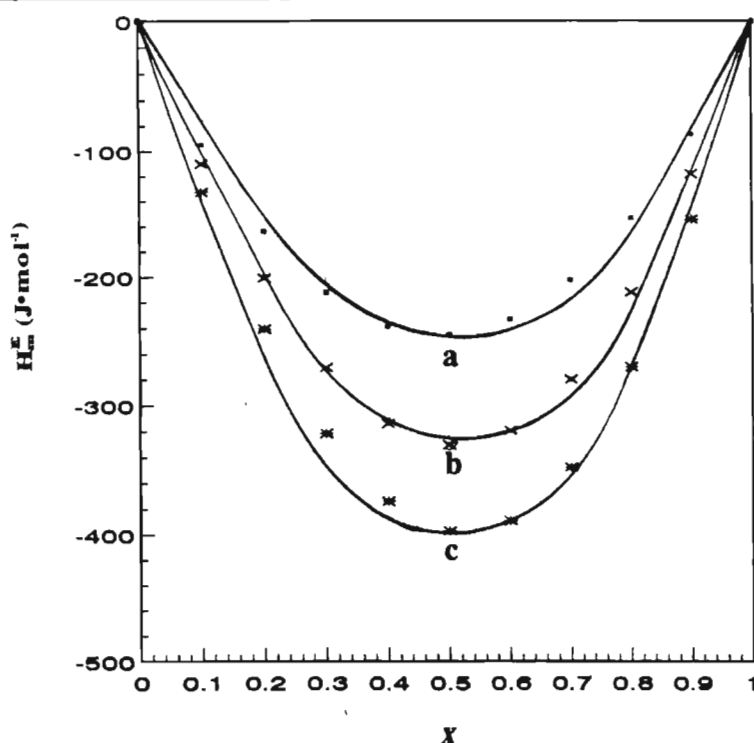
Figure 6.7 The predicted and experimental H_m^E for (x 1-C_7H_{12} + (1-x) (a) IPE or (b) TBME or (c) TAME).
The experimental points were fitted by the curve predicted by the Flory equation.
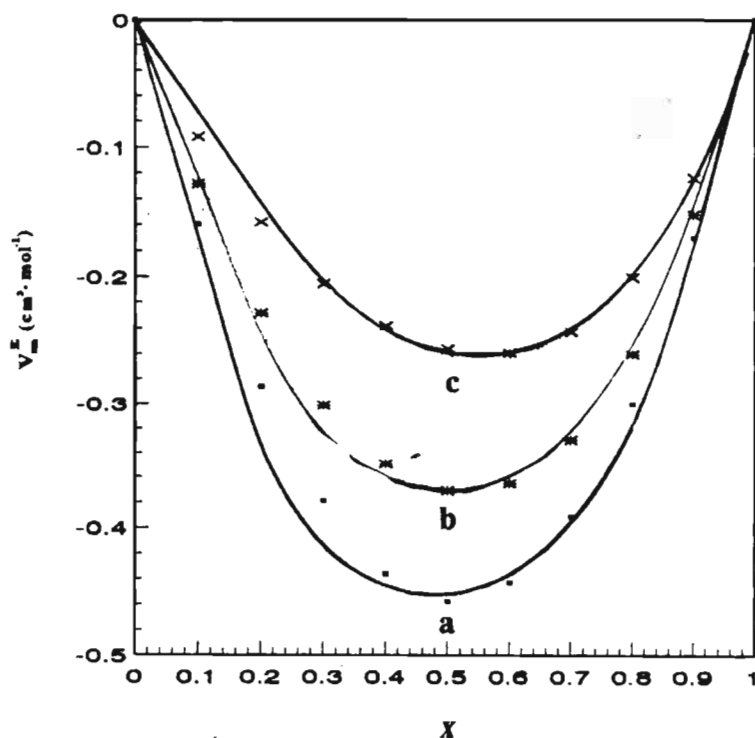
Figure 6.8 The predicted and experimental V_m^E for (x 1-C_7H_{12} + (1-x) (a) IPE or (b) TBME or (c) TAME). The
experimental points were fitted by the curve predicted by the Flory equation.

Figure 6.9 The predicted and experimental H_m^E for (x 1-C_8H_{14} + (1-x) (a) IPE or (b) TBME or (c) TAME. The experimental points were fitted by the curve predicted by the Flory equation.
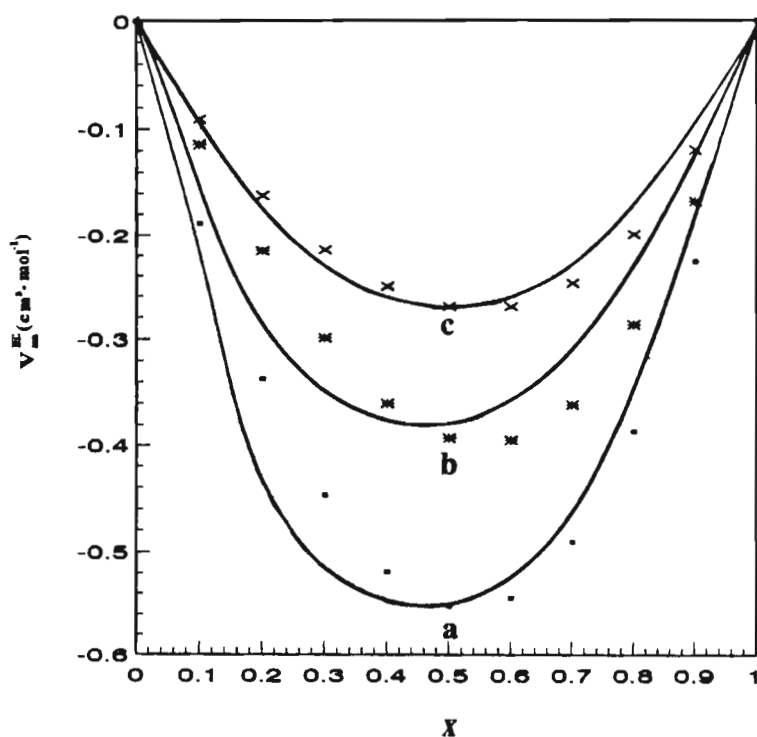
Figure 6.10 The predicted and experimental V_m^E for (x 1-C_8H_{14} + (1-x) (a) IPE or (b) TBME or (c) TAME. The experimental points are fitted by the curve predicted by the Flory equation.

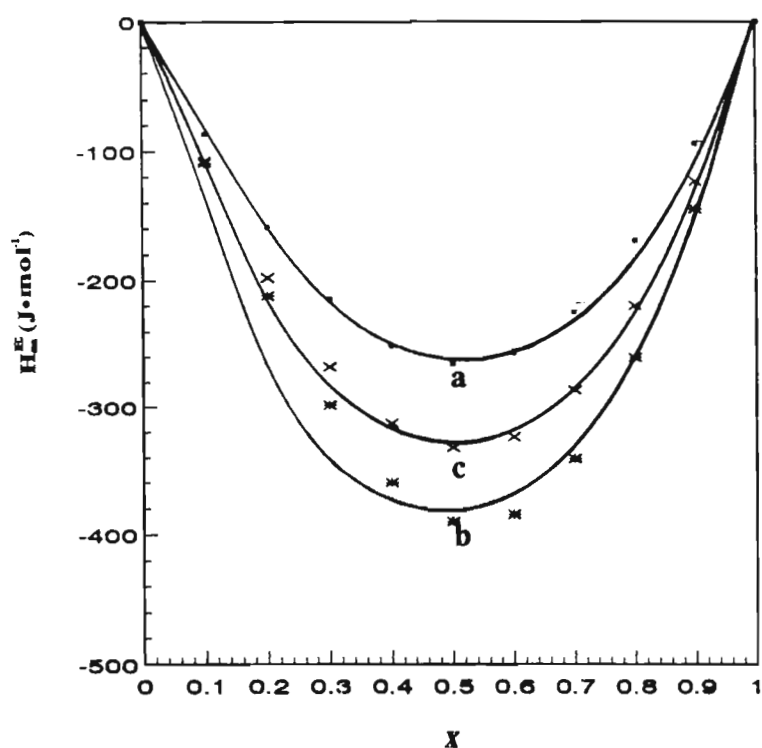### 6.3.3 The Prigogine Flory Patterson(PFP) Theory

The PFP theory relates V_m^E to three contributions : (a) an interaction term which is proportional to the interaction parameter X_{12}; (b) a free volume contribution which arises from the dependence of the reduced volume upon the reduced temperature as a result of the difference between the degree of expansion of the two components and (c) the internal pressure which depends both on the difference of the characteristic pressures and of the reduced volumes of the components. The PFP theory has been described in chapter 5 and the PFP expressions given by equations 5.57 to 5.63.

A procedure identical to Davolio et al[335] and Garg[344,345] and Ahluwahlia[239] and Diaz Pena et al.[333] was employed in the testing of the PFP theory. This involved the calculation of the contributions of the free volume and the P^* effect to V_m^E from the expression given in equation 5.63. The contribution of the interactional term was then estimated by using the experimental equimolar values of V_m^E and the free volume and P^* effect contribution. The estimated value of interactional contribution (to V_m^E) was used to obtain X_{12} from equation 5.63. The various parameters involved in equations 5.57 to 5.63 for the pure components and the mixtures are listed in Table 6.10. The PFP theory was tested for systems of {(an alkanol or a secondary amine) + (a branched chain ether or a cyclic ether)}.

TABLE 6.10 Characteristic parameters of pure components for the PFP theory at 298.15K

Component	V_{mol}	V^*	T^*	P^*	$\tilde{V}$
	cm³·mol⁻¹		K	J·cm⁻³	
methanol	40.74	31.70	4776	469.2	1.285
ethanol	58.68	46.31	4980	454.9	1.267
propan-1-ol	75.15	60.06	5183	471.8	1.251
propan-2-ol	76.96	61.09	5069	443.9	1.260
diethylamine	104.5	77.60	4248	562.9	1.347
di-n-propylamine	138.0	105.5	4555	547.7	1.308
IPE	142.2	326.4	4853	326.4	1.278
TBME	119.9	94.39	4946	346.8	1.270
TAME	133.4	107.5	5332	226.5	1.241
THF	81.56	66.75	5638	406.4	1.222
THP	98.19	81.83	6070	352.1	1.200
1,4-dioxane	85.70	72.22	6380	407.3	1.187

6.3.3.1 Mixtures of {an alkanol + (a branched chain or a cyclic ether)}

The calculated equimolar values of the three contributions to V_m^E according to equation 5.57 together with the X_{12} values are listed in Table 6.11 for the systems {(methanol or ethanol or propan-1-ol or propan-2-ol) + (IPE or TBME or TAME or THF or THP or 1,4-dioxane)}.

Inspection of the separate terms listed in Table 6.11 offers a partial explanation of the origin of V_m^E in the various mixtures. The short chain alkanols are strongly self associated and exist as equilibrium mixtures of monomer, dimer and higher multimers[346,347] and the associative equilibria of the alkanol molecules contribute largely to the overall V_m^E in binary solutions. V_m^E for the alkanol binary mixtures may be explained on the following basis: (a) the breaking of the alkanol self-association upon mixing, (b) the breaking of the the physical dipole-dipole interaction in the alkanol molecules, (c) the specific interaction between the OH group of the alkanol and the O group on the ether and (d) the change in the free volume and interstitial accommodation of the ethers in the alkanol multimers. Processes (a) and (b) are associated with a positive contribution to V_m^E and processes (c) and (d) will lead to a negative V_m^E depending on the nature, extent and strength of the interactions.

Analysis of the three terms in Table 6.11 shows that for all the systems studied here, at equimolar concentration, the free volume term is negative and makes the smallest contribution to the excess volume. This indicates that the dominant contribution to the V_m^E is the specific interaction between the functional groups of the component species for systems showing negative experimental V_m^E. For the systems with positive experimental V_m^E the interaction term becomes less significant. For all the systems investigated $P_1^* \equiv P_2^{*(11,12)}$ and the P^* effect is small making a minor contribution to the overall V_m^E. The small P^* and the free volume terms indicate that V_m^E depends to a large extent on the interaction term. This means that the interactions between unlike molecules in the binary mixture are the major determinant in V_m^E.

TABLE 6.11 Calculated values of X_{12} and the three contributions to the predicted V_m^E by the PFP theory (equation 5.57) for {an alkanol + branched chain or cyclic ether} at 298.15K

Mixture	X_{12}	Interaction	Free Volume	P^* effect
	$J \cdot cm^{-3}$	10^{-1}	10^{-2}	10^{-2}
methanol				
+ IPE	-71.46	-9.81	-0.11	3.39
+ TBME	-54.60	-6.74	-0.46	5.71
+ TAME	-55.74	-7.74	-4.25	41.06
+ THF	-20.70	-1.85	-6.78	10.03
+ THP	-27.68	-2.62	-13.95	29.61
+ 1,4-dioxane	34.65	2.86	-16.95	15.74
ethanol				
+ IPE	-41.06	-7.31	-0.32	-6.18
+ TBME	-30.87	-4.90	-0.02	-1.20
+ TAME	-31.74	-6.35	-1.98	32.93
+ THF	-4.28	-0.49	-4.26	7.05
+ THP	-11.90	-1.46	-10.59	26.21
+ 1,4-dioxane	-1.43	-0.15	-14.03	12.68

TABLE 6.11 *Continued*

Mixture	X_{12} J·cm^{-3}	Interaction 10^{-1}	Free Volume 10^{-2}	P* effect 10^{-2}
propan-1-ol				
+ IPE	-39.75	-7.82	-2.22	-19.68
+ TBME	-30.11	-5.24	-0.97	-10.55
+ TAME	-29.50	-6.39	-0.33	15.67
+ THF	-4.37	-0.55	-2.04	6.93
+ THP	-15.07	-2.06	-7.01	26.35
+ 1,4-dioxane	7.03	0.82	-10.37	15.61
propan-2-ol				
+ IPE	-16.46	-3.53	-1.02	-11.16
+ TBME	-10.63	-2.01	-0.06	-4.55
+ TAME	-17.17	-4.04	-1.15	26.52
+ THF	12.45	1.70	-3.46	5.36
+ THP	2.97	4.40	-9.64	24.57
+ 1,4-dioxane	23.20	2.93	-13.40	10.44

6.3.3.2 Mixtures of {(a secondary amine) + (a branched chain ether or a cyclic ether)}

Table 6.12 lists the calculated equimolar values of the interaction, free volume and P^* contributions to V_m^E for the systems {(diethylamine or di-n-propylamine) + (IPE or TBME or TAME or THF or THP or 1,4-dioxane)}. Like the alkanols, the amines exhibit self association but to a far lesser degree.[227,230] For all the mixtures it appears that the interactional term predominates over the free volume or P^* term i.e the interaction term contributes the largest negative value to the overall V_m^E. The values of the interaction X_{12} and the free volume terms are negative for all the cases.

$P_1^* > P_2^{*(11,12)}$ leads to a positive P^* term and a positive effect in V_m^E for all the systems. The P^* term for {(diethylamine or di-n-propylamine) + TAME} shows the largest positive value indicating the decrease of molecular surface area of the TAME molecule. This reflects what is most likely taking place i.e. steric crowding of the groups within the TAME molecule results in a reduced flexibility of this highly branched molecule. The bulky nature of the symmetrical secondary amines[107] may also contribute to the large positive P^* effect.

TABLE 6.12 Calculated values of X_{12} and the three contributions to the predicted V_m^E by the PFP theory (equation 5.57) for {a secondary amine + branched chain or cyclic ether} at 298.15 K

Mixture	X_{12}	Interaction	Free Volume	P^* effect
	$J \cdot cm^{-3}$	10^{-1}	10^{-1}	10^{-1}
diethylamine				
+ IPE	-24.78	-6.79	-1.65	8.82
+ TBME	-20.21	-4.90	-1.85	8.01
+ TAME	-61.72	-17.35	-3.56	21.95
+ THF	-22.50	-3.81	-3.96	7.17
+ THP	-43.71	-8.09	-6.15	13.60
+ 1,4-dioxane	-22.56	-3.61	-6.89	9.57
di-n-propylamine				
+ IPE	-20.95	-6.12	-0.34	4.13
+ TBME	-16.47	-4.22	-0.50	4.22
+ TAME	-45.07	-13.38	-1.49	14.92
+ THF	-18.34	-3.27	-2.06	5.05
+ THP	-37.13	-7.39	-3.62	10.54
+ 1,4-dioxane	-8.35	-1.46	-4.36	7.44

6.4   The Extended Real Associated Solution (ERAS) Model

6.4.1 <u>Introduction</u>

The ERAS model has been applied successfully to mixtures containing either one and/or two associating components.[20,21,227,230] In this work the ERAS model is applied to mixtures containing (a) a strongly self-associating component with a non self-associating component (i.e. an alkanol + a branched chain or a cyclic ether) and (b) a weakly self-associating component and a non self-associating component (i.e. a secondary amine + a branched chain or a cyclic ether). The theory of ERAS as applied to mixtures containing two associating components has been described in Chapter 5 through equations 5.64 to 5.90. The ERAS parameters h_{AB}^*, v_{AB}^*, K_{AB} and X_{AB} were adjusted simultaneously to experimental H_m^E and V_m^E. In all the systems studied here the ether was assumed to be an inert component without self association ($K_B = 0$) but cross association was possible ($K_{AB} \neq 0$).

6.4.2 <u>Mixtures of (an alkanol + (a branched chain or a cyclic ether)</u>

The ERAS model has been applied to {(methanol or ethanol or propan-1-ol or propan-2-ol) + (IPE or TBME or TAME or THF or THP or 1,4-dioxane)} systems. For all the alcohols an average value of -25 kJ·mol⁻¹ for the enthalpy of hydrogen bonding Δh_A^* was assumed. This value has been used by a number of workers in ERAS model calculations with alkanol mixtures.[20,231,232,348] The value of Δv_A^* for each of the four alkanols was used from literature sources as given in Table 6.13. The pure component properties are listed in Tables 6.7, 6.10 and 6.13 and the adjustable parameters for all the binary systems are listed in Table 6.14.

TABLE 6.13 Pure component properties for the alkanols at 298.15 K

Component	Δh^* kJ·mol^{-1}	Ref.	Δv^* cm^3·mol^{-1}	Ref.	K_{298}	Ref.
methanol	-25.1	231	-5.6	231	986	231
ethanol	-25.1	231	-9.3	348	317	231
propan-1-ol	-25.1	231	-7.6	227	197	231
propan-2-ol	-25.1	231	-5.6	231	131	231

For the {methanol + (IPE or TBME or TAME)} mixtures the calculated V_m^E curves agree well with the experimental data. The largest deviation between the predicted and experimental results of about 0.09 cm^3·mol^{-1} is observed for the {methanol + TAME} system. For all the {methanol + (THF or THP or 1,4-dioxane)} mixtures, the V_m^E curves calculated using the ERAS model fails to describe the shape and the size of the experimental curves. The predicted V_m^E curve for the (methanol + THP) system is skewed towards the alkanol poor mole fraction range and the deviations between the predicted and calculated curves are of the order 0.06 cm^3·mol^{-1}. The chemical contribution seems to significantly affect the symmetry of the predicted V_m^E curves. The magnitude of the chemical contribution depends on the terms present in the V_{chem}^E expression (equation 5.90) i.e. dependent on K_{AB} and on the α and κ_T properties of the pure components.

The predicted H_m^E curves for {methanol + (IPE or TBME or TAME)} are qualitatively reproduced i.e. the exothermic behaviour of the experimental curves in the alkanol rich region is adequately predicted. However the magnitude of the predicted exothermic behaviour was larger than those experimentally determined. The ERAS model correctly predicts the endothermic H_m^E behaviour up to alkanol mole fraction of x = 0.65.

For all the {methanol + a cyclic ether} systems the predicted H_m^E curves are in agreement with the experimental H_m^E data except for the {methanol + THF} system. The {methanol + THF} system is inaccurately predicted at $x > 0.9$ alkanol mole fraction. For all the binary systems reported in this section the ERAS model expresses the chemical contribution as the dominant term for the endothermic H_m^E behaviour. In molecular terms this chemical contribution is interpreted as the breaking of the hydrogen bonds (self association) between the alkanol molecules.

For the {(ethanol or propan-1-ol or propan-2-ol) + (IPE or TBME or TAME)}, the calculated V_m^E and H_m^E curves are of the same endothermic sign as the experimental curves as shown in figure 6.13, 6.15 and 6.17. However, large deviations in the symmetry of the predicted V_m^E curves are observed. From all the systems, the {(ethanol or propan-2-ol) + TAME} mixtures exhibit the worst V_m^E prediction with the shape, size and symmetry of the predicted curve in disagreement with the experimental V_m^E curves. For all the {(ethanol or propan-1-ol or propan-2-ol) + a branched chain ether} systems the ERAS model predicts accurately the endothermic H_m^E behaviour of the systems up to an $x = 0.6$ alkanol mole fraction. At $x > 0.7$ the calculated H_m^E curves indicate small exothermic behaviour which is in disagreement with the experimental H_m^E. Consequently, deviations between calculated and experimental H_m^E curves are as large as 190 J·mol^{-1} in some cases.

The predictions of the V_m^E curves for {(ethanol or propan-1-ol) + (THF or THP or 1,4-dioxane)} systems are quantitatively reproduced in alkanol-poor regions as shown in figures 6.14 and 6.16. In particular, for all the {ethanol + (THF or THP or 1,4-dioxane)} systems the model qualitatively reproduces the S-shaped concentration dependence of the experimental V_m^E. However the magnitudes of the calculated curves at $x > 0.45$ alkanol mole fraction are greater than that experimentally determined. For the {propan-2-ol + (THF or THP or 1,4-dioxane)} systems the ERAS model fails at $x > 0.6$ alkanol mole fraction in the prediction of V_m^E as shown in figure 6.18.

The experimental H_m^E curves for {(ethanol or propan-1-ol or 2-propan-2-ol) + (THF or THP or 1,4-dioxane)} systems with the exception of the {ethanol + THF} mixture are symmetrical around x = 0.5 while the model predicts asymmetrical concentration dependence, skewed towards the low alkanol region. For the {ethanol + THF} system the asymmetrical behaviour of the experimental curve is accurately predicted.

TABLE 6.14 ERAS model parameters characterising mixture properties of $\{x$ an alkanol $+ (1-x)ROR'\}$ where ROR' is a branched chain or cyclic ether at 298.15 K

Mixture	X_{AB} J·cm^{-3}	$-\Delta h_{AB}^{*}$ kJ·mol^{-1}	$-\Delta v_{AB}^{*}$ cm^{3}·mol^{-1}	K_{AB}
methanol				
+ IPE	7.8	24.5	9.6	350
+ TBME	11.8	23.7	8.4	350
+ TAME	11.8	23.3	9.8	350
+ THF	3.8	19.3	6.6	90
+ THP	8.0	16.9	8.4	45
+ 1,4-dioxane	9.0	14.3	7.6	75
ethanol				
+ IPE	2.8	21.9	11.0	220
+ TBME	5.0	21.0	10.7	128
+ TAME	15.0	21.0	14.7	38
+ THF	11.0	15.6	9.5	21
+ THP	5.0	14.9	9.8	23
+ 1,4-dioxane	8.0	5.2	9.1	15

TABLE 6.14 *Continued*

Mixture	X_{AB}	$-\Delta h^*_{AB}$	$-\Delta v^*_{AB}$	K_{AB}
	$J \cdot cm^{-3}$	$kJ \cdot mol^{-1}$	$cm^3 \cdot mol^{-1}$	
propan-1-ol				
+ IPE	5.0	21.6	10.0	108
+ TBME	3.0	20.2	9.1	700
+ TAME	2.0	19.6	10.0	50
+ THF	3.6	14.1	7.3	22
+ THP	2.6	15.4	8.0	29
+ 1,4-dioxane	10.9	6.5	6.7	19
propan-2-ol				
+ IPE	5.0	19.5	11.0	60
+ TBME	2.8	18.1	10.7	50
+ TAME	3.8	18.4	14.7	40
+ THF	9.2	13.6	9.5	20
+ THP	9.0	15.3	9.8	30
+ 1,4-dioxane	14.0	7.6	9.1	22

(a)

(b)

(c)
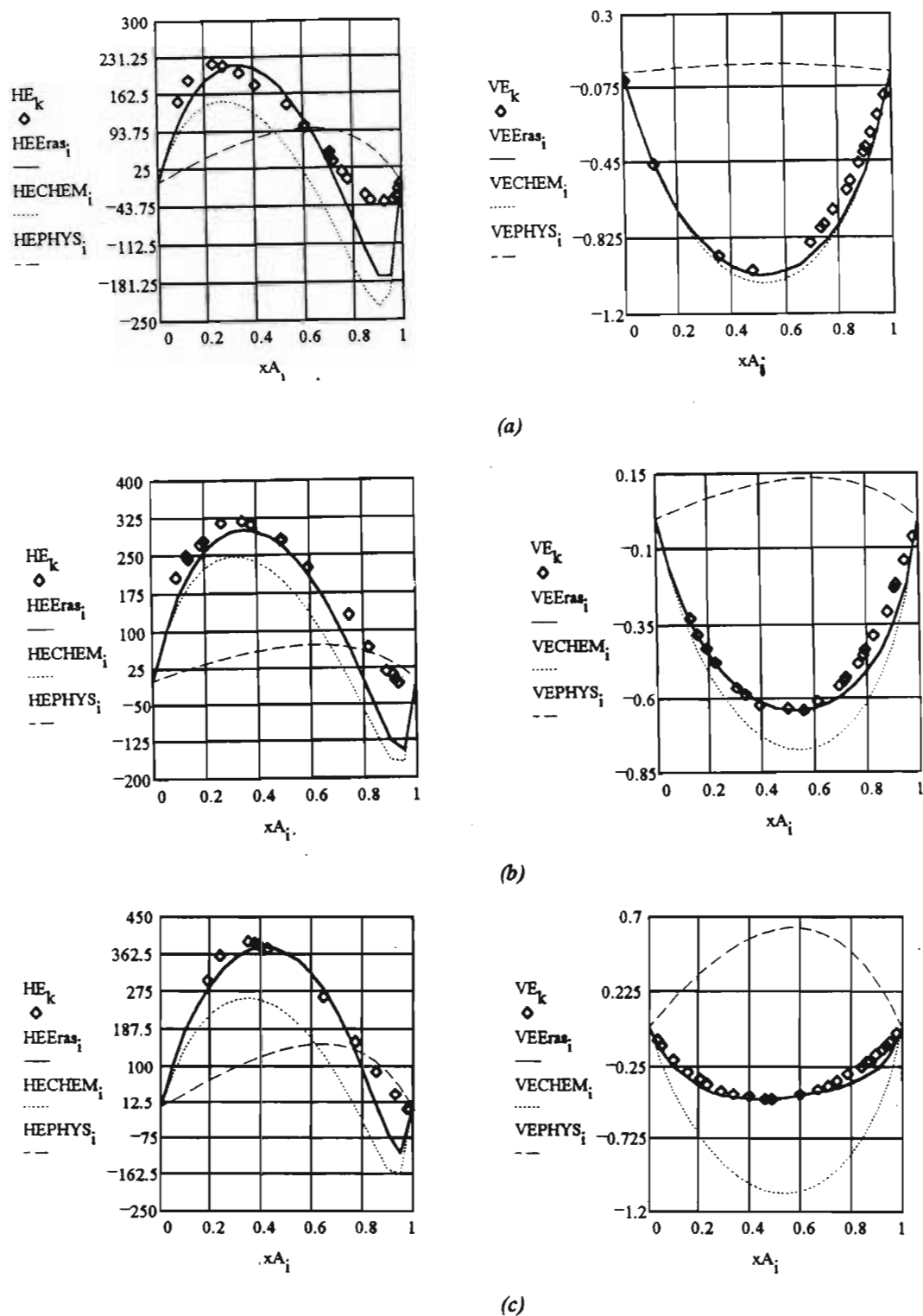
Figure 6.11 H_m^E and V_m^E ERAS model description of (x methanol + (1-x) {(a) IPE, (b) TBME and (c) TAME}) at 298.15 K: ◇, experimental data; ———, ERAS model; ......, chemical contribution; ———, physical contribution.
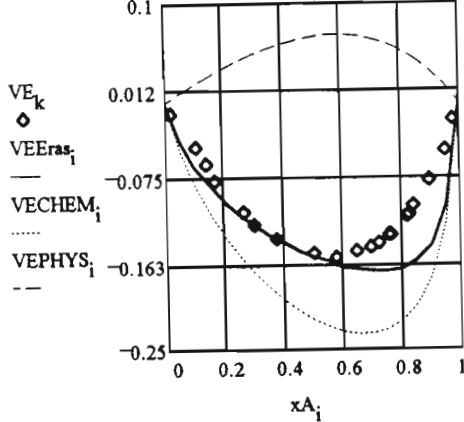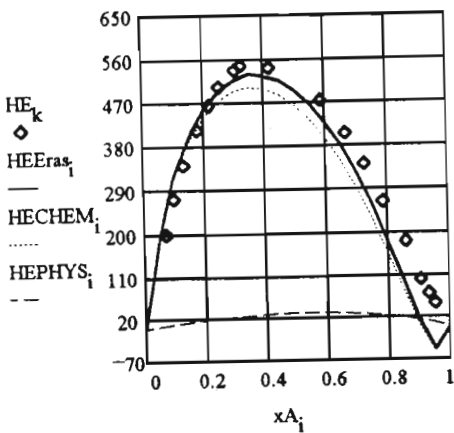
(a)

(b)

(c)

Figure 6.12 H_m^E and V_m^E ERAS model description of(x methanol + (1-x) {(a) THF, (b) THP and (c) 1,4-dioxane}) at 298.15 K: ◇ , experimental data; ———, ERAS model; ······, chemical contribution; ———, physical contribution.
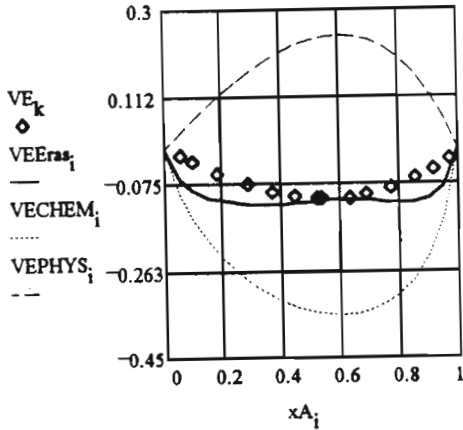
(a)

(b)

(c)

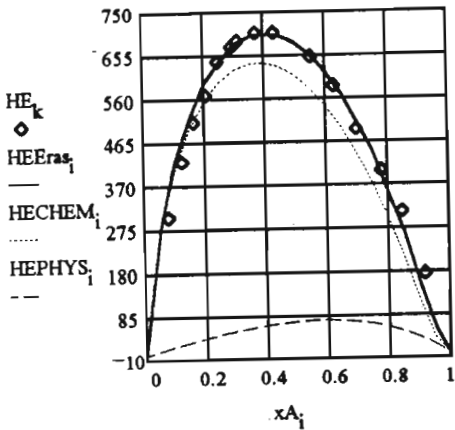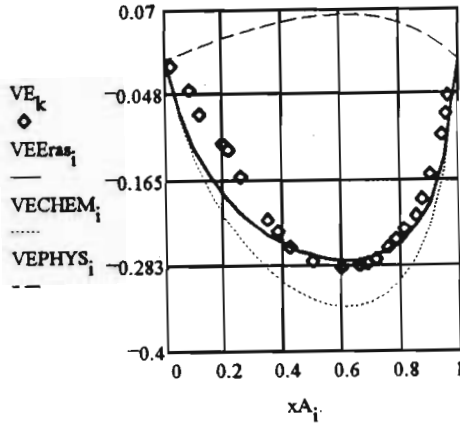*Figure 6.13 H_m^E and V_m^E ERAS model description of (x ethanol + (1-x) {(a) IPE, (b) TBME and (c) TAME}) at*
298.15 K: ◇, experimental data; ———, ERAS model; ······, chemical contribution; -------,
physical contribution.

(a)

(b)

(c)

Figure 6.14 H_m^E *and* V_m^E *ERAS model description of (x ethanol + (1-x) {(a) THF, (b) THP and (c) 1,4-dioxane})*
at 298.15 K: ◇ *, experimental data;* ——— *, ERAS model;* ······ *, chemical contribution;* ———,
physical contribution.

(a)

(b)

(c)
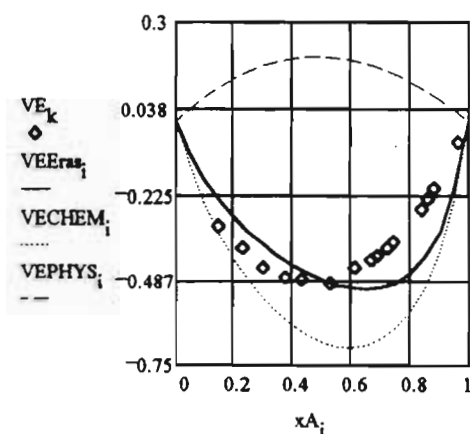
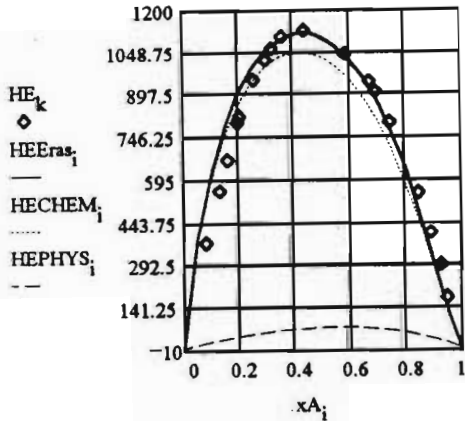*Figure 6.15 H_m^E and V_m^E ERAS model description of (x propan-1-ol + (1-x) {(a) IPE, (b) TBME and (c) TAME})*
at 298.15 K: $\diamond$, experimental data; ———, ERAS model; ⋯⋯, chemical contribution; ———,
physical contribution.
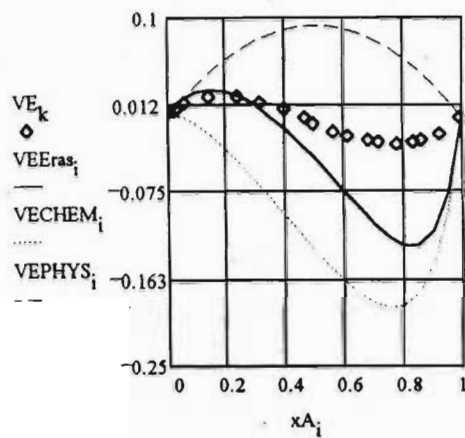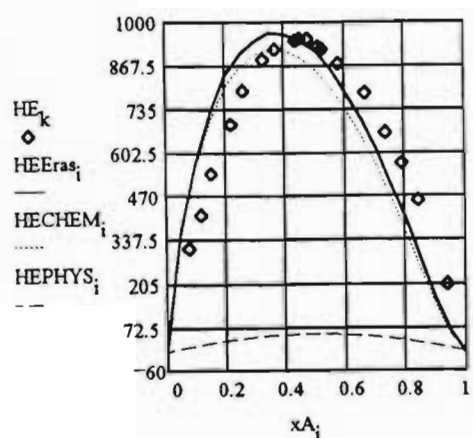
(a)
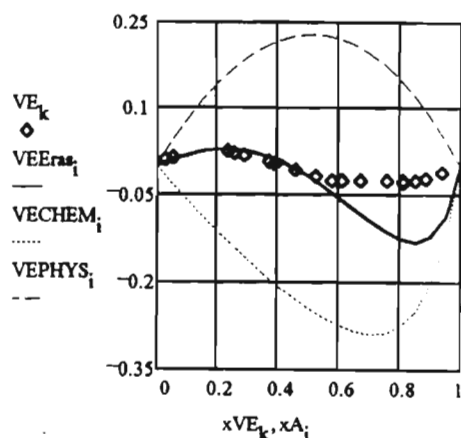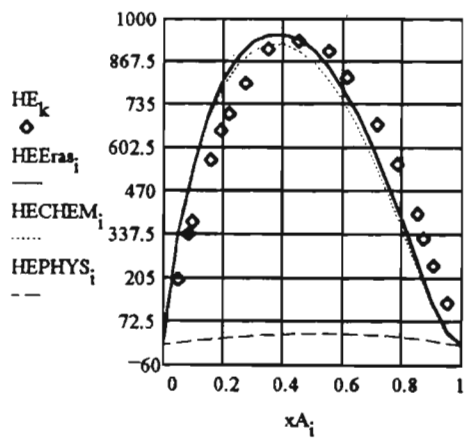
(b)
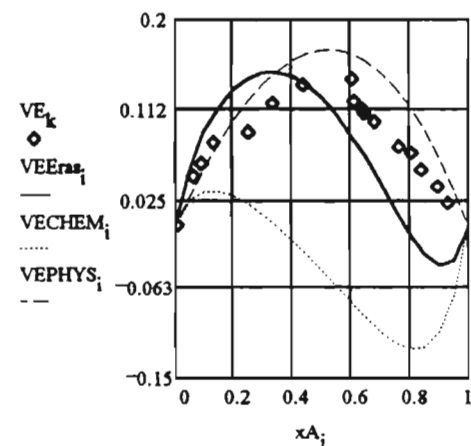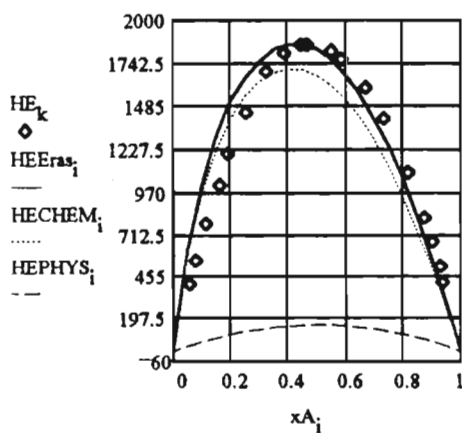
(c)

Figure 6.16 H_m^E and V_m^E ERAS model.description of (x propan-1-ol + (1-x) {(a) THF, (b) THP and (c) 1,4-dioxane}) at 298.15 K: ◇ , experimental data; ———, ERAS model; ······, chemical contribution; ———, physical contribution.
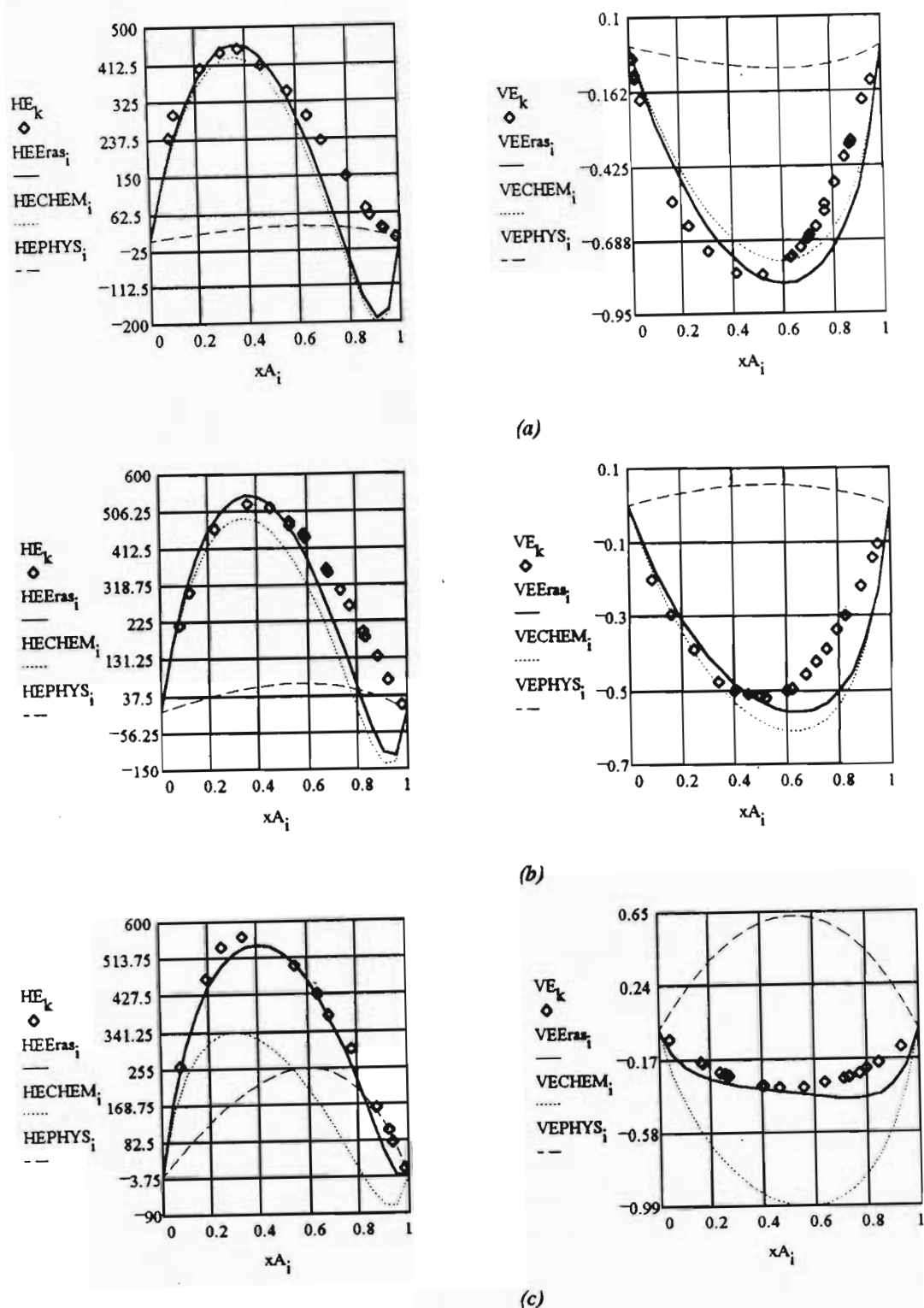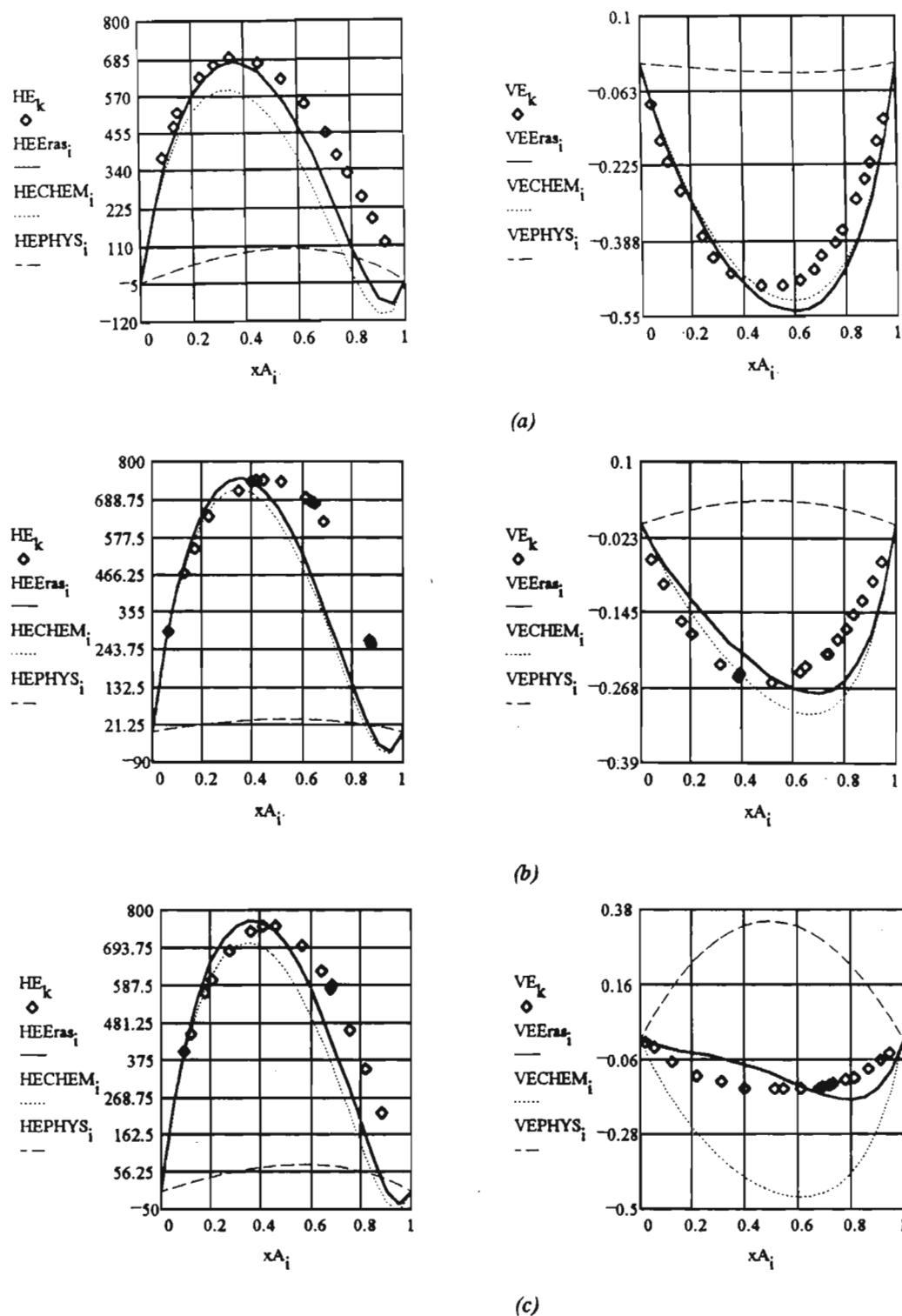
Figure 6.17 H_m^E *and* V_m^E *ERAS model description of (x propan-2-ol + (1-x) {(a) IPE, (b) TBME and (c) TAME})* *at 298.15 K:* $\diamond$, *experimental data;* ———, *ERAS model;* ······, *chemical contribution;* ———, *physical contribution.*
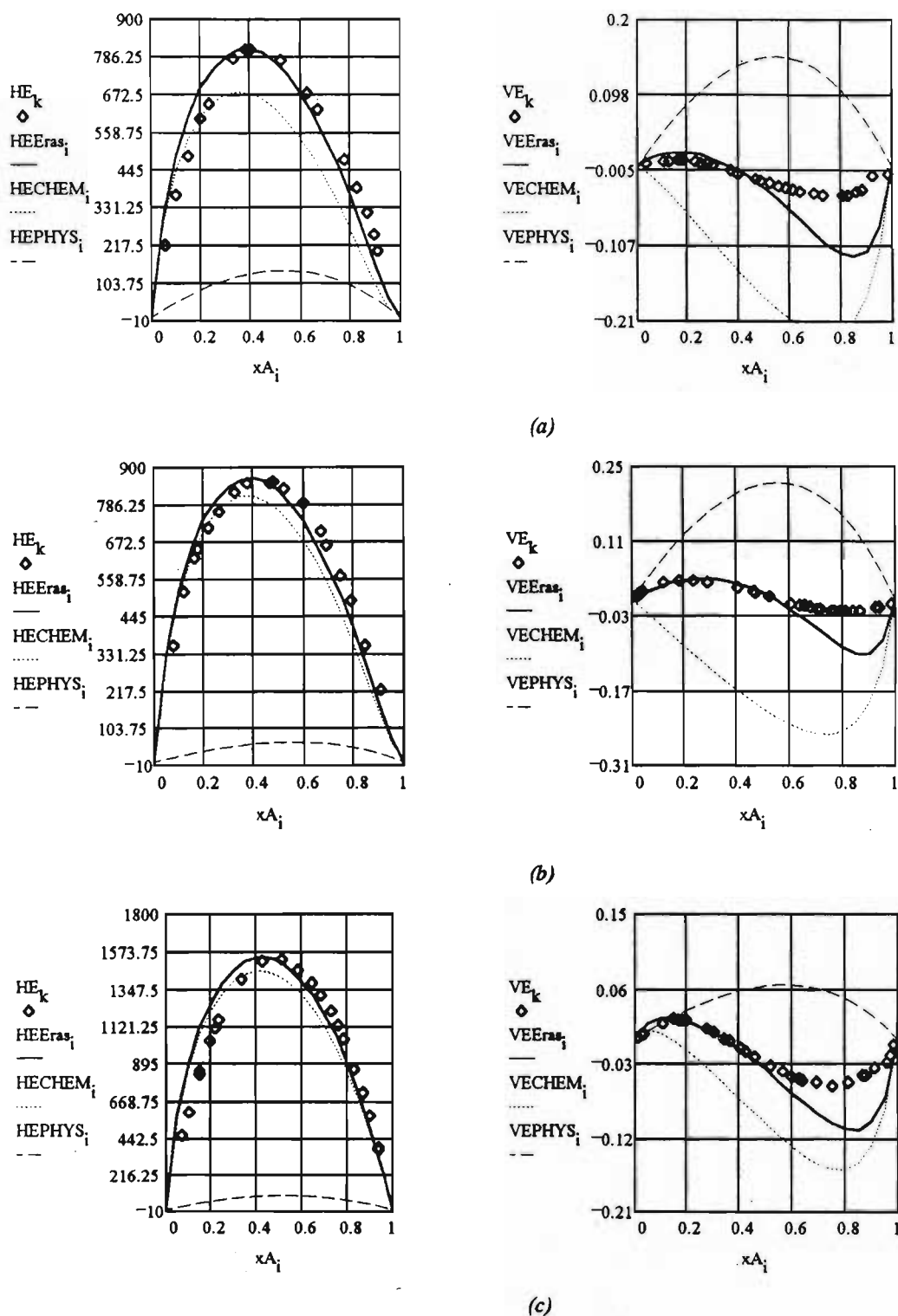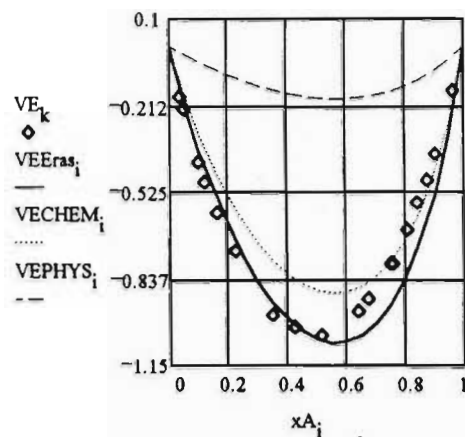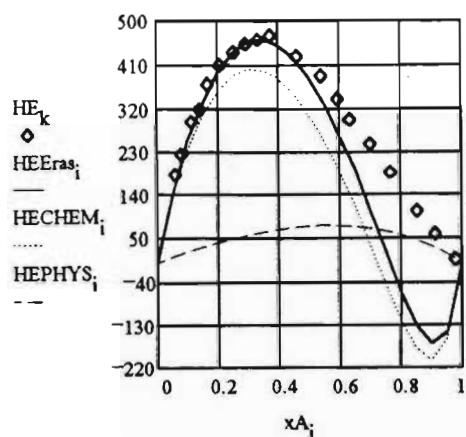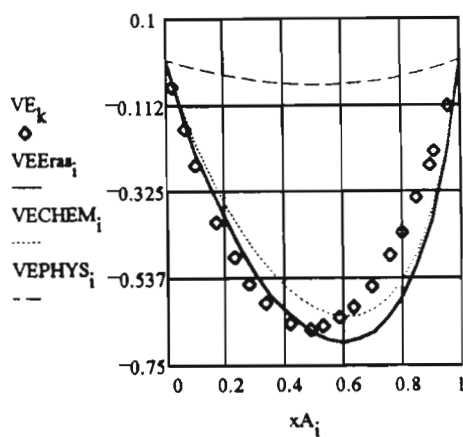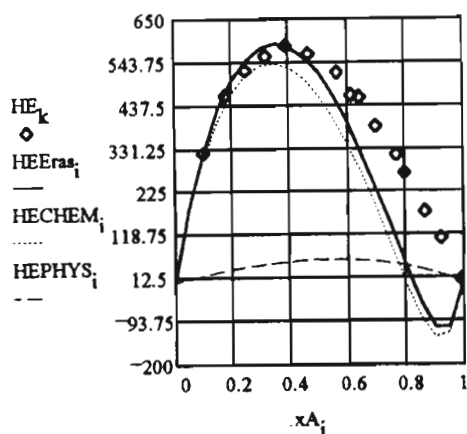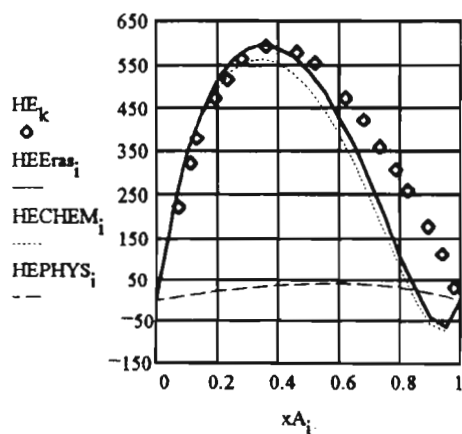
Figure 6.18 H_m^E and V_m^E ERAS model description of (x propan-2-ol + (1-x) {(a) THF, (b) THP and (c) 1,4-dioxane}) at 298.15 K: ◇, experimental data; ———, ERAS model; ······, chemical contribution; ———, physical contribution.

### 6.4.3 Mixtures of (a secondary amine + a branched chain or a cyclic ether)

The ERAS model has been applied to {(diethylamine or di-n-propylamine) + (IPE or TBME or TAME or THF or THP or 1,4-dioxane)} systems. For the secondary amines the enthalpy of hydrogen bonding h_A^* and the molar volume effect due to hydrogen bonding v_A^* are listed in Table 6.15. The pure component properties are listed in Tables 6.7, 6.10 and 6.15 and the adjustable parameters for all the binary systems are listed in Table 6.16.

TABLE 6.15 Pure component properties for the secondary amines at 298.15 K

Component	Δh^* kJ·mol^{-1}	Ref.	Δv^* cm^3·mol^{-1}	Ref.	K_{298}	Ref.
diethylamine	-8.5	104	-4.7	104	0.84	227
di-n-propylamine	-7.5	232	-4.2	232	0.55	232

A comparison of the calculated and experimental V_m^E and H_m^E functions for the systems {(diethylamine or di-n-propylamine) + (IPE or TBME)} from figures 6.19 and 6.21 indicates that the ERAS model adequately describes the excess properties quantitatively. In particular for mixtures containing IPE and TBME the strong symmetrical concentration dependence of V_m^E is reproduced accurately with the ERAS model. For the system {(diethylamine or di-n-propylamine) + TAME} the model fails in its prediction of both V_m^E and H_m^E as shown in figures 6.19 and 6.21.

For all the {(diethylamine or di-n-propylamine) + (THF or THP or 1,4-dioxane)} systems the calculated V_m^E curves are symmetrical around x = 0.5. This is in

contrast to the experimental V_m^E curves which are skewed towards the amine rich region. For the {(diethylamine or di-n-propylamine) + THF} systems the model fails to predict the S-shaped concentration dependence of V_m^E in the dilute amine region.

The ERAS model showed only partial success in H_m^E description for all the systems except {(diethylamine or di-n-propylamine) + 1,4-dioxane}. Again the model could not reproduce the details (S-shaped curves with $H_m^E = 0$ at $x \equiv 0.7$ mole fraction) of the experimental H_m^E curves of {diethylamine + THP} and {di-n-propylamine + THF} systems. The large endothermic H_m^E behaviour of {(diethylamine or di-n-propylamine) + 1,4-dioxane} is accurately reproduced by the ERAS model as shown in figures 6.20 and 6.22.

TABLE 6.16 ERAS model parameters characterising mixture properties of {x a secondary amine + (1-x) ROR'} where ROR'is a branched chain or cyclic ether at 298.15 K

| Mixture | X_{AB} | $-\Delta h_{AB}^*$ | $-\Delta v_{AB}^*$ | K_{AB} |
	$J \cdot cm^{-3}$	$kJ \cdot mol^{-1}$	$cm^3 \cdot mol^{-1}$	
diethylamine				
+ IPE	1.1	6.4	4.8	0.83
+ TBME	1.2	6.8	4.0	0.65
+ TAME	0.5	10.5	17.1	0.74
+ THF	1.0	5.8	5.8	0.83
+ THP	2.2	7.8	9.5	0.80
+ 1,4-dioxane	1.0	0.3	5.8	0.81

TABLE 6.16 *Continued*

Mixture	X_{AB}	$-\Delta h_{AB}^{*}$	$-\Delta v_{AB}^{*}$	K_{AB}
	$J \cdot cm^{-3}$	$kJ \cdot mol^{-1}$	$cm^{3} \cdot mol^{-1}$	
di-n-propylamine				
+ IPE	0.35	6.2	4.3	0.54
+ TBME	2.0	7.2	4.1	0.38
+ TAME	0.2	9.2	16.1	0.55
+ THF	0.3	4.7	5.0	0.56
+ THP	2.6	6.5	9.0	0.55
+ 1,4-dioxane	19.5	1.9	6.3	0.55
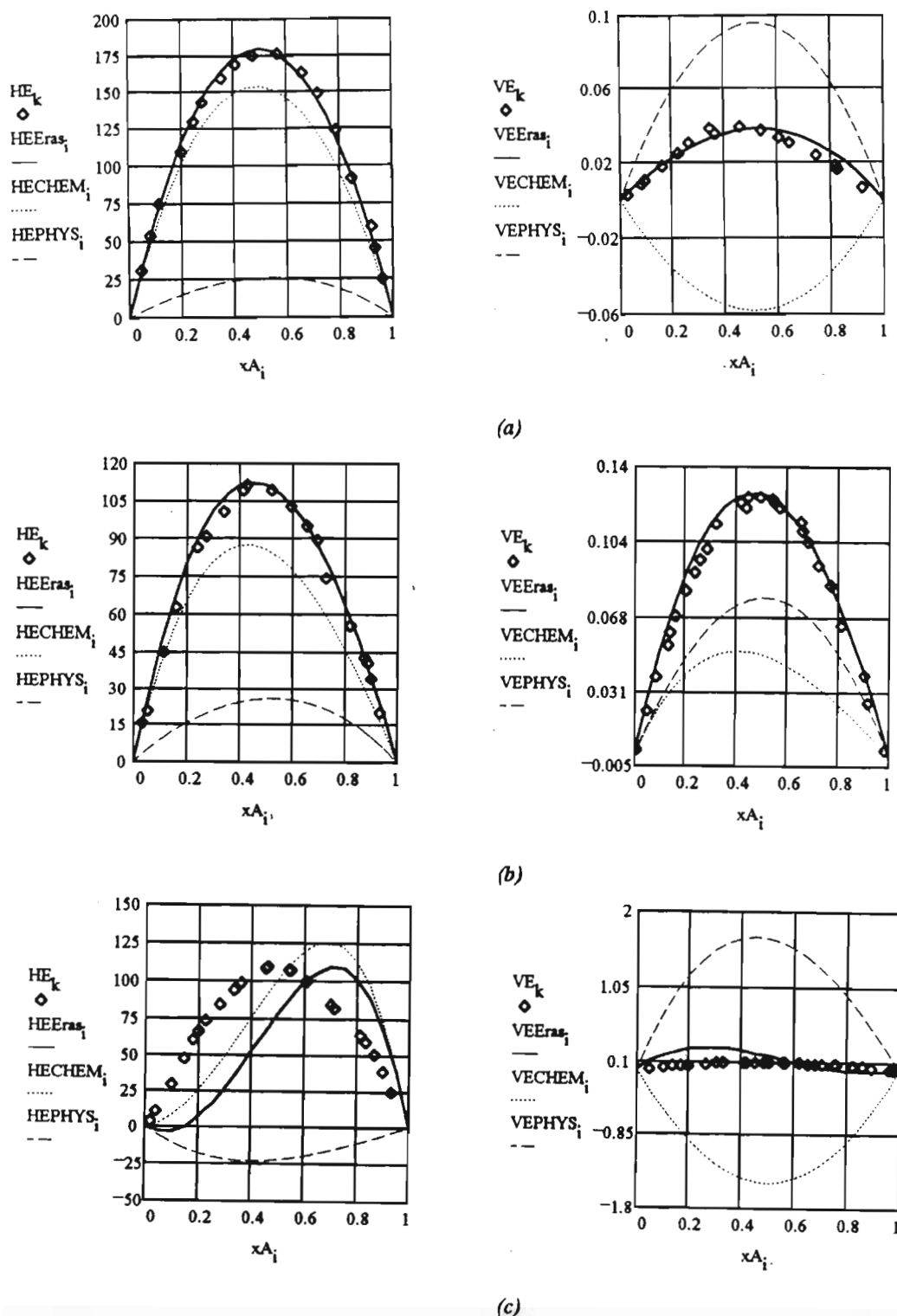
Figure 6.19 H_m^E and V_m^E ERAS model description of (x diethylamine + (1-x) {(a) IPE, (b) TBME and (c) TAME}) at 298.15 K: ◇, *experimental data;* ———, *ERAS model;* ······, *chemical contribution;* ———, *physical contribution.*
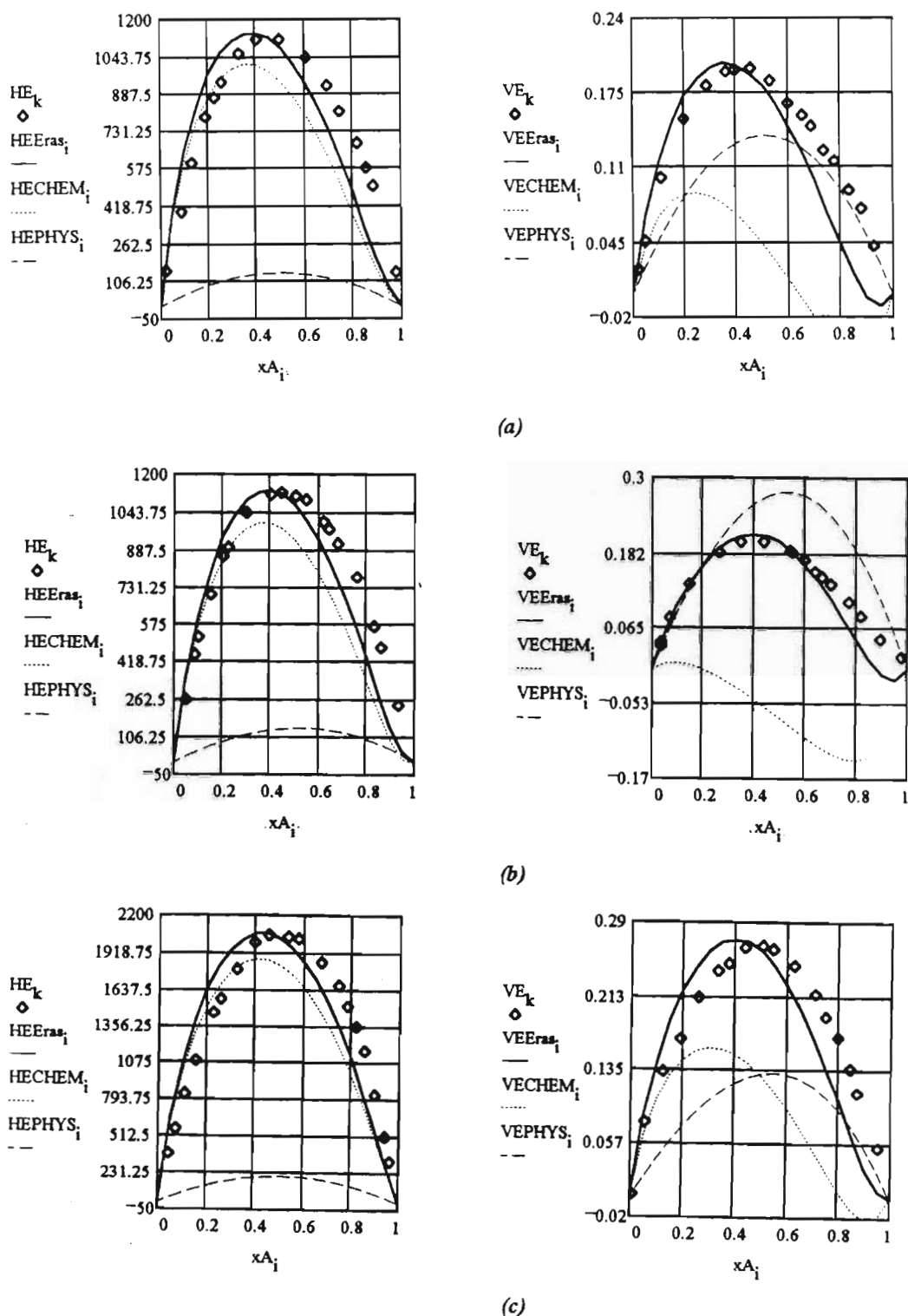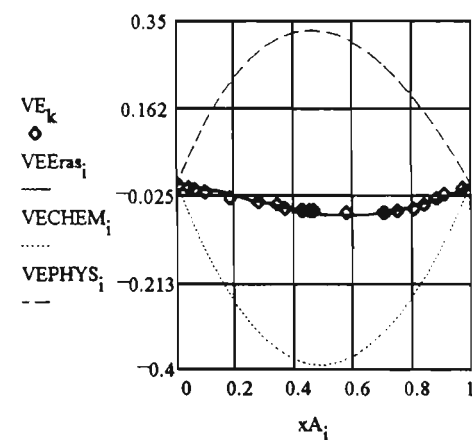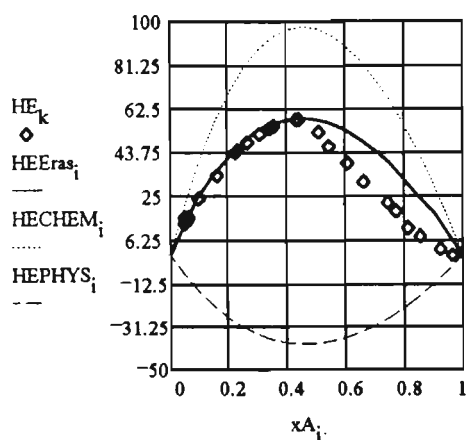
(a)
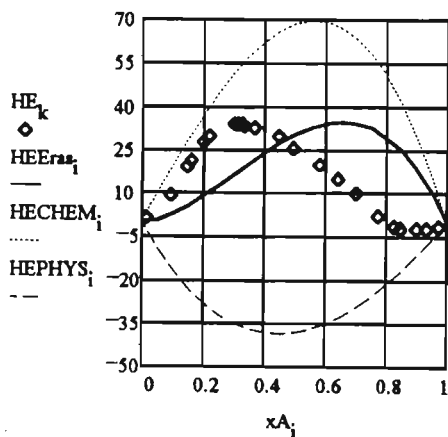
(b)
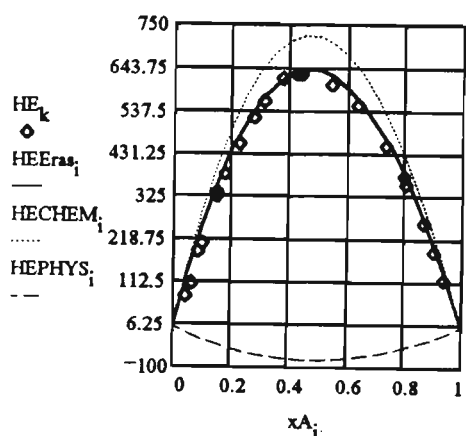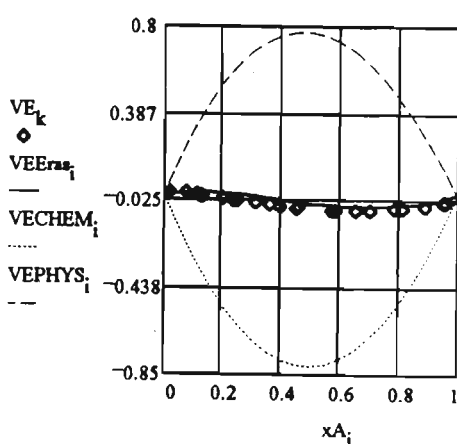
(c)
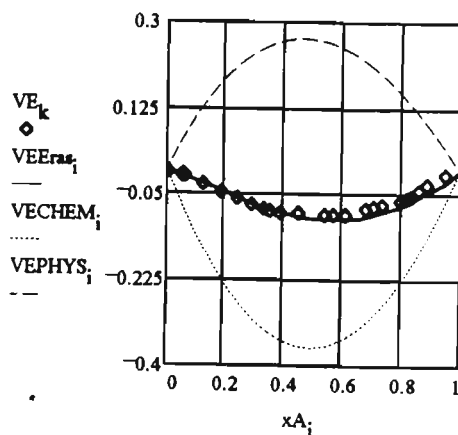
Figure 6.20 H_m^E and V_m^E ERAS model description of (x diethylamine + (1-x) {(a) THF, (b) THP and (c) 1,4-dioxane}) at 298.15 K: ◇ , experimental data; ———, ERAS model; ······, chemical contribution; ———, physical contribution.
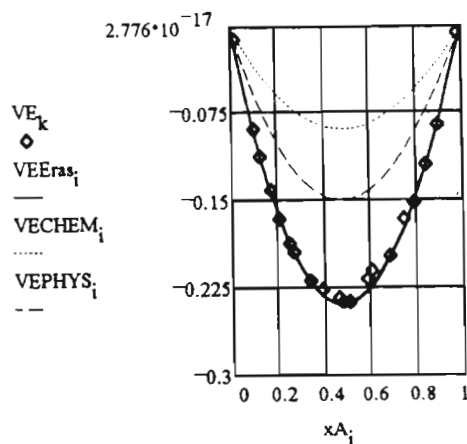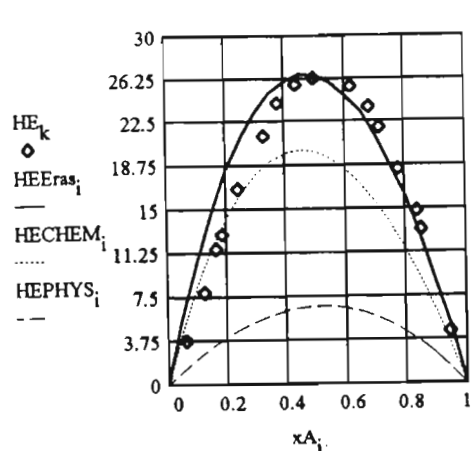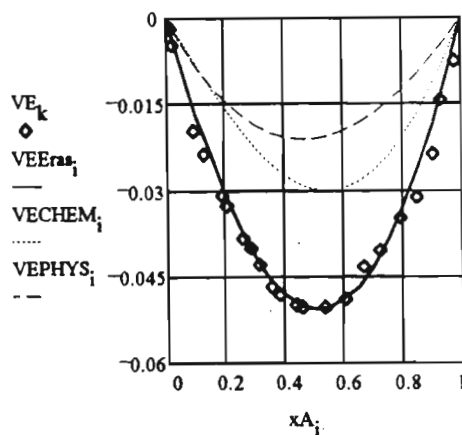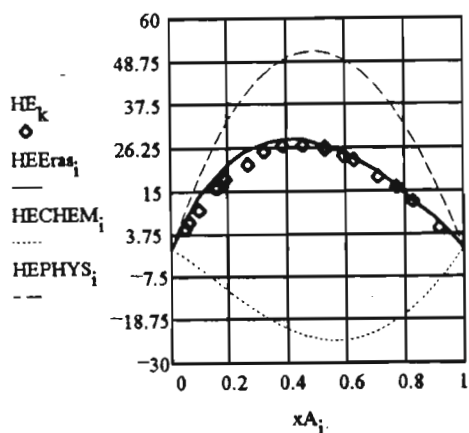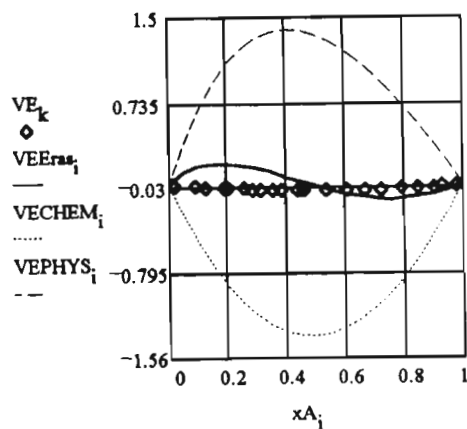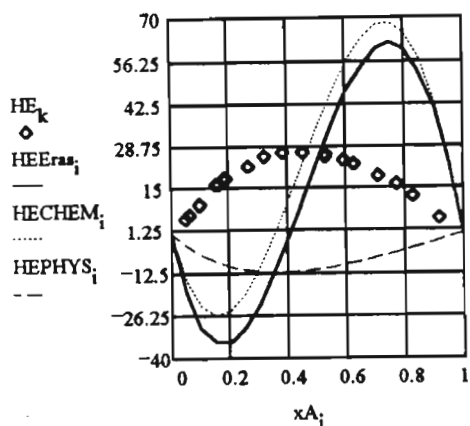
Figure 6.21 H_m^E and V_m^E ERAS model description of (x di-n-propylamine + (1-x) {(a) IPE, (b) TBME and (c) TAME}) at 298.15 K: $\diamond$ *, experimental data;* ——*, ERAS model;* ⋯⋯*, chemical contribution;* ——*, physical contribution.*
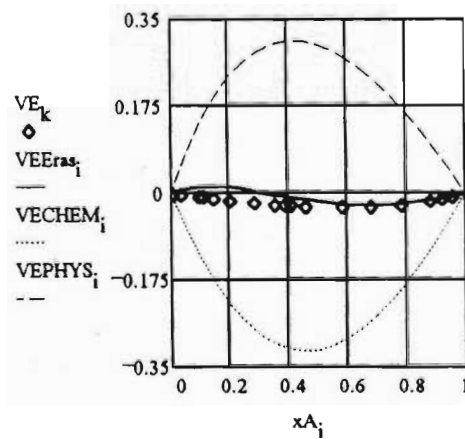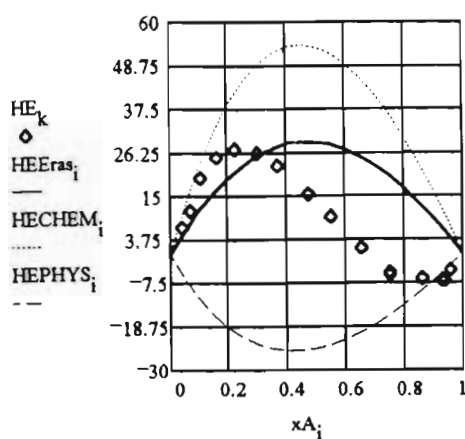
(a)
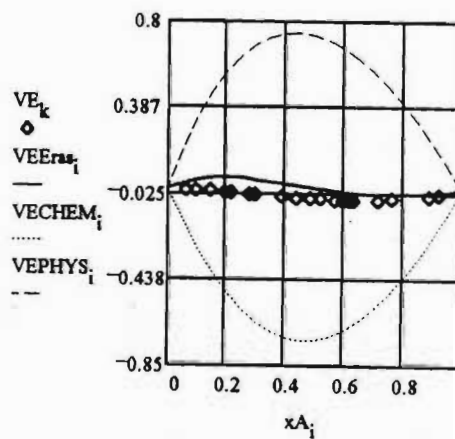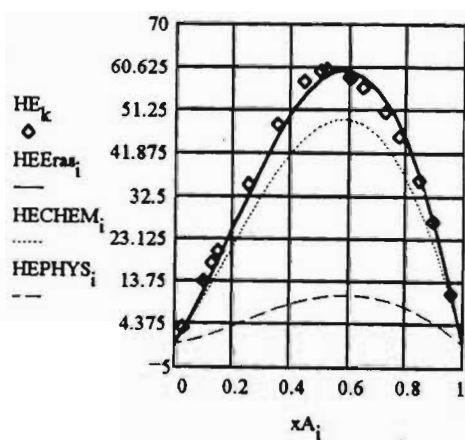
(b)
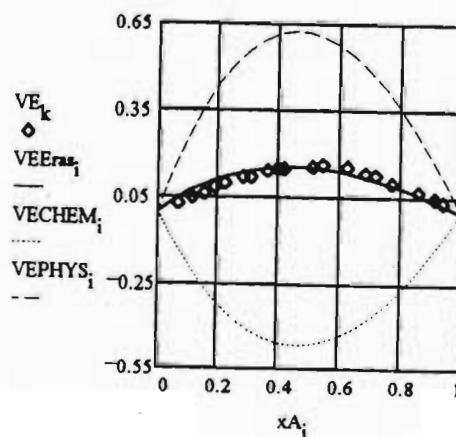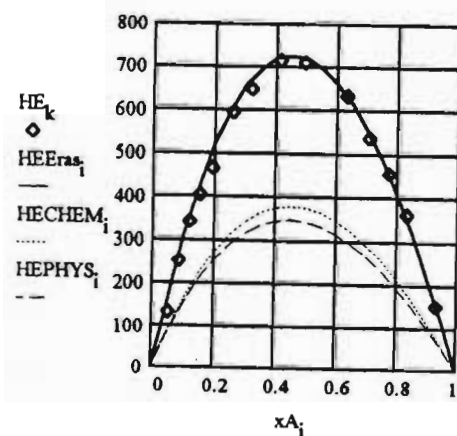
(c)

Figure 6.22 H_m^E and V_m^E ERAS model description of (x di-n-propylamine + (1-x) {(a) THF, (b) THP and (c) 1,4-dioxane}) at 298.15 K: ◇, *experimental data;* ——, *ERAS model;* ......, *chemical contribution;* ——, *physical contribution.*

The Principle of Congruence

7.1   Introduction

The principle of congruence was formulated by Bronsted and Koefoed[22] as a very simple way of relating the thermophysical properties of a mixture of *n*-alkanes to those of a representative pure *n*-alkane. In its most general form[22,349], the theory of congruence asserts that the configurational properties of members of a homologous series and of mixtures of members of such a series at a given temperature and pressure are a function only of the number average chain length. Thus for an excess property, X_m^E, such as volume or enthalpy, we may write

$$X_m^E \ (T, \ p, \ x_1, \ x_2 \ ..., \ n_1, \ n_2, \ ...) \ = \ X_m^E \ (T, \ p, \ \textstyle\sum x_i n_i) \tag{7.1}$$

The usefulness of the principle is that it allows the prediction of the properties of a mixture by equating them to the pure fluid at the same pressure and temperature. Hence formulations based on the principle of congruence are simple compared with any other method devised for describing fluid mixtures(cf. chapter 5).[349] The principle has been used to estimate densities,

excess enthalpies, excess volumes and activity coefficients of many binary systems[350] and to some special cases of multicomponent mixtures. The simplest kinds of multicomponent systems to which one might expect it to apply are ternary mixtures of members of a homologous series.[351] For such systems, several possible experimental tests of the principle of congruence suggest themselves, some of which are [350]: (a) null experiments involving mixing of a binary mixture with its congruent pure homologue e.g. the excess volume and excess enthalpy of pure *n*-hexane in any proportion with any mixture of alkanes of chain length n_1 and n_2 and composition such that $n_1x_1 + n_2(1 - x_1) = 6$, to be equal to zero; and (b) experiments in which a binary pseudo-*n*-alkane[350] **(A)** of integral average chain length n_1 is mixed with a number of other *n*-alkanes **(B, C, ...)** of various chain lengths $n_2, n_3, \ldots\ldots$ Here the excess functions for such experiments would be expected to be the same as those for binary mixtures of pure component of chain length n_1 in the same proportions with the alkanes of chain length $(n_2, n_3, n_4, \ldots\ldots)$[350]

The work reported here is an extension of the principle of class (b) above and involves ternary mixtures obtained by mixing a single component with an equimolar mixture. A novel set of mixtures involving accurately made up pseudo-ethers and pseudo-ketones has been used to test the principle. A pseudo-ether or pseudo-ketone of carbon number m was mixed with an ether or ketone of carbon number m over the whole mole fraction range. The V_m^E s and H_m^E s values for $m = 3, 4$ and 5 for the ethers and $m = 2, 3$ and 4 for the ketones, are reported in this work over the whole composition range and the results were used to test the principle of congruence.

7.2 Theory

7.2.1 Short description of the congruence principle and the application to ternary mixtures

First proposed by Bronsted and Koefoed in 1946[22], the principle of congruence asserts that a mixture of chain molecules from a given homologous series may be characterized by an index n and that, at a given temperature and pressure, mixtures with the same index have the same values for certain of their properties. For n-alkanes,[352] n-alcohols,[195] perfluoro-n-alkanes,[353] 1-alkenes,[354] 1-chloroalkenes[260] and methylalkanoates,[355] the index, n has been identified as the average number of carbon atoms per molecule, defined by

$$n = \sum_i x_i n_i \qquad (7.2)$$

where x_i is the mole fraction of the member of the series containing n_i carbon atoms. Mixtures of the same average chain length n are said to be congruent.[22,350] Equation 7.1, for a mixture of members of a homologous series, is the basic equation to the principle of congruence. The principle may be further developed by rewriting equation 7.1 in the form:

$$X_m^E(T,p,n;1,...,c) = X_m(T,p,x_1,...,x_c) -$$

$$\sum_i x_i X_i^*(T,p) - \qquad (7.3)$$

$$\Delta X_m^{id}(T,p,x_1,...,x_c)$$

where the X_m^{id} and X_i^* refer to the ideal mixture and the pure substance, respectively. For

enthalpy and volume $\Delta X_m^{id} = 0$, and this indicates that a function f(n) exists such that

$$X_m^E(T, p, n; 1,..., c) = f(T, p, n; 1,..., c) -$$

$$\sum_i x_i f(T, p, n_i)$$

(7.4)

Various forms and expansions for f(n) have been proposed, the most widely applicable and used forms being those by McGlashan[356], Hijmans and Hollemans[357] and by Diaz Pena et al.[358] McGlashan[356] proposed an expansion of the type

$$f(n) = \sum_{i=0}^{s} A_r n^{r+2}$$

(7.5)

whereas Hijmans and Holleman[357] proposed an expansion in descending powers of n-2 or

$$f(n) = a_1(n-2) + a_0 + \frac{a_{-1}}{(n-2)} + \frac{a_{-2}}{(n-2)^2} + ...$$

(7.6)

Following from equation 7.5, McGlashan[356] reported an equation for the excess property of the form

$$X_m^E(n;1, 2) = -[(n_2 - n_1)^2 x_1 x_2 \sum_{r=0}^{s} A_r] \times [\sum_{i=0}^{r} (x_1 n_1 + x_2 n_2)^i] \times [\{n_2^{r-i+1} - n_1^{r-i+1}\}/n_2 - n_1]$$

(7.7)

in which the principle of congruence was applicable to mixtures which have asymmetric excess property versus mole fraction curves. This author applied equation 7.7 to the system (*n*-hexane + *n*-hexadecane) at 20 °C and a fit to the data gave the following equation for the excess enthalpy:

$$H_m^E = (n_1 - n_2)^2 x_1 x_2 \{8.08 - 0.088 [(1 + x_1)n_1 + (1 + x_2)n_2]\}$$

(7.8)

In the application of the congruence principle to ternary mixtures for the n-alkanes, the above system has been extensively examined as a reference for other mixtures.[351]

Hijmans and Holleman[357] reported the excess property relation corresponding to equation 7.6 as

$$X_m^E(n_1, n_2, n, T) = [\frac{-(n - n_1)(n_2 - n)}{(n_1 - 2)(n_2 - 2)(n - 2)}] \cdot$$

$$[a_{-1}(T) + a_{-2}(T)(\frac{1}{n_1 - 2} + \frac{1}{n_2 - 2} + \frac{1}{n - 2})] \tag{7.9}$$

A good fit with the excess volume of five mixtures of n-alkanes {(decane + dodecane) or (decane + tetradecane) or(decane + hexadecane) or (dodecane + tetradecane) or (dodecane + hexadecane)} at 298.15 to 338.15 K was obtained using equation 7.9. It has been suggested that equation 7.9 has superior characteristics to equation 7.7 as it requires only two constants against four to fit data.

Diaz Pena et al.[195,358] tested the principle of congruence on excess enthalpy data at 298.15 K for five binary mixtures of the *n*-alcohols with methanol. For the f(n) function they used

$$f(n) = \sum_{i=0} A_{i-2} n^{(1-i)} \tag{7.10}$$

which leads to

$$X_m^E(n:1,2) = -\frac{(n_1-n_2)^2 x_1 x_2}{n n_1 n_2} \sum_{i=0} A_i H_i \tag{7.11}$$

where

$$H_i = \frac{1}{i} \sum_{s=1}^{i} (n^{-s} + n_1^{-s} + n_2^{-s}) H_{1-s} \tag{7.12}$$

and $H_0 = 1$. Equation 7.12 gave a good fit to the experimental data. Pope et al.[359] also tested equation 7.12 against the excess enthalpy and excess volume at 298.15 K of 11 binary n-alcohol mixtures and found satisfactory results for all the systems investigated.

Ternary mixtures may be most simply tested for conformity with the principle of congruence by considering them as being constituted from two components, one of which is a binary mixture and the other may be a single component or a binary mixture. Two kinds of experimental tests may be used, a null test or a comparative test. Various versions[51] of these two tests are listed in Table 3.1 where components A, B, C, D, E and F are homologues. In a null test, components 1 and 2 (from the table) are congruent and should yield no observable change on mixing for properties such as volume or enthalpy. In a comparative test, components 1 and 2 are not congruent, and a change observed on mixing is compared against a binary mixture with which it is congruent. These changes observed on mixing should be the same if the principle of congruence is valid.[22]

TABLE 7.1 Summary of the various tests for ternary mixtures.

Component 1	Component 2	Test Type
$(A + B)$, $n = n_c$	C	Null Test
$(A + B)$, $n = n_c$	$(D + E)$, $n = n_c$	Null Test
$(A + B)$, $n = n_c$	D	Comparative-
i.e. C	D	Test
$(A + B)$, $n = n_c$	$(D + E)$, $n = n_F$	Comparative-
i.e. C	F	Test

Looi *et al*[351] initiated the application of the congruence principle to ternary mixtures in which the comparative test [(A + B) + C] was conducted on a ternary mixture consisting of a [(1-x)C_6H_{14} + x (0.5$C_{13}H_{28}$ + 0.5$C_{19}H_{40}$)] mixture. They called the binary mixture (0.5$C_{13}H_{28}$ + 0.5$C_{19}H_{40}$) a "pseudo-n-hexadecane". The V_m^E and H_m^E results are compared with that of system *n*-hexadecane with *n*-hexane. The excess volumes are in good agreement with the results of Diaz Peña et al.[358] and also with those of Gomez-Ibanez and Liu.[360] A slightly poorer correlation was obtained between the excess enthalpies and those of Larkin et al.[361] and those interpolated from the data of McGlashan and Morcom, [362]as shown in figure 7.1.

In a later paper, Lim and Williamson[363] reported V_m^E data at 303.15 K on quaternary mixtures of pseudo-n-hexadecane + pseudo-n-hexane which were in excellent agreement with the data for pure n-hexane + pure n-hexadecane and the principle of congruence. The pseudo-n-hexane and the pseudo-n-hexadecane was composed of a binary mixture of (0.6667C_5H_{12} +

0.3333C_8H_{18}) and (0.2C_8H_{18} + 0.8$C_{18}H_{38}$), respectively. These workers[363] concluded that the excellent agreement between their work and those reported for the pure n-alkane mixtures confirms the applicability of the principle of congruence to the volumetric behaviour of mixtures containing a wide range of components of very different chain lengths.[363]
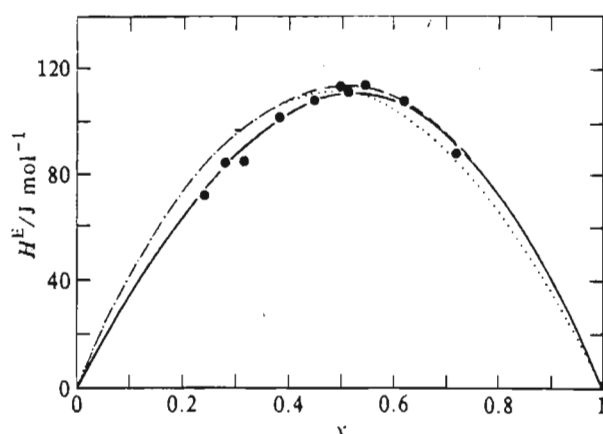
Figure 7.1 Excess enthalpies. ·, *(1-x)C_6H_{14} + x(0.5$C_{13}H_{28}$ + 0.5$C_{19}H_{40}$) at 298.15 K; ——, (1-x)C_6H_{14} + x$C_{16}H_{34}$: results of Larkin et al:* ····, *(1-x)C_6H_{14} + x$C_{16}H_{34}$: results of McGlashan et al. copied from reference 351*

The work of this thesis extends the work done by Letcher et al.[364] for the (*n*-alkane + pseudo-*n*-alkane) system and the present author[365] for the (cycloalkane + pseudo-cycloalkane) system to include the symmetrical di-*n*-ethers and di-*n*-ketones. Letcher et al.[364] reported studies done on the application of the congruency null test to a ternary mixture obtained by mixing a pseudo-*n*-alkane of carbon number *m* with the *n*-alkane of carbon number *m* over the whole composition range. The excess molar volumes and excess molar enthalpies for $\{x(0.5C_kH_{2k+2} + 0.5C_lH_{2l+2}) + (1-x)C_mH_{2m+2}\}$ where m = (k + 1)/2 were reported to be 0 ±0.005 cm³·mol⁻¹ and 0 ±1.1 J·mol⁻¹, respectively.[363] The results show that V_m^E and H_m^E

for (an *n*-alkane of carbon number *m* + a pseudo-*n*-alkane of the same carbon number) are relatively small and can be interpreted as confirmation of the application of the principle of congruence to homologous mixtures of widely differing chain length.[364] The present author[365] reported small positive excess enthalpies and small negative excess volumes for the mixtures (a cycloalkane + a pseudo-cycloalkane). These systems did not satisfy the null test of the congruence principle as well as the *n*-alkanes have been shown to do.

This work reports experimental V_m^E and H_m^E values for (pseudo $C_3H_7OC_3H_7$ [0.5 $C_2H_5OC_2H_5$ + 0.5 $C_4H_9OC_4H_9$] + $C_3H_7OC_3H_7$) or (pseudo $C_4H_9OC_4H_9$ [0.5 $C_5H_{11}OC_5H_{11}$ + 0.5 $C_3H_7OC_3H_7$] + $C_4H_9OC_4H_9$) or (pseudo $C_5H_{11}OC_5H_{11}$ [0.5 $C_8H_{17}OC_8H_{17}$ + 0.5$C_2H_5OC_2H_5$] + $C_5H_{11}OC_5H_{11}$) for the ethers and for (pseudo $C_2H_5COC_2H_5$ [0.5 $C_3H_7COC_3H_7$ + 0.5CH_3COCH_3] + $C_2H_5COC_2H_5$) or (pseudo $C_3H_7COC_3H_7$ [0.5 $C_4H_9COC_4H_9$ + 0.5$C_2H_5COC_2H_5$] + $C_3H_7COC_3H_7$) or (pseudo $C_4H_9COC_4H_9$ [0.5 $C_5H_{11}COC_5H_{11}$ + 0.5$C_3H_7COC_3H_7$] + $C_4H_9COC_4H_9$) or (pseudo $C_3H_7COC_3H_7$ [0.5 $C_5H_{11}COC_5H_{11}$ + 0.5CH_3COCH_3] + $C_3H_7COC_3H_7$) for the ketones by a novel null method and used to test the principle of congruence.

7.3 Experimental

7.3.1 Materials and Apparatus

The cyclopentane was obtained from Fluka (>99 % GC), the cyclohexane from SARchem (99 % GC), the cycloheptane from Aldrich (>99 % GC), the cyclooctane from Janssen Chemicals (>99 % GC), and the cyclodecane from Fluka (99 % GC). All the liquids

were analyzed by g.l.c. after being fractionally distilled. The V_m^E and H_m^E values were measured using an Anton Paar DMA 601 vibrating-tube densimeter and the Thermometric 2277 Thermal Activity Monitor, respectively. The methods have been described in Section 2.3.2.1.

7.3.2 Preparation of mixtures

The pseudo-ether and pseudo-ketone mixtures were made up to within 1 x 10^{-3} of $x =$ 0.5, in each case. The bottles were weighed on a Mettler AT 250 (accurate to 0.001 g). The liquids were degassed just before use by immersing the flask in a sonic bath for 10 to 15 minutes. All the mixtures were made up in 5 cm^3 bottles, and care was taken to keep the vapour space to a minimum. In all cases the least volatile component was added to the bottle first. The experimental error expected with the additional problem of making up equimolar solutions is estimated to be less than 1 x 10^{-4} in x , and in V_m^E is of the order 0.005 cm^3·mol^{-1} and in H_m^E it is of the order 0.2 J·mol^{-1} or 1 % whichever is the greater.

7.4 Results

The V_m^E results are given in Table 7.2 for all the ether mixtures and in Table 7.3 for all the ketone mixtures. The H_m^E results are listed in Table 7.4 and 7.5 for the ether and ketone mixtures, respectively. Each of the measured properties are given together with their deviations, δ, calculated from the Redlich-Kister polynomial (eqn. 2.8). The coefficients A_r and B_r are given in Table 7.6 for the excess volume and excess enthalpy data, respectively.

TABLE 7.2 Experimental excess molar volumes, V_m^E for binary mixtures of $\{x$ [0.5 $C_kH_{2k+1}OC_kH_{2k+1}$ + 0.5 $C_lH_{2l+1}OC_lH_{2l+1}$] + (1-x) $C_mH_{2m+1}OC_mH_{2m+1}$ } where m = (k+l)/2 at 298.15 K.

x	$\dfrac{V_m^E}{cm^3 \cdot mol^{-1}}$	x	$\dfrac{V_m^E}{cm^3 \cdot mol^{-1}}$	x	$\dfrac{V_m^E}{cm^3 \cdot mol^{-1}}$

$x[0.5C_2H_5OC_2H_5 + 0.5C_4H_9OC_4H_9] + (1-x)C_3H_7OC_3H_7$

x	V_m^E	x	V_m^E	x	V_m^E
0.008	-0.0151	0.226	0.0007	0.664	0.0037
0.014	-0.0136	0.350	0.0034	0.774	-0.0012
0.044	-0.0147	0.419	0.0041	0.847	-0.0029
0.068	-0.0110	0.533	0.0033	0.893	-0.0048
0.138	-0.0014	0.586	0.0038	0.992	-0.0017

$x[0.5C_5H_{11}OC_5H_{11} + 0.5C_3H_7OC_3H_7] + (1-x)C_4H_9OC_4H_9$

x	V_m^E	x	V_m^E	x	V_m^E
0.091	-0.0040	0.545	0.0110	0.826	-0.0052
0.251	-0.0080	0.600	0.0065	0.884	-0.0042
0.338	0.0091	0.711	0.0027	0.894	-0.0011
0.361	-0.0067	0.725	0.0079	0.985	-0.0056
0.406	0.0091	0.765	-0.0017	0.987	-0.0060
0.451	0.0013	0.781	-0.0016		

$x[0.5C_8H_{17}OC_8H_{17} + 0.5C_2H_5OC_2H_5] + (1-x)C_5H_{11}OC_5H_{11}$

x	V_m^E	x	V_m^E	x	V_m^E
0.099	-0.0076	0.403	-0.0011	0.675	-0.0038
0.172	-0.0021	0.469	-0.0030	0.749	-0.0031
0.250	-0.0012	0.500	-0.0046	0.835	-0.0025
0.289	-0.0022	0.622	-0.0035	0.990	-0.0036

TABLE 7.3 Experimental excess molar volumes, V_m^E for binary mixtures of $\{x [0.5\ C_kH_{2k+1}COC_kH_{2k+1} + 0.5\ C_lH_{2l+1}COC_lH_{2l+1}] + (1-x)\ C_mH_{2m+1}COC_mH_{2m+1} \}$ where m = (k+l)/2 at the temperature 298.15 K.

x	V_m^E cm$^3\cdot$mol^{-1}	x	V_m^E cm$^3\cdot$mol^{-1}	x	V_m^E cm$^3\cdot$mol^{-1}
		$x[0.5C_2H_5OC_2H_5 + 0.5C_4H_9OC_4H_9] + (1-x)C_3H_7OC_3H_7$			
0.129	-0.0041	0.439	-0.0114	0.911	-0.0060
0.197	-0.0065	0.479	-0.0115	0.932	-0.0056
0.203	-0.0071	0.505	-0.0115	0.953	-0.0039
0.207	-0.0074	0.581	-0.0114	0.977	-0.0023
0.302	-0.0097	0.670	-0.0106	0.987	-0.0026
0.303	-0.0097	0.755	-0.0090	0.994	-0.0013
0.377	-0.0108	0.789	-0.0085		
		$x[0.5C_2H_5OC_2H_5 + 0.5C_4H_9OC_4H_9] + (1-x)C_3H_7OC_3H_7$			
0.006	0.0037	0.364	0.0024	0.728	-0.0038
0.065	0.0036	0.407	0.0005	0.777	-0.0001
0.126	-0.0013	0.477	-0.0003	0.881	-0.0010
0.141	0.0006	0.531	-0.0020	0.941	-0.0009
0.178	-0.0024	0.600	-0.0030	0.989	-0.0016
0.221	0.0005	0.637	-0.0034		
0.281	0.0007	0.702	-0.0036		
		$x[0.5C_2H_5OC_2H_5 + 0.5C_4H_9OC_4H_9] + (1-x)C_3H_7OC_3H_7$			
0.009	-0.0024	0.356	-0.0007	0.587	-0.0002
0.045	-0.0005	0.380	-0.0007	0.699	-0.0006
0.163	-0.0009	0.468	-0.0017	0.720	-0.0003
0.203	-0.0008	0.499	-0.0003	0.895	-0.0020
0.280	-0.0000	0.529	-0.0010	0.995	-0.0014
		$x[0.5C_2H_5OC_2H_5 + 0.5C_4H_9OC_4H_9] + (1-x)C_3H_7OC_3H_7$			
0.012	-0.0067	0.495	-0.0044	0.786	-0.0109
0.105	-0.0096	0.555	-0.0014	0.833	-0.0091
0.294	-0.0107	0.599	-0.0070	0.868	-0.0057
0.402	-0.0077	0.697	-0.0108	0.942	-0.0115
0.485	-0.0060	0.748	-0.0085	0.995	-0.0152

TABLE 7.4 Experimental excess molar enthalpies, H_m^E for binary mixtures of $\{x\ [0.5\ C_kH_{2k+1}OC_kH_{2k+1} + 0.5\ C_lH_{2l+1}OC_lH_{2l+1}] + (1-x)\ C_mH_{2m+1}OC_mH_{2m+1}\}$ where $m = (k+l)/2$ and the deviations δH_m^E at the temperature 298.15 K.

x	H_m^E	δH_m^E	x	H_m^E	δH_m^E	x	H_m^E	δH_m^E
	J·mol⁻¹	J·mol⁻¹		J·mol⁻¹	J·mol⁻¹		J·mol⁻¹	J·mol⁻¹

$$x[0.5C_2H_5OC_2H_5 + 0.5C_4H_9OC_4H_9] + (1-x)C_3H_7OC_3H_7$$

x	H_m^E	δH_m^E	x	H_m^E	δH_m^E	x	H_m^E	δH_m^E
0.083	0.89	-0.17	0.510	4.14	0.03	0.764	2.72	-0.09
0.155	1.91	-0.02	0.606	3.89	-0.01	0.871	1.70	0.05
0.194	2.49	0.14	0.700	3.35	-0.00	0.907	1.32	0.11
0.284	3.18	-0.02	0.755	2.85	-0.04	0.920	1.05	0.00
0.430	4.02	0.00						

$$x[0.5C_5H_{11}OC_5H_{11} + 0.5C_3H_7OC_3H_7] + (1-x)C_4H_9OC_4H_9$$

x	H_m^E	δH_m^E	x	H_m^E	δH_m^E	x	H_m^E	δH_m^E
0.063	0.60	-0.16	0.503	3.70	-0.01	0.674	3.20	-0.04
0.133	1.50	-0.04	0.507	3.70	-0.00	0.744	2.79	0.01
0.211	2.40	0.09	0.527	3.72	0.02	0.798	2.38	0.06
0.298	3.05	0.05	0.601	3.50	-0.06	0.865	1.71	0.06
0.406	3.54	0.01	0.650	3.32	-0.04	0.905	1.14	-0.04

$$x[0.5C_8H_{17}OC_8H_{17} + 0.5C_2H_5OC_2H_5] + (1-x)C_5H_{11}OC_5H_{11}$$

x	H_m^E	δH_m^E	x	H_m^E	δH_m^E	x	H_m^E	δH_m^E
0.078	8.75	0.26	0.332	27.79	1.21	0.750	19.79	0.47
0.122	11.95	-0.75	0.411	29.44	0.72	0.810	15.52	0.34
0.156	15.40	-0.37	0.412	29.04	0.32	0.897	8.44	0.04
0.175	16.76	-0.54	0.518	28.22	-0.60	0.934	5.89	0.43
0.256	23.01	0.09	0.611	24.90	-1.57			

TABLE 7.5 Experimental excess molar enthalpies, H_m^E for binary mixtures of $\{x$ [0.5 $C_kH_{2k+1}COC_kH_{2k+1}$ + 0.5 $C_lH_{2l+1}COC_lH_{2l+1}$] + $(1-x)$ $C_mH_{2m+1}COC_mH_{2m+1}$ $\}$ where m = (k+l)/2 and the deviations, δH_m^E at the temperature 298.15 K.

x	H_m^E ($J \cdot mol^{-1}$)	δH_m^E ($J \cdot mol^{-1}$)	x	H_m^E ($J \cdot mol^{-1}$)	δH_m^E ($J \cdot mol^{-1}$)	x	H_m^E ($J \cdot mol^{-1}$)	δH_m^E ($J \cdot mol^{-1}$)
			$x[0.5C_3H_7COC_3H_7 + 0.5CH_3COCH_3] + (1-x)C_2H_5COC_2H_5$					
0.050	1.84	0.22	0.411	5.92	0.03	0.775	3.49	-0.13
0.128	3.28	-0.12	0.444	5.90	0.04	0.817	3.16	0.07
0.176	4.20	-0.14	0.497	5.63	-0.10	0.893	2.00	0.00
0.210	4.89	0.10	0.607	5.14	-0.03	0.921	1.76	0.23
0.280	5.45	-0.01	0.644	4.95	0.05	0.943	1.01	-0.12
0.333	5.90	0.15	0.713	4.25	-0.04			
			$x[0.5C_4H_9COC_4H_9 + 0.5C_2H_5COC_2H_5] + (1-x)C_3H_7COC_3H_7$					
0.126	1.61	-0.18	0.412	4.62	0.16	0.785	2.03	-0.04
0.184	2.44	-0.16	0.443	4.62	0.11	0.829	1.61	0.06
0.225	3.13	0.04	0.527	4.19	-0.14	0.904	1.00	0.29
0.290	3.79	0.03	0.627	3.60	-0.17	0.973	0.27	0.12
0.359	4.43	0.18	0.701	2.89	-0.16			
			$x[0.5C_5H_{11}COC_5H_{11} + 0.5C_3H_7COC_3H_7] + (1-x)C_4H_9COC_4H_9$					
0.090	-0.19		0.406	-0.07		0.831	-0.13	
0.100	-0.11		0.510	0.10		0.869	0.24	
0.214	0.07		0.615	-0.10		0.892	0.06	
0.259	-0.03		0.748	0.91				
			$x[0.5C_5H_{11}COC_5H_{11} + 0.5CH_3COCH_3] + (1-x)C_3H_7COC_3H_7$					
0.029	-0.34	-0.89	0.221	5.88	0.19	0.551	10.78	0.20
0.071	1.09	-0.43	0.325	8.34	-0.06	0.625	10.07	-0.46
0.094	1.64	-0.46	0.345	8.96	0.15	0.674	9.46	-0.39
0.124	3.04	0.13	0.422	10.21	0.05	0.800	6.58	-0.33
0.173	4.75	0.43	0.509	11.16	0.23	0.836	5.89	0.08
0.198	4.96	-0.06	0.511	11.14	0.20	0.911	4.10	0.87

TABLE 7.6 Coefficients $A_r(cm^3 \cdot mol^{-1})$ and $B_r(J \cdot mol^{-1})$ for V_m^E and H_m^E $\{x$ [0.5 $C_kH_{2k+1}OC_kH_{2k+1}$ + 0.5 $C_lH_{2l+1}OC_lH_{2l+1}]$ + (1-x) $C_mH_{2m+1}OC_mH_{2m+1}$ $\}$ and $\{x$ [0.5 $C_kH_{2k+1}COC_kH_{2k+1}$ + 0.5 $C_lH_{2l+1}COC_lH_{2l+1}]$ + (1-x) $C_mH_{2m+1}COC_mH_{2m+1}$ $\}$where m = (k+l)/2 at the temperature 298.15 K by equation 2.8.

Mixture	A_0	A_1	A_2
x[0.5C$_3$H$_7$COC$_3$H$_7$ + 0.5CH$_3$COCH$_3$] + (1-x)C$_2$H$_5$COC$_2$H$_5$	-0.0455	-0.0100	-0.0151

Mixture	B_0	B_1	B_2
x[0.5C$_2$H$_5$OC$_2$H$_5$ + 0.5C$_4$H$_9$OC$_4$H$_9$] + (1-x)C$_3$H$_7$OC$_3$H$_7$	16.462	0.154	-3.481
x[0.5C$_3$H$_7$OC$_3$H$_7$ + 0.5C$_5$H$_{11}$OC$_5$H$_{11}$] + (1-x)C$_4$H$_9$OC$_4$H$_9$	14.822	0.451	-1.971
x[0.5C$_2$H$_5$OC$_2$H$_5$ + 0.5C$_8$H$_{17}$OC$_8$H$_{17}$] + (1-x)C$_4$H$_9$OC$_4$H$_9$	116.045	-17.251	-17.601
x[0.5CH$_3$COCH$_3$ + 0.5C$_3$H$_7$COC$_3$H$_7$] + (1-x)C$_2$H$_5$COC$_2$H$_5$	22.904	-7.019	5.696
x[0.5C$_2$H$_5$COC$_2$H$_5$ + 0.5C$_4$H$_9$COC$_4$H$_9$] + (1-x)C$_3$H$_7$COC$_3$H$_7$	17.859	-4.648	-8.874
x[0.5CH$_3$COCH$_3$ + 0.5C$_5$H$_{11}$COC$_5$H$_{11}$] + (1-x)C$_3$H$_7$COC$_3$H$_7$	43.590	9.417	-16.955

7.5   Discussion

The V_m^E and H_m^E results for all the systems investigated are represented in figures 7.2 and 7.3 respectively, where the mole fraction of the pseudo-ether and pseudo-ketone are calculated by using the mean molar mass, respectively and regarding the pseudo-compound as a single pure substance.

The results show a small positive excess enthalpy, 4.2 J·mol⁻¹ < $H_{m(max)}^E$ < 29 J·mol⁻¹ for all the mixtures investigated here except the $x[0.5C_5H_{11}OC_5H_{11}$ + $0.5C_3H_7OC_3H_7]$ + $(1-x)C_4H_9OC_4H_9$ ether system and the $x[0.5C_5H_{11}COC_5H_{11}$ + $0.5C_3H_7COC_3H_7]$ + $(1-x)C_4H_9COC_4H_9$ ketone system. The enthalpic behaviour of the latter two mixtures over the whole composition range was small(0.9 J·mol⁻¹ < $H_{m(max)}^E$ < 3.7 J·mol⁻¹) and suggests confirmation of the congruence principle for pseudo mixtures containing constituent liquids which do not differ from one another by more than one -CH₂- group. The H_m^E data for the remainder of the mixtures, in general, seem to confirm that the greater the disparity in the carbon number, the greater the divergence from the congruence principle for example $H_{m(max)}^E$ for x [0.5 (CH_3COCH_3) + 0.5 $(C_5H_{11}COC_5H_{11})$ + $(1-x)$ $C_3H_7COC_3H_7$ is 11.2 J·mol⁻¹ while $H_{m(max)}^E$ for $x[0.5$ (CH_3COCH_3) + 0.5 $(C_3H_7COC_3H_7)]$ + $(1-x)$ $C_2H_5COC_2H_5)$ is 5.9 J·mol⁻¹.

The V_m^E data for all the systems investigated here show little trend and the data are scattered around ±0.01 cm³·mol⁻¹, except for the $x[0.5C_3H_7COC_3H_7$ + $0.5CH_3COCH_3]$ + $(1-x)C_2H_5COC_2H_5$ system. In this latter system the V_m^E curves are symmetrical around x = 0.7 with $V_{m(max)}^E$ = -0.012 cm³·mol⁻¹.

The results for (an alkane of carbon number m + a pseudo-alkane of the same carbon number) reported by Letcher et al.[364] show the V_m^E and H_m^E within a limit of 0 ±0.01 cm³·mol⁻¹ and 0 ± 1.1 J·mol⁻¹, respectively, while the results presented here are within 0 ±0.01 cm³·mol⁻¹ and 0.2 - 29 J·mol⁻¹, respectively. The work done by the present author[365] for cycloalkane mixtures are of the order 0.0005 - 0.002 cm³·mol⁻¹ and 0.04 - 48 J·mol⁻¹, in V_m^E and H_m^E, respectively. In general the V_m^E and H_m^E for the *n*-alkanes, cycloalkanes, ethers and ketone mixtures, the congruence principle is obeyed in the order: *n*-alkanes > > > > ethers ≥ ketones > > cycloalkanes.[364,365]
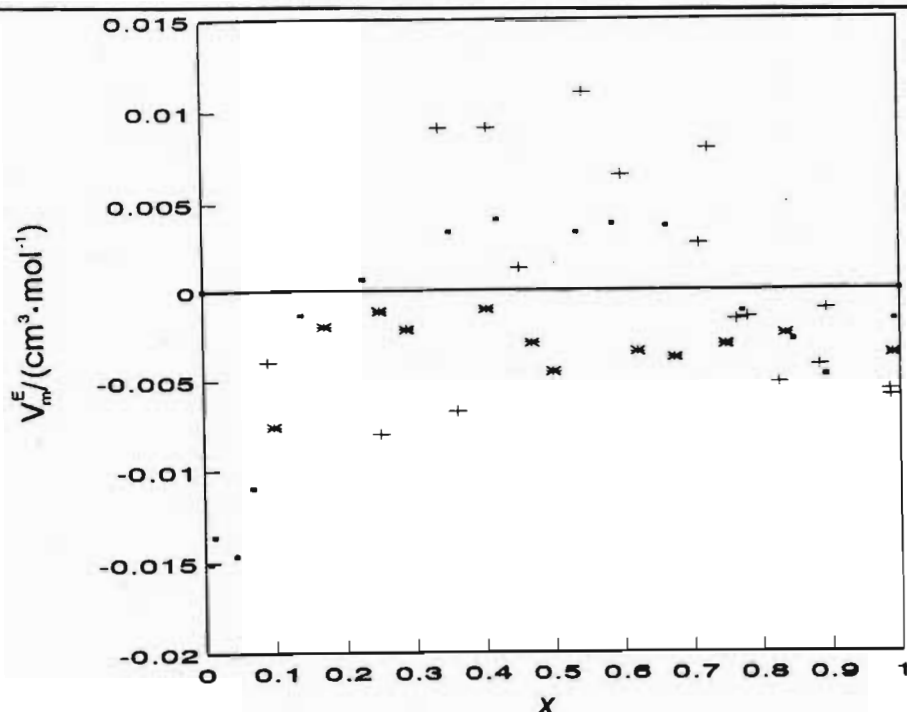
Figure 7.2 Excess molar volume V_m^E for: ■ *{x[0.5C₂H₅OC₂H₅ + 0.5C₄H₉OC₄H₉] + (1-x)C₃H₇OC₃H₇} ;* + *{x[0.5C₃H₇OC₃H₇ + 0.5C₅H₁₁OC₅H₁₁] + (1-x)C₄H₉OC₄H₁₁ } and* ✳ *{x[0.5C₂H₅OC₂H₅ + 0.5C₆H₁₃OC₆H₁₃] + (1-x)C₅H₁₁OC₅H₁₁} at 298.15 K*
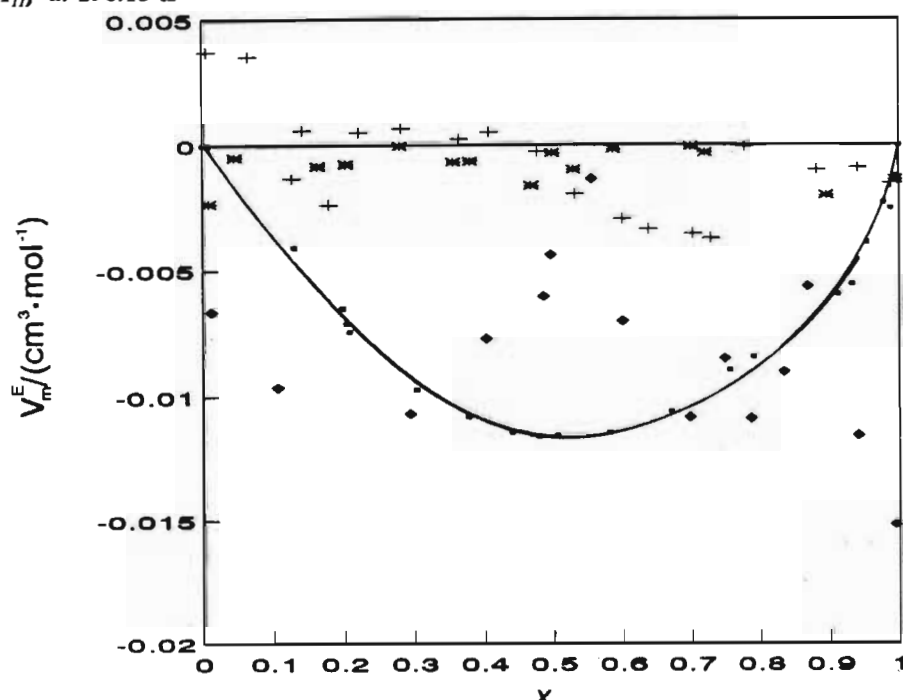
Figure 7.3 Excess molar volume V_m^E for: ■ *{x[0.5CH₃COCH₃ + 0.5C₃H₇COC₃H₇] + (1-x)C₂H₅COC₂H₅} ;* + *{x[0.5C₂H₅COC₂H₅ + 0.5C₄H₉COC₄H₉] + (1-x)C₃H₇COC₃H₇} ;* ✳ *{x[0.5C₃H₇COC₃H₇ + 0.5C₅H₁₁COC₅H₁₁] + (1-x)C₄H₉COC₄H₉} and* ◆ *{x[0.5CH₃COCH₃ + 0.5C₅H₁₁COC₅H₁₁] + (1-x)C₃H₇COC₃H₇} at 298.15 K*
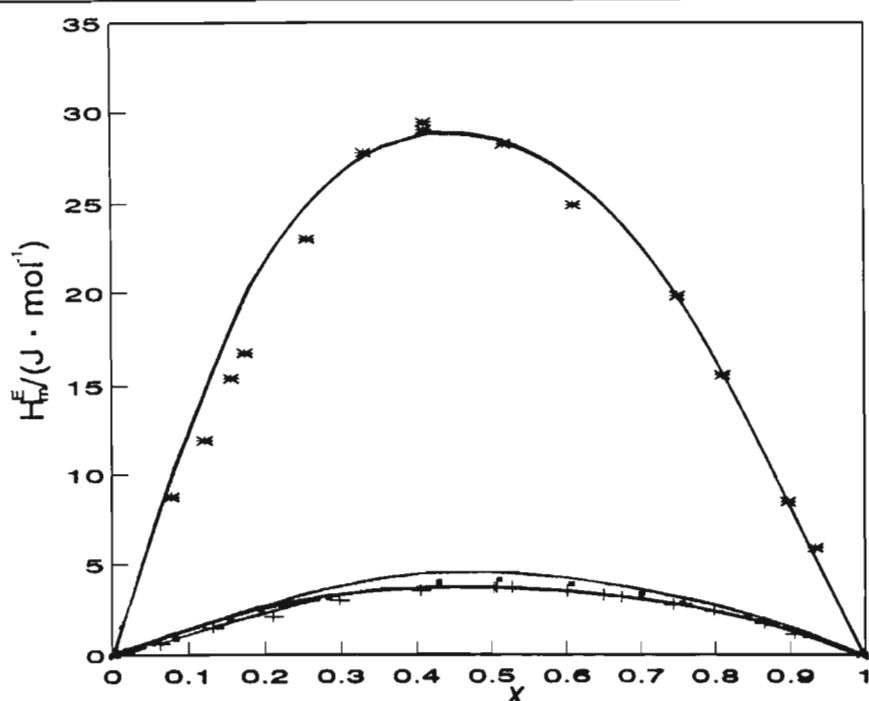
Figure 7.4 Excess molar enthalpy H_m^E for: ■ *{x[0.5C$_2$H$_5$OC$_2$H$_5$ + 0.5C$_4$H$_9$OC$_4$H$_9$] + (1-x)C$_3$H$_7$OC$_3$H$_7$}* ; +

{x[0.5C$_3$H$_7$OC$_3$H$_7$ + 0.5C$_5$H$_{11}$OC$_5$H$_{11}$] + (1-x)C$_4$H$_9$OC$_4$H$_{11}$ } and ✳ *{x[0.5C$_2$H$_5$OC$_2$H$_5$ + 0.5C$_8$H$_{17}$OC$_8$H$_{17}$] + (1-*

x)C$_5$H$_{11}$OC$_5$H$_{11}$} at 298.15 K
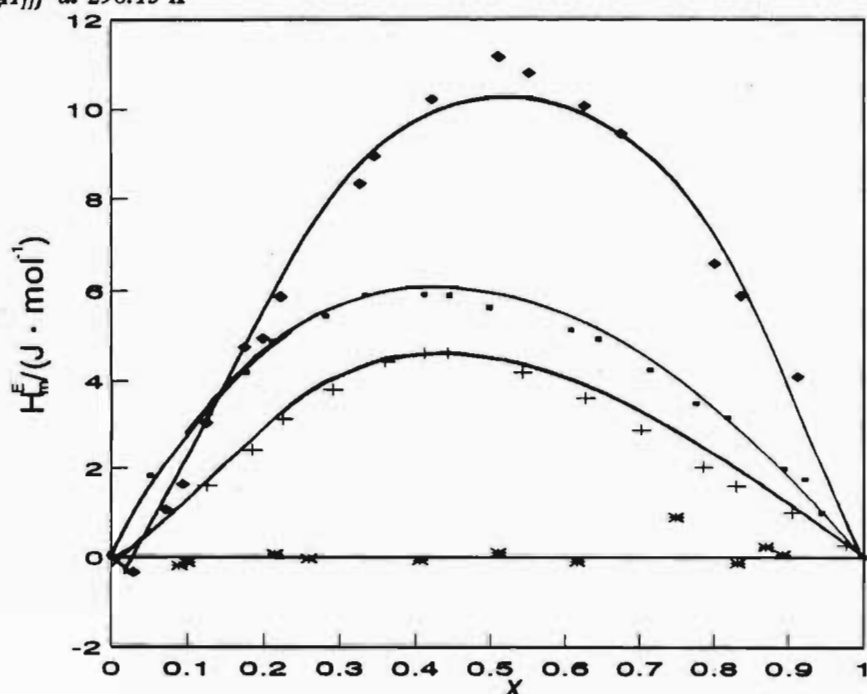
Figure 7.5 Excess molar enthalpy H_m^E for: ■ *{x[0.5CH$_3$COCH$_3$ + 0.5C$_3$H$_7$COC$_3$H$_7$] + (1-x)C$_2$H$_5$COC$_2$H$_5$}* ; +

{x[0.5C$_2$H$_5$COC$_2$H$_5$ + 0.5C$_4$H$_9$COC$_4$H$_9$] + (1-x)C$_3$H$_7$COC$_3$H$_7$} ; ✳ *{x[0.5C$_3$H$_7$COC$_3$H$_7$ + 0.5C$_5$H$_{11}$COC$_5$H$_{11}$] + (1-*

x)C$_4$H$_9$COC$_4$H$_9$} and ◆ *{x[0.5CH$_3$COCH$_3$ + 0.5C$_5$H$_{11}$COC$_5$H$_{11}$] + (1-x)C$_3$H$_7$COC$_3$H$_7$} at 298.15 K*

Conclusions

8.1 Mixtures of (an alkanol + a branched chain ether)- chapters two and three

The V_m^E data for {(methanol or ethanol or propan-1-ol or propan-2-ol) + (IPE or TBME or TAME)} are negative over the whole mole fraction range and this is explained in terms of (a) a more organized packing effect in the mixture and (b) stronger specific interactions between the -OH in the alkanol and the -O- in the ether. The H_m^E data for all the systems are positive over the whole mole fraction range except for the (methanol + IPE or TBME or TAME) system where a small exothermic effect is found in the methanol rich region. The results suggest that the H_m^E data reported in this thesis depend on the balance between two opposing contributions, (a) a positive term from the rupture of alkanol-alkanol hydrogen bonds and ether-ether interactions and (b) a negative term from the formation of -OH·····O- hydrogen bonded complexes.

8.2 Mixtures of (an alkanol + a cyclic ether) - chapters two and three

The V_m^E data for {(methanol or ethanol or propan-1-ol or propan-2-ol) + (THF or THP or 1,4-dioxane)} range from large and negative for the methanol mixtures to sine shaped to large positive for the propan-2-ol mixtures over the whole mole fraction range. The positive effect is explained in terms of the structure breaking effect becoming dominant when the

alkanol concentration is smaller than that of the cyclic ether while the negative effect is explained in terms of more efficient packing of the methanol molecule in the heterocyclic ring. The H_m^E data for all the systems are positive over the whole alkanol mole fraction range. The results suggest that the H_m^E depends on three effects: (a) endothermic contributions from the disruption of alkanol-alkanol hydrogen bonds and (b) endothermic contributions from the disruption of ether-ether interactions and (c) exothermic contribution from the association between alkanol-ether molecules.

8.3   Mixtures of (a secondary amine + a branched chain or cyclic ether)

The V_m^E and H_m^E results for the mixtures {(diethylamine or di-n-propylamine) + (IPE or TBME or TAME or THF or THP or 1,4-dioxane)} seem to indicate that as the aliphatic chain length of the secondary amine increases, (a) the packing and association effects between the amine and the ether become less dominant and (b) the breakdown of the self association in both the amine and the ether dictate the thermodynamic behaviour of the system.

8.4   Mixtures of (1-alkyne + a branched chain ether)

The V_m^E and H_m^E results for the mixtures {(1-hexyne or 1-heptyne or 1-octyne) + (IPE or TBME or TAME)} are all negative and this is most likely due to the superimposition of two effects: (a) the hydrogen bond capability between the terminal hydrogen in the 1-alkyne and the oxygen in the ether and (b) the $\pi\cdots n$ interaction between the carbon-carbon triple bond in the 1-alkyne and the lone pair electrons of the oxygen in the ether.

A comparison of the V_m^E and H_m^E data for all the -OH or -NH or $\equiv CH\cdots O$ interacting systems seems to indicate that the 1-alkyne systems display the largest hydrogen donor capability while self association effects in mixtures containing an alkanol or an amine molecule

seem to significantly dictate V_m^E and H_m^E behaviour.

8.5 Density, Isothermal Compressibility and Cubic Expansion Coefficient of branched chain ethers - chapter four

For all the ethers investigated in this work, the cubic expansion coefficients decrease with an increase in temperature or pressure while the isothermal compressibilities increase with an increase in temperature or pressure over the temperature and pressure ranges used in this work. Linear isotherms of density are observed for all the investigated liquids.

8.6 Application of the Theories of Liquid Mixtures - chapters five and six

For the majority of the (an alkanol + a branched chain or cyclic ether) mixtures the Modified UNIFAC model is successful in reproducing the main features of the experimental data although quantitative agreement is not achieved. In particular, for the (methanol + a branched chain ether) system, the Modified UNIFAC model fails to reproduce the small exothermic behaviour in the methanol-rich region resulting in very high absolute relative deviations. For the (a secondary amine + a cyclic ether) mixtures the Modified UNIFAC model fails to correctly reproduce the experimental H_m^E data and gives large absolute average deviations. The large differences in size and shape of the amine and ether molecules could possibly account for the poor representation by the model.

For the (a 1-alkyne + branched chain ether) mixture the Flory one-parameter equation provides a surprisingly good fit of the experimental V_m^E and H_m^E results. For all the (an alkanol or a secondary amine + a branched chain or a cyclic ether) the PFP theory suggests that the calculated V_m^E depends to large extent on the interaction term.

For most of the (an alkanol + a branched chain or cyclic ether) the ERAS model is

sufficiently accurate in the representation of the V_m^E and H_m^E experimental results. However in some instances deviations as large as 190 J·mol^{-1} in H_m^E have been described. For the (diethylamine or di-n-propylamine + a branched chain or cyclic ether) mixtures the ERAS model adequately describes the excess thermodynamic properties. The theoretical analysis presented here seems to indicate that the ERAS model is sufficiently rigorous and accurate for both strongly and weakly associating systems.

8.7   The Congruence Theory - chapter seven

The principle of congruence is not as well obeyed for H_m^E as it is for V_m^E. The results show a small positive excess enthalpy, 4.2 J·mol^{-1} < $H_{m(max)}^E$ < 29 J·mol^{-1} for all the mixtures investigated here except the $x[0.5C_5H_{11}OC_5H_{11} + 0.5C_3H_7OC_3H_7] + (1-x)C_4H_9OC_4H_9$ ether system and the $x[0.5C_5H_{11}COC_5H_{11} + 0.5C_3H_7COC_3H_7] + (1-x)C_4H_9COC_4H_9$ ketone system. The enthalpic behaviour of the latter two mixtures over the whole composition range was small (0.9 J·mol^{-1} < $H_{m(max)}^E$ < 3.7 J·mol^{-1}) and suggest confirmation of the congruence principle for pseudo mixtures containing constituent liquids which do not differ from one another by more than one -CH$_2$- group. The V_m^E data for all the systems investigated here satisfy the principle of congruence and the results are scattered around ±0.01 cm^3·mol^{-1}, except for the $x[0.5C_3H_7COC_3H_7 + 0.5CH_3COCH_3] + (1-x)C_2H_5COC_2H_5$ system. Comparing the work in this thesis with that published for *n*-alkanes and cycloalkanes mixtures, the congruence principle is obeyed in the order: *n*-alkanes > > > > ethers ≥ ketones > > cycloalkanes. The decision of whether the principle of congruence is obeyed or not ultimately rests on an arbitrary choice of limits. These in turn are dependent on the limits of experimental precision. In this work the arbitrary limits were chosen as 5 J·mol^{-1} for H_m^E and 0.01 cm^3·mol^{-1} for V_m^E.

References

1. Trampe D.M.; Eckert C.A.; *J. Chem. Eng. Data* (1991), **36**, 112

2. Pfeffer T.; Lowen B.; Schulz S.; *Fluid Phase Equilibria* (1995), **106**, 139

3. Prausnitz J.M.; *Ber. Bunsenges. Physik. Chem.* (1994), **98(11)**, 1461

4. Heminger W.; Hohne G.; Calorimetry: *Fundamentals and Practice* (1984), Verlag Chemie, Weinheim, New York.

5. Randzio S.L. Grolier J.P.E.; Quint J.R.; Eatough D.J.; Lewis E.A.; Hansen L.D.; *Int. J. of Thermophysics* (1994), **15(3)**, 415

6. Randzio S.L.; *Experimental Thermodynamics Vol. IV, Solution Calorimetry* (1994), Edited by K.N. Marsh and P.A.G. O'Hare; Blackwell Scientific, Oxford, London.

7. Hallen D.; *PhD Thesis* (1989), Lund University, Lund, Sweden.

8. Tomiska J.; Wang H.; *Ber. Bunsenges. Physik. Chem.* (1995), **99(8)**, 633

9. Homendra N.; *PhD Thesis* (1989), Indian Institute of Technology, New Delhi, India.

10. Mercer Chalmers J.; *PhD Thesis* (1993), Rhodes University, South Africa

11. Van H.T.; Patterson D.; *J. Soln. Chem.* (1982), **11**, 793

12. Costas M.; Patterson D.; *J. Soln. Chem.* (1982), **11**, 807

13. Walas S.M.; *Phase Equilibria in Chemical Engineering* (1985), Butterworth Publishers, Stoneham, MA, 02180, USA.

14. Renon H.; Prausnitz J.M.; *AIChE* (1968), **14(1)**, 135

15. Abrams F.; Prausnitz J.M.; *AIChE* (1975), **21(1)**, 116

16.   Nagata I.; Kawamura Y.; *Z. Physik. Chem Neue Folge* (1977), **107**, 141

17.   Weidlich U.; Gmehling J.; *Ind. Eng. Chem. Res.* (1987), **26(7)**, 1372

18.   Freudenslund A.; Jones R.L.; Prausnitz J.M.; *AIChE* (1975), **21(6)**, 1086

19.   Flory P.; *J. Am. Chem. Soc.* (1965), **87**, 1833

20.   Heintz A.; *Ber. Bunsenges. Phys. Chem.* (1985), **89**, 172

21.   Reimann R.; Heintz A.; *J. Soln. Chem.* (1991), **20**, 29

22.   Bronsted J.N.; Koefoed J.; *K. Dan. Vidensk. Selsk. Mat-Fys. Medd.* (1946), **22(17)**, 1

23.   Battino R.; *Chem Reviews* (1971), **71(1)**, 5.

24.   Handa Y.P.; Benson G.C.; *Fluid Phase Equilibria* (1979), **3**, 185.

25.   McGlashen M.L.; *Chemical Thermodynamics* (1979), Academic Press Inc., London.

26.   Letcher T.M.; *Chem SA* (1975), **1**, 226.

27.   Stokes R.H.; Marsh K.N.; *Ann. Rev. Phys. Chem* (1972), **23**, 65.

28.   Marsh K.N.; *Ann. Rep. R.S.C. Sect. C* (1980), **77**, 101.

29.   Marsh K.N.; *Ann. Rep. R.S.C. Sect. C* (1984), **81**, 209.

30.   Bauer N.; Lewin S.Z.; *Physical Methods of Organic Chemistry* (1959), **1**, Part 1, Third edition, EDITOR: Weissberger, Interscience, New York.

31.   Wood S.E.; Brusie J.P.; *J. Am. Chem. Soc.* (1953), **65**, 1891.

32.   Scatchard G.; Wood S.E.; Mochel J.M.; *J. Am. Chem. Soc.* (1946), **68**, 1957.

33.   Hepler L.; *J Phys. Chem.* (1957), **61**, 1426.

34.   Battino R.; *J. Phys Chem.* (1966), **70**, 3408.

35.   Kimura T.; Takagi S.; *J. Chem. Thermodynamics* (1979), **11**, 119.

36.   Ashcroft S.J.; Booker D.R.; Turner J.C.R.; *J. Chem. Soc. Faraday Trans.* (1990), **86(1)**, 145.

37.   Leopold H.; Jelinek R.; Tilz G.P.; *Biomedizinische Ttechnik* (1977), **22**, 231.

38.   Leopold H.; *Electronik* (1970), **19**, 297.

39.   Kratky O.; Leopold H. Stabinger H.; *Z. Angew. Phys.* (1969), **27**, 273.

40.   Keyes D.B.; Hildbrand J.H.; *J. Am. Chem. Soc.* (1917), **39**, 2126.

41.   Prausnitz J.M.; *Molecular Thermodynamics of Fluid Phase Equilibria*, 1969, Prentice Hall, New Jersey, USA.

42.   Duncan W.A.; Sheridan J.P.; Swinton F.L.; *Trans Faraday Society* (1966), **62**, 1090.

43.   Stookey D.J.; Sallak H.M.; Smith B.D.; *J. Chem. Thermodynamics* (1973), **5**, 741.

44.   Geffcken W.; Kruis A.; Solana L.; *Z. Phys Chem. B* (1937), **35**, 317.

45.   Desmyter A.; van der Waals J.H.; *Rec. Trav. Chim. Pays-Bas.* (1958), **77**, 53.

46.   Pflug H.D.; Benson G.C.; *Can. J. Chem.* (1968), **46**, 287.

47.   Pasfield W.H.; *J. Phys Chem.* (1965), **69**, 2406.

48.   Beath L.A. O Neill S.P.; Williamson A.G.; *J. Chem. Thermodynamics* (1969), **1**, 293.

49.   Stokes R.H.; Levien B.J.; Marsh K.N.; *J. Chem. Thermodynamics* (1970), **2**, 43.

50.   Kumaran M.K.; McGlashan M.L.; *J. Chem. Thermodynamics* (1977), **9**, 259.

51.   Bottomley G.A.; Scott R.L.; *J. Chem. Thermodynamics* (1974), **6**, 973.

52.   Tanaka R.; Kiyohara O.; D'Arcy P.J.; Benson G.C.; *Can. J. Chem.* (1975), **53**, 2262.

53.   Perrin D.D.; Perrin D.R.; Armarego W.L.F.; *Purification of Laboratory Chemicals* (1980), Pergamon Press, Oxford.

54.   Riddick J.A.; Bunger W.B.; Sakano T.K.; *Organic Solvents: Physical Properties and Methods of Purification* (1986), Wiley Interscience, New York.

55.   Timmermans J.; *Physico-Chemical Constants of Pure Organic Compounds* (1950), Elsevier Publishing Company, Amsterdam.

56.   Furniss B.S.; Hannaford A.T.; Rogers V.; Smith P.W.G.; Tatchell A.R.; *Vogels*

Textbook of Practical Inorganic Chemistry (1981), Fourth Edition, Longmans, New York.

57.   Battino R.; *J. Phys Chem.* (1968), **72**, 4496.

58.   Treszczanowicz T.; Lu B.C.Y.; *Bull. Acad. Pol. Sci.* (1981), **29(5-6)**, 285.

59.   Villamanan M.A.; Van Ness H.C.; *Fluid Phase Equilibria* (1986), **27**, 181.

60.   Arm, H.; Bankay, D.; Schaller, R.; Waelti, M.; *Helv. Chim. Acta* (1966), **49**, 2598.

61.   Rowlinson, J.S.; *Liquids and Liquid Mixtures* (1969), Second Edition, Butterworths, London.

62.   Mecke, R.; *Dicuss. Faraday Society* (1950), **9**, 161.

63.   Swani, G.N.; Dharmaraju, G.; Raman G.K.; *Can. J. Chem.* (1980), **58**, 229

64.   Panayiotou, C.; *J. Chem. Soc. Faraday Trans.II* (1984), **80**, 1435

65.   Goates F.R.; Show R.L.; Bott J.; *J. Phys Chem.* (1962), **66**, 1301

66.   Marsh K.N.; Kohler F.; *J. Mol. Liquids* (1985), **30**, 13.

67.   Prigogine I.; DeFay R.; *Chemical Thermodynamics* (1965), Wiley Interscience, New York.

68.   Panayiotou C.G.; *J. Phys Chem.* (1988), **92**, 2960.

69.   Tanaka R.; Toyama S.; Murakami S.; *J. Chem. Thermodynamics* (1986), **18**, 63.

70.   Treszczanowicz A.; Benson G.C.; *J. Chem. Thermodynamics* (1977), **9**, 1189

71.   Van Ness H.C.; Soczek C.A.; Kocher N.K.; *J. Chem. Eng. Data* (1967), **12**, 346

72.   Brown I.; Fock W.; Smith F.; *J. Chem. Thermodynamics* (1969), **1**, 273

73.   Marsh K.N.; Burfitt C.; *J. Chem. Thermodynamics* (1975), **7**, 955

74.   Zielkiewicz J.; *J. Chem. Thermodynamics* (1993), **25**, 1243

75.   Kleeberg H.; Kocak O.; Luck W.A.P.; *J. Soln. Chem* (1982), **11**, 611.

76.   Zielkiewicz J.; *J. Chem. Thermodynamics* (1994), **26**, 959

77. Hepler L.G.; Kooner Z.S.; Roux Desgranges G.; Grolier J.P.E.; *J. Soln. Chem* (1985), **14**, 576.

78. Grolier J.P.E.; Roux Desgranges G.; Kooner Z.S; Hepler L.G.; *J. Soln. Chem* (1987), **16**, 745.

79. Rowlinson J.S.; Swinton F.L.; *Liquids and Liquid Mixtures* (1982), Third Edition, McGraw-Hill, New York.

80. Beath L.A.; Williamson A.G.; *J. Chem. Thermodynamics* (1969), **1**, 51.

81. Grolier J.P.E.; Roux Desgranges G.; Berkane M.; Wilhelm E., *J. Soln. Chem* (1994), **23(2)**, 153

82. Beath L.A.; O'Neill S.P.; Williamson A.G.; *J. Chem. Thermodynamics* (1969), **1**, 293

83. Treszczanowicz T.; *Thermochimica Acta* (1990), **160**, 253

84. Pintos M.; Amigo A.; Bravo R.; *J. Chem. Thermodynamics* (1993), **25**, 337

85. Pintos M.; Amigo A.; Bravo R.; Calvo E,; *J. Chem. Thermodynamics* (1994), **26**, 803

86. Andrews A.W.; Morcom K.W.; *J. Chem. Thermodynamics* (1971), **3**, 513

87. Deshpande D.; Oswal S.L.; *J. Chem. Thermodynamics* (1975), **7**, 155

88. Meyer R.; Giusti G.; Meyer M.; Vincent E.J.; *Thermochimica Acta* (1975), **13**, 379

89. Amigo A.; Bravo R.; Pintos M.; *J. Chem. Eng. Data* (1993), **38**, 141

90. Guillen M.P.; Olosa C.G.; *J. Chem. Thermodynamics* (1978), **10**, 567

91. Solimo H.N.; Marigliano A.C.G.; *J. Soln. Chem* (1993), **22(10)**, 951

92. Blanco S.F.; Embid J.M.; Otin S.; *J. Chem. Thermodynamics* (1994), **26**, 23

93. Nakashini K.; Nakasato K.; Toba R.; Shirai H.; *J. Chem. Eng. Data* (1967), **12**, 440

94. Farkova I.; Linek J.; Wichterle I.; *Fluid Phase Equilibria* (1995), **109**, 53

95. *CRC Handbook of Chemistry and Physics*, Ed. R. C. Weast, 49th edition(1969), Chemical Rubber Publishing Company, Cleveland, Ohio, USA

96. Amigo A.; *PhD Thesis* (1991), Universidad de Santiago, Spain.

97. Nakashini K.; Shirai H.; *Bull. Chem. Soc. Japan* (1970), *43*, 1634

98. Singh P.P.; Verna D.V.; Arora P.S.; *Thermochimica Acta* (1976), **15**, 267

99. Ling T.D.; Van Winkle M.; *J. Chem. Eng. Data* (1958), **3**, 88

100. Wolff V. H.; Landeck H.; *Ber. Bunsenges. Physik. Chem.* (1977), **81(10)**, 1054

101. Wolff V.H.; Hopfner A.; Hopfner H.M.; *Ber. Bunsenges. Physik. Chem.* (1964), **68(4)**, 410

102. Wolff V.H.; Schmidt U.; *Ber. Bunsenges. Physik. Chem.* (1964), **68(6)**, 579

103. Nagata I.; Rogalski M.; Miyamoto K.; *Thermochimica Acta* (1993), **224**, 43

104. Nagata I.; Tamura K.; *Thermochimica Acta* (1986), **101**, 305

105. Cibulka I.; Tamura K.; Nagata I.; *Fluid Phase Equilibria* (1988), **39**, 39.

106. Cibulka I.; Nagata I.; *Fluid Phase Equilibria* (1987), **35**, 19

107. Kehiaian H.V.; Pintos M.; Bravo R.; Paz Andrade M.I.; *J. Chim. Phys.* (1980), **77(9)**, 797

108. Letcher T.M.; *J. Chem. Thermodynamics* (1972), **4**, 159

109. Handa Y.; Benson G.C.; *Fluid Phase Equilibria* (1979), **3**, 185

110. Panayiotou G.C.; *J. Soln. Chem* (1991), **20(1)**, 97

111. Letcher T.M.; Domanska U.; Govender P.; *J. Chem. Thermodynamics* (1994), **26**, 1019

112. Letcher T.M.; Domanska U.; *J. Chem. Thermodynamics* (1994), **26**, 1241

113. Inglese A.; Marongiu B.; *Thermochimica Acta* (1987), **122**, 19

114. Meyer E.F.; Aielinski W.M.; *J. Chem. Thermodynamics* (1982), **14**, 403

115. Meyer E.F.; Gens T.H.; *J. Chem. Thermodynamics* (1979), **11**, 719

116. Wilhelm E.; Inglese A.; Grolier J.P.E.; Kehiaian H.V.; *Monatschefte fur Chemie*

(1978), **109**, 435

117. Wilhelm E.; Inglese A.; Grolier J.P.E.; Kehiaian H.V.; *Monatschefte fur Chemie* (1978), **109**, 235

118. Pimentel G.C.; McClellan A.L.; *The Hydrogen Bond* (1960), W. H. Freeman. San Francisco, USA.

119. Harris H.G.; Prausnitz J.M.; *Ind. Eng. Chem. Fundament.* (1969), **8**, 180

120. Anderson R.; Cambio R.; Prausnitz J.M.; *AIChE* (1962), **8**, 66

121. Hirth L.J.; Harris H.G.; Prausnitz J.M.; *AIChE* (1968), **14**, 812

122. Desplanches H.; Chevalier J.L; Llinas R.; *J. Chim. Phys* (1977), **74**, 219

123. Woycicki W.; Rhensius P.; *J. Chem. Thermodynamics* (1979), **11**, 153

124. Otsa E,; Kudrjawzewa L.S.; Eisen O.G.; *Monatschefte fur Chemie.* (1980), **111**, 37

125. Letcher T.M.; Scoones B.W.H.; *J. Chem. Thermodynamics* (1982), **14**, 189

126. Letcher T.M.; Baxter R.; *J. Chem. Thermodynamics* (1987), **19**, 321

127. Letcher T.M.; Prasad A.K.; *J. Chem. Thermodynamics* (1991), **23**, 643

128. Letcher T.M.; Schoobaert F.E.Z.; Mercer-Chalmers J.D.; *J. Chem. Thermodynamics* (1990), **22**, 815

129. Letcher T.M.; Schoobaert F.E.Z.; Bean B.; *Fluid Phase Equilibria* (1990), **61**, 111

130. Letcher T.M.; Mercer-Chalmers J.D.; Govender P.U.; Radloff S.E.; *Fluid Phase Equilibria* (1993), **91**, 313

131. Pinnick H.R.; Falling C.R.; Allred G.C.; Parrish W.R.; *J. Chem. Eng. Data* (1995), **40**, 950

132. Kumaran J.; Wang L.; Benson G.C.; Lu B.C.Y.; *Thermochimica Acta* (1993), **223**, 35

133. Jangkamo I., Kulchai A., Allred G.C.; Parrish W.R.; *J. Chem. Eng. Data* (1991),

36, 481

134.   Obama M.; Odera Y.; Kohama N.; Yanese T.; Salto Y.; Kusano K.; *J. Chem. Eng. Data* (1985), **30**, 1

135.   Fortier J.C.; Benson G.C.; *J. Chem. Eng. Data* (1979), **24**, 34

136.   Ross P.D.; *Biochimica et Biophysica Acta* (1973), **313**, 106

137.   Marsh K.N.; *Chemical Thermodynamics* (Specialist Periodical Reports), Editor: M.L. McGlashan, Vol II. Chapter 1, (1978), The Chemical Society, London.

138.   Williamson A.G., *An Introduction to Non-Electrolyte Solutions* (1967), Oliver and Boyd, London.

139.   Letcher T.M.; Bayles J.W.; *J. Chem. Eng. Data* (1971), **16**, 266

140.   Letcher T.M.; Bayles J.W.; *J. South African Chem. Inst.* (1972), **25**, 53

141.   McGlashan M.L.; *Experimental Thermochemistry* (1967), Volume 2, Chapter 15, Editor: H.R. Skinner, Interscience, London.

142.   Becker F.; *Thermochimica Acta* (1980), **40**, 1

143.   Skinner H.R.; Sturtevant J.M.; , Sunner S.; *Experimental Thermochemistry* (1967), Volume 2, Chapter 9, Interscience, London.

144.   Armitage D.A.; Morcom K.W.; *Trans. Faraday Society* (1969), **65**, 688.

145.   Raal J.D.; Naidoo P.; *Fluid Phase Equilibria* (1990), **57**, 147

136.   Christensen J.J; Gardner J.W.; Izatt R.M.; *Rev. Sci. Instum.* (1973), **44**, 481

147.   Christensen J.J; Hansen L.D.; Izatt R.M.; Eatough D.J.; Hart R.M.; *Rev. Sci. Instum.* (1981), **52(8)**, 1226

148.   Wittig I.; Schmatz S.; *Z. Electrochem* (1959), **63**, 470

149.   Mrazek R.V.; Van Ness H.C.; *AIChE* (1961), **6(3)**, 190

150.   Christensen J.J; Johnston H.D.; Izatt R.M.; *Rev. Sci. Instum.* (1968), **39**, 1356

151. Winterhalter D.R.; Van Ness H.C.; *J. Chem. Eng. Data* (1966), **11**, 189

152. Scatchard G.; Ticknor L.B. Goates J.R.; McCartney E.R.; *J. Am. Chem. Soc.* (1952), **74**, 3721

153. Thacker R.; Rowlinson J.S.; *Trans, Faraday Society* (1956), **50**, 1036

154. Van der Waals J.H.; Hermans J.J.; *Rec. Trav. Chim. Pays-Bas* (1950), **69**, 949

155. Larkin J.A.; McGlashan M.L.; *J Chem. Soc.(A)*, (1961), 3425

156. Wadso I.; *Pure and Appl. Chem.* (1980), **52**, 465

157. Rose V.C.; Storvick T.S.; *J. Chem. Eng. Data* (1966), **11(2)**, 143

158. Picker P.; Jolicoeur C.; Desnoyers J.E.; *J. Chem. Thermodynamics* (1969), **1**, 469

159. Monk P.; Wadso I.; *Acta Chem. Scanda.* (1968), **22**, 1842

160. McGlashan M.L.; Stoeckli H.F.; *J. Chem. Thermodynamics* (1969), **1**, 589

161. Hsu K.; Clever H.L.; *J. Chem. Thermodynamics* (1975), **7**, 435

162. IUPAC Commission on Thermodynamics and Thermochemistry, *Bull. Thermod. Thermochem.* (1970), **13**, 507

163. Randzio S.; Tomaszkiewicz I.; *J. Phys Eng. Sci Instrum.* (1980), **13**, 1292

164. Siddiqi M.A.; Lucas K.; *J. Chem. Thermodynamics* (1982), **14**, 1183

165. Raal J.D.; Webley P.A.; *AIChE* (1987), **33(4)**, 604

166. Marsh K.N.; Stokes R.H.; *J. Chem. Thermodynamics* (1969), **1**, 223

167. Grolier J.P.E.; Benson G.C.; Picker P.; *J. Chem. Thermodynamics* (1975), **7**, 89

168. Christensen J.J.; Izatt R.M.; *Thermochimica Acta* (1984), **73**, 117

169. Picker P.; *Can. Res. Dev.* (1974), 11

170. Naumann E.B.; Buffham B.A.; *Mixing in Continuous-Flow Systems* (1983), Wiley Interscience, New York.

171. Villamanan M.A.; (1979), *PhD Thesis*, University of Valladolid, Spain.

172. Villamanan M.A.; Roux Desgranges R.H.; Grolier J.P.E.; *Int. Data Series, Ser A, No. 2*(1984), 118

173. Kehiaian K.S.; Hryniewicz H.; Kehiaian H.V.; *Bull. Acad. Pol. Sci. Ser Sci. Chem.* (1969), **17**, 185.

174. Kehiaian H.V.; Kehiaian K.S.; Hryniewicz H.; *J. Chim. Phys. Physicochim. Biol.* (1971), **68**, 922

175. Tresczanowicz T.; *Bull. Acad. Pol. Sci. Ser Sci. Chem.* (1975), **23**, 2

176. Kehiaian H.V.; Tine M.R.; *Fluid Phase Equilibria* (1990), **59**, 223

177. Kehiaian H.V.; Tine M.R.; *Fluid Phase Equilibria* (1987), **32**, 211

178. Tresczanowicz T.; Benson G.C.; Lu B.C.Y.; *J. Chem. Eng. Data* (1988), **33**, 379

179. Kehiaian H.V.; Tine M.R.; Lepori L.; Matteoli E.; Marongiu B.; *Fluid Phase Equilibria* (1989), **46**, 131

180. Zhu S.; Shen S.; Benson G.C. Lu B.C.Y.; *J. Chem. Thermodynamics* (1994), **26**, 35

181. Stevanovic A.K.; Jin Z.L.; Benson G.C.; Lu B.C.Y.; *J. Chem. Thermodynamics* (1995), **27**, 423

182. Zhu S.; Shen S.; Benson G.C. Lu B.C.Y.; *J. Chem. Eng. Data* (1994), **39**, 302

183. Zhu S.; Shen S.; Benson G.C. Lu B.C.Y.; *Fluid Phase Equilibria* (1994), **94**, 217

184. Zhu S.; Shen S.; Benson G.C. Lu B.C.Y.; *Can. J. Chem.* (1994), **72**, 1111

185. Wang L.; Benson G.C.; Lu B.C.Y.; *J. Chem. Thermodynamics* (1992), **24**, 1305

186. Wang L.; Benson G.C.; Lu B.C.Y.; *J. Chem. Eng. Data* (1992), **37**, 403

187. Nagata I,; *J. Chem. Thermodynamics* (1994), **26**, 779

188. Tusel Langer E.; Garcia Alonso J.M.; Villamanan M.A.; Lichtenthaler R.N.; *J. Soln. Chem.* (1991), **20**, 153

189. Oba M.; Murakami S.; Fiushiro R.; *J. Chem. Thermodynamics* (1977), **9**, 407

190. Blanks R.F.; Prausnitz J.M.; *J. Phys. Chem.* (1963), **67**, 1154

191. Christiansen J,J, Hanks R.W.; Izatt R.M.; *Handbook of Heats of Mixing: Supplementary Volume* (1988), Wiley Interscience, New York.

192. Brown N.G.; Ziegler W.T.; *J. Chem. Eng. Data* (1979), **24**, 319

193. Villamanan M.A.; Casanova C.; Roux A.H.; Grolier J.P.E.; *J. Chem. Thermodynamics* (1982), **14**, 251

194. Diogo H.P.; Minas da Piedade, Moura Ramos J.A. Simono J.A.; Martinho Simoes J.A.; *J. Chem. Ed.* (1993), **70**, A227.

195. Diaz Pena M.; Fernandez-Martin F.; *An. R. Soc. Esp. Fis. Quim. Ser. B.* (1964), **60**, 9

196. Christiansen J,J, Hanks R.W.; Izatt R.M.; *Handbook of Heats of Mixing* (1982), Wiley Interscience, New York.

197. Grolier J.P.E.; Inglese A.; Wilhelm E.; *J. Chem. Thermodynamics* (1984), **16**, 67

198. Inglese A.; Wilhelm E.; Grolier J.P.E.; Kehiaian H.V.; *J. Chem. Thermodynamics* (1980), **12**, 1047

199. Wilhelm E.; Inglese A.; Grolier J.P.E; Kehiaian H.V.; *J. Chem. Thermodynamics* (1982), **14**, 517

200. Sharma S.C.; Tormar M.; Singh J.; *J. Soln. Chem.* (1993), **22(4)**, 391

201. Chao J.P.; Dai M.; *J. Chem. Thermodynamics* (1989), **21**, 977

202. Matous J.; Zivny A.; Biros J.; *Coll. Czech Comm.* (1972), **37**, 3960

203. Arm H. Banjay D.; Schaller R.; Waelti M.; *Helv. Chim. Acta* (1966), **49**, 2598

204. Keller M.; Heintz A.; Lichtenthaler R.N.; *J. Chem. Thermodynamics* (1992), **24**, 1197

205. Dai M.; Chao J.P.; *Fluid Phase Equilibria* (1985), **23**, 321

206. Singh P.P.; Verna D.V.; Arora P.S.; *Thermochimica Acta* (1976), **15**, 267

207. Kortum G.; Valent V.; *Ber. Bunsenges. Phys. Chem.* (1977), **81**, 752

208. Belousov V.P.; Makarova W.L.; *Vestnik Lenin-Grad Univ, Ser. Fiz. Khim.* (1970), **4**, 101

209. Inglese A.; Wilhelm E.; Grolier J.P.E.; Kehiaian H.V.; *J. Chem. Thermodynamics* (1980), **12**, 217

210. Nagata I.; Kazuma K.; *J. Chem. Eng. Data* (1977), **22**, 79

211. Battler J.R.; Clark W.M.; Rowley R.L.; *J. Chem. Eng. Data* (1985), **30**, 254

212. Dai M.; Chao J.P.; *Fluid Phase Equilibria* (1985), **23**, 315

213. Kehiaian K.S.; Orzel K.; Kehiaian H.V.; *Bull. Acad. Pol. Sci. Ser Sci. Chem.* (1966), **14**, 711

214. Velasco I.; Otin S.; Losa C.G.; *J. Chim. Phys. Physicochim. Biol.* (1978), **75**, 706

215. Sarmiento F.; Bravo R.; Paz Andrade M.I.; Kechavarz R.; Dubes J.P.; Tachoire H.; *Thermochimica Acta* (1983), **68**, 273

216. Paz Andrade M.I.; Sarmiento F.; *Int. Data Series of Mixtures* (1984), 110

217. Nunez L.; Barral L.; Gomez Orellana I.; Ramil Rio P.E.; Paz Andrade M.I.; *J. Chem. Thermodynamics* (1989), **21**, 739

218. Fernandaz I.; Paz Andrade M.I.; Pintos M.; Sarmiento F.; Bravo R.; *J. Chem. Thermodynamics* (1983), **15**, 581

219. Wang L.; Benson G.C.; Lu B.,C.Y.; *J. Chem. Thermodynamics* (1989), **21**, 147

220. Berti P.; Lepori L.; Matteoli E.; *Fluid Phase Equilibria* (1989), **44**, 285

221. Letcher T.M.; Domanska U.; Govender P.; *J. Chem. Thermodynamics* (1994), **26**, 681

222. Ghassemi M.H.; Grolier J.P.E.; Kehiaian H.V.; *J. Chim. Phys. Physicochim. Biol.* (1976), **73**, 923

223.   Kehiaian H.V.; *Thermochemistry and Thermodynamics* (International Review of Science), 1972, Editor : H.A. Skinner, Butterworths, London

224.   Renon H.; Prausnitz J.M.; *Ind. Eng. Chem. Res.* (1969), **8**, 413

225.   Domanska U.; Domański K.; Klofutar C.; Paljk S.; *Thermochimica Acta* (1990), **164**, 227

226.   Marquardt D.; *J. Soc. Appl. Math.* (1963), **11**, 431

227.   Nath A.; Bender E.; *Fluid Phase Equilibria* (1981), **7**, 275

228.   Nath A.; Bender E.; *Fluid Phase Equilibria* (1981), **7**, 289

229.   Nath A.; Bender E.; *Fluid Phase Equilibria* (1983), **10**, 43

230.   Funke H.; Wetzel M.; Heintz A.; *Pure and App. Chem.* (1989), **61**, 1429

231.   Letcher T.M.; Mercer Chalmers J.D.; Schnabel S.; Heintz A.; *Fluid Phase Equilibria* (1995), **112**, 131

232.   Letcher T.M.; Bricknell B.; *J. Chem. Eng. Data* (1995), submitted for publication.

233.   Aicart E.; Van Tra H.; Andreoli-Ball L.; Patterson D.; *J. Soln. Chem.* (1994), **23(11)**, 1183

234.   Diaz Pena M.; Tardajos G.; *J. Chem. Thermodynamics* (1979), **11**, 441

235.   Goldberg R.N.; Weir R.N.; *Pure and App. Chem.* (1992), **64**, 1545

236.   Sharma K.N.; Jain K.K.; Bandyopadhyay A.K.; Jager J.; *J. Phys. E: Sci. Instrum.* (1988), **21**, 635

237.   *NBS Standard Reference Materials Catalogue*: NBS Special Publication 260 (1988-1989); Editor: Sewrard R.W.;Department of Commerce, Washington DC.

238.   Banipal T.S.; Garg S.K.; Ahluwalia J.C.; *J. Chem. Thermodynamics* (1991), **23**, 923

239.   Garg S.K.; Ahluwalia J.C.; *J. Soln. Chem.* (1995), **24**, 153

240.   Diaz Pena M.; Tardajos G.; *J. Chem. Thermodynamics* (1978), **10**, 19

241. Baonza G.V.; Alonso M.C.; Delgado J.N.; *J. Chem Soc. Faraday Trans.* (1994), **90(4)**, 553

242. Minassian L.T.; Bouzer K.; Alsa C.; *J. Phys Chem.* (1988), **92**, 487

243. Garg S.K.; Banipal T.S.; Ahluwalia J.C.; *J. Chem. Thermodynamics* (1993), **25**, 57

244. Obama M.; Odera y.; Kohama N.; Yanase T.; Salto Y.; Kusano K.; *J. Chem. Eng. Data* (1985), **30**, 1

245. Spanneda A.; Lepori L. Mattteoli E.; *Fluid Phase Equilibria* (1991), 69, 209

246. *TRC Thermodynamic Tables - Non-Hydrocarbons* (1988); Thermodynamics Research Centre, Texas A&M University System; College Station, TX, a5030

247. Kehiaian H.V.; *Pure and App. Chem.* (1985), **57(1)**, 15

248. Gmehling J.; Fischer K.; Schiller M.; Li J.; *Pure and App. Chem.* (1993), **65(5)**, 919

249. Kehiaian H.V.; *Fluid Phase Equilibria* (1983), **13**, 243

250. Gmehling J.; *Fluid Phase Equilibria* (1995), **107**, 1

251. Vera J.H.; Sayegh S.G.; Ratcliff G.A.; *Fluid Phase Equilibria* (1977), **1**, 113

252. Rasmussen H.K.H.P.; Freudenslund A.; Schiller M.; Gmehling J.; *Ind. Eng. Chem. Res.* (1991), **30(10)**, 2352

253. Prausnitz J.M.; Lichtenthaler R.N.; Gomes de Azevedo E.; *Molecular Thermodynamics of Fluid Phase Equilibria* (1986), Prentice Hall, New Jersey, USA.

254. Van Laar J.J.; *Z. Phys. Chem.* (1910), 72, 723

255. Scatchard D.; *Chem. Rev.* (1949), **44**, 7

256. Hildebrand J.H.; Scott R.L.; *The Solubility of Non-Electrolytes* (1950), Third Edition, Reinhold Publishing Corporation, New York.

257. Hildebrand J.H.; Scott R.L.; *Regular Solutions* (1962), Prentice Hall, New Jersey, USA.

258. Flory P.J.; *J. Phys. Chem.* (1942), **10**, 51

259. Hildebrand J.H.; Prausnitz J.M.; Scott R.L.; *Regular and Related Solutions* (1970), Van Nostrand Reinhold, New York.

260. Coursey B.M.; Heric E.L.; *Can. J. Chem.* (1971), **49**, 2631

261. Huggins M.; *Ann. N.Y. Acad. Sci.* (1942), **43**, 9

262. Prigogine I.; (with collaboration of A. Bellemans and V. Mathot) *The Molecular Theory of Solutions* (1957), North Holland, Amsterdam.

263. Guggenheim E.A.; *Mixtures* (1952), Oxford, Oxford University Press, London.

264. Guggenheim E.A.; *Trans. Faraday Society* (1937), **33**, 151

265. Guggenheim E.A.; *Application of Statistical Mechanics* (1966), Oxford, Oxford University Press, London.

266. Barker J.A.; *Lattice Theories of the Liquid State* (1963), MacMillan Publishing Company, New York.

267. Wilson G.M.; *J. Amer. Chem. Soc.* (1964), **86**, 127

268. Langmuir I.; *The Distribution and Orientation of Molecules* (1925), Third Colloid Symposium Monograph, The Chemical Catalogue Co. Inc., New York.

269. Redlich O.; Derr E.L.; Pierotti G.; *J. Amer. Chem. Soc.* (1959), **81**, 2283

270. Derr E.L.; Papadopoulus M.; *J. Amer. Chem. Soc.* (1959), **81**, 2285

271. Derr E.L.; Deal C.H.; *I. Chem. E. Symp. Ser. No. 32* (1969), **3**, 40

272. Derr E.L.; Deal C.H.; *Advan. Chem. Ser.* (1973), **124**, 11

273. Wilson G.M.; Deal C.H.; *Ind. Eng. Fundamentals* (1962), **1**, 20

274. Ronc M.; Ratcliff G.A.; *Can J. Chem. Eng.* (1971), **49**, 875

275. Soave G.; *Chem. Eng. Sci.* (1972), **27**, 1197

276. Peng D.Y.; Robinson D.B.; *Ind. Eng. Chem. Fundam.* (1976), **15**, 59

277. Kehiaian H.V.; Grolier J.P.E; Keechavarz M.R.; Benson G.C.; *Fluid Phase Equilibria* (1981), 5, 159

278. Guieu R.; *PhD Thesis* (1982), University of Marseille, France.

279. Flory P.J.; Orwoll R.A.; Vrij A.; *J. Amer. Chem. Soc.* (1964), **86**, 3507

280. Abe A.; Flory P.J.; *J. Amer. Chem. Soc.* (1965), **87**, 1838

281. Oswal S.L.; Indian J. Chem. (1979), 18(A), 353

282. Renon H.; Prausnitz J.M.; *Chem. Eng. Sci.* (1967), **22**, 299; errata, **22**, 1891 (1967)

283. Kehiaian H.V.; Treszczanowicz A.; *Bull. Acad. Polon. Sci. Chim.* (1968), **16**, 445

284. Scott R.L.; *J. Chem. Phys.* (1956), **25**, 193

285. Kehiaian H.V.; Grolier J.P.E; Benson G.C.; *J. Chim. Phys.* (1978), **75**, 1031

286. DECHEMA Chemistry Data Series, *VLE Data Collection* (1979), Part 6A and 6B, Germany.

287. Anderson F.; Prausnitz J.M.; *Ind. Eng. Process. Des. Dev.* (1980), **19**, 1

288. Anderson F.; Prausnitz J.M.; *Ind. Eng. Process. Des. Dev.* (1978), **17**, 552

289. Kretschmer C.B.; Wiebe R.; *J. Amer. Chem. Soc.* (1949), **71**, 3176

290. Kretschmer C.B.; Wiebe R.; *J. Chem. Phys.* (1954), **22**, 425

291. Kehiaian H.V.; Treszczanowicz A.; *Bull. Soc. Chem. France* (1969), **15**, 1561

292. Mecke R.; *Z. Elektrochem.* (1948), **52**, 269

293. Bagley E.B.; Nelson T.P.; Scigliano J.A.; *J. Phys. Chem.* (1973), **77**,. 2794

294. Treszczanowicz A.; *Bull. Acad. Polon. Sci. Chim.* (1973), **21**, 189

295. Kehiaian H.V.K.; Treszczanowicz A.; *Bull. Acad. Polon. Sci. Chim.* (1966), **14**, 891

296. Bondi A.; *J. Phys Chem.* (1964), **68**, 441

297. Nagata I.; *Fluid Phase Equilibria* (1977), **1**, 93

298. Lien T.R.; *PhD Thesis* (1972), University of Toronto, Ontario, Canada.

299. Nagata I.; *J. Chem. Eng. Japan* (1973), **6**, 18

300. Nagata I.; *Z. Physik. Chem. (Liepzig)* (1973), **254**, 273

301. Nitta T.; Katayama T.; *J. Chem. Eng. Japan* (1973), **6**, 1

302. Nguyen T.H.; Ratcliff G.A.; *Can. J. Chem. Eng.* (1971), **49**, 120

303. Nguyen T.H.; Ratcliff G.A.; *Can. J. Chem. Eng.* (1974), **52**, 641

304. Nagata I.; Ohta N.; *Chem. Eng. Sci.* (1978), **33**, 177

305. Freudenslund A.; Gmehling J.; Rasmussen P.; *Vapor Liquid Equilibria using UNIFAC* (1977), Elsevier, Amsterdam.

306. Gmehling J.; Rasmussen P.; *Ind. Eng. Chem. Fundam.* (1982), **21**, 186

307. Magnussen T.; Rasmussen P.; Fredenslund A.; *Ind. Eng. Process. Des. Dev.* (1981), **20**, 331

308. Kikic I.; Alessi P.; Rasmussen P.; Fredenslund A.; *Can. J. Chem. Eng.* (1980), **58**, 253

309. Kikic I.; Alessi P.; Fredenslund A.; Rasmussen P.; *Can. J. Chem. Eng.* (1982), **60**, 300

310. Thomas E.R.; Eckert C.A.; *Ind. Eng. Process. Des. Dev.* (1984), **23**, 194

311. Gmehling J.; Li Jiding, Schiller M.; *Ind. Eng. Chem. Res.* (1993), **32(1)**, 178

312. Abe A.; Flory P.J.; *J. Amer. Chem. Soc.* (1966), **88**, 2887

313. Eyring H.; Hirschfelder J.; *J. Phys. Chem.* (1937), **41**, 249

314. Hirschfelder J.; Stevenson D.P.; Eyring H.; *J. Chem. Phys.* (1937), **5**, 896

315. Prigogine I.; Trappeniers N.; Mathot V.; *Discuss. Faraday Soc.* (1953), **15**, 93

316. Prigogine I.; *J. Chem. Phys.* (1953), **21**, 559

317. Prigogine I.; Mathot V.; *J. Chem. Phys.* (1952), **20**, 49

318. Letcher T.M.: Perkins D.M.; *Thermochimica Acta* (1984), **77**, 263

319. Letcher T.M.; Baxter R.; *J. Chem. Thermodynamics* (1987), **19**, 321

320. Benson G.C.; Murukami S.; Lam V.T.; Singh J.; *Can. J. Chem.* (1970), **48**, 211

321. Rajagopal E.; Subramaryam S.V.; *J. Chem. Thermodynamics* (1974), **6**, 873

322. Howell P.J.; Skillerne de Bristowe B.J.; Stubley D.; *J. Chem. Soc. (A) Inorg. Phys. Theory,* (1971), 397

323. Benson G.C.; Pflug H.D.; *J. Chem. Eng. Data* (1970), **15**, 382

324. Lam V.T.; Pflug H.D.; Murakami S.; Benson G.C.; *J. Chem. Eng. Data* (1973), **18**, 63

325. Patterson D.; Delmas G.; *Disc. Faraday Soc.* (1970), **49**, 98

326. Letcher T.M.; Baxter R.; *J. Soln. Chem.* (1989), **18**, 65

327. Nagata I.; Katoh K.; *Fluid Phase Equilibria* (1981), **5**, 225

328. Schmelzer J.; Liebermirth I.; *Fluid Phase Equilibria* (1982), **9**, 67

329. Letcher T.M.; Goldon A.; *Fluid Phase Equilibria* (1996), accepted for publication.

330. Prigogine I.; Defay R.; *Chemical Thermodynamics* (1954), London, Longmans, Green and Company.

331. Jones D.E.G.; Weeks I.A.; Benson G.C.; *Can. J. Chem.* (1971), **49**, 2481

332. Subramaryam S.V.; Rajgopal E.; *Z. Phys. Chem.* (1973), **85**, 256

333. Diaz Pena M. Menduiana C.; Nunez J.; *An Chim* (1979), **72**, 8

334. Dhillon M.S.; *Indian J. Chem. Soc.* (1975), **52**, 905

335. Schaefer C.R.; Davalio F.; Katz M.; *J. Soln. Chem.* (1990), **19(3)**, 289

336. Schiller M.; *PhD Thesis* (1992), University of Dortmund, Federal Republic of Germany

337. Gmehling J.; Tiegs D.; Knipp U.; *Fluid Phase Equilibria* (1990), **54**, 147

338. Treszczanowicz A.; Benson G.C.; *Fluid Phase Equilibria* (1985), **23**, 117

339. Hals T.C.; Ellender T.N.; *J. Chem. Thermodynamics* (1976), **8**, 1177

340. Aicart E.; (1991), personal communication

341. Sahli B.; Gager H.; Richard A.J.; *J. Chem. Thermodynamics* (1976), **8**, 179

342. Redlich O.; Kister P.; *Ind. Eng. Chem.* (1948), **40**, 345

343. Baxter R.; *PhD Thesis* (1989), Rhodes University, Grahamstown. South Africa.

344. Garg S.K.; *PhD Thesis* (1994), Indian Institute of Technology, New Delhi, India.

345. Banipal T.S.; Garg S.K.; Ahluwalia J.C.; *J. Chem. Thermodynamics* (1991), **23**, 923

346. Heintz A.; Dolce E.; Lichtenthaler R.N.; *Fluid Phase Equilibria* (1986), **27**, 61

347. Cabanas A.; Coto B.; Renuncio J.A.R.; *Ber. Bunsenges. Phys. Chem.* (1994), **98(6)**, 777

348. Mier W.; Oswald G.; Tusel Langer E.; Lichtenthaler R.N.; *Ber. Bunsenges. Phys. Chem.* (1995), **99(9)**, 1123

349. Peters C.J.; Florusse L.J.; de Roo J.L.; de Swaan Arons J.; Levelt Sengers J.M.H.; *Fluid Phase Equilibria* (1995), **105**, 193

350. Koh S.P.; Williamson A.G.; *Chem. Eng. J.* (1980), **19**, 85

351. Looi C.K.; Mayhew C.J.; Williamson A.G.; *J. Chem. Thermodynamics* (1974), **6**, 117

352. Hutchings R.S.; Alexander van Hook W.; *J. Chem. Thermodynamics* (1985), **17**, 523

353. Dantzler E.M.; Knobler C.M.; *J. Phys. Chem.* (1969), **73**, 1335

354. Pandya M.W.; Williamson A.G.; *Aust. J. Chem.* (1971), **24**, 465

355. Koefoed J.; *Discuss. Faraday Soc.* (1953), **15**, 207

356. McGlashan M.L.; *Mol. Phys.* (1961), **4**, 87

357. Hijmans J.; Holleman Th.; *Mol. Phys.* (1961), **4**, 91

358. Diaz Pena M.; Trigueros R.; *An. R. Soc. Esp. Fis. Quim. Ser. B.* (1971), **67**, 467

359. Pope A.E.; Pflug H.D.; Dacre B.C.; Benson G.C.; *Can. J. Chem.* (1967), **45**, 2665

360. Gomez-Ibanez J.D.; Liu C.T.; *J. Phys. Chem.* (1963), **67**, 1388

361. Larkin J.A.; Fenby D.V.; Gilman T.S.; Scott R.L.; *J. Phys. Chem.* (1966), **70**, 1959

362. McGlashan M.L.; Morcom K.W.; *Trans. Faraday Soc.* (1961), **57**, 581

363. Lim C.B.; Williamson A.G.; *J. Chem. Thermodynamics* (1980), **12**, 65

364. Letcher T.M.; Mercer-Chalmers J.; Battino R.; *J. Chem. Thermodynamics* (1992), **24**, 65

365. Letcher T.M.; Mercer-Chalmers J.; Govender U. P.; Battino R.; *Thermochimica Acta* (1993), **224**, 39

Appendices

Appendix 1

Error Analysis

Using the notation in the GWBASIC computer programme:

$$V^E = \{X_A.M_A + (1-X_A)M_B\}/D_U - (X_A.M_A)/D_A - \{(1-X_A)M_B\}/D_B$$

where V^E is the excess molar volume, X_A is the mole fraction of A, X_B is the mole fraction of B M_A is the molar mass of A, M_B is the molar mass of B, D_U is the density of the mixture, D_A is the density of A, and D_B is the density of B.

$$X_A = \{(B_A-B_o)/M_A\}/\{(B_A-B_o)/M_A + (B_B-B_A)/M_B\}$$

where B_o is the mass of the weighing bottle, B_A is the mass of B_o + A, and B_B is the mass of B_A + B.

$$D_U = C(\tau_u^2 - \tau_w^2) + D_W$$

where C is the densimeter constant (0.542394), τ_u is the periodicity value obtained from the densitometer for the mixture, τ_w is the periodicity value for distilled and deionised water, and D_W is the density of the water.

$$D_A = C(\tau_A^2 - \tau_w^2) + D_W$$

where τ_A is the periodicity value obtained for A.

$$D_B = C(\tau_B^2 - \tau_w^2) + D_W$$

where τ_B is the periodicity value for B.

$$V_\phi = \{1000(d - d_o)\}/(C_1 d_o) + M_1/d_o$$

where V_ϕ is the apparent molar volume, d is the density of the solution, d_o is the density of the pure solvent, C_1 is the concentration of the solution, and M_1 is the molar mass of the solute.

Calculation of errors

Here Δ represents the error in the quantity, and an example of a typical (average value) calculation is given.

$$(\Delta X_A)^2 = (\partial X_A/\partial B_o)^2(\Delta B_o)^2 + (\partial X_A/\partial B_A)^2(\Delta B_A)^2 + (\partial X_A/\partial B_B)^2(\Delta B_B)^2$$

$$(\partial X_A/\partial B_o) = -[M_A.M_B(B_B-B_A)]/[M_B(B_A-B_o) + M_A(B_B-B_A)]^2$$
$$= - [100.40(1.0)]/[40(1.0) + 100(1.0) + 100(1.0)]^2$$
$$= -0.20408$$

$$(\partial X_A/\partial B_A) = [M_A.M_B(B_B-B_o)]/[M_B(B_A-B_o) + M_A(B_B-B_A)]^2$$
$$= [100.40(1.0)]/[40(1.0) + 100(1.0)]^2$$
$$= 0.20408$$

$$(\partial X_A/\partial B_B) = -[M_A.M_B(B_A-B_o)]/[M_B(B_A-B_o) + M_A(B_B-B_A)]^2$$
$$= -[100.40(0.1)]/[40(1.0) + 100(1.0)]^2$$
$$= -0.20408$$

Thus, $\Delta X_A = 0.000004$ moles

$$(\Delta D_U)^2 = (\partial D_U/\partial \tau_u)^2 (\Delta \tau_u)^2 + (\partial D_u/\partial \tau_w)^2 (\Delta \tau_w)^2$$

$$(\partial D_U/\partial \tau_u) = 2\tau_u = 2(1.780000) = 3.56000$$

$$(\partial D_U/\Pi \tau_w) = 2\tau_w = 2(1.739781) = 3.47956$$

$$(\Delta D_U)^2 = (3.56000)^2 (0.00002)^2 + (3.47956)^2 (0.00002)^2$$

Thus, $\Delta D_U = 0.00001$ g.cm^{-3}

Similarly, ΔD_A and ΔD_B are equal to 0.00001 g.cm^{-3}

$$(\Delta V^E)^2 = (\partial V^E/\partial X_A)^2 (\Delta X_A)^2 + (\partial V^E/\partial D_U)^2 (\Delta D_U)^2 + (\partial V^E/\partial D_A)^2 (\Delta D_A)^2 + (\partial V^E/\partial D_B)^2 (\Delta D_B)^2$$

$$(\partial V^E/\partial X_A) = (M_A - M_B)/D_U - M_A/D_A + M_B/D_B = 60/0.9 - 100/0.8 + 40/0.8 = -8.33333$$

$$(\partial V^E/\partial D_U) = -[X_A . M_A - (1-X_A M_B . D_U]/(D_U)^2 = -[0.5(100) - (0.5)40(0.9)]/(0.9)^2 = 39.50617$$

$$(\partial V^E/\partial D_A) = -M_A/(D_A)^2 . (\_D_A) = -[100/(0.8)^2](-0.8) = 125$$

$$(\partial V_E/\partial D_B) = -[\{(1-X_A)M_B\}/(D_B)^2\}(-D_B)] = -[0.5.40.(-0.8)]/(0.8)^2 = 25$$

Thus, $\Delta V^E = 0.00132$ cm^3.mol^{-1}

$$(\Delta V_\phi)^2 = (\partial V_\phi/\partial d_o)^2 (\Delta d_o)^2 + (\partial V_\phi/\partial d)^2 (\Delta V_\phi)^2 + (\partial V_\phi/\partial C_1)(\Delta C_1)^2$$

$$(\partial V_\phi/\partial d_o) = [-1000(d-d_o)(d_o)]/[C_1(d_o)^2] - (M_1.d_o)/(d_o)^2 = [-1000(0.9-0.8)(0.8)]/[0.05.(0.8)^2]$$

$$(\partial V_\phi/\partial d) = 1000/(C_1 d_o) = 1000/(0.05.0.8)$$

$$(\partial V_\phi/\partial C_1) = -[1000(d-d_o)C_1]/(C_1^2 d_o) = [-1000(0.9-0.8)(0.05)]/[(0.05)^2(0.8)]$$

Thus, $\Delta V_\phi = 0.025$ cm^3.mol^{-1}

Appendix 2

Calibration of the Hewlett-Packard 2804 A Quartz Thermometer

The Hewlett Packard quartz thermometer was used for all the accurate temperature measurements in this work, and was calibrated against a Tinsley platinum resistance thermometer, which had been previously calibrated by the CSIR-South Africa. The resistance of the platinum thermometer at any temperature, T, was measured with an FE Smith difference bridge. This is a modification of a Kelvin double bridge. This and other Wheatstone bridge type assemblies have been discussed by Hall and Barber.[316] The off-balance current was amplified using a PYE Galvanometer Photocell preamplifier, and was fed to a PYE Scalamp galvanometer. A 2V source was used to drive the circuit.

The heating effects could not be neglected for accurate readings. To a first approximation the heating effect at different temperatures is constant if the current in the thermometer bulb is kept constant. This is only true if the conditions of heat transfer between the bulb and its surroundings remain approximately the same. For this reason calibration was carried out in an environment closely resembling that in which later measurements would be made. The calibration of the quartz thermometer was carried out at 5 K intervals over the temperature range 273 K to 323 K in a thermostatted bath similar to the one described in Chapter 2.

To eliminate any stray emf's it was necessary to take resistance readings of both the platinum resistance thermometer and of the standard resistance with the current flowing in both directions in turn; that is four readings, x_i, for each temperature. The resistance, R_T, of the thermometer at the temperature, T, is given to a good approximation by:

$$R_T = [(x_3 + x_4)/2] - [(x_1 + x_2)/2] \qquad \text{B.1}$$

where the first term in equation B.1 corresponds to the average of the resistance of the

standard resistance, R, with the current flowing in both directions, and the second term is with respect to the platinum resistance thermometer at the temperature, T.

Resistance readings were converted to temperature values using the iterative relationship:

$$T^* = [(R_T - R_o)/\alpha R_o] + \delta[(T/100) - 1)](T/100) \qquad \textbf{B.2}$$

together with:

$$\cdots\cdots\cdots\cdots\ t_{68} = T^* + 0.045(T^*/100)[(T^*/100) - 1][(T^*/630.74) - 1] \qquad \textbf{B.3}$$

where α, δ and R_o are the constants for the platinum resistance thermometer. In this case: $\alpha = 3.9214 \times 10^{-3}, \delta = 1.4962$ and $R_o = 24.9573\Omega$.

Appendix 3

GW Basic Computer Program to determine excess molar volumes from period and density measurements

```
10    REM ****************************************************************
20    REM THE FOLLOWING PROGRAM IS WRITTEN IN GWBASIC FOR ANY IBM PC 100%
30    REM COMPATIBLE WITH IBM PERSONAL COMPUTERS.
40    REM THIS PROGRAM CALCULATES EXCESS VOLUMES FOR BINARY LIQUID MIXTURES
50    REM FROM DENSITY MEASUREMENT, BY THE FOLLOWING SIMPLE RELATIONSHIP :
60    REM
70    REM    VE = ((XA*MA + XB MB) / P.UNKNOWN) - (CA + CB)
80    REM
90    REM
100   REM WHERE : P.UNKNOWN IS THE DENSITY OF THE MIXTURE
110   REM   C1 = ((XA*MA) / P.A)
120   REM   C2 = ((XB*MB) / P.B)
130   REM
140   REM
150   REM (AN ANTON PAAR VIBRATING TUBE DENSITOMETER WAS USED IN THIS STUDY)
160   REM

170   REM ORIGINALLY WRITTEN FOR APPLE BY : R C BAXTER, RHODES UNIVERSITY
180   REM CONVERTED TO GWBASIC FOR IBM BY : B BEAN    , RHODES UNIVERSITY
185   REM ADAPTED FOR EXP USE BY            : PENNY GOVENDER-NATAL UNIVERSITY
190   REM
200   CLS
210   PRINT "THE FOLLOWING PROGRAM CALCULATES EXCESS VOLUMES"
220   PRINT
230   PRINT "INPUT THE FOLLOWING CONSTANTS:"
240   PRINT "-----------------------------"
250   PRINT
260   REM ****************************************************************
270   REM INPUT CONSTANTS
280   REM ****************************************************************
290   PRINT"(MA AND MB - MOLAR MASSES, T-PERIODS FOR WATER(W), FOR STD(S),"
300   PRINT"AND FOR COMPOUNDS A AND B,"
310   PRINT"DW AND DS - THE DENSITIES OF WATER AND STD RESPECTIVELY,"
320   PRINT"B-MASSES OF SAMPLE CONTAINER(BO), CONTAINER+A(BA), CONTAINER+B(BB).
330   PRINT"T-PERIOD FOR UNKNOWN(U)"
340   PRINT
350   PRINT" NOTE :- SEPARATE VALUES BY COMMAS" : PRINT
360   PRINT" INPUT YOUR VALUES FOR: MA,MB,TW,TS,TA,TB,DW,DS"
370   INPUT MA,MB,TW,TS,TA,TB,DW,DS
380   PRINT : PRINT" INPUT YOUR VALUES FOR: BO,BA,BB,TU"
390   INPUT BO,BA,BB,TU
393   REM
394   REM
395   GOTO 1500 : REM ************      CALCULATE ANSWERS      ************
396   REM
397   REM
400   REM ****************************************************************
401   REM
402   REM                         PRODUCE OUTPUT
403   REM
404   REM ****************************************************************
420   CLS
430   LPRINT"THE CONSTANTS ARE :"
440   LPRINT"-------------------"
450   LPRINT""
460   LPRINT"MA :",MA," MB :",MB,"
470   LPRINT"TW :",TW," TS :",TS,"
480   LPRINT"TA :",TA," TB :",TB,"
490   LPRINT"DW :",DW," DS :",DS,"
500   LPRINT"BO :",BO," BA :",BA,"
510   LPRINT"BB :",BB," TU :",TU,"
520   LPRINT""
530   LPRINT"THE RESULTS ARE :-"
540   LPRINT"------------------"
550   LPRINT""
560   LPRINT"DENSITY OF MIXTURE = ",DU
570   LPRINT"--------------------"
580   LPRINT"MOLE FRACTION OF COMPONENT A = ",XA
```

```
600   LPRINT"EXCESS VOLUME = ",VE
1000  INPUT "ENTER OUTPUT DATA FILENAME.[<ENTER> TO SKIP]";FLNM$
1010  IF FLNM$ = "" GOTO 2000
1020  OPEN "O",#1,FLNM$
1030  PRINT#1,"THE CONSTANTS ARE :"
1040  PRINT#1,"--------------------"
1050  PRINT#1,""
1060  PRINT#1,"MA :",MA," MB :",MB
1070  PRINT#1,"TW :",TW," TS :",TS
1080  PRINT#1,"TA :",TA," TB :",TB
1090  PRINT#1,"DW :",DW," DS :",DS
1100  PRINT#1,"BO :",BO," BA :",BA
1110  PRINT#1,"BB :",BB," TU :",TU
1120  PRINT#1,""
1130  PRINT#1,"THE RESULTS ARE :-"
1140  PRINT#1,"------------------"
1150  PRINT#1,""
1160  PRINT#1,"DENSITY OF MIXTURE = ",DU
1170  PRINT#1,"-------------------- "
1180  PRINT#1,"MOLE FRATION OF COMPONENT A = ",XA
1190  PRINT#1,"----------------------------- "
1200  PRINT#1,"EXCESS VOLUME = ",VE
1210  PRINT#1,"--------------- "
1220  CLOSE#1
1230  GOTO 2000
1400  REM
1410  REM
1420  REM
1500  REM ************************************************************************
1510  REM
1520  REM                         PERFORM CALCULATIONS
1530  REM
1540  REM
1550  REM ************************************************************************
1560  REM CALCULATE MOLE FRACTIONS
1570  REM ************************************************************************
1580  XA = ((BA - BO) / MA) / ((BA - BO) / MA + (BB - BA) / MB)
1590  XB = 1 - XA
1600  REM ************************************************************************
1610  REM CALCULATE EXCESS VOLUME
1620  REM ************************************************************************
1630  C = (DW - DS) / (TW^2 - TS^2)
1640  DU = C * (TU^2 - TW^2) + DW
1650  DA = C * (TA^2 - TW^2) + DW
1660  DB = C * (TB^2 - TW^2) + DW
1670  VE = (XA * MA + XB * MB)/DU - XA*MA/DA - XB*MB/DB
1680  REM ************************************************************************
1690  REM END OF CALCULATIONS
1700  REM ************************************************************************
1710  REM RETURN TO PRODUCE OUTPUT
1720  REM ************************************************************************
1730  GOTO 400
2000  PRINT
2010  INPUT "DO YOU WANT TO USE THE PROGRAM AGAIN ?>";YN$
2020  IF (YN$="YES") OR (YN$="Y") OR (YN$="yes") OR (YN$="y") GOTO 2040
2030  IF (YN$="NO") OR (YN$="N") OR (YN$="no") OR (YN$="n") GOTO 2200
2035  GOTO 2010
2040  PRINT
2050  PRINT "DO YOU WANT TO EMPLOY THE SAME CONSTANTS IN YOUR NEXT CALCULATION?
2060  INPUT ">";YN$
2070  IF (YN$="YES") OR (YN$="Y") OR (YN$="yes") OR (YN$="y") GOTO 380
2080  IF (YN$="NO") OR (YN$="N") OR (YN$="no") OR (YN$="n") GOTO 360
2090  GOTO 2050
2200  END
```

Appendix 4

TABLE 4.1 R_k and Q_k parameters and group interaction parameters of (an alkanol + a branched chain ether) for Modified UNIFAC

Main Group				Group			
Parameters	Type			Parameters			
System	(n or m)	R_k	Q_k	n amd m	a_{mn}	b_{mn}	c_{mn}
methanol + IPE	CH$_3$OH	0.8585	0.9938	CH$_3$OH-CH$_3$	82.593	-0.486	0.0
	CH$_3$	0.6325	1.0608	CH$_3$-CH$_3$OH	2409.4	-3.0099	0.0
	CH	0.6325	0.3554	CH$_3$-OCH	233.10	-0.3155	0.0
	OCH	1.1434	0.8968	OCH-CH$_3$	-9.654	-0.0324	0.0
methanol + TBME	CH$_3$OH	0.8585	0.9938	CH$_3$OH-CH$_3$	82.593	-0.4857	0.0
	CH$_3$	0.6325	1.0608	CH$_3$-CH$_3$OH	2409.4	-3.0099	0.0
	C	0.6325	0.0000	CH$_3$OH-OCH$_3$	-87.480	-0.5522	0.0
	OCH$_3$	1.1434	1.6022	OCH3-CH$_3$OH	475.20	0.1198	0.0
				CH$_3$-OCH$_3$	233.10	-0.3155	0.0
				OCH$_3$-CH$_3$	-9.654	-0.0324	0.0
methanol + TAME	CH$_3$OH	0.8585	0.9938	CH$_3$OH-CH$_2$	82.593	-0.4857	0.0
	CH$_2$	0.6325	0.7081	CH$_2$-CH$_3$OH	2409.4	-3.0099	0.0
	C	0.6325	0.0000	CH$_3$OH-OCH$_3$	-87.48	-0.5522	0.0
	CH$_3$	0.6325	1.0608	OCH$_3$-CH$_3$OH	475.20	0.1198	0.0
	OCH$_3$	1.1434	1.6022	CH$_2$-OCH$_3$	233.10	-0.3155	0.0

TABLE 4.1   (continued)

Main Group				Group Int.			
Parameters	Type			Parameters			
System	(n or m)	R_k	Q_k	n amd m	a_{mn}	b_{mn}	$c_{mn}\cdot10^3$
				OCH_3-CH_2	-9.654	-0.3242	0.0
ethanol + IPE	OH_p	1.2302	0.8927	OH_p-CH_2	1606.0	-4.7460	9.180
-	CH	0.6325	0.3554	CH_2-OH_p	2777.0	-4.6740	1.551
	OCH	1.1434	0.8968	OH_p-OCH	1102.0	-7.1760	9.698
	$CH_2$0.8585	0.6325	0.7081	OCH-OH_p	1631.0	-7.3260	11.760
	CH_3	0.6325	1.0608	CH_2-OCH	233.10	-0.3155	0.0
				OCH-CH_2	-9.6540	-0.0324	0.0
ethanol + TBME	OCH_3	1.1434	1.6022	OH_p-CH_2	1606.0	-4.7460	9.18
	CH_3	0.6325	1.0608	CH_2-OH_p	2777.0	-4.6740	1.551
	CH_2	0.6325	0.7081	OH_p-OCH_3	1102.0	-7.1760	9.698
	OH_p	0.8585	0.9938	OCH_3-OH_p	1631.0	-7.3620	11.760
	C	0.6325	0.0000	CH_2-OCH_3	233.10	-0.3155	0.0
				OCH_3-CH_2	-9.6540	-0.0324	0.0
ethanol + TAME	CH_3	0.6325	1.0608	OCH_3-OH_p	1631.0	-7.3620	11.76
	OCH_3	1.1434	1.6022	OH_p-OCH_3	1102.0	-7.1760	9.698

TABLE 4.1 (continued)

Main Group				Group Inter.			
Parameters	Type			**Parameters**			
System	(n or m)	R_k	Q_k	n amd m	a_{nm}	b_{nm}	$c_{nm} \cdot 10^3$
	C	0.6325	0.0000	OH_P-CH_2	1606.0	-4.7460	0.918
	CH_2	0.6325	0.7081	CH_2-OH_P	2777.0	-4.6740	1.551
	OH_P	1.2302	0.8927	CH_2-OCH_3	233.10	-0.3155	0.0
				OCH_3-CH_2	-9.654	-0.0324	0.0
2-propanol + IPE	CH0.8585	0.6325	0.3554	OH_s-CH	1606.0	-4.7460	0.918
	CH_3	0.6325	1.0608	CH-OH_s	2777.0	-4.6740	1.551
	OCH	1.1434	0.8968	OCH-OH_s	1631.00	-7.3620	11.76
	OH_s	1.0630	0.8663	OH_s-OCH	1102.0	-7.1760	9.698
				CH-OCH	233.10	-0.3155	0.0
				OCH-CH	-9.654	-0.0324	0.0
2-propanol+ TBME	OH_s	0.8585	0.9938	OCH_3-OH_P	1631.0	-7.3620	11.760
	C	0.6325	0.0000	CH_2-OCH_3	233.10	-0.3155	0.0
	CH	0.6325	0.3554	OCH_3-CH_2	-9.6540	-0.0324	0.0
	CH_3	0.6325	1.0608	OCH_3-CH_3OH	475.20	0.1198	0.0
				OH_P-CH_2	1606.0	-4.746	0.918
				CH_2OH_P	2777.0	-4.6740	1.551

TABLE 4.1   (continued)

Main Group				Group Inter.			
Parameters	Type			Parameters			
System	(n or m)	R_x	Q_a	n amd m	a_{nm}	b_{nm}	$c_{nm} \cdot 10^3$
2-propanol+TAME	OH_s	1.0630	0.8663	$CH-OCH_3$	233.10	-0.3155	0.0
	C	0.6325	0.0000	OCH_3-CH	-9.654	-0.0324	0.0
	CH	0.6325	0.3554	OH_s-CH	1606.0	-4.7460	0.918
	CH_3	0.6325	1.0608	$CH-OH_s$	2777.0	-4.6740	1.551
	OCH_3	1.1434	1.6022	OH_s-CH_3O	1102.00	-7.1760	9.698
				CH_3O-OH_s	1631.0	-7.3620	11.76

TABLE 4.2 R_k and Q_k parameters and group interaction parameters of (an alkanol + a cyclic ether) for Modified UNIFAC

Main Group Parameters System	Type (n or m)	R_k	Q_k	Group Parameters n amd m	a_{nm}	b_{nm}	c_{nm}
methanol + THF	CH₃OH	0.8585	0.9938	CH₃OH-c-CH₂	68.972	-0.420	0.0
	c-CH₂	0.7136	0.8635	c-CH₂-CH₃OH	2540.7	-3.5236	0.0
	c-COC	1.7023	1.8784	CH₃-c-COC	-308.7	1.7454	-0.0
				c-COC-CH₃	952.24	-3.3287	0.0
methanol + THP	CH₃OH	0.8585	0.9938	CH₃OH-c-CH₂	68.972	-0.4200	0.0
	c-CH₂	0.7136	0.8635	c-CH₂-CH₃OH	2540.7	-3.5236	0.0
	c-COC	1.7023	1.8784	CH₃OH-c-COC	-308.70	1.7454	-0.0
				c-COC-CH₃OH	952.24	-3.329	0.0
methanol + 1,4-dioxane	CH₃OH	0.8585	0.9938	CH₃OH-c-COC	-308.7	1.7454	-0.0
	c-COC	1.7023	1.8784	c-COC-CH₃OH	952.24	-3.3287	0.0
ethanol + THF*	OH'	1.2302	0.8927	OH$_P$-CH₂	1606.0	-4.746	0.0
	CH₂	0.6325	0.7081	CH₂-OH$_P$	2777.0	-4.674	0.0
	CH₃	0.6325	1.060	OH$_P$-c-CH₂	3856.0	-17.97	0.0
	c-CH₂	0.7136	0.8635	c-CH₂-OH$_P$	3246.0	-4.937	-0.0
	c-COC	1.7023	1.8784	OH$_P$-c-COC	401.89	-0.4363	-0.0

* the same group and interaction parameters are used for (propan-1-ol + a cyclic ether) mixture

TABLE 4.2 Continued

Main Group				Group			
Parameters	Type			Parameters			
System	(n or m)	R_k	Q_k	n amd m	a_{mn}	b_{mn}	c_{mn}
ethanol + THF*				c-COC-OH$_p$	-238.4	5.00	-0.0
				CH$_2$-c-CH$_2$	-680.9	4.0194	-0.0
				c-CH$_2$-CH$_2$	1020.8	-6.075	0.0
				c-COC-CH$_2$	186.7	-1.3546	0.0
				CH$_2$-c-COC	79.51	0.7089	-0.0
ethanol + THP*	OH$_p$	1.2302	0.8927	OH$_p$-CH$_2$	1606.0	-4.746	0.0
	CH$_2$	0.6325	0.7081	CH$_2$-OH$_p$	2777.0	-4.674	0.0
	CH$_3$	0.6325	1.060	OH$_p$-c-CH$_2$	3856.0	-17.97	0.0
	c-CH$_2$	0.7136	0.8635	c-CH$_2$-OH$_p$	3246.0	-4.937	-0.0
	c-COC	1.7023	1.8784	OH$_p$-c-COC	401.89	-4.674	0.0
				c-COC-OH$_p$	-238.36	5.00	-0.0
				CH$_2$-c-CH$_2$	-680.95	4.0194	-0.0
				c-CH$_2$-CH$_2$	1020.8	-6.075	0.0
				CH$_2$-c-COC	79.51	0.7089	-0.0
				c-COC-CH$_2$	186.71	-1.3546	0.0
ethanol + 1,4-dioxane*	OH$_p$	1.2302	0.8927	OH$_p$-CH$_3$	1606.0	-4.746	0.0

* the same group and interaction parameters are used for (propan-1-ol + a cyclic ether) mixture

TABLE 4.2 Continued

Main Group Parameters System	Type (n or m)	R_k	Q_k	Group Parameters n amd m	a_{nm}	b_{nm}	c_{nm}
ethanol + 1,4-dioxane[*]	CH₃	0.6325	1.0608	CH₃-OH_P	2777.0	-4.674	0.0
	CH₂	0.6325	0.7081	OH_P-c-COC	401.89	-0.4363	-0.0
	c-COC	1.7023	1.8784	c-COC-OH_P	-238.36	5.00	-0.0
				c-COC-CH₃	186.7	-1.3546	0.0
				CH₃-c-COC	79.51	0.7089	-0.0
propan-2-ol + THF[**]	OH_S	1.063	0.8663	OH_S-CH	1606.0	-4.746	0.0
	CH	0.6325	0.3554	CH-OH_S	2777.0	-4.674	0.0
	CH₃	0.6325	1.060	OH_S-c-CH₂	3856.0	-17.97	0.0
	c-CH₂	0.7136	0.8635	c-CH₂-OH_S	3246.0	-4.937	-0.0
	c-COC	1.7023	1.8784	OH_S-c-COC	401.89	-0.4363	-0.0
				c-COC-OH_S	-238.36	5.00	-0.0
				CH-c-CH₂	-680.95	4.0194	-0.0
				c-CH₂-CH	1020.8	-6.075	0.0
				CH-c-COC	79.51	0.7089	-0.0
				c-COC-CH	186.71	-1.3546	0.0
propan-2-ol + 1,4-dioxane	OH_S	1.063	0.8663	OH_S-CH	1606.0	-4.746	0.0

[*] the same group and interaction parameters are used for propan-1-ol

[**] the same group and interaction parameters are used for (propan-2-ol + THP) mixture

TABLE 4.2 Continued

Main Group Parameters System	Type (n or m)	R_k	Q_k	Group Parameters n amd m	a_{mn}	b_{mn}	c_{mn}
propan-2-ol + 1,4-dioxane	CH$_3$	0.6325	1.0608	CH-OH$_3$	2777.0	-4.674	0.0
	CH	0.6325	0.3554	OH$_3$-c-COC	401.89	-0.4363	-0.0
	c-COC	1.7023	1.8784	c-COC-OH$_3$	-238.36	5.00	-0.0
				c-COC-CH	186.7	-1.3546	0.0
				CH-c-COC	79.51	0.7089	-0.0

TABLE 4.3 R_k and Q_k parameters and group interaction parameters of (diethylamine or di-n-propylamine + a cyclic ether) for Modified UNIFAC

Main Group				Group			
Parameters	**Type**			**Parameters**			
System	(n or m)	R_k	Q_k	n amd m	a_{mn}	b_{mn}	c_{mn}
diethylamine + THF or THP[*]	CH$_2$	0.6325	0.7081	c-CH$_2$-CH$_2$NH	350.58	0.0667	0.0
	CH$_3$	0.6325	1.0608	CH$_2$NH-c-CH$_2$	207.26	-1.091	0.0
	CH$_2$NH	1.368	1.0805	CH$_2$-c-CH$_2$	-680.95	4.0194	-0.0
	c-CH$_2$	0.7136	0.8635	c-CH$_2$-CH$_2$	1020.8	-6.075	0.0
	c-COC	1.7023	1.8784	CH$_2$-c-COC	79.51	0.7089	-0.0
				c-COC-CH$_2$	186.71	-1.3546	0.0
				CH$_2$NH-c-CH$_2$	154.5	-0.9466	0.0
				c-CH$_2$-CH$_2$NH	528.30	-0.3991	0.0
				CH$_2$NH-c-COC	-186.98	0.0	0.0
				c-COC-CH$_2$NH	295.07	0.0	0.0
diethylamine + 1,4-dioxane[*]	CH$_2$	0.6325	0.7081	CH$_2$-CH$_2$NH	350.58	0.06773	0.0
	CH$_3$	0.6325	1.0608	CH$_2$NH-CH$_2$	207.26	-1.0916	0.0
	CH$_2$NH	1.368	1.0805	CH$_2$-c-COC	79.51	0.7089	-0.0
	c-COC	1.7023	1.8784	c-COC-CH$_2$	186.71	-1.3546	0.0
				CH$_2$NH-c-COC	-186.98	0.0	0.0
				c-COC-CH$_2$NH	295.07	0.0	0.0

[*] the same group and interaction parameters are used for (di-n-propylamine + a cyclic ether) mixture